CONDUCTION IN MYELINATED AND DEMYELINATED SINGLE OPTIC AXONS

by

KATHRYN AILSA ROSE

A thesis submitted for the degree of

Doctor of Philosophy

of the Australian National University

November 1995

This thesis describes the results of a research project carried out under the supervision of Professor W.R. Levick in the Visual Neurosciences Unit, John Curtin School of Medical Research at the Australian National University.

The experiments and analysis presented in this thesis are my own original work. The complex electrophysiological experiments required that two people be present and I acknowledge the part played by colleagues in assisting with these experiments. The work described has not been submitted previously for a degree at this or any other university.

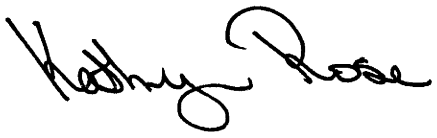

Kathryn Rose

ACKNOWLEDGMENTS

The contribution of the following individuals is gratefully acknowledged:

Professor W.R. Levick, Visual Neurosciences Unit, JCSMR for supervision and training, incisive comment and advice;

Professor L. Burke, University of Sydney for providing the animals with the pressure-lesioned optic nerve and one other, and for his good humour;
Dr W.M. Carroll, Perth, for providing the animals with anti-galactocerebroside lesion and the results of his histological analysis.

I would like to thank the other members of my supervisory panel:
Dr Ian Morgan, Centre for Visual Sciences, RSBS, ANU for giving freely of his time, not just over lunch, expertise, for friendship and unwavering belief in my ability to do it
Dr Geoff Henry, Visual Neurosciences Unit, JCSMR, ANU for helpful and pragmatic advice.

I also wish to express my gratitude to Dr Juleen Cavanaugh, who gave of her time and help in adverse circumstances, provided friendship and support over long lunches and at strange hours of the day.

I wish to express thanks to several people who gave assistance, expertise and encouragement:
Shigang He, Roger McCart, Robert Tupper, Dr Arnie Leon and Ray Brokenshire.

Finally I would to thank my family for their continued tolerance. A wife and mother doing a PhD is not always the easiest person to understand.

ABSTRACT

This thesis presents electrophysiological studies of single myelinated optic axons in the cat, recorded extracellularly in the retina and stimulated from various sites in the optic pathway. The conduction properties of latency and refractory period of transmission were examined in both normal fibres, and fibres undergoing demyelination and remyelination.

The refractory period of transmission of BT/T1 and BS/T2 optic fibres were observed to be the same, while the conduction velocity of BT/T1 fibres is approximately double that of the BS/T2 fibres. This contradicts the widely held view (Paintal, 1965, 1966) that the absolute refractory period is inversely related to the conduction velocity of a fibre. However, an examination of the literature, and data from the non-brisk/T3 fibres in this study, suggests that an increase in refractoriness may occur for fibres whose conduction velocity is less than 15-20 m/s. The conduction velocities of BT/T1 optic fibres were observed to vary between the optic nerve and the tract, with increases in conduction velocity in the tract predominating.

An experimental paradigm utilising the collision of impulses was adapted to examine the refractory periods of transmission of spatially limited regions of the single optic axons, by producing delays in the electrical initiation of antidromic impulses relative to the recording of the spontaneously occuring orthodromic impulses. The space-time diagram was an important device for explaining events associated with the interaction of impulses in the collison paradigm. The use of a simple geometric representation of events allowed simple interpretations of the rules governing the successful transmission of antidromic impulses.

This method of interpretation was crucial when applied to the even more complex situation of understanding collisions through regions of reduced safety factor for conduction created by physiological and pathological lesions of the optic pathway. The application of the collision paradigm in axons with lesions demonstrated that increases in the refractory period of transmission occured within the lesion, and that lesioned axons generally had normal conduction properties in the segment of axon that lay upstream from the lesion. Analysis using the space-time diagrams suggested that some lesioned axons had multiple regions of differing abnormal refractoriness.

Conduction vulnerability for antidromic impulses at the junction of the myelinated and unmyelinated segments of optic axons was not demonstrated in any of the measures regional refractory periods of transmission, when using the optic tract or chiasm stimulating electrodes. Minor vulnerability could be demonstrated only by the application of three closely spaced impulses stimulated from the retrobulbar optic nerve.

Recovery of conduction in optic axons demyelinated by micro-injection of anti-galactocerebroside, occured prior to remyelination. Recovery of conduction also appeared to occur in two stages. Firstly, in axons that were initially unable to conduct impulses, the ability to conduct impulses returned but conduction parameters remained abnormal. Later latency and refractory periods of transmission measurements attained normal values.

Some retinal ganglion cells demonstrated sluggish but atypical non-brisk responses to visual stimulation. The majority of these retinal ganglion cells were unable to transmit impulses. A few were able to conduct impulses downstream from the lesion at conduction latencies that were consistent with T1 latencies. It is suggested that these retinal ganglion cells are in fact "sick BTs", that is BT/T1 retinal ganglion cells whose visual responses have been altered by retrograde changes to the cell body and dendrites.

These advances in our understanding of conduction in normal and lesioned central fibres may ultimately provide approaches to the more effective management of conduction deficits in human neurological diseases.

TABLE OF CONTENTS

GLOSSARY

A1	first antidromic impulse
A2	second antidromic impulse
anti-GC	antigalactocerebroside
4-AP	4-aminopyridine
ARP	Absolute refractory period
BS	brisk sustained retinal ganglion cell
BT	brisk transient retinal ganglion cell
CAP	compound action potential
CNS	Central nervous system
CV	Conduction velocity
D1	delay one, collision paradigm
D2	delay two, collision paradigm
d.a.p.	depolarising after-potential
EAE	allergic encephalomyelitis
GR	geometric ratio of axonal diameters
HRP	horseradish peroxidase
IMP	intra-membranous particle
IRI	inter-response interval
ISI	inter-stimulus interval
LGN	dorsal nucleas of the lateral geniculate
MS	multiple sclerosis
MTP	mid-time point
OD	optic disc
ON	optic nerve
OT	optic tract
OX	optic chiasm
PNS	Peripheral nervous system
R1	time to recording of response to first stimulus
R2	time to recording of response to second stimulus
RGC	retinal ganglion cells
RPT	refractory period of transmission
RRP	relative refractory period
rRPT	regional refractory period of transmission
S1	first stimulus
S2	second stimulus
SC	superior colliculus
SS	sluggish sustained retinal ganglion cell
ST	sluggish transient retinal ganglion cell
TEA	tetraethylammonium

T1	fast conducting optic axons
T2	mediun/slow conducting optic axons
T3	very slow conducting optic axons

CHAPTER 1.

INTRODUCTION.

The axon is the link between the cell body, which integrates information inputs onto its dendrites, and the destination of that integrated information which is output at a synapse. Its integrity is crucial for the conveyance of neural information. However, until the latter half of this century, knowledge of the structure of axons and the processes underlying the transmission of neural information along axons was relatively elementary. Progress in our understanding has followed the development of a battery of techniques that are now used to elucidate the functional architecture of axons. Modern electrophysiological techniques, in conjunction with a variety of pharmacological and biochemical agents, have been used to demonstrate the nature of ion channels in neurons. Axonal ultrastructure has been revealed with the development of electron microscopy and freeze fracture techniques. The recent use of antibodies against components of the ionic channels has enabled an increased understanding of axonal function at the molecular level.

It has become clear that the apparently simple conveyance of an action potential, along what is often thought of as merely a conduit, is in fact a more complex and varied process than originally believed. This thesis adds to existing knowledge of the ways in which neurons will conduct impulses in a variety of normal circumstances and pathological conditions. The majority of previous information has been derived from the peripheral nervous system (PNS), particularly in invertebrate and amphibian species. There has also been a bias in these studies towards larger axons caused by two main technical limitations: in single axonal studies the larger axons have been more easily visualised and dissected out; in studies of whole nerves, the earliest and highest peak of the compound action potential (CAP) is that of the fastest and largest axons and is therefore more readily identified. This study, using the many opportunities provided by the cat visual pathway, examines questions of conduction in the relatively small single axons of the mammalian central nervous system (CNS).

The cat visual system has been used extensively in experimental research and as such is particularly well characterised. The anatomy of the pathway is well documented and there is a comprehensive classification of cat retinal ganglion cells (RGC). The arrangement of the axons in the retina facilitates the use of microelectrode recording of

single axons and the anatomical feature of an unmyelinated axon becoming myelinated in the nerve proper also provides a unique opportunity to examine propagation of impulses through the junction of the myelinated and unmyelinated segments. An electrophysiological study of the visual system of mammals is particularly relevant to the demyelinating diseases of the CNS such as multiple sclerosis (MS).

In this chapter there will be an examination of research on the propagation of action potentials and their after effects. Recent studies of axons, particularly myelinated axons, have revealed that the axolemma is a heterogeneous structure, and that the myelin may not be a simple insulating wrap. The consequences of demyelination on the propagation of impulses and the plasticity of the neuron and myelin during the process of recovery is discussed. Consideration is given to the physiologically normal axonal structures that might also modify impulse transmission in a meaningful way. Finally, aspects of the anatomy of the cat optic pathway relevant to the experimental aspects of this thesis are discussed.

1.1 CONDUCTION PARAMETERS

There are two parameters of conduction that are functionally important for the temporal and spatial coding of information in the nervous system. They are the conduction velocity (CV) and maximum frequency at which impulses can be transmitted. The CV of a particular axon sets the time at which impulses arrive at their destination. Individual axons within a bundle of neurons may receive information simultaneously but transmit that data at different rates, according to the structure of that axon. It is possible that the differing times of arrival may represent a form of information coding. Alternatively, the differing times of arrival could pose a problem for the nervous system, which could be compensated for, in part, by systematic variations in conduction properties. The arrival of a burst of impulses, suppression of impulses or even the rhythmic pattern and frequency of discharge could encode information. The maximum frequency at which an axon can carry trains of impulses determines the operating range of that system in the frequency domain.

1.1.1 Conduction velocity.

Conduction velocity is an easily performed and reliable measure of neuronal function. It is now apparent that all nerve fibres do not conduct at the same rate, and it is generally accepted that fibres with larger diameters conduct impulses faster than smaller fibres. However, the exact relationship between the diameter of fibres and the CV of impulses is not so clear. During the propagation of an action potential, the resistive and capacitive properties of a nerve fibre will slow the passive spread of depolarisation and therefore limit the rate of transmission of an impulse. Changes in the diameter of an axon affect the resistive properties of the core of the axon, and the resistive and capacitive properties of the axon membrane.

1.1.1a Conduction velocity in unmyelinated axons.

The most studied unmyelinated axon is the giant axons of cephalopods, which are up to 400 microns (μm) in diameter, and easily visible under the light microscope. In 1938, Pumphrey and Young measured the CV of axons from the cephalopods *Sepia* and *Loligo*. The CV of an impulse was calculated from the difference in latencies between the recording electrodes placed at varying distances along the axon. Those axons with larger diameters were measured in the fresh state, while the smaller axons were measured after fixation. By studying the change in CV with diameter, Pumphrey and Young suggested that CV was likely to be proportional to the square root of the diameter. Hodes (1953) conducted a similar experiment on the undissected giant squid axon and, contrary to Pumphrey and Young, found a linear relationship of CV to diameter.

Using a procedure of action potential reconstruction, Gasser (1950) determined that diameter was linearly related to CV for small (<1.3 μm) unmyelinated C fibres arising from the cat dorsal root ganglia, but stated that this was not at odds with the square-root relationship suggested for the large invertebrate unmyelinated axons. Cottrell (1984) also found a linear relationship of CV to diameter for C fibres that supply the duodenum in sheep and rabbit. The discrepancies in the results of experimental studies of CV and diameter in unmyelinated axons have not been resolved.

In an elegant theoretical examination of conduction in myelinated axons, Rushton (1951) suggested that CV should be proportional to the square root of the diameter of the unmyelinated fibre. Hodgkin and Huxley (1952) also predicted that CV should vary

as the square root of the diameter of a fibre, after deriving an expression for CV that took account of the resistance of the axoplasm and the capacitance of the axon membrane. In their model, the spread of excitation was dependent upon the passive spread of depolarisation along the axon by local circuit current flow from the active region of the axolemma to the adjacent inactive zones. The rate of conduction was contingent on the time taken by the current flow to depolarise the axolemma to threshold so that the self-regenerative action potential could propagate. An increase in axon diameter increased the membrane capacitance per mm in proportion to the diameter, but at the same time axial resistance decreased in proportion to the square of the diameter (Rushton, 1951). The sum effect of these changes is an overall increase in local circuit current flow which increases the rate of depolarisation and therefore speeds up the rate of transmission of an impulse.

It is worthwhile noting at this point that the threshold of excitation is lower in axons that have faster CVs and therefore larger diameters, whether they are myelinated or unmyelinated (Bishop and Heinbecker, 1928). Injected extracellular current tends to follow the path of least resistance, which is primarily through the extracellular fluid. However a small amount of current enters the axon, flows along the axon cylinder and out at a region closer to the cathode. As already discussed, a larger axon's axial resistance decreases with the square root of the diameter, which will allow greater current flow. This tends to increase the rate of depolarisation of the axon membrane. Even though more current must flow to charge the increased membrane capacitance of the larger axon, the requirement for current increases only linearly with diameter, so that the proportion of capacitive current required to the total available current is less. The overall effect is to decrease the threshold for excitation with an increase in diameter.

1.1.1b Conduction velocity in myelinated axons.

Myelination of nerve fibres is a characteristic primarily of the vertebrate nervous system. The cells that ensheath the axon are of two types. In the CNS, a single oligodendrocyte spirally wraps several axons and forms many internodal segments. In the PNS the Schwann cell surrounds a single axon with many layers and forms only one internodal segment (Bunge, 1968). However, CNS and PNS myelin are functionally similar. In myelinated nerve fibres there are four regions at which current flows must be considered: across the nodal membrane, across the myelin, along the axon cylinder and

through the extracellular environment.

Tasaki and Takeuchi (1941; 1942) found that the myelin sheath was a relatively high resistance and low capacitance structure. So, in myelinated axons, the local circuit current tends to flow ahead of the impulse along an inexcitable internode, until it reaches an excitable region, the next node of Ranvier. With the continued depolarisation of this previously inactive node, threshold for excitation is reached and then this node will contribute to the further propagation of the impulse.

1.1.1c Dependence of conduction velocity on axonal diameter.

Rushton's (1951) important theoretical examination of the effects of changes in diameter on conduction parameters, assumed that the nodal membrane, the axoplasm and external environment were constant, while internodal length varied proportionally with respect to the diameter. Rushton concluded that CV would be proportional to diameter in myelinated axons. Experimental studies of populations of mammalian peripheral myelinated nerve fibres (Gasser and Grundfest, 1939; Hursh, 1939a; Boyd and Davey, 1968; Tackmann et al., 1976) and of frog single axons (Tasaki, 1953; Hutchinson et al., 1970) indicate that CV varied in a linear fashion, proportional to fibre diameter. Hursh (1939a) showed that the largest and fastest fibres of various peripheral nerves of cat and kitten had CVs (in metres per second, m/s), that were 6 times the fibre diameter in μm. There are some suggestions that the relationship of CV to diameter is not linear but that smaller diameter fibres have a lower CV to diameter ratio (Boyd and Davey, 1968; Coppin and Jack, 1972) which may be due to differences in specific membrane properties (Jack, 1975). Jack (1976) suggested that the most likely factors to vary with the diameter of myelinated fibres was the maximal membrane conductances, and the dimensions of the nodal area. Boyd and Kalu (1979) proposed that the important factors might be a combination of changes in membrane conductances and relative myelin thickness.

1.1.1d Dependence of conduction velocity on myelin thickness.

Hodler et al., (1952) showed experimentally that the rate of spread of current between nodes, or the internodal conduction time, was determined by the capacitance of

the myelin sheath and the axial resistance. The thickness of the myelin sheath in particular contributes to the lowering of internodal membrane capacitance.

Rushton (1951) had theorised that there would be an optimal ratio of axonal diameter to outer fibre diameter (the g ratio) of 0.6 which maximised CV. Subsequent theoretical studies have predicted similar optimal g ratios of between 0.60-0.75 (Hodgkin, 1964; Goldman and Albus, 1968; Selektor and Khodorov, 1979; Smith and Koles, 1970). Previous observations of mammalian peripheral axons were in general agreement with this prediction (Gasser and Grundfest, 1939). Sanders (1948), using light microscopy, observed that myelin thickness did not always vary linearly with diameter, primarily because the relation for axons <1 μm in diameter was very steep.

Rushton (1951), noting Sander's measurements of g ratio, concluded that those fibres below the critical diameter of 1 μm might conduct faster if they were unmyelinated. In peripheral nerves, myelinated fibres of < 1 μm are not common (review Berthold, 1978), so this conclusion was apparently supported by experimental observation. However, Waxman and Bennett (1972), using evidence provided by electron microscopy of small fibres in the CNS and PNS, showed that the g ratio remained constant as the diameter of fibres decreased. Waxman and Bennett revised Rushton's analysis and concluded that the benefits of myelination would commence at the critical diameter of 0.2 μm. This contention is supported by electron microscopic evidence of the existence of myelinated fibres of diameter <1 μm in the CNS (review Hirano and Dembitzer, 1978).

If the g ratio were not constant, the experimentally observed linear relationship between CV and fibre diameter would not have been seen. However, if the g ratio is constant while there is some non-linearity in the relationship of diameter to CV, then variation of fibre geometry cannot account for changes in the relationship of diameter to CV and other properties of myelinated fibres would have to vary systematically with diameter.

1.1.1e Dependence of CV on other factors.

The density of sodium ion (Na^+) channels in the nodal membrane will affect the speed of generation of the propagating action potential. Increases in nodal Na^+ channel

density will result in greater nodal Na+ conductance which will be reflected in the more rapid rate of the rising phase of the action potential. If the rise time of a propagating action potential is short, it reduces the time constant of the axon, and will therefore increase CV. The rise time of the action potential has been observed to vary with CV and therefore, possibly with diameter, both in frog (Blair and, Erlanger, 1933) and cat (Paintal, 1966) peripheral nerves. As Paintal (1978) indicated, differences in rise time with diameter are apparently compensated for by a linear relationship between internodal distance and fibre diameter. That is, the smaller diameter fibres with shorter rise times also have short internodal lengths so that internodal conduction time does not vary greatly with diameter in normal fibres (Tasaki, 1953; Rasminsky and Sears, 1972). Moore et al. (1978) simulated the effects of increased excitable nodal area on CV and found that the resultant increased nodal capacitance was offset by an equal increase in voltage-sensitive conductance. They concluded that changes in nodal area are not as effective at altering CV as changes in internodal dimensions.

Changes in internodal length may have little impact on CV in peripheral fibres (Vizoso and Young, 1948; Moore et al., 1978). Huxley and Stampfli (1949) concluded that a particular nodal spacing would maximise CV, but that considerable deviations from the optimum spacing would not alter CV greatly. Rushton (1951) reached the same conclusion and further predicted that the ratio of internodal distance to diameter of fibres would be relatively constant over a wide range of myelinated fibres. In peripheral nerve fibres, the nodes are spaced relatively far apart (minimum 200-400 μm, Ritchie, 1982) and the internodal distance has been observed to be proportional to diameter (Boycott, 1904; Hursh, 1939a; Vizoso and Young, 1948) with a ratio of between 100-146 variously estimated (Schalow, 1989; Waxman, 1972, derived from Hursh, 1939a; Tasaki, 1953). A linear relationship between diameter and internodal length has also been found in CNS fibres (McDonald and Ohlrich, 1971; Murray and Blakemore, 1980), although in some regions of the CNS there are axons with very short internodal segments (Waxman and Melker, 1971; Fraher, 1978; Fried and Erdelyi, 1984).

Brill et al. (1977), simulating the effect of changes in internodal distances on CV, predicted that fibres with a low ratio of internodal length to diameter would be more sensitive to changes of internodal distance than those fibres with more usual nodal spacing. Ritchie (1982) pointed out that in the PNS, the minimum internodal length is limited by the size of the Schwann cell but in the CNS, because one oligodendrocyte forms many internodes, no such limit on minimum length applies. The determinant of

internodal length in the CNS is unknown but shortened internodes could have a great effect upon the facilitation of conduction of impulses into regions of conduction vulnerability (Waxman and Brill, 1978), such as junctions of unmyelinated and myelinated sections of axons, branching axons or regions of focal demyelination.

Despite extensive experimental and theoretical examination of CV, its dependence on the properties of the individual axon is not yet completely understood. This is particularly true for myelinated fibres, where the roles of specific nodal membrane properties and nodal width, internodal distance, myelin thickness and fibre diameter are likely to be interwoven and interdependent. Discrepancies between experimental studies contribute some confusion. These differences may in part be attributed to significant physiological and histological sources of error that can occur in the experimental calculation of the relationship between CV and diameter (Hodes, 1953; Boyd and Davey, 1968; Jack, 1975). In addition, there are methodological difficulties in experimentally studying small diameter fibres, both in isolating such fibres and in interpreting their small amplitude, broad waveforms when embedded in a CAP. Yet examination of the factors that affect CV in small fibres is important for an overall understanding of the relationship between axonal structure and CV.

1.1.2 Refractory period.

The structure-function relationship of nerve fibres is also significant for other aspects of conduction, such as accommodation (Hill, 1936), which is the failure to elicit an impulse when using a slowly rising current to stimulate a nerve, and for refractory period and the related ability of an axon to conduct trains of impulses. By the end of the 19th century, it was known that the second of a pair of stimuli, if applied at a close interval, would fail to propagate (Gotch and Burch, 1899). Absolute refractory period (ARP) has been defined as the interval of time during which a second stimulus of any strength will be unable to elicit a response (Forbes et al., 1923). There are problems with this definition of ARP, as the use of an infinite amount of strength to elicit a response is not feasible, both to produce such a stimulus intensity and because of the effects of high stimulus intensity on biological tissue. Operationally ARP is usually calculated by measuring the interval between the first and second shocks, generally of 1.2-3 times threshold strength, that just fails to produce a detectable response to the second stimulus.

The generation of a second response is dependent upon a sufficient fraction of Na^+ channels returning to rest, via inactivation, after the generation of the first action potential. The number of channels available for activation is related to the time since the first or conditioning stimulus and the strength of current used to generate the first response. The ability to activate sufficient Na^+ channels to depolarise the membrane to threshold a second time is, in turn, dependent on the strength of the second or test stimulus. Normally a few milliseconds (ms) after a conditioning stimulus of threshold strength, a test stimulus of the same intensity would be able to generate a response of the same amplitude as the first response. At a shorter inter-stimulus interval (ISI), the amplitude of the second response would be reduced. If the strength of the test stimulus was increased, a second response of normal amplitude could then be produced at a shorter ISI. The period of time after the conditioning stimulus over which there is a raised threshold for excitation and a reduced amplitude of the test response is known as the relative refractory period (RRP).

Many theories for the underlying mechanism of the refractory phases of nerve have been suggested. Tait (1910) proposed that stimulation of the nerve caused its partial destruction which activated the ARP, followed by a gradual repair process which was the RRP. By contrast, Gotch (1910) suggested that the refractory process was of two origins, a fatigue phenomena of both the site of excitation and the propagating impulse. Lucas (1912) by initiating the first and second impulses at differing locations, showed that the refractory state could be a feature of the propagating impulse alone. Lillie (1920) used an iron wire analogue of nerve to argue that the neuronal membrane might be permeable to ions during the action current. He deduced that the ARP & RRP were likely to be caused by two distinct processes. Adrian (1921) tested a variety of nerve and muscle tissues at different temperatures and found that the duration of the action potential and the ARP coincided and that the RRP commenced at the end of the potential change. For the next three decades Adrian's conclusions were not contested, even though they did not fit all experimental observations.

A more satisfactory explanation for the mechanisms of ARP and RRP awaited the elegant work of Hodgkin and Huxley (1952), who quantified the ionic hypothesis of the resting membrane and action potential by using a voltage clamp technique on giant unmyelinated axon of the squid *Loligo*. This enabled the region of axon under investigation to change potential without propagation occurring. They showed that in response to a stimulus, local changes occurred in the nerve. Depolarisation of the axonal

membrane initially caused a transient increase in the membrane permeability to Na^+. This rise in Na+ conductance accelerated as the inward Na+ current caused further depolarisation, leading to the generation of an action potential. Limiting the level to which Na+ conductance could be raised was the process of inactivation of the membrane Na^+ channels. In addition, there was a delayed, slower rise in potassium (K) conductance which tended to repolarise the axonal membrane by providing a hyperpolarising current. Both these processes contribute to the refractory period of axons.

The role of K+ conductance in repolarisation of the membrane potential in myelinated axons has been re-considered after experimental observations of the relative absence of K+ conductance at the mammalian node of Ranvier (Horackova et al., 1968; Chiu et al., 1979; Brismar, 1980). It is now well established that the contribution of voltage-dependent fast K^+ channels to the repolarisation of the axonal membrane is negligible in mammalian myelinated nerve, compared to their contribution in unmyelinated axons. The absence of a fast voltage-dependent K+ conductance suggested that the repolarisation of the membrane should have been prolonged in mammalian myelinated axons, which is not the case. The solution lay with the faster Na^+ channel inactivation found in mammalian myelinated fibres (Chiu et al., 1979) and the operation of, what were initially known as, passive leak channels (Frankenhaeuser and Huxley, 1964). It now seems that the leak current is not a transmembrane ionic current but rather a capacitive current driven by the recharging of the nodal capacity by the larger internodal capacity (Baker et al., 1987). These currents acting across the myelin via a possible periaxonal pathway (Barrett and Barrett, 1982; Blight, 1985) would limit activation of Na^+ channels. They may also play a vital role in the prevention of reexcitation of the node by any persistence of depolarisation at the paranode. It is the kinetics of these processes which must determine the refractory period of mammalian myelinated axons.

In addition to the faster Na^+ channel inactivation, the node of Ranvier has a large resting membrane conductance (contributed to by the paranodal K^+ channels) which shortens the membrane time constant, thereby reducing the need for a fast voltage dependant K+ conductance. The large passive leak K+ conductance also contributes to the repolarisation of the membrane.

1.1.2a Refractory period of transmission.

The conditions that affect the ARP described thus far apply to the initiation of an impulse at the stimulus site. While these processes will also affect the propagation of a second impulse in the wake of a preceding impulse, it is important to note that other factors also affect the propagation of two closely spaced impulses. Tasaki (1953) observed that an impulse may fail to propagate until it has attained 40% of the normal action potential amplitude. However, even if a second stimulus fails to propagate, a local response to the stimulus may occur (known sometimes as an abortive spike) and this spike is still followed by its own refractory period at the site of stimulation. Tasaki (1953) described this period in the RRP when an impulse can be evoked at the stimulus site but not propagated, as the "critical interval for conduction". Paintal (1966) has called the interval to the initiation of an impulse, ARP1 and to its propagation, the ARP. If the definition of the ARP is the minimum interval possible between closely spaced shocks for the *initiation* of two impulses, then this would be significantly less than the time taken to produce a *propagating* impulse (Tasaki, 1953; Paintal, 1966; Kimura, 1981).

In whole animal experiments or in the clinical study of pathological disorders of nerves, it is difficult to establish the maximum interval for the failure of the initiation of an impulse, so ARP in these circumstances usually applies to the interval between the conditioning stimulus and the test stimulus that just fails to produce a detectable propagating impulse. ARP is sometimes used to describe both the refractory period at the site of initiation and the refractory period of propagating impulses. The classic refractory period of transmission (RPT) described by McDonald and Sears (1970) determines the ability of an individual axon to transmit the second of two closely spaced impulses. The concept of RPT is useful in describing not only those factors that may affect the refractory period at the point of initiation of the impulses, but also those that affect the passage of two impulses, particularly through a region of nerve that is physiologically or pathologically vulnerable.

Of course, the placing of two impulses at a closely spaced interval does, in itself, increase the vulnerability of the tested axon or nerve trunk. The first conditioning impulse will leave in its wake, axolemma in a state of partial recovery. As the test (second) impulse approaches the region previously traversed by the conditioning (first) impulse, the local circuit current, generated by the test impulse, attempts to depolarise the refractory membrane. The success of this attempt is governed by two factors: the

first is the number of Na^+ channels at rest and therefore available for the generation of an action potential; and the second is the size of the local circuit current. An action potential propagating in a relatively refractory axon has a reduced amplitude because of the limited number of Na^+ channels available to generate that action potential. In these circumstances, a second action potential will fail to propagate when its local circuit current is unable to activate sufficient Na^+ channels to cause regeneration of the impulse.

1.1.2b Safety factor for conduction.

Tasaki (1953) noted, in his experiments on single nodes of Ranvier in frog, that the action current developed at each node by the propagating impulse was 5 times greater than the amount of current that was just sufficient to excite the next node. He defined the safety factor for conduction as the ratio of initial action potential amplitude to the critical amplitude that is required for an action potential to excite the next node (Tasaki, 1982). A region of low safety factor for conduction has a decreased likelihood of an impulse propagating. This can be caused by an increase in threshold or a decrease in local circuit current at vulnerable regions, such as would occur at the junction of the axon hillock and cell body, at the branching of an axon, or at areas of trauma or demyelination (Goldstein, 1978; Waxman, 1972; Rasminsky and Sears, 1972). It is to be noted that the standard two shock test for RPT indicates the refractory period for that region of axon which has the lowest safety factor for the secure transmission of impulses.

1.1.2c Latency of the second impulse.

Gotch (1910) made extensive observations on the behaviour of a second impulse propagating in the wake of the first impulse in frog sciatic nerve. He noted that the rate of propagation of the second impulse was increasingly delayed the closer the application of the second stimulus to the refractory period of the first impulse. He attributed the delay to local changes at the point of initiation of the first stimulus and to more subtle changes associated with previous activity along the axon pathway. This was disputed by Lucas (1910), Forbes et al. (1923) and Gasser and Erlanger (1925). Gasser and Erlanger found no additional delay in setting up a second impulse at the stimulus site, when compared to the time taken to set up the first. They found that the interval between the first and second response (or inter-response interval, IRI) was increased with longer

conduction distance and a shorter ISI. The greatest rate of change in velocity of the second response occurred in the first few centimetres of conduction distance. This implied that the delay in the IRI was a feature of travelling in the refractory period of the preceding impulse.

Tasaki (1953) confirmed the results of Gasser and Erlanger. He noted that the second impulse is transmitted more slowly than the first and that the separation between the two will progressively increase from the point of stimulation. With the gradual increase in IRI, the second impulse will start to encounter axon in a more complete state of recovery, progressively allowing the second impulse to increase speed. Tasaki concluded that the velocity of the second impulse would eventually approach a normal conduction rate. In single fibres of myelinated mammalian peripheral nerves Paintal (1965) observed that 95% of normal CV was reached by the second impulse in 3 ms, for fast fibres (conduction velocity of 84 m/s) and in 5 ms in slower fibres travelling at 11 m/s. This suggested that the rate of recovery of the conduction velocity of the second impulse was marginally slower in more slowly conducting fibres. This finding also implies that the distance over which normal CV was attained was shorter for the slower fibres.

If the second impulse does finally reach a constant velocity, the question arises whether the second impulse maintains a fixed distance or time from the preceding impulse. This question has implications for the transmission of trains of impulses and for temporal coding of information in the nervous system. Adrian and Lucas (1912) had noted that the RRP was succeeded by a phase of greater excitability. They named this phase "the period of supernormality" (SNP), which is due to what is now known as the depolarising after potential (see next section) and is believed to be due to the passive discharge of the internodal membrane capacitance. The rate of conduction during this period has been found to exceed the normal CV in a variety of nerves and species (Graham, 1934; Bullock, 1951; Swadlow et al. 1978; Kocsis et al., 1979). It could be supposed that an impulse initiated at a minimum ISI after a conditioning impulse may eventually travel at a constant IRI due to the stabilising effects on its velocity of the RRP and SNP. The RRP will cause an initial deceleration of the second impulse and when the IRI widens sufficiently to cause the impulse to travel in the SNP, it will then accelerate (Kocsis et al., 1979). This would not be expected to happen over short conduction distances, such as occurs in the CNS, as there would be insufficient time for the second impulse to fall far enough behind the first impulse, to then conduct within the SNP.

1.1.2d Refractory period vs diameter of fibres.

That refractory period varies with the diameter of axons has been widely accepted since Paintal (1965; 1966), in a study of *cooled* single fibres of the vagus and saphenous nerves of cat, found that the ARP varied inversely with CV. The expectation from this result would be that, in fibres at *normal physiological* temperatures, the refractory period should also be inversely related to CV and therefore to diameter of fibres. Earlier authors had made experimental observations of only very small variations in refractory period; in the order of 0.6 ms with a fivefold variation in fibre size (Gasser and Grundfest, 1939). Erlanger and Gasser (1937) had earlier examined frog nerve fibres and reported that those peripheral fibres conducting impulses at 17 m/s, or less, had a steeply inverse relationship between CV and ARP. Erlanger and Gasser also indicated that ARP measurements for fibres conducting slower than 6-7 m/s were questionable because of the strong stimulus that was required to excite the slower and less excitable axons. If Hursh's data (Table 3. 1939b) from kitten and cat saphenous and cervical sympathetic nerve fibres is assessed, excluding fibres with CV less than 7 m/s, then in this example the range of ARP is from 0.40 to 0.85 ms for a fivefold decrease in CV.

Hursh (1939b) also found very little variation in ARP, from 0.58 to 0.40 ms, in fibres that conducted at rates from 18-60 m/s. Those fibres that were conducting slower than 18 m/s, however, had ARP that increased markedly with declining conduction rate, paralleling Erlanger and Gasser's finding. Paintal (1965) had also noted that for fibres with CV greater than 30 m/s, the change in ARP was small or insignificant. In rabbit CNS, visual callosal fibres that conducted impulses at a maximum 12.9 m/s showed a similar trend for a short refractory period to occur with the faster fibres (Swadlow and Waxman, 1976), though this population of fibres contained some 45% unmyelinated fibres. A later study of monkey callosal efferent fibres, which were all thought to be myelinated, revealed again a general trend of shorter refractory periods to be associated with faster conducting fibres (Swadlow et al., 1978).

Rushton, in his 1951 paper, discussing the effects of fibre size on aspects of conduction in myelinated nerves, theorised that fibres possessing the same membrane properties but with varying diameters should have similar refractory periods. Whereas CV is dependent upon axonal diameter, myelin sheath thickness and internodal length, the refractory period is correlated to the time course of the process of recovery from the

initiation and passage of a preceding impulse. So if refractoriness is to vary with CV and diameter, then it is anticipated that there would have to be appropriate changes in the kinetics of Na^+ channel inactivation and K+ conductances linked to diameter. Smith and Schauf (1981b) voltage clamped the single fibres of the sciatic or tibial nerves from frog and found that the large K^+ currents seen in large fibres (Frankenhaeuser and Huxley, 1964) did not persist, but disappeared in a graded fashion with decreasing diameter of fibres. The significance of this finding for duration of refractory period in mammalian myelinated fibres, where only a small fast nodal K+ conductance has been found (Baker et al., 1987), is not clear. If such a size-dependent variation in mammalian nodal and paranodal ion channel type and distribution does exist, it may be that it is not a progressive variation with size, but rather a step variation that occurs at a critical diameter of approximately 3 μm in mammalian myelinated axons (derived from Hursh, 1939a & b).

1.1.3 Summary

CV and RPT have been used extensively in experimental studies as electrophysiological measures of axonal activity and as clinical measures of neuronal performance in a wide variety of neuronal disorders. Even though they are a valuable tool, our understanding of the specific structural features of neurons that determine these measures of function is not complete. Although Hodgkin and Huxley made great strides in explaining the ionic processes underlying conduction in unmyelinated axons, later studies of mammalian myelinated axons have revealed that they have a more elaborate architecture than unmyelinated axons and therefore more complex processes underlying the generation of an action potential and the process of recovery.

1.2 CONDUCTION IN MYELINATED AXONS.

Before the membrane organisation of myelinated fibres was understood, it was already known that the exchange of Na^+ and K^+ through uniformly distributed ion channels underpinned the continuous mode of conduction in unmyelinated axons. In myelinated axons, breaks in the myelin called nodes of Ranvier had been seen as early as the turn of the century and the saltatory mode of conduction of impulses in peripheral myelinated fibres was described in the 1930s. However, the complexity of the ion

channel organisation in myelinated fibres has been progressively elucidated only in the last three decades. The non-uniform distribution of Na^+ and K^+ channels in myelinated fibres is now widely accepted but further detail of their complex nature and distribution has recently come to light. The complex nature and distribution of channels in myelinated axons has implications for normal physiological function, as well as for conduction disrupted by disorders of myelin, and in particular, the pathophysiology of demyelinating diseases.

1.2.1 Role of ion channels in unmyelinated axon.

Basic understanding of how action potentials are generated comes from experimental studies conducted on the giant axon of the squid *Loligo*. Using the large unmyelinated axon as a convenient subject, Cole and Curtis (1939) found that the ionic conductance of the axonal membrane rose dramatically during the course of an action potential. In the early 50s, Hodgkin and Huxley published the first comprehensive analysis of the ionic fluxes underlying the action potential in unmyelinated axons. They proposed that the shifts in conductance seen during the passage of an action potential were due to depolarisation generating changes in the permeability of the axonal membrane to Na^+ and K^+. Depolarisation caused a transient increase in Na+ conductance accounting for the rapidly rising phase of the action potential. The time course of this phase was a function of the membrane time constant. The time constant is a measure of the time taken for the membrane potential to reach 63% (ie 1 -1/e) of its final value and is dependent upon the membrane resistance and capacitance. A high resistance and high capacitance membrane will have a large time constant. After the peak of Na+ conductance, and during the inactivation of the voltage-sensitive Na^+ channels, the slower rise of the K+ conductance contributes to the falling phase of the action potential.

Once an impulse has been generated, its conduction along an axon is caused by a passive, decremental spread of depolarisation called electrotonic conduction. The impulse is propagated by local circuit current flow from the active region of the axolemma to the adjacent inactive regions (Hodgkin, 1937b). The efficiency of this process is measured by the length (or space) constant, which is the distance along the axon that an impulse will travel before the membrane potential has decayed to 37% (ie 1/e) of its original value. The length constant is dependent upon the ratio of the membrane resistance to the internal or axial resistance of any particular axon. The less

the axial resistance and the higher the membrane resistance, the further the current will flow, with less current leaking across the axonal membrane, and hence increasing the length constant.

While the generation and propagation of action potentials in unmyelinated axons is adequately described by the mechanisms mentioned above, the explanation of conduction for myelinated axons has proved to be more complex.

1.2.2 Saltatory conduction.

In 1934, Erlanger and Blair, recording from myelinated fibres of the sciatic nerve of frog, found indications that nodes of Ranvier were sites of greater excitability than the internodal regions of axons. At that time, the notion that conduction was saltatory was dismissed on the basis of two popularly held notions: the first, that the nerve fibre itself was the sole conductor of activity, so that no activity spread to the extracellular environment; and second, that while the myelin of peripheral fibres was known to be segmented, myelin of central fibres was thought to be continuous. The saltatory form of conduction and its possible advantage for speed of conduction had been proposed by Lille (1925) who used an analogue of nerve composed of an iron wire enclosed in a glass tube interrupted at regular intervals and placed in a conducting solution. He noted that activation appeared to leap from one interrupted area to the next and that transmission was much faster than in a continuously insulated or bare wire. Even though the connection between the diameter of nerve fibres and conduction velocity was known (Gasser and Erlanger, 1927), saltatory conduction was not immediately seen as the solution to the apparent contradiction of high conduction velocity in small diameter myelinated fibres.

However, during the 1930s, two other laboratories independently began to study the issue of conduction in myelinated fibres. In England, Hodgkin (1937 a;b) concluded from a study of conduction block by cold or pressure in the sciatic nerve of frog, that impulses could be transmitted beyond the block by the spread of electrotonic currents. In Japan, Kato and colleagues had developed a technique for the dissection of single fibres of the nerves of toads, allowing more direct electrophysiological approaches to the problem. Tasaki, one of Kato's co-workers, found evidence that local circuit currents developed at active nodes (1939). He concluded that the impulse jumped from one node

of Ranvier to the next. While studying action currents in short lengths of single myelinated fibres, it was found that the node was traversed by an inwardly directed current, demonstrating that the nodes were the sites of activation in myelinated fibres (Tasaki and Takeuchi, 1941; 1942). Using single fibre dissection in conjunction with voltage clamping, Huxley and Stampfli (1949) working at Cambridge, provided evidence to confirm the theory of saltatory conduction.

1.2.3 Ion channel distribution in myelinated axon.

1.2.3a The role of myelin in conduction.

Classically it has been considered that myelin functions as an insulator of leaky internodal axolemma. Only negligible amounts of current flow were measured at the myelinated internode, as the high resistance, low capacitance myelin effectively seals off the internodal axonal membrane from direct investigation. The major path for transmembrane current flow was the node (reviews Stampfli, 1981; Tasaki, 1953; 1982). Confining current flow to the nodes of Ranvier has at least three advantages. Firstly, a myelinated axon generally has a greater length constant and shorter time constant than an unmyelinated axon of the same diameter and can therefore transmit information at higher conduction velocity. Secondly, small diameter myelinated axons will allow a greater amount of information to be rapidly transmitted within the physical constraints of the overall volume of an organism, such as occurs in the optic nerve (ON). With more axons, there is more sampling of information leading to the greater fidelity of information transmitted. Thirdly, less metabolic energy is required to return internal axonal ionic concentrations to their resting state in comparison to a fibre with ion channels distributed along all its length. However the evolution of myelin has required compensatory alterations in axolemmal structure, in particular, in ion channel distribution.

1.2.3b Voltage-dependent sodium channels.

In myelinated axons, studies using a variety of morphological and physiological techniques have revealed that voltage-dependent Na^+ channels are aggregated at the nodes of Ranvier. The internode has a low density of Na^+ channels, lower than that estimated for unmyelinated axons (Waxman and Ritchie, 1985; Black et al., 1990).

Following the definition by Hodgkin and Huxley of the ionic currents involved in the generation of the action potential in unmyelinated axon, Frankenhaeuser and colleagues used voltage clamp experiments in the toad to demonstrate that an inward Na+ current was present at the node of Ranvier. Studies of mammalian nodes, indicated that a transient inward current was responsible for the initial fast depolarising phase of the action potential (Horackova et al., 1968; Chiu et al., 1979; Brismar, 1980). This paralleled the findings from amphibian axons (Hodgkin and Huxley, 1952; Frankenhaeuser and Huxley, 1964). However, in contrast to the giant squid axon or toad sciatic nerve, the outward current consisted of passive leak current only. It was thought that repolarisation of the mammalian myelinated axonal membrane was brought about by more rapid Na^+ channel inactivation, induced at more negative membrane potentials (Chiu et al, 1979; Brismar, 1980) than in the amphibians. It was not clear whether differences in the Na^+ channel kinetics between amphibians and mammals represented different types of Na^+ channels. Chiu (1980) found that the kinetics of activation in the rabbit node were similar to those of the frog. Neumcke and colleagues (1982; 1987) concluded that mammalian voltage dependent Na^+ channels had similar gating properties but higher single channel conductance than amphibian voltage dependent Na^+ channels.

Neumcke and Stampfli (1982) estimated by voltage clamping rat sciatic nerve and measuring ionic currents that there were approximately 21,000 Na^+ channels per node. Binding of tritium-labelled saxitoxin has been used to estimate the density of Na^+ channels at nodes of Ranvier in rabbit sciatic nerve at 12,000 per μm^2 while the density at the internode was no more than 25 per μm^2 (Ritchie and Rogart, 1977). Later, saxitoxin was found to bind to glia also (Ritchie and Rang, 1983; Shrager et al., 1985), suggesting that the original calculations of nodal Na^+ channel density may have overestimated the number of channels at the node. Pellegrino and Ritchie (1984) compared saxitoxin-binding capacity in normal rabbit ON and a crush preparation that caused axonal degeneration. They found that central glia, at least in the ON after Wallerian degeneration, did not bind saxitoxin and estimated that nodal Na^+ channel density was 400-700 channels per μm^2. Estimates in PNS axons now place the value a little higher at 1,000-2,000 per μm^2 (Howe and Ritchie, 1990). The evidence from saxitoxin-binding studies supports the conclusion that the density of Na^+ channels is highest at the node. Using a modification of a ferric ion-ferrocyanide stain (Landon and Langley, 1971), it has been shown cytochemically that dense aggregation of the stain occurs at nodes in rat peripheral axons and at the electrically excitable nodes of the

axons of the electric organ of the gymnotid fish (Quick and Waxman, 1977). This stain appears to demonstrate a structural heterogeneity in the axolemma of myelinated fibres which is probably due to aggregations of Na^+ channels (Waxman and Foster, 1980).

Examination of axolemma at the electron microscope level using the technique of freeze fracturing of membrane has revealed that the outer face of the fractured membrane (E-face) exhibits protuberances called intra-membranous particles (IMPs). These IMPs are thought to be integral membrane proteins and are likely to indicate the presence of Na^+ channels (Rosenbluth, 1981). In unmyelinated axons, there is a uniform distribution of IMPs (Black et al., 1981), but in myelinated axons the IMPs on the E-face have a heterogeneous distribution with the incidence of IMPs at the node 9 to 18 times greater than that seen in the internode (Rosenbluth, 1976). The more recent development of a polyclonal antibody directed against a purified Na^+ channel protein from rat brain, has demonstrated intense immunoreactivity at the nodes of Ranvier in contrast to the internodal membrane, in peripheral (Ritchie et al., 1990) and central (Black et al., 1989) mammalian myelinated axons. Because of differences in methodology it is difficult to be precise about the numbers of nodal Na^+ channels, however, these studies demonstrated the presence of Na^+ channels predominantly confined to the node in sufficient numbers to guarantee the generation and propagation of action potentials.

To examine the physiological status of Na^+ channels in the internodal membrane it was necessary to remove the myelin to expose the channels to direct investigation. Chiu and Ritchie (1982) and others have used lysolecithin, an agent that causes demyelination, to expose the internodal axolemma. Chiu and Ritchie's voltage clamp examination of the demyelinated internode of frog sciatic axon failed to reveal any Na^+ current. However, Grissmar (1986) found a small internodal Na^+ current in frog PNS nerves demyelinated *in vitro* with lysolecithin and estimated that within 1 hour of demyelination the internodal Na^+ channel density was approximately 500 times less than that at the node. Employing a loose voltage clamp technique, Shrager (1987) by contrast, estimated that the internodal density of Na^+ channels was 1/25 that of the node in frog PNS nerves that had been demyelinated *in vivo*, then removed and examined 1-8 days after the lysolecithin injection. Chiu and Schwarz (1987) also recorded a transient Na^+ current from the internode of rabbit fibres demyelinated *in vitro* and calculated from the peak Na+ current that the Na^+ channel density in the internodal axolemma was 1/30 that at the node.

The differences in the calculated internodal Na^+ channel density found in these

studies are difficult to resolve on the basis of a single factor, such as diameter of axons, inter-species differences or time elapsed since demyelination. However, the conclusions drawn from these studies were similar in principle. Na^+ channels do exist in the internode at a density of approximately 20-25 μm^2, which is a much lower density than in the node and is a value consistent with the earlier saxotoxin binding studies. During normal conduction it is unlikely that the internodal Na^+ channels play any part in the flow of current as they are present in numbers too small and their direct connection with the extracellular environment is restricted by the myelin wrap, limiting their ability to contribute to the rapid rising phase of the action potential.

1.2.3c Voltage-dependent potassium channels at the node.

Voltage clamp studies of the nodes of Ranvier in mammalian peripheral nerve indicated that there were no or very few fast voltage-dependent K^+ channels present at the nodes in rat (Horackova et al., 1968; Brismar 1980) or rabbit (Chiu et al., 1979). Brismar (1980) noted that the permeability of nodal membrane to K^+ in mammals was approximately 1/5th that found in the frog and squid. The small amount of outward current seen in normal mammalian nodes was not affected by the application of tetraethylammonium (TEA) (Bostock et al., 1978; Chiu and Ritchie, 1980) which is known to block voltage-dependent K^+ channels (Hille, 1967).

Both TEA or the more potent voltage-dependent K^+ channel blocker, 4-aminopyridine (4-AP) also did not affect the action potential waveform or refractory period of central myelinated axons (Kocsis and Waxman 1980) or the single fibre action potential activated in peripheral myelinated fibres (Bostock et al., 1981). However, Baker et al., (1987) found that at strong depolarisations of mammalian PNS fibres, rapid K+ current associated with the small numbers of nodal K+ channels could be abolished with the application of 4-AP. These studies all indicated that repolarisation in mammalian myelinated axons is primarily associated with Na^+ channel inactivation and a passive leak current and that (unlike unmyelinated axons and frog myelinated axons), voltage-dependent K^+ channels are present in only low concentration at the mammalian node.

1.2.3d Voltage-dependent potassium channels in the internode.

Internodal voltage-dependent K^+ channels were revealed by Chiu and Ritchie (1980) who employed procedures designed to loosen the paranodal myelin from the axonal membrane of rat nerve fibres. As these treatments proceeded, a sudden increase in outward current occurred. This current was suppressed by internal or external TEA and internal caesium (Cs) ions and was sensitive to external K^+ concentrations (Chiu and Ritchie, 1981). Sherratt et al. (1980) also demonstrated the presence of 4-AP sensitive voltage-dependent K^+ channels in demyelinated internodes. Chiu and Ritchie (1981) speculated that the function of these K^+ channels was to prevent re-excitation of nodal membrane by any lingering depolarisation located in the paranodal membrane. Chiu and Ritchie (1984) also conducted a theoretical analysis of the passive electrical properties of normal myelinated fibres and suggested that the nodal resting potential is, in fact, maintained by an internodal resting potential mediated by voltage-dependent internodal channels.

So, in parallel with the discovery of the heterogeneous nature of Na^+ channel distribution in the axolemma of myelinated axons, the heterogeneity of voltage-dependent K^+ channel distribution was documented (reviews Waxman and Foster, 1980; Waxman and Ritchie, 1985). At this time, the function of internodal voltage-dependent K^+ channels was particularly uncertain because they were normally masked by the myelin, and therefore would apparently have little effect on conduction in normal axons, but would have a profound effect on conduction in demyelinated axons.

1.2.3e Depolarising after-potential and the periaxonal current path.

Barrett and Barrett (1982) recorded intracellularly from the internodal region of peripheral myelinated fibres of frog and lizard. Following an action potential, they noted a slow and prolonged depolarising after-potential (d.a.p.) with a decay half time of 20-100 msec. They attributed the d.a.p. to the passive discharge of capacitance from the internodal axolemma. It was suggested that the d.a.p. was similar in time and nature to the period of superexcitability or supernormality that follows an action potential (Adrian and Lucas, 1912) and that the d.a.p. contributes to the supernormal period. D.a.ps have been recorded in the mammalian central nervous system (Blight and Someya 1985) and in mammalian and amphibian peripheral nerve (Bowe et al., 1987b).

As already discussed, myelin has traditionally been thought to be a high resistance, low capacitance insulator of the internodal axolemma. Numerous models of the myelinated axon have in the past considered the resistive and capacitive properties of the combined internodal axolemma and intact myelin sheath to be one and the same, largely because the internodal axolemma was thought to be completely masked by the myelin and therefore played no significant role in the generation of action potential waveforms unless unmasked by demyelination. Because the sum of the capacitance of the combined internodal axolemma and myelin is low, and the capacitance of the node is also relatively low due to its small area and its high conductance, the time constant of current flow through these paths is, by definition, short. The classical concept of the resistive and capacitive properties of myelin and internodal axolemma cannot, therefore, satisfactorily explain those passive currents that have long time constants.

Barrett and Barrett (1982) proposed new low resistance pathways along the internodal periaxonal space, emerging near the nodes and/or through the myelin sheath, to allow the discharge of the capacitive charge stored on the internodal axolemma. This model yielded a d.a.p. similar to that recorded, without distortion of the action potential. However, the structure of the termination of myelin at its junction with the node is such that this region would not ready allow communication of the periaxonal space with the extracellular environment of the node (Landon, 1981). The suggestion that the myelin has a lower resistance than traditionally supposed was supported by Funch and Faber (1984) who made microelectrode recordings of action potentials within the myelin sheath of the goldfish Mauthner axon. This concept of a low resistance pathway (Barrett and Barrett, 1982, Baker et al., 1987) has significantly changed our view of how myelinated fibres work.

Blight (1985) emphasised that the most important function of the myelin sheath was its ability to reduce the overall capacitance of the internode, not just to act as a resistive barrier to the flow of current through the leaky internodal membrane. Blight's model of an axon with myelin of lower than conventional resistance could account for the d.a.p. while its primary effect was to lessen the effective internodal time constant for a given nodal resistance. But it is not clear what route the current may take to remove charge from the internodal axolemma as the ultrastructure of myelinated axons (Berthold, 1978, Landon, 1981) would appear not to facilitate such a path.

1.2.3f Differentiation of types of potassium channels.

In 1980, Ilyin and colleagues, and then Dubois (1981) reported that repolarisation in frog peripheral myelinated axons had several components, including a fast and slow K+ conductance. Dubois found that the slow phase was not blocked by external 4-AP and persisted for several hundred milliseconds. The fast phase lasted some 20 ms and was blocked by external 4-AP. He suggested the possibility that the fast phase could comprise a further two components. The finding of K+ conductances with different kinetics and pharmacological sensitivities suggested the possibility that there were two structurally different K^+ channels. In confirmation, Grissmar (1986), while examining the current flows at internodes demyelinated with lysolecithin, recorded a two component K^+ current. The fast component was blocked by 4-AP and he noted that the slow component of the K^+ current was twice as large in the internode as that found in the node.

In 1987, Baker and colleagues recording both intra and extracellularly from myelinated axons in rat spinal roots, used a variety of pharmacological agents to determine the nature, function and location of a number of rectifying channels. The term rectification has been used to describe conductances of different sizes with reversed polarity, evoked by depolarisation or hyperpolarisation of the axonal membrane.

In response to depolarisation, two 4-AP sensitive outward rectifying currents were found, a rapid current consistent with K^+ channels previously recorded from the node (Brismar, 1980) and a slow rectifying current. The fast component (time constant 0.5 ms) was thought to be mainly located in the internodal and nodal membrane. Roper and Schwarz (1989) later investigated this current by voltage clamping single axons from the sciatic nerve of rats before and after demyelination. Calculations of channel density lead them to conclude that the fast, 4-AP sensitive K^+ channels were located predominantly in the paranodal region of the axon. Because application of 4-AP is known to promote bursts of impulses in response to a single stimulus, it was thought that these channels might control inappropriate repetitive firing of axons (Baker et al., 1987). A paranodal location ideally places them to prevent re-excitation of the node via current flow through the periaxonal space (Roper and Schwarz, 1989).

The slow 4-AP sensitive outward current appeared to originate from internodal K+ channels and were responsible for the effects on the d.a.p.. These internodal channels may also assist in the maintenance of the resting membrane potential (Chiu and Ritchie,

1984; Baker et al., 1987; Roper and Schwarz, 1989).

A slow outward rectifying current that is blocked by TEA or barium is thought to be too slow to affect action potential duration but is responsible for a small hyperpolarising afterpotential at 20-80 ms (Baker et al., 1987; Eng et al. 1988). The additional hypothesis, that it may be important in the process of accommodation, has been supported by dendrotoxin reduction of accommodation (Poulter et al., 1989). The TEA sensitive channels appeared to be predominantly nodal in origin (Baker et al., 1987; Schwarz et al., 1991) and their internodal density was estimated to be 1/31 of their nodal density (Roper and Schwarz, 1989). The persistence of the effect of TEA on developing axons after myelination also supported the idea of a nodal location for the slow TEA sensitive channels (Eng et al., 1988). An important purpose of this rectifying current may also be the prevention of repetitive firing of the node of Ranvier (Black et al., 1990; Awiszus, 1990) .

A further rectifying current was found by Baker and colleagues (1987). It was a slow inward rectification which was blocked by caesium and it was presumed that the channels responsible were located in the internode. Eng et al., (1990) found a similar inward rectifying current in response to a hyperpolarising pulse in rat ON. This current was also sensitive to Cs^+, but not barium, and was both Na^+ and K^+ dependent. Both groups hypothesised that the possible function of this current was to limit hyperpolarisation of the membrane caused by excessive outward rectifying current induced by trains of impulses. If unchecked, this could block conduction during intense activity.

All these experiments were conducted on peripheral axons, however, Gordon et al. (1988), recording single intracellular potentials and compound action potentials from rat ON, found a differential effect of 4-AP and TEA on action potential duration and postspike activity. This suggested that there might be two pharmacologically distinct K^+ channels in mammalian central myelinated axons as well.

1.2.4 Summary

The discovery that a nodal K^+ current was not responsible for the restoration of the nodal resting potential of myelinated axons has lead to an examination of the distribution and function of ion channels in myelinated axons. The existence of myelin would appear

to call for compensatory alterations of the uniform channel distribution found in unmyelinated axons. Na^+ channel aggregation at the node of Ranvier, at sufficient density to ensure action potential generation, may in itself limit the nodal area available for K^+ channels, the primary source of repolarisation in unmyelinated axons. Repolarisation in myelinated axons appears to be mediated by rapid Na^+ channel inactivation and the recharging of the nodal capacitance by the large internodal capacitive current.

1.3 CONDUCTION IN VULNERABLE AXONS.

Action potentials will propagate along a uniform axon at a constant velocity and retain their amplitude and duration. However, most fibres do not retain a uniform geometry over their entire length. They taper, expand in diameter, branch and in some regions myelinated fibres become unmyelinated. It is, however, probable that the majority of axonal pathways are designed to secure conduction and that the safety factor for a single impulse will exceed 1 in most situations.

Disease states, such as demyelination or injury, can also affect the margin for safety of conduction. On encountering regions of non-uniformity, impulses will speed up or slow down so that impulses may still be transmitted albeit less reliably and in some instances, in an altered form. If an axon is disconnected from its destination or if the safety factor for conduction has fallen below unity, impulses will be blocked and function is lost.

1.3.1 Conduction through regions of varying diameter.

Gradual increases in fibre diameter tend to progressively reduce CV because the decrease in core resistance will allow a greater fraction of the available current to flow down the axon cylinder, thereby reducing the amount of available current to cross the axolemma. This causes less local circuit current to flow and there is less driving current available to depolarise the adjacent membrane, which also has increased capacitance because of the increase in membrane area (Goldstein and Rall, 1974).

This is accentuated if there is an abrupt increase in diameter, such as might occur at the branching of axons. Another well-known example is the antidromic activation of the axon hillock-soma region of the motoneurons. Impulses invading this initial segment can be slowed or even blocked if the axon is refractory (Coombs et al., 1957a). The potential success of impulse propagation through a region of increased diameter depends upon the geometric ratio (GR) of the adjacent regions. If the GR is ≤ 1 in regions with similar conductances and of reasonable length then conduction will proceed unhindered. If GR is >1, the sudden increase in membrane area per unit length and decrease in input resistance will decrease the velocity and amplitude of the approaching impulse. Reduction in safety factor of conduction at a region of increased diameter may be revealed by an increased refractory period. Conduction has been predicted to block if the step-like expansion of diameter increases six fold (Khodorov and Timin, 1975).

Goldstein and Rall (1974) predicted that, in regions that would marginally permit conduction, propagation of impulses may occur in both the forward and reverse directions. The key feature of a reflected impulse is the delay experienced by the action potential at the edge of the region of axonal heterogeneity. With arrival of the impulse at the point of increasing diameter, the smaller axon directly behind the action potential is still refractory. However with the longer delay of the impulse at the edge of the region of heterogeneity, this refractoriness will subside to the point where an impulse can be generated in the reverse direction also. Such reflected impulses have also been predicted in the qualitative analysis of Khodorov and Timin (1975) who also suggested that even if the reflected impulse failed to propagate due to persistent refractoriness, then it may delay the recovery of the axonal membrane. Reflected impulses have been seen experimentally in the axon hillock-soma region (Fuortes et al., 1957) and from regions of segmental demyelination (Howe et al., 1976).

1.3.2 Conduction from a myelinated to unmyelinated axon.

The junction of a myelinated and unmyelinated segment occurs normally in the terminal branches of the motor nerve fibres in the skeletal muscles. Such a region is subject to an apparent impedance mismatch because of the considerable area of unmyelinated terminal membrane that must be charged by the current generated by the penultimate node. Despite this, conduction of impulses into the terminal occurs with a relatively small delay (Katz and Miledi, 1965). The velocity of impulses is slowest at the junction of the myelinated axon and the unmyelinated terminal, and this region also displays a low safety factor for propagation of trains of impulses (Braun and Schmidt, 1966).

The structure of the early portion of the terminal and the preterminal region of the motor nerve fibres appears to have partially solved the problem of impedance mismatch by the adoption of three mechanisms to assist the impulse invasion of the terminal. The first mechanism is the narrowing of the terminal compared to the diameter of the myelinated axon (Khodorov and Timin, 1975). The second is the shortening of internodal segments in the preterminal area (Waxman, 1972; Fried and Erdelyi, 1984). The third is the apparent development of a specialised heminode, just beyond the termination of the myelin. Extracellular recording and pharmacological blockage of K^+ and Na^+ channels, have shown that the membrane just beyond the furthermost extent of myelin possesses a concentration of Na^+ channels. K^+ channels were only present at the terminal endings (Brigant and Mallart, 1982). At the ultrastructural level, the transition region has also been shown to contain a cytoplasmic undercoating similar to that seen at nodes of Ranvier by electron microscope (Waxman, 1974). The terminal heminode therefore appears to have a specialised structure that resembles that of a node and that extends several microns into the unmyelinated terminal.

Specialisation of structure has also been noted at other sites of transition from unmyelinated to myelinated fibres, such as occurs in the transition from the PNS to the CNS of dorsal root C fibres (Carlstedt, 1977), where the larger diameter fibres (0.6-0.8 um) after being invested by myelin have several internodes <10 μm in length. Hildebrand et al. (1985) examined the junction of the unmyelinated and myelinated portions of rat ON fibres and also found that the internodal distances of the axons in the transition zone were very short. The presence of shortened internodes, decreasing diameter and of a specialised heminode with a high concentration of Na^+ channels will increase the safety

factor of conduction at the heminode, though CV may be reduced. It also suggests that sites of initial investiture of myelin on unmyelinated axons may be subject to variation of the developmental factors that normally govern the regular internodal length and axonal diameter relationship (Quick et al., 1979).

1.3.3 Conduction in demyelinated axons.

As first described by Charcot in 1877, the pathophysiology of demyelinating diseases is characterised by discrete areas of destruction of myelin and the retention of the intact axon cylinder. Loss of myelin occurs as a consequence of diseases such as multiple sclerosis (MS) or idiopathic polyneuritis, or can arise secondarily through anoxia, oedema or trauma (for review see Traugott and Raine, 1984). The degree of demyelination can extend from loosening of paranodal myelin to the entire removal of myelin over many internodes.

Experimental demyelination of axons is induced by a wide variety of agents and means. These include injection of whole brain, white matter or purified myelin basic protein producing experimental allergic encephalomyelitis (EAE), diphtheria toxin, lysolecithin (Hall and Gregson, 1978), antigalactocerebroside antisera (anti-GC) (review Saida, 1985) and nerve compression (review Raine, 1984), to name just a few. Lesions can be induced in either the PNS and CNS, and despite the differences in myelination between the two systems and differences in the agents used, it is generally considered that experimental electrophysiological findings are relevant to all situations where demyelination occurs.

1.3.3a - Demyelination and symptoms.

Individuals afflicted with demyelinating diseases typically display abnormalities of motor and sensory neuronal function. The resultant symptoms have been attributed to conduction defects associated with the loss of myelin in focal areas, known as plaques. Plaques occur in the PNS and CNS or, as in the case of MS, exclusively in the CNS with a predilection for the ONs as well as the corticospinal tracts, cerebellar pathways, dorsal columns of the spinal cord and subcortical white matter. Clinical signs in persons suffering demyelinating disorders appear to be attributable to conduction block (Cragg

and Thomas, 1964; McDonald and Sears, 1969), or in less severe lesions; reduced CV (McDonald, 1963; Lehmann and Ule, 1964; Cragg and Thomas, 1964), lengthening of the refractory period (Lehmann, 1969; McDonald and Sears, 1970) and impairment of the transmission of high frequency trains of impulses (McDonald and Sears, 1970; Davis, 1972; Bostock and Grafe, 1985). Other symptoms, known as paroxysmal phenomena (Halliday and McDonald, 1977), cannot be explained by deficits of conduction, and our understanding of their mechanism is presently limited to speculation. It has been reported that mechanically generated or spontaneous bursts of impulses can occur from within a demyelinated lesion (Smith and Hall, 1980) but Bostock et al. (1983) was unable to detect any hyperexcitability within the regions of rat spinal roots demyelinated by diphtheria toxin.

While it is apparent that demyelination can cause abnormalities of conduction, there is evidence from a number of sources indicating that symptoms are not always manifest in the presence of a demyelinating lesion. Pathological examination often reveals a wider distribution of demyelinating lesions than the manifest clinical symptoms would suggest (Namerow and Thompson, 1969; Waxman, 1981). Similarly, delays in visually evoked potentials of up to 40 ms can be detected in MS patients with no visual symptoms and no history of optic neuritis (Halliday et al., 1972; Nuwer and Namerow, 1981). However, symptoms are often the manifestation of gross abnormalities, that is minor alterations of CV within a portion of a nerve trunk may in fact not give rise to overt signs noticed by the individual. It requires more subtle clinical tests to demonstrate any abnormality in these cases.

It has also been observed clinically that symptoms can be acutely exacerbated or relieved over a short period of time, much less than the time scale for the process of demyelination and remyelination. The transitory relief of symptoms can be induced by alterations of acid-base balance caused by hyperventilation, or by the intravenous administration of sodium bicarbonate or decreases in calcium concentration, using disodium edetate (Davis et al., 1970), or symptoms can be exacerbated by increases in body temperature (reviewed by Halliday and McDonald, 1977).

Rasminsky (1973) showed that increases of temperature within physiological range caused reversible conduction block preceded by increased CV in experimentally demyelinated rat PNS fibres. This apparently anomalous finding is consistent with known descriptions of ion channel kinetics. Huxley (1959) had shown that elevation of

temperature speeded up both Na^+ channel inactivation and K^+ channel activation, with the latter progressively overtaking Na^+ channel activation. Consequently while CV is initially increased by a rise in temperature, eventually conduction block occurs.

The most likely explanation for the conduction block is a lowering of safety factor due to the decreased duration of the action current at the demyelinated node, which reduces the current flow available for regeneration of the impulse (Rasminsky, 1973; Davis and Shauf, 1981). In the demyelinated axon, rises in temperature alter the balance between increased CV and lowered safety factor. These findings all strongly suggest that conduction deficit in demyelinating diseases is not a reflection of destruction of axonal continuity. Rather, it is state in which many axons within a nerve fibre bundle will have a safety factor for conduction that is close to or less than unity.

1.3.3b Conduction and loss of myelin.

Conduction defects such as blocking of impulses, reduced CV and extended RPT may be related to either a decrease in local circuit current and/or an increase in threshold of the demyelinated region of the axon. It is thought that removal of the myelin greatly increases the capacitance and conductance of the axolemma (Tasaki, 1955) and as a consequence reduces the spread of the local circuit current. Thus, more current is required to charge the increased capacitance and more current will be shunted from the axon core, across the exposed internodal membrane, thereby reducing the length constant of the axon. With less current available, the adjacent, as yet unexcited node, will experience a reduction in the normal outward current flow and, therefore take longer to reach threshold (Rasminsky and Sears, 1972). Less severe losses of current will permit conduction to continue, but at a cost in the speed at which an impulse can be generated. Rasminsky and Sears (1972) concluded, from their study of external currents in single fibres from rat ventral roots, that internodal conduction time could increase twenty-five fold before conduction block would occur.

It has also been indicated that conduction block may be due to an increase in the current required to reach threshold, due to membrane hyperpolarisation (Bostock and Grafe, 1985). In addition to the loss of the capacitive and resistive properties of myelin, demyelination also unmasks the voltage-dependent K^+ channels normally concealed by the myelin (Ritchie and Chiu, 1981). As an impulse approaches the demyelinated region,

depolarisation activates all voltage-gated channels including internodal K^+ channels. The opening of these channels provides hyperpolarising drive to the membrane potential. Koles and Rasminsky (1972) observed that paranodal demyelination was the most destructive to continued conduction, probably due to the paranodal location of fast outward rectifying channels in myelinated axon (Baker et al., 1987).

Computer simulations of demyelinated axons yield some qualitative predictions on structural factors that can affect conduction. Schauf and Davis (1974) predicted from their model of a demyelinated axon with inexcitable internodal membrane, that even if K+ conductance in the demyelinated region was reduced by 50%, the action potential would be prolonged by only 10% and CV would not change. However, Waxman and Wood (1984) simulated various ion conductances in the internode and their effects upon securing conduction into regions of focal demyelination and found that a substantial decrease in the K^+ channel density at the junction of the myelinated and unmyelinated segments facilitated conduction into the unmyelinated zone. This latter prediction is interesting in light of the suggestion of Schwarz et al. (1991) that in chronic EAE demyelination, changes may occur in the relative contribution of fast and slow K^+ channels. In particular, reduction in concentration of the paranodal fast K^+ channels might assist conduction in the manner predicted by Waxman and Wood.

Waxman (1977) examined a model of demyelinated axon, which included an electrically excitable internode with intrinsic characteristics similar to nodal membrane uniformly extended along the two demyelinated internodes. Despite this wealth of Na^+ channels, conduction still failed at the demyelinated region. This failure was thought to be due to impedance mismatch between the myelinated and demyelinated segments, caused by the abrupt increase in membrane capacitance and the current density produced at the last normal node being too low to depolarise the exposed membrane to threshold. Stephanova (1989), similarly using elongation of the node to simulate demyelination, predicted that conduction was affected when the area of demyelination was increased from 10 μm to 30 μm and suggested that increase in the refractory period may be caused by both reduction in local circuit current per unit area and a rise in threshold current.

Quandt and Davis (1992) used a model that progressively reduced the myelin thickness. They predicted reduction of local circuit current and following the passage of the first impulse, a delay in repolarisation of the node prior to the demyelinated segment, due to the conducted current from the node distal to demyelinated segment. This

prolongs Na^+ channel inactivation, delays recovery from inactivation and slows closure of K^+ channels, all combining to generate an increase in the RPT at the node prior to the demyelinated segment.

In a study of single fibres from the cat spinal cord, McDonald and Sears (1970) found that RPTs were significantly affected by demyelination, as did Smith and Hall (1980) in demyelinated PNS fibres. Rasminsky and Sears (1972) suggested that the RPT will reflect the refractory period of the most severely affected internode, whereas CV denotes the status of the length of fibre tested. Smith and Hall (1980) also found that RPT was correlated with the histology of demyelinated fibres and concluded that RPT reflected more truly the degree of clinical deficit than CV did. In addition, they stated that fidelity of transmission would be more dependent upon security of conduction than would be the speed at which impulses were transmitted. Refractory period measurements have been used as a clinical tool (Gilliat and Willison, 1963; Kimura, 1981). Shefner and Dawson (1990) in reviewing the use of a variety of clinical measures of conduction concluded that refractory period may be a more sensitive measure of some neuropathies than other more conventional measures. While the examination of the ability of demyelinated axons to transmit trains of impulses would perhaps prove an even more sensitive measure, high frequency impulses tend to be very unpleasant for conscious individuals, restricting their use to non-clinical situations.

The lengthening of the RPT and the inability to transmit high frequency stimulation trains are related, but not the same. If the frequency at which demyelinated axons appear to block is 50 Hz (Bostock and Grafe, 1985; Kaji et al., 1988) and if the maximum RPT recorded from demyelinated axons is in the order of 3-4.2 ms (Smith and Hall, 1980 and McDonald and Sears, 1970) then these RPTs roughly indicate a possible carrying capacity of 250 Hz, well above the rate established. While it is known that multiple impulses will reduce safety factor in an axon with already marginal security of conduction, it is likely that another mechanism is being induced by the tetanic stimulation. The mechanism of blocked trains of impulses in demyelinated fibres has been an issue of some contention. It was suggested by Rasminsky and Sears (1972) that the failure to continue to transmit trains of impulses was due to a gradual accumulation of intracellular Na^+ during activity which reduced the Na^+ equilibrium potential, and that this would lead to a progressive decline of inward current.

Davis (1972) observed that reduction of the amplitude of CAPs occurred when demyelinated and pressure-injured mammalian myelinated fibres were subjected to trains of impulses at frequencies as low as 10-25 and 50 Hz, respectively. He attributed this effect to block of conduction in demyelinated fibres caused by decreased local circuit current flow and shunting of current through the demyelinated internode. This mechanism had been earlier suggested by Tasaki (1953) for lightly anaesthetised nodes. Another possibility is the loosening of paranodal myelin by high frequency repetitive stimulation, as has been seen in rat sciatic nerve stimulated at a rate of 200 Hz (Moran and Mateu, 1983), which apparently exposed the paranodal 4-AP sensitive K^+ channels.

Brismar (1981) found by voltage clamping fibres of demyelinated rat sciatic nerve that the Na^+ equilibrium potential was normal but that the delayed outward K^+ currents were increased. Brismar concluded that these large K^+ currents may cause the accumulation of extracellular K^+ during repetitive stimulation. Kocsis et al. (1983) noted a reduction in excitability of the parallel fibres of the cerebellum when stimulated at 50 Hz and attributed this to an increase in extracellular K^+. Bostock and Grafe (1985) used intracellular and ion-sensitive extracellular electrodes to record from single rat ventral root fibres demyelinated by diphtheria toxin. Their experiments showed that a rise in threshold was all important and that the local circuit current did not significantly alter during stimulation at a frequency high enough to block conduction. Bostock and Grafe directly demonstrated that a major factor in producing block in demyelinated fibres was the hyperpolarisation that follows activation of the electrogenic Na^+/K^+ pump during repetitive stimulation. This pump normally counteracts the passive leakage of Na^+ into and K^+ out of a cell.

In general, experimental results and computer simulation studies appear to indicate that both reduction of local circuit current and increases in membrane threshold in the demyelinated region of the axon, by mechanisms not yet determined, cause conduction block, extended refractory period and failure to transmit trains of impulses. When the safety factor for conduction is less than 1, conduction will fail because the minimum current required to activate the next node is not attained. Agents or procedures that can alter the safety factor will have a profound effect on the numbers of axons able to transmit impulses through a region of demyelination.

1.3.3c The pharmacology of demyelination.

If deficits of conduction are induced by impedance mismatch at the site of demyelination, it follows that agents that can prolong the action potential duration, or lower the threshold for excitation, would alleviate symptoms. The effects of these agents on demyelinated fibres also yield valuable information on the kinetics of action potentials in demyelinated axons. The action potential duration in mammalian demyelinated fibres can be extended by one of two mechanisms: either by delaying Na^+ channel inactivation; or by reducing K+ conductance. Bostock et al. (1978) found that the venom of the scorpion *Leiurus quinquestriatus*, known to suppress Na^+ channel inactivation, could raise the blocking temperature of rat spinal roots demyelinated by diphtheria toxin. Amantadine, an anti-viral drug, has also been implicated in the possible slowing of Na^+ channel inactivation and improvement of conduction across regions of demyelination (Schauf, 1987). Clinical trials of the drug in patients with MS have not reported relief of symptoms associated with improved conduction (Plaut, 1987), though some improvement of the non-specific symptom of fatigue has been reported (Rosenburg and Appenzeller, 1988; Cohen and Fisher, 1989).

Aminopyridines and TEA, which are known to block voltage-dependent K^+ channels, have also been used. Sherratt et al. (1980) and Bostock et al. (1981) have demonstrated that 4-AP and TEA increased the temperature at which conduction block occurred in rat spinal roots demyelinated by diphtheria toxin. They deduced that K^+ channels must be present in internodal axolemma and their blockage could assist conduction in cases of marginal conduction block. Another agent, gallamine triethiodide, has also been shown to block neuronal K^+ conductance in amphibian and mammalian fibres (Smith and Schauf, 1981a). However, the ability of this powerful neuromuscular blocking agent to cross the blood brain barrier is questionable, even though the barrier may be compromised in MS. This, and its paralysing action, rule out gallamine's use as a drug to relieve the symptoms of demyelination.

Recent clinical trials of orally administered 4-AP and 3,4 diaminopyridine (DAP) have shown improvement in performance and symptoms particularly for those patients whose symptoms are temperature sensitive (Davis et al., 1990; van-Diemen et al., 1992, Bever, 1994). These subjects only showed mild adverse reactions to orally administered 4-AP, most commonly reporting paraesthesia, while Polman et al., (1994) suggested that 4-AP was more tolerated than DAP. The generation of bursts of impulses when 4-AP is

applied to sensory fibres (Kocsis et al., 1981) may suggest a possible mechanism for the paraesthesia reported.

Another avenue of possible therapeutic benefit is suppression of the Na^+/K^+ pump. This would have two effects in MS. As previously discussed, the pump is implicated in the failure of conduction due to membrane hyperpolarisation caused by tetanic stimulation in demyelinated axons. Inhibition of the pump may alleviate this, as well as increasing the membrane potential, by preventing the pump playing its normal role in maintaining the resting membrane potential (review by Thomas, 1972). Somatosensory evoked potentials were assessed in rats with spinal cord anti-GC lesions (Kaji and Sumner, 1989) that were administered ouabain systemically. Ouabain, a known specific pump inhibitor, appeared to be effective in removing conduction block and rate-dependent conduction block, and in improving CV. An initial clinical trial, administering single dose digitalis (digoxin) to patients with MS, has met with only limited success (Kaji et al., 1990), possibly because the therapeutic dose is rather close to the toxic dosage.

The primary disadvantage of a pharmacological approach to improving conduction in demyelinated axons is that agents which alter the kinetics of ion channels, thereby altering the membrane threshold and action potential generation and duration, have a global effect when administered systemically. Unpleasant side-effects, often neurological in origin and including convulsions (Ball et al., 1979; Sears and Bostock, 1981), can be the consequence of using these pharmacological agents. However, it is possible that drugs that do not normally cross the blood brain barrier may find entry where the barrier is potentially compromised by the process of demyelination thereby limiting their action to the site of demyelination. This is more likely to occur in active lesions rather than established inactive plaques. Steroids are widely used to suppress active inflammatory processes in MS but play no role in restoring lost function. Another possibility which has not yet been explored is that of agents that would promote remyelination of axons.

1.3.3d Remyelination

Remyelination of the demyelinated fibres would be expected to restore function if demyelinating neuropathies simply destroyed the myelin without breaching axonal continuity. In the PNS, remyelination takes place relatively rapidly and effectively both in

disease-induced (Weller, 1967) and experimental demyelination (review by Ludwin, 1981). Migrating Schwann cells have been seen to remyelinate spinal cord axons (Bunge, 1968; Feigin and Ogata, 1971). Normally in the CNS remyelination does not occur readily (Ludwin, 1981; Raine, 1984). However, experimental remyelination of CNS fibres by oligodendrocytes has been demonstrated (Koenig et al., 1967; Gledhill et al., 1973; Smith et al., 1979; Blakemore and Murray, 1981) and limited remyelination has been seen at the edges of MS plaques (Prineas and Connell, 1979).

Remyelinated fibres have been characterised by thin myelin and shorter than normal internodal lengths in both the PNS (Vizoso and Young, 1948; Wisniewski and Raine, 1971; Hildebrand, 1989) and the CNS (Suzuki et al., 1969; Gledhill et al., 1973; Ludwin, 1978; Blakemore and Murray, 1981). Studies simulating reduction in myelin thickness have shown that increases in the conductance and capacitance of the myelin sheath as it is thinned do cause disruption to conduction. Koles and Rasminsky (1972) and Schauf and Davis (1974) found that CV decreased as myelin became progressively thinner and Koles and Rasminsky calculated that conduction would stop when myelin reached 2.7% of its original thickness. Quandt and Davis (1992) predicted from their model that the ARP would increase as myelin was progressively reduced to less than 25% of its original thickness. The significance of these calculations is unclear, but variable myelin thickness has been reported in demyelinating diseases (Ludwin, 1981). The implication is that conduction could continue despite substantially thinned myelin such as occurs in remyelinating axons.

Further examination of this question (Waxman and Brill, 1978) showed that impedance mismatch could be alleviated by the presence of at least two shortened internodes proximal to the demyelinated zone. Invasion of the demyelinated zone would occur if the two internodes were one-third or less of their normal length. Conduction would then proceed in a continuous manner across the demyelinated zone until myelinated axon was encountered and saltatory conduction would then be re-established. While such shortened internodes do not speed up CV, they increase security of conduction.

But the question remained as to whether remodelling of internodes occurs and whether it would guarantee secure conduction. Smith and Hall (1980) examined a demyelinating lesion created by intraneural injection of lysophosphatidyl choline in the rat sciatic nerve. Initially, conduction block coincided with demyelination, but then

conduction began to recover. Histological examination revealed thinner than normal myelin and shortened nodes. Conduction was eventually restored to the control level. A subsequent study of an equivalent lesion in the spinal cord of cat (Smith et al., 1981) showed the same recovery of CV and RPT. Saida et al. (1980) conducted a combined electrophysiological and morphological study of rat PNS fibres demyelinated with anti-GC, and found that conduction recovered when myelin thickness had been restored to approximately the value (2.7%) predicted by Koles and Rasminsky (1972). Saidi et al. (1980) also noticed that the demyelinated axons had smaller diameters in the region of the focal demyelination, as has also been seen in MS plaques (Prineas and Connell, 1978). As this occurred early in the process of demyelination and was not associated with return of conduction (Saidi et al. 1980), it was unlikely to cause recovery of conduction by itself, but may assist in improving safety factor in conjunction with other modifications of axonal structure.

Despite thinned myelin, which would serve to increase the capacitance and conductance of the internode, the shortened internodes may reduce the internodal capacitance, improving the safety factor for conduction. Further, if the new nodes had a 'normal' complement of Na^+ channels, then the time constant for conduction would be greatly improved. The exact structure of these new nodes is uncertain although their apparent 4-AP sensitivity in remyelinated (Hildebrand et al., 1985) and regenerated nerves (Kocsis and Waxman, 1981) with shortened internodes, implies the presence of 4-AP sensitive K^+ channels either in the new nodes or in the paranodal axolemma, the latter becoming accessible to 4-AP due to changes in the paranodal axo-glial junction.

1.3.3e Are functional sodium channels present in the internode?

In considering how conduction block or slowing of CV can occur, it is important to determine the nature of the internodal axonal membrane, that is, whether it is excitable or not. In the healthy myelinated axon, the capacity of the internodal membrane to generate action current is not relevant. The low capacitance, relatively high resistance myelin sheath inhibits any rapid ionic exchange across the internodal membrane that might be associated with impulse generation. It is only when this insulating cover is lost that the possible existence of internodal Na^+ channels has a bearing upon the potential for the denuded axolemma to contribute to continued conduction. Internodal Na^+ channels might be implicated in the remitting nature of symptoms in persons suffering from MS,

in the CNS, remissions appear to occur despite limited remyelination (McDonald, 1974). Such channels may also account for continuing function and absence of symptoms despite extensive plaques seen post-mortem in patients with MS (Waxman, 1981).

As previously discussed, there is evidence from a variety of electrophysiological and morphological sources suggesting that even though there are Na^+ channels in the internode, their low density precludes any possibility of propagation of impulses across demyelinated internodes. Grissmer (1986) estimated that the internodal density of Na^+ channels for frog was 4-10/ μm^2 and Shrager (1989) calculated 20-25 channels/ μm^2 for rat sciatic nerve. Ritchie and Rogart (1977) had also estimated <25 channels/ μm^2 for rabbit sciatic nerve using saxitoxin binding. However, Waxman et al. (1989) estimated the level of saxitoxin binding in premyelinated rat ON as 2 binding sites/ μm^2 in small (0.2 μm) diameter axons and yet found that conduction was blocked by low concentrations of saxitoxin, suggesting that the saxitoxin-sensitive channels were responsible for electrogenesis. They suggested that the low density of Na^+ channels in very small developing axons supported conduction in a possibly microsaltatory fashion. So the possibility exists that conduction may continue across demyelinated internodes with a relative scarcity of Na^+ channels, particularly if the axon diameter is small.

Rasminsky and Sears (1972) reported that conduction remained saltatory in rat ventral root fibres 12-23 days after demyelination with diphtheria toxin. This implied that the internodal axolemma was inexcitable. However, Bostock and Sears (1976; 1978) detected continuous conduction within an internode of rat ventral root fibres only 3-14 days after a similar demyelination procedure, which suggested that the internodal axolemma was excitable. Bostock and Sears (1978) stated that their technique of recording improved the spatial resolution of the longitudinal membrane currents (to 240 um) and pointed out that the fibres in their study were smaller than those studied by Rasminsky and Sears (1972). They suggested that the conflicting results may represent a difference in internodal Na^+ channel distribution, related to axonal diameter. In view of the small number of Na^+ channels normally in the internode, Bostock and Sear's studies suggested that Na^+ channels may be redistributed or new channels generated in response to demyelination.

Smith and Hall (1980) observed that restoration of conduction occurred prior to remyelination of mouse sciatic nerve following demyelination by lysolecithin. Bostock et al. (1980) found that the same lesion developed foci of inward current up to 300 μm

apart prior to remyelination. These 'phi nodes' were physiologically the same as normal nodes but could be distinguished by their shorter spacing (Sears and Bostock, 1981). These findings were confirmed by Smith et al. (1982) who noted that conduction was restored up to 3 days before remyelination. However, in the CNS return of conduction appeared to coincide with remyelination (Smith et al., 1979; 1980), though Kaji et al. (1988) did indicate some recovery of function prior to remyelination in rat spinal cord demyelinated with anti-GC. These findings indicate that, at least in the PNS, myelination is not essential for conduction, and suggest that a redistribution of Na^+ channels within the demyelinated region may facilitate conduction prior to remyelination.

There is also morphological evidence of Na^+ channel reorganisation. Freeze-fracture studies have shown nodal-like elements to be redistributed along the chronically demyelinated internode of CNS fibres (Blakemore and Smith, 1983; Rosenbluth and Blakemore, 1984; Black et al., 1987). Foster et al. (1980) used the ferric ion-ferrocyanide cytochemical technique to examine rat sciatic nerve demyelinated by crush. They found evidence of uniform and clumped areas of stain along internodal membrane. Aggregations of nodal elements were also seen in Blakemore and Smith's (1983) freeze-fracture study.

Meiri et al. (1985) used immunofluoresence with a Na^+ channel specific monoclonal antibody to examine rat sciatic nerve. Three to six weeks after lead induced demyelination, they observed that stain intensity was not uniform in the demyelinated area, but that there were several regions stained as strongly as the nodes, suggesting possible Na^+ channel aggregation. Utilising a polyclonal antibody to the tetrodotoxin-binding protein of Na^+ channels, England et al., (1990), have also shown that in goldfish PNS axons demyelinated by doxorubicin, multiple regions of specific immunoreactivity occurred, again suggestive of Na^+ channel aggregation. In response to demyelination, new Na^+ channels may be synthesised and then reorganised in the internodal axolemma prior to remyelination, thereby facilitating conduction. All evidence indicates that conduction may occur in the absence of myelination when nodal elements are redistributed.

1.3.3f Possible sources of 'new' sodium channels.

The origins of the internodal Na^+ channels seen after demyelination are unknown.

It has been suggested that they may derive from an extracellular source, are synthesised *de novo* or are simply are existing channels redistributed. Shrager (1987) estimated from amphibian PNS, that there were 40 times as many Na^+ channels in the total internode as compared to the node. In mammalian PNS, this factor was variously estimated to be 30 times for rabbit (Chiu and Schwarz, 1987) and 20-25 times for rat (Shrager, 1989). It is possible that these channels may be reorganised to form new or so called 'phi' nodes. Another existing source of Na^+ channels is the nodes themselves. Diffusion of channels from nodes is supported by Saida et al. (1984) who observed that within 3 hours of demyelinating rat sciatic nerve with anti-GC, ferric ion-ferrocyanide stain had extended into the exposed paranodal region with decreased density of the stain in the nodal region. The spread of nodal elements into the paranodal region has been shown in freeze-fracture by Black et al. (1987) in mammalian CNS fibres affected by EAE and by Ishise and Rosenbluth (1987) in amphibian PNS fibres after crush injury.

The suggestion that all demyelinated internodal Na^+ channels are rearranged pre-existing channels is contradicted by Ritchie et al. (1981), who compared total saxitoxin-binding sites in homogenised control and demyelinated rabbit sciatic nerve and determined that there was a more than twofold increase in binding sites per mm following remyelination. This is consistent with the formation of new Na^+ channels but not with the diffusion of channels from pre-existing nodes. A loose patch-clamp study of ionic currents of demyelinated and remyelinating frog sciatic nerve axons (Shrager, 1989) has indicated that the nodes continued to have a high Na^+ channel density despite the formation of 'phi' nodes. These findings, while they do not completely rule out possible reorganisation of some existing Na^+ channels, would seem to indicate that new channels must be synthesised within the cell or synthesised elsewhere and transported to sites within the demyelinated internodal axolemma.

The method by which Na^+ channels might be synthesised is not specifically known but the cell body of the neuron is certainly implicated as the site of manufacture (Brismar and Gilly, 1987). Generally speaking genetic information from the nucleus is transcribed into messenger ribonucleic acid (mRNA) which moves into the cytoplasm, where it will be translated into a variety of proteins, including proteins destined to be incorporated into the membrane of the neuron. The synthesis of such proteins occurs on the rough endoplasmic reticulum. There the protein is glycosylated and then is passed into the Golgi apparatus for completion. The glycoprotein is then budded off as a vesicle for transport out of the cell body. This process may take several hours (for a comprehensive

description see Hille, 1992, ch 19).

A newly synthesised glycoprotein will most commonly be associated with fast anterograde transport via the microtubular domain (Schnapp and Reese, 1986). The fast axonal transport system has been specifically implicated in the movement of Na^+ channels by Lombet et al. (1985) who reported that, within 24 hours, tetrodotoxin-binding sites accumulated either side of a ligature placed below the dorsal root or nodose ganglia in rat. Liverant and Meiri (1990) used an axonal cuff of colchicine (a fast axonal transport blocker) and demyelination of the axon distal to the cuff to demonstrate larger accumulation of Na^+ channel monoclonal antibody binding sites on the proximally side of the cuff than was seen with the cuff alone, implying greater production of Na^+ channels in response to demyelination. In addition, 8 days after demyelination conduction of impulses had failed to recover when a colchicine cuff was used, but conduction recovered in the case of demyelination alone or when a control cuff was used suggesting that recovery of conduction was dependent upon fast axonal transport of Na^+ channels. Ochs (1972) found that the maximum rate of fast transport in mammalian PNS nerves was 410 mm/day. This rate appears to be consistent amongst a variety of peripheral nerves, while the rate of fast transport reported for the CNS is slower (review by Grafstein and Forman, 1980). The time frame of these processes suggests that Na^+ channels could be manufactured and arrive at new locations in the axonal membrane within 48 h, certainly within the period of several days from demyelination to restoration of conduction that have been reported.

England et al. (1991) used a sensitive radioimmunoassay to study any changes that might occur in the total number of Na^+ channels in goldfish PNS myelinated axons demyelinated *in vivo* with doxorubicin. At 14 days postinjection, a significant increase in Na^+ channel concentration was seen, compared to the control. Querfurth et al. (1987) found in regenerating cat ventral spinal roots that exhibit shortened internodal lengths, that there was also a concomitant increase in saxitoxin binding sites. The number of Na^+ channels detected was more consistent with the synthesis of new Na^+ channels than the redistribution of existing channels. Autoradiography, using tritiated saxitoxin to study Na^+ channel densities of demyelinated pathways from the CNS of patients who suffered from multiple sclerosis, has demonstrated a four-fold increase in densities compared to the healthy control (Moll et al., 1991). However Rubstein and Shrager (1990) found that recovery of conduction in demyelinated frog sciatic nerve can occur despite transection of the nerve 6 days prior to remyelination on day 17. They suggest that synthesis and

transport of Na^+ channels from the cell body is not required for at least 6 days prior to recovery, though this can not exclude the arrival of Na^+ channels at the demyelinated zone in sufficient numbers in the 11 days prior to transection to create new nodes in conjunction with remyelination.

The detection of voltage-gated Na^+ and K^+ channels in cultured Schwann cells (Chui et al., 1984) and cultured cortical astrocytes (Bevan et al., 1985), but not oligodendrocytes (Barres et al., 1988), has raised the possibility that some glial cells may act as a source of Na^+ channels for the axonal membrane. The transport of large molecules between the glial cells and axon is well known (Grossfeld, 1991, review) and Schwann cells form a dense hexagonal inwardly directed array of microvilli at their junction with the nodal axolemma (Landon, 1981), providing a possible biochemical and anatomical link for the transfer of channel proteins (Shrager et al., 1985). In addition, studies using a polyclonal antibody **7493** directed against rat CNS Na^+ channel protein have localised Na^+ channels in the nodes of Ranvier and paranodal processes of Schwann cells in rat sciatic nerve (Ritchie et al., 1990) and in the nodes and perinodal astrocytic processes of rat ON (Black et al., 1989).

For the glial Na^+ channels to have some relationship to the neuronal voltage-gated Na^+ channels it would be important to determine if they have similar characteristics. In Schwann cells and astrocytes, Na^+ channels have been found to have similar properties to neuronal channels, however, with significantly different kinetics and voltage-dependance (Bevan et al., 1985, Ritchie, 1992). It is unclear, however, whether it is possibile that glial channels could alter their characteristics when inserted into the axonal membrane or whether there are quite different neuronal and glial channels, as suggested by Barres et al., (1989) for the ON type-1 astrocytes. It certainly does not appear to be a CNS versus PNS division, as the voltage-dependent Na^+ channels of the Muller (glial) cells of the retina have recently been shown to have voltage-dependent kinetics similar to those of neuronal Na^+ channels (Chao et al., 1994). In addition, recent evidence from the expression of brain voltage-dependent Na^+ channel mRNAs in astrocytes from rat ON and spinal cord both *in vivo* and *in vitro* (Sontheimer et al., 1994) implies the possible synthesis of neuronal-like Na^+ channel elements within glia cells.

The exact role of glial voltage gated channels is still unclear, although there is increasing evidence that they may be involved in the regulation of external K^+ concentration (Sontheimer et al., 1994). In Schwann cells it is unlikely that the channels are involved directly in any electrogenesis due to their low resting potential which will inactivate the Na^+ channels (Chui et al., 1984). In astrocytes the resting potential is higher, but the low density of Na^+ channels and high capacitance of the cell ensures that the cell would be unlikely to generate a response to any but a large non-physiological depolarisation (Ritchie, 1992). Their role as a primary source of neuronal-like Na^+ channels elements following demyelination is questionable, following demonstration of new Na^+ channel distributions without any glial interaction (England et al., 1990). However, this does not preclude the possibility that the glia may be a secondary source of Na^+ channels for neurons.

1.3.3h Regulation of the sites for sodium channels.

There are two ways in which ion channels might maintain their heterogeneous organisation in the axolemma. One possibility is that contact with glia is necessary to segregate the types of channels. A second is that the subaxolemmal cytoskeleton may provide the guidance for the location of the channels. In addition, this cytoskeleton may require closely associated glial cells to retain its normal integrity. Reorganisation of ion channels in the absence of myelination could reflect either the generation of an active signal to synthesise and redistribute Na^+ channels, or may simply be the result of the withdrawal of regulatory factors. Which of these possibilities is correct is still not certain, although there are some indications to be drawn from recent research.

Several of the morphological studies examining Na^+ channel distribution in demyelinated axons have noted that the 'phi' nodes are often found in association with the precursors of glial cells or astrocytes (Blakemore and Smith, 1983; Rosenbluth and Blakemore, 1984; Black et al., 1991). These astrocytes and glia also appear to be a strong determinant of the segregation of ion channels during development (Waxman, 1987). Freeze-fracture examination of the ultrastructure of axolemma in myelin-deficient rats has shown that where the myelin is absent, the axolemma fails to show the normal pattern of ion channel segregation (Rosenbluth, 1985; Waxman et al., 1990). Waxman et al. (1990), however argued that because some clustering of nodal-like elements occurred, an intrinsic neuronal factor must play some part in channel regulation. This

would of course fit with the observations of conduction recovery before remyelination.

It has been shown that glial protein fractions can inhibit the growth of neurites in mammalian CNS (Caroni and Schwab, 1988), which indicates a powerful trophic reaction on neurons by glia. More specifically, Noebels et al. (1991) have shown that deletion of the myelin basic protein gene results in an excess of Na^+ channels in the dysmyelinated axons of the CNS of the mutant shiverer mouse. As the glial plasma membrane was still adhering to the axon, it was apparent that simple apposition of axon and glia was insufficient to control ion channel proliferation and that one of the deleted components of myelin must be, at least in part, responsible for control of Na^+ channel density.

In confirmation of the regulatory role of glia on Na^+ channels, Joe and Angelides (1992) have cultured dorsal root ganglia neurons and located with immunofluoresence specific antibodies to Na^+ channels. The specific antibodies, ankyrin and spectrin, are cytoskeletal elements linked to Na^+ channels (Srinivasan et al., 1988). With the introduction of Schwann cells into the culture, the uniform distribution of Na^+ channels changed to aggregation of channels. Joe and Angelides concluded that specific interaction of the glia and neuron must be occurring, by a mechanism as yet unknown. More recently Dugandzija-Novakovic et al. (1995) have observed that clustering of Na+ channels in demyelinated rat sciatic nerve appeared only at the edges of the remyelinating Schwann cell. This evidence would support the suggestion that glia cells play a vital role in the re-location of Na+ channels in the demyelinated axolemma.

1.3.4 Summary

It is now apparent that the loss of myelin in the process of demyelinating diseases implies more than the loss of just a high capacitance and relatively high resistance insulator. The exposure of internodal K^+ channels, by removal of myelin, would appear also to have a detrimental effect on the propagation of action potentials and this effect can be modified by the use of agents that block K^+ channels. Such agents continue to be clinically tested. The recovery of demyelinated axons is characterised by thinned myelin, shorter than normal internodal length, and the redistribution and aggregation of Na^+ channels. While the thinner than normal myelin is not ideal, such plasticity of the remyelinated axon can assist the recovery of conduction. It may also be that such

variations could occur in normal axonal morphology and increase safety factor for conduction at physiologically vulnerable regions of axons.

1.4 THE RETINOGENICULATE PATHWAY.

The visual pathway provides unique opportunities to study propagation of impulses through a variety of different anatomical structures, as well as giving much needed information on the characteristics of conduction in a central pathway. In the following description of the visual system, emphasis will be given, where possible, to studies of the anatomy of the cat optic pathway, as this animal is the experimental subject of this thesis. The cat has been commonly used as an experimental subject in vision research because it presents some features of the human visual system, including large binocular overlap of visual fields, unmyelinated intraretinal axons, decussation of optic fibres and branching of fibres to the superior colliculus (SC). As a result considerable information on the cat visual system is available. In addition, the induced demyelination of the normally myelinated fibres of the ON of the cat is an informative animal model of the plaques of demyelination characteristic of the disease MS. These plaques often form in the optic pathways of humans and episodes of optic neuritis can be one of the first signs of multiple sclerosis. The cat optic pathway is therefore an ideal system in which to study conduction in a variety of situations.

1.4.1 The fundus of the cat.

The fundus of the cat is distinguished by the presence of a tapetum. This layer of cells has a high absolute reflectivity and can cause the pigmented retina to appear light yellow green, particularly when photographed or examined with a bright light source (see Fig. 2.1.). The nasal portion of the tapetum extends 40^{0} into the nasal retina and only 25^{0} in the temporal retina (Bishop et al., 1962d). The tapetum is largely confined to the upper retina and its lower boundary is relatively horizontal on the temporal side of the retina and usually passes the lower margin of the optic nerve head.

The optic disc (OD) is roughly circular and is 0.7 mm in diameter in small cats (Prince et al., 1960) and has a mean of 0.93 mm in cats weighing approximately 2-5 kg (Bishop et al., 1962d). There are three main arterio-venous bundles that exit at the disc

margin, one going up and medially, and the other two passing downwards, one going medially and the other laterally. The branches of these vessels extend in a curved course and some converge towards the area centralis which is itself free of blood vessels. The area centralis lies 3-3.42 mm above and temporal to the OD (Prince et al., 1960; Bishop et al., 1962d; Hughes, 1975).

1.4.2 The retina.

The retina is composed of ten distinct layers. Of these, three contain the somata of the neuronal elements of the retina. These are, in order from the outside (towards the sclera) to the inside (towards the vitreous):

1. The outer nuclear layer which contains the rods and cones, which are the sensory receptors known as the photoreceptors. The retinal rod and cone photoreceptors hyperpolarise in response to light. Each rod and cone makes contact with at least one bipolar cell.

2. The bipolar cell somas are in the inner nuclear layer. Sharing this layer are the retinal horizontal cells and amacrine cells, which have an integrative neural function. They are thought to be vital in the formation of the diverse responses of the different classes of RGC. The different types of visual receptive fields are discussed in detail in Chapter 2.

The on and off cone bipolars form separate on and off channels and these make direct contact with the appropriate on and off beta and alpha RGC. There is only one type of rod bipolar (on). The scotopic on response of beta and alpha RGC is generated by rod biplar input to the AII amacrine cells which then form gap junctions with the cone bipolar cells (Sterling et al., 1986, review). The scotopic off response is generated by the release of the inhibitory transmitter glycine either directly upon off-RGC or indirectly via cone bipolars terminals (Muller et al., 1988). The centre of the concentric receptive field appears to be generated by these pathways, while the surround is thought to be mediated by the retinal interneurons, the amacrine and horizontal cells (Dowling and Boycott, 1966). Hamasaki and Maguire (1985) suggested that the periphery effect may be generated via complex retinal circuits involving the A19 amacrine cells.

3. The RGC are located in the final somatic layer. These cells send their axons, via

the ON, to the dorsal nucleus of the lateral geniculate (LGN) for relay to the cortex. The axons also send collaterals to other parts of the brain including the SC. The axons of the RGC pass inwards (towards the vitreous) and turn tangential to the inner surface of the retina, to form the stratum opticum or the nerve fibre layer, which is separated from the vitreous by the final thin layer of the retina, known as the internal limiting membrane.

The axons tend to form bundles which follow an arcuate course towards the OD (Laties and Sprague, 1966). The fibres from the nasal portion of the area centralis extend straight to the optic nerve head, while the remainder pass in an arciform manner above or below the straight fibres, depending on the particular location of their cells of origin. There is a fibre-free raphe that starts from the area centralis and slopes upwards into the temporal retina. There is no raphe on the nasal side of the retina, as fibre bundles from this region tend to travel to the optic nerve head in relatively straight lines. Stone and Hansen (1966) noted that, as an obvious consequence of the fibre arrangement, the fibre bundles thickened as they approached the optic nerve head. They attributed this to the increasing number of axons picked up as the bundle passed cells. The arciform organisation was confirmed by the electrophysiological mapping of many receptive fields of RGC recorded intraretinally from one point along an axon bundle (Ogawa et al., 1969).

The cat does not possess a fovea, as do humans. But the area centralis is a region, <1 mm in diameter, where there is a dense aggregation of RGC (Stone, 1965; Hughes 1975) and extending from this area is a horizontal region of increased ganglion cell density known as the visual streak (Hughes, 1975). The total number of RGC in the retina has been variously estimated to be between 90,000 (Stone, 1965) and 217,000 (Hughes, 1973). The reason for such variation lies in part in the difficulties of correctly identifying RGC, avoiding inclusion of amacrine cells and glia, and also in differences in methodology. Taking account of these possible errors, Hughes (1985) reviewed the available data from a variety of sources and concluded that the best estimate was in the vicinity of a mean 170,000 RGC per retina.

The RGC layer has been shown to contain at least three different morphological types of ganglion cells, the alpha, beta and gamma classes, identified from a study of Golgi stained cells by Boycott and Wassle (1974). The alpha cell was observed to have a dendritic field that extended up to 1,000 μm in diameter in the peripheral retina and had the largest soma of all cells at any retinal position. The alpha cells comprised less than

5% of the total population of RGC (Wassle et al., 1975) and had their greatest density at the area centralis with a region of augmented density coinciding mainly with the horizontal meridian. The beta cells had smaller somata and a dendritic spread of 25-250 μm with a perikaryon of 12-23 μm in diameter (Wassle et al., 1981). They comprised approximately 55% of the total number of ganglion cells in the retina (Fukuda and Stone, 1974; Wassle et al., 1983). The gamma cell class was thought to comprise the rest of the ganglion cells forming as much as 40% of the total population of RGC (Illing and Wassle, 1981). They had dendritic fields extending from 180-800 μm (Boycott and Wassle, 1974) and were the most morphologically diverse group of RGC with widely varying cell body dimensions, though most were smaller than the other two classes (Kolb et al., 1981).

Based upon the work of Boycott and Wassle (1974), electrophysiological studies by Cleland and Levick (1974a, b) and Fukuda and Stone (1974) have proposed that the receptive field characteristics of RGC are correlated to the morphological divisions of the retinal cells. The alpha class of cells corresponded with the brisk transient, Y receptive field properties, the beta class to the brisk sustained, X and the gamma class to the sluggish concentric and rarely encountered units recorded in the retina (for a more complete discussion of the receptive field classes see Chapter 2). This view was strengthened by the results of Cleland et al. (1975), Peichl and Wassle (1981) and Wassle et al. (1981). Saito (1983) directly confirmed the correlation by recording intracellularly from brisk transient, Y-, brisk sustained, X-, and one sluggish, W- cell and labelling the cells with lucifer yellow.

Boycott and Wassle (1974) and Hughes (1981) showed that the cell bodies of the alpha and beta classes of cells became smaller, closer to the area centralis, while the cell bodies of the gamma class of cell tended to remain constant. This results in some overlap of the size distributions of the beta and gamma classes of cells towards the area centralis. The axonal diameter of RGC tends to reflect the size of their somata (Stone and Hollander, 1971; Boycott and Wassle, 1974) and Stone and Hollander (1971) observed that the axons from the central retina were on average smaller than those emanating from the peripheral retina. Similarly, it has been observed that the axons of cells located in different parts of the retina conduct at different rates. Stone and Freeman (1971) found that while fast axons of peripheral retinal origin had an average CV of 34 m/s, fast axons originating from the area centralis had slower CVs, in the range of 20-30 m/s. A similar difference was observed in the slower conducting axonal populations. This finding has

been confirmed by others (Fukuda and Stone, 1974; Cleland and Levick, 1974a; Rowe and Stone, 1976). Kirk et al. (1975) extended this conclusion by showing that there was a continuous gradation of CV in axons within each class from the centre to the periphery of the retina.

The intraretinal portions of the optic axons are unmyelinated in the cat and numerous other species (Prince et al., 1960). It follows that the CV of impulses in this portion of the optic axons will be considerably slower than in the myelinated extraocular portion of the nerve. This has been confirmed by intraretinal recordings of cat optic axons,where an 8 to 10-fold slowing of CV in the retina compared to the extra-retinal CV, and two CV groupings has been observed (Dodt, 1956; Motokawa et al., 1957; Ogawa et al., 1969; Stone and Freeman, 1971). Stone and Freeman found the range of CVs for the fast fibres from 3.5 to 4.9 m/s and for the slow fibres from 2.0 to 3.0 m/s.

Despite the reduced conduction time in the retinal portion of the axons, absence of myelin in the retina may confer some advantages. Myelin is refractile by nature. Its absence may prevent scattering of light before it reaches the photoreceptors which lie under the nerve fibre layer. The advantage of the clarity of images received by the photoreceptors presumably far outweighs any slowing of the conduction of impulses. There is also a probable advantage in terms of the bulk of the fibres leaving the eye through a relatively small optic nerve head. Increased bulk, due to the myelin, could create a larger OD and could also limit the maximum permissible number of RGC, thereby decreasing the number of sampling elements in the retina and reducing the overall quality of images transmitted to the higher centres.

There is also a suggestion that the unmyelinated axolemma of RGC may in fact be of a specialised nature. Hildebrand and Waxman (1983) while studying the ultrastructure of rat retinal axons, observed that the membrane showed localised regions of electron-dense subaxolemmal undercoating. These regions had a limited distribution and extended between 0.5-5.0 μm along the axon. These specialised regions had characteristics in common with those observed at nodes of Ranvier and at 'phi' nodes seen in remyelinating axolemma. They also noted a possible interaction between the fibres and the glial cells of the retina and processes of the Muller cells (Black et al., 1984). The implication of this finding is that the unmyelinated intraretinal axons of mammals may in fact have node-like distributions of sodium channels along their length. This may be advantageous for the speed of propagation and security of conduction for impulses in the retina.

1.4.3 The optic nerve head.

The optic axons extend towards the OD and leave the eye via the optic nerve head, to form the ON. The nerve passes through the retina, choroid and sclera and emerges medial to the posterior pole of the eye. The scleral portion of the nerve contains the lamina cribrosa, a sieve-like structure up to 0.4 mm thick (Prince et al., 1960), that acts as support for the nerve bundles or fascicles as they pass through it. All axons become progressively myelinated (Hughes and Wassle, 1976) by oligodendrocytes in the first 1-1.5 mm of the post-laminar portion of the nerve (Blunt et al., 1965). Astrocytes, however, are associated with the nerve at the scleral level of the lamina cribrosa.

The ultrastructure of the junction of the unmyelinated and myelinated portions of the ON in the cat has not been studied, but there are observations from the rat which may shed some light upon this region of the nerve in mammals generally. Hildebrand and colleagues (Black et al., 1985; Hildebrand et al., 1985) have observed in detail the initial myelination of the optic axons. They noted that there was no uniform front of myelination. While some axons were closely apposed only by processes of oligodendrocytes, others were surrounded by myelin layers which were thinner than normal and had internodal lengths as short as 3.3 μm long. The axons also tended to have larger diameters in their myelinated portion than in the pre-myelinated area. Localised areas of increased density of E-face intramembranous particles were also seen in the pre-myelinated region. In addition a variety of axon and glial associations were observed suggesting that the transition zone in optic axons has a complex morphology.

1.4.4 The optic nerve

The number of fibres within the ON has been variously estimated to be 86,000 by Donovan (1967) (who counted only those fibres greater than 1 μm in diameter) to 120,000 by Bishop et al. (1953) who included those fibres smaller than 1 μm that could be resolved with the light microscope. However, Bishop et al. (1969) using electron microscopy reported that the mode of fibre diameter in the nerve was 1 μm, so the earlier studies would have underestimated the total number of fibres. In a later electron microscopic study, Hughes and Wassle (1976) estimated 193,000 fibres, and then used fibre isodensity maps to revise this to a mean of 184,000 fibres. Later, Hughes (1985) pooled all available electron microscopy data from different laboratories and concluded

that the number of fibres in the ON would be 158,000 ± 27,000.

The observation of at least two prominent well defined waves in the CAP elicited by electrical stimulation and recorded both in the ON and optic tract (OT) has prompted attempts to find groups of optic axons aggregated on the basis of size, the rationale being that the two waves are thought to be formed by two groups of fibres with differing CV and therefore separate diameter spectrums (Gasser and Erlanger, 1927). Bishop and McLeod (1954) introduced the terminology T1, for the fast conducting and therefore presumably large optic axons and T2, for slower conducting and smaller axons. While studying both anti and orthodromic CAPs Bishop et al. (1969) found an additional third wave on the declining phase of the gross potential with very slow CV which they labelled T3. Though other terms have been suggested, this nomenclature has proven to be the most convenient and enduring. They arranged the three conduction groups as; the fast (T1) axons, with the peak of the wave's velocity ranging from 28-50 m/s, the medium/slow (T2) from 14-27 m/s and the very slow (T3) group from 3-8 m/s.

This division of conduction groups of optic axons into T1, T2 and T3 fitted with the later classification of the alpha, beta and gamma classes of RGC (Boycott and Wassle, 1974). It also proved to be convenient to classify the receptive fields of RGC into a similar triad (Y, X, W), though such a limited division of the diverse receptive field classes is not always informative. The classification of receptive fields is discussed in detail in Chapter 2 of this thesis, with particular reference to the scheme used in this experimental study.

Attempts to find a trimodal distribution of fibre diameter spectrum have proven not to be straightforward. An early electron microscopic study of this question by Bishop and Clare (1955) found that the distribution was unimodal. However, in 1976 Hughes and Wassle observed that the core of the nerve had more small fibres than the outer zone, with the average diameter of fibres increasing progressively towards the periphery of the nerve. This supported the notion that fibres from the central retina appear to travel in the centre of the ON. Hughes and Wassle determined that the diameters of the peripheral ON fibres had a trimodal distribution, unlike the unimodal distribution found for the core and the nerve as a whole. They found that 53% of the fibres were <2.25 μm, 42% from 2.25-5.0 μm, and a tail of fibres with diameters >5.0 μm, and that these groupings appeared to coincide with the proportions of alpha, beta and gamma fibres in the retina (Boycott and Wassle, 1974). Williams and Chalupa (1983) performed a high

resolution analysis of a large number of electron micrographs of cat ON and found a trimodal distribution of fibre diameters for the *whole* nerve. Using high resolution techniques, they found a similar proportional distribution of fibre diameter as had been estimated by Hughes and Wassle (1976) for the peripheral region of the nerve alone.

The measurement of discrete ranges of CV for conduction groups has varied substantially between laboratories. Levick and Thibos (1983, Table 1) presented a thorough review of the various studies to that date. A number of those studies estimated the range of CVs for the various groups while recording CAPs. Spehlmann (1967) found that a variety of CAP waveforms could be produced by varying the stimulation voltage, and with adjustment of the placement of stimulating electrodes within the optic pathway. This means that the determination of the ranges of the various conduction groups is problematical when observing CAPs. Errors in calculating CV may also arise either because conduction distance may be too short or the complex pathway of fibres in the chiasm (see below) can result in the distances travelled by different fibres being quite varied.

However, variation is not confined to CAP studies. Single axonal studies of CV in optic axons have also shown considerable overlap in the CVs and latencies measured from the axons of RGC with the various types of receptive fields (Stone and Freeman, 1971; Hoffman, 1973; Cleland and Levick, 1974a; Ogawa and Takahashi, 1981; Hada and Hayashi, 1990). In addition to the errors mentioned above, these studies may also suffer from selective recording procedures, either in the retina or in the pathway where fibres appear to occupy segregated locations on the basis of size. An examination of these studies does, however, reveal a pattern of CV ranges; the slow axons (T3), 2-18 m/s, the medium/slow axons (T2), 15-25 m/s and the fast fibres (T1), >20 m/s. As most of these ranges were calculated with a view to the receptive field classification of axons, it may be that there is not a discrete but an overlapping grouping of axonal diameters and therefore CVs attributable to classes of RGC.

1.4.5 Anatomy of the optic chiasm.

The optic axons continue to course away from the eye, moving posteriorly and medially, until they reach the optic chiasm (OX). At the chiasm, over half the ON fibres cross to the opposite OT (Polyak, 1957). The decussating fibre bundles turn towards

each other and as they cross to the opposite tract, they interweave in a basket-like pattern (Aebersold et al., 1981). In the chiasm the thinner fibres cross in the anterior of the OX while the thicker fibres cross in the posterior half. Aebersold and colleagues also found that the fibres from various retinal areas tended to stay together, so that despite some rotation (90^{0}) and decussation, the crossing was not just random and a new binocular retinotopic order was made. The crossing of the fibre bundles is, however, not straightforward. Most bundles loop during the process of crossing over. The most prominent loop is the anterior loop into the contralateral ON (Polyak, 1957).

The decussation of the ON fibres has a precise arrangement in terms of the position of the ganglion cells of origin. Basically, fibres from the nasal portion of the retina cross to the contralateral OT and temporal fibres continue into the ipsilateral tract. The vertical boundary between the two hemifields is in the region of the area centralis (Stone, 1966; Laties and Sprague, 1966). However, there is an overlap of the distribution of the crossed and uncrossed cells of varying extent for the different classes of RGC (Kirk et al., 1976 a,b). Nasal to the region of overlap, 100% of the fibres go to the contralateral OT. Early observations of fibres that appeared to branch at the chiasm and send collaterals into both tracts have not been confirmed by either horseradish peroxidase (HRP) staining or by electrophysiological studies.

1.4.6 Anatomy of the optic tract.

In the chiasm the retinal fibres have been divided so that each OT contains the fibres from homolateral visual hemifields. In addition, it appears that the fibres have been sorted according to their fibre diameter class. Bishop et al. (1953) observed that the uppermost region of the OT appeared to contain only smaller fibres in stained sections. The lower region contained the larger fibres with some smaller ones intermingled. Bishop and Clare (1955) confirmed this segregation by size. They also observed that fibres ranged from 11 μm to <0.5 μm, with the mode at 1-1.5 μm. Guillery et al. (1982) made detailed assessment, by both light and electron microscopy of the topographical organisation of the tract confirming the dorsal/ventral segregation of fibres according to diameter. They also observed a ventrolateral zone which appeared to contain most of the finest axons. Sur and Sherman (1982) made intracellular injections of HRP into physiologically identified ganglion cell fibres and found that the thinner X axons lay dorsal to the larger Y axons.

Baker and colleagues have reported that the diameter of the largest fibres of the ferret increase systematically from the ON to the OT with a resultant change in CV (Baker and Stryker, 1990). However, it is possible that if there were large fibres originating from the parabigeminal nucleus, and they occurred in sufficient numbers, they may contribute to the changes in diameter and CV observed. This kind of systematic variation in fibre diameter has yet to be observed in the cat. However, it has been suggested that the failure to find distinct clusters of axons with diameters corresponding to the CV groupings in cat could be attributed to fibre diameter varying along the length of an axon, therefore obscuring groupings assessed from transverse sections of the ON and OT (Bishop and Clare, 1955; Stone and Hollander, 1971). Using polarising light interference microscopy with reconstruction of the dimensions of fixed and unteased optic fibres from serial longitudinal sections, Freeman (1978) showed that optic fibres had both abrupt and gradual changes in diameter and shape. Freeman noted that myelin sheath thickness tended to vary less dramatically than axonal diameter, and concluded that myelin thickness may therefore be a more reliable indicator of average axonal diameter than measurements of axonal diameter. The distribution of myelin thicknesses showed 5 peaks, which Freeman attempted to correlate to conduction in a possible four latency groups. However, this has not been confirmed by later studies. Difficulties in establishing fibre diameter distributions that correlate to the three peaks in the optic pathway CAP may lie in the heterogeneity of the fibres themselves (Baker and Styker, 1990).

1.4.7 Summary

The unique arrangement of axons in the retina permits access to relatively small axons, so that conduction of impulses in single central mammalian fibres can be studied. The optic pathway of the cat is a well characterised part of a mammalian visual system which has situations where physiological conduction vulnerability may be demonstrated, such as the junction of the myelinated and unmyelinated segments of the optic axons.

CHAPTER 2.
METHODS.

2.1. ANAESTHESIA AND MAINTENANCE OF THE PREPARATION.

Electrophysiological experiments were conducted on 40 mature cats, weighing from 2.0 and 3.4 kilograms. Anaesthesia was induced and maintained with 1-4% halothane (Fluothane, ICI) in a mixture of nitrous oxide:oxygen:carbon dioxide (70:28.5:1.5 respectively) delivered through a face mask. Prior to neuromuscular blockade, the gaseous anaesthetic mixture was delivered via a cannula inserted through a tracheotomy. The vago-sympathetic trunks were divided bilaterally to minimise eye movements from fluctuations in the tone of smooth muscle in the orbit and to avoid vagal reflex effects on the heart, in order to improve the stability of recordings (Rodieck et al., 1967). The halothane was discontinued when surgical procedures were completed, but was kept available. The use of nitrous oxide as the sole anaesthetic agent was originally considered sufficient to maintain anaesthesia during the non-surgical phase of the experiment (Venes et al., 1971). A later study (Hammond, 1978) demonstrated that nitrous oxide on its own was not quite sufficient and the use of additional anaesthesia was recommended. Therefore, before halothane was discontinued, a continuous intravenous supplement of alpha-chloralose (15-30 $mg.kg^{-1}$ day^{-1}) was commenced.

A venous cannula was placed in the cephalic vein to provide continuous intravenous infusion at the rate of approximately 97 $ml.day^{-1}$, using a Palmer infusion pump. To maintain the well-being of the animal the infusion contained L-amino-acids (Synthamin 13, 8%, Travenol, Australia, approximately 95 $ml.day^{-1}$), 5% (w/v) D-glucose, multi-vitamins (M.V.I.12, Rorer, Australia, 2 $ml.day^{-1}$), porcine insulin (Nuralin, Commonwealth Serum Laboratories, 2 $units.day^{-1}$), dexamethasone (Dexadreson, Intervet, Holland, 1 $mg.day^{-1}$) and an anti-coagulant (Heparin, Commonwealth Serum Laboratories, 48 $units.day^{-1}$) and included a neuromuscular blocking agent (see below). Intramuscular amoxycillin (Amoxil, Beecham, 15 $mg.day^{-1}$) was administered routinely to prevent infection. Cicatrin powder (Wellcome, Australia) was dusted on all incisions prior to closure, as a precautionary measure against infection.

The depth of anaesthesia was continuously monitored by heart rate and by recording the electroencephalogram (EEG). An insulated screw was placed through a burr hole in the skull at Horsley-Clarke coordinates (H-C) 3 posterior and 3 left, for extradural recording of the EEG. A stainless steel plate was inserted underneath the scalp posteriorly, to ground the preparation. The heart rate was monitored using subcutaneous electrodes located on either side of the heart and recorded on a electrocardiograph. During recording, depth of anaesthesia was also regularly evaluated by monitoring pupillary reflexes in the unoperated eye. If the pupil remained slit-like, if the heart rate was unvaried for extended periods, if the EEG showed a periodically synchronised slow, large amplitude wave pattern and if none of these signs changed with bright light or abrupt sound or mildly noxious stimuli such as paw pressure, then the level of anaesthesia was deemed to be sufficient.

Intense neuromuscular blockade was required to control eye movement so that recording from single axons could be maintained for sufficient time to complete data collection. Initial paralysis of the cat was produced by the administration of alcuronium chloride (Alloferin, Roche) in a single dose of 1.5 $mg.kg^{-1}$. Neuromuscular blockade was maintained with alcuronium chloride (6 $mg.kg^{-1}.day^{-1}$) given intravenously. The animal was artificially ventilated by a respiratory pump (Palmer) at a rate of approximately 33 $strokes.min^{-1}$. The stroke volume was adjusted to achieve an end-tidal concentration of 4% CO_2 as measured by an analyser (Normocap, Datex, Finland). The range of stroke volumes used was 20 to 40 ml. The lungs were frequently hyperinflated (3-5 strokes) to prevent alveolar collapse.

The anaesthetised animal was placed on a padded cradle. To prevent ventral pressure, the trunk of the animal was suspended by a 15 gauge needle passed through the interspinous ligament, caudal to the seventh cervical spinous process, and the needle was supported by a stirrup. Core temperature was continuously recorded by a sub-scapular thermistor probe and maintained at a constant 37.5^{0} C by a feedback-controlled electric blanket wrapped around the animal's trunk. The comfort of the animal was maximised by wrapping in cotton wool and towelling, which also minimised heat loss. The animal was set up so that the head was aligned in H-C stereotaxic planes (Reinoso-Suarez, 1961) and so that the animal's visual field was almost free of obstruction.

During the experiments which lasted between 2-5 days, it was necessary to manually express urine 2-3 times daily so that renal function would not be perturbed and to minimise discomfort and therefore promote ocular stability. Urine was collected in a plastic bag placed around the hindquarters of the animal. The volume of urine was measured daily as an indicator of the animals fluid balance and urine was also assessed for colour and clarity as indicators of normality.

2.2 PREPARATION OF THE RECORDING ELECTRODE.

Clear plastic contact lenses were used to prevent drying of the cornea, to provide protection during manipulations and to maintain good optical quality. The lenses had zero refractive power, a radius of curvature of the concave surface of 8.00-9.00 mm and a chord diameter of 13-14 mm. Access to the eye was gained by performing a lateral canthotomy. The nictitating membrane was retracted with 2.5% phenylephrine (1 drop, Neosynephrine, Winthrop) and the pupil was dilated and accommodation paralysed with atropine (1 drop, Atropt 1%, Sigma).

To immobilise the eye, an appropriately sized, insulated, chromium-plated metal ring was loosely clamped to a small block at the side of the animals head. The block was, in turn, clamped to the headstage. The ring was secured to the eye at the limbus by bringing forward a fold of bulbar conjunctiva and wrapping it back over the ring and securing it with six well-spaced stitches. The eye ring was positioned to minimise any strain upon the eye and then all points of attachment were firmly clamped in place. Also attached to the block was a small oval plate with a central hole and two smaller holes at either end. An elastic band was threaded through the two outer holes. The plate was placed such that the central hole was 6.5 mm behind the limbus and then clamped in position.

After placement of the stimulating electrodes (see next section), a small buttonhole incision was made in Tenon's capsule through the central hole of the plate and the sclera was exposed. The electrode holder consisted of an 18 gauge cannula, with a stylet occupying its centre, and an attached mono-dimensional microdrive. The cannula was inserted into the eye through the central hole in the plate. A small nylon ball on the shaft of the cannula rested in the central hole and the whole assembly was attached to the plate with the elastic band. The whole assembly was then attached to two manually-operated hydraulic systems to allow for fine adjustments of position of

the electrode within the eye. The microelectrode was then placed inside a 21 gauge needle, which acted as a protective carrier. The stylet was removed and the carrier then inserted through the cannula until the carrier just emerged from the tip of the cannula within the eye. Initially the microelectrode was advanced by hand towards the retinal surface whilst being directly viewed with an ophthalmoscope, using parallax to judge proximity to the retina. The space between the cannula and the carrier needle was sealed with petroleum jelly.

A modified tungsten-in-glass microelectrode (Levick, 1972) was used to make extracellular recordings from single intra-retinal ganglion cell axons at the optic disc (OD) margin (Fig. 2.1a). The recording location was chosen to maintain a relatively constant distance from the stimulating electrodes to the recording site and to minimise the amount of unmyelinated axon included in the conduction path. In some animals the electrode was moved to the peripheral retina (Fig. 2.1b.). This was to enable comparison of conduction in myelinated and unmyelinated segments of the cat's optic axons.

The full evaluation of several conduction parameters required that stable recordings be obtained for some time. This necessitated a modification of the electrode to maximise selectivity and durability of recording. The ideal electrode proved to be an unbroken pipette pulled from glass tubing with an outer diameter of 0.4 mm (Hilgenberg, Germany) and a tip some 1.5 μm in outside diameter. Through this was passed an etched tungsten wire with a rounded tip of 0.5-0.8 μm diameter. The wire protruded beyond the glass for a distance of 1-2 μm. The wire was then fixed to the glass using cyanoacrylate adhesive (Super fast hobby super glue, Magic, Technical Adhesives, Melbourne, Australia) both at the broad end and at the fine tip. The latter was achieved by suspending a drop of glue from the end of a needle and syringe over the tip of the electrode and using capillary action to draw glue into the tip. The electrode was allowed to air dry. Then gold was chemically deposited on the tip of tungsten, using a commercial gold plating solution (Atomex, Engelhard Industries, Australia) to achieve a resistance in the range of 100-300 Mohms. These electrodes successfully recorded single retinal ganglion cell (RGC) axons at the optic nerve head (ONH), frequently without signs on the oscilloscope or loudspeaker, of the electrode having penetrated the internal limiting membrane (ILM). Presumably the electrode recorded axons just below the surface of the retina by pressing into the ILM. This method appeared to increase the durability of recordings.

FIGURE 2.1 Position of the recording electrodes

A A tungsten-in-glass recording micro-electrode placed close to the optic disc margin. The shaft of the electrode crosses the optic disc from above and the tip touches the nasal retina, and is positioned just below the horizontal mid-line. Note the central retinal arteries and veins and the reflective tapetum.

B A similar recording electrode placed in the peripheral nasal retina.

POSITIONS OF THE RECORDING ELECTRODES.

A.

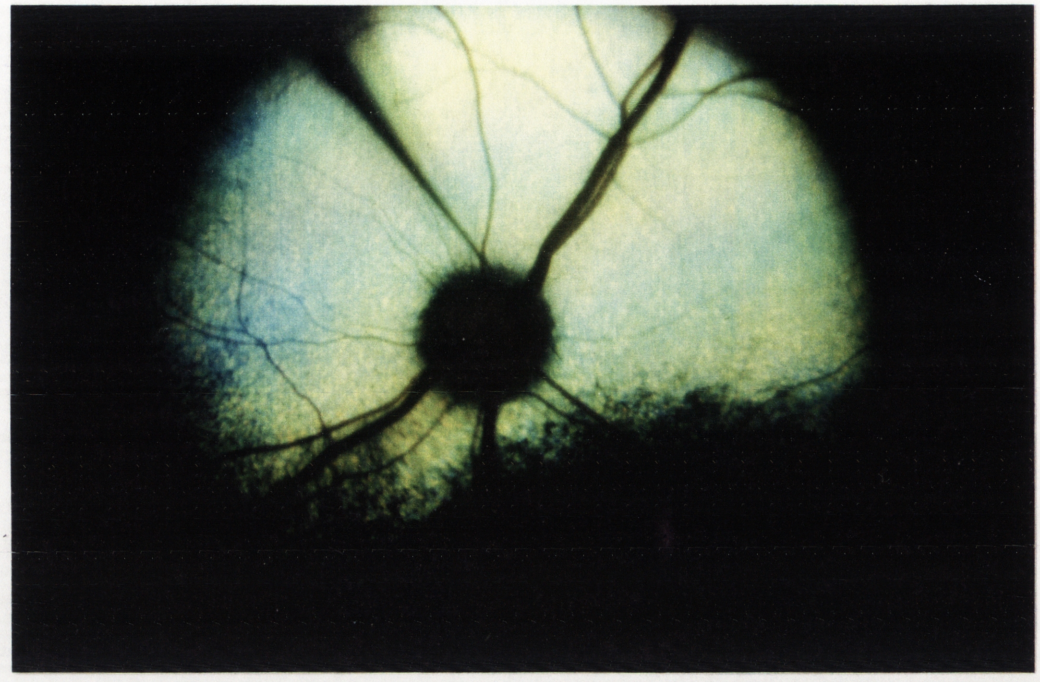

B.

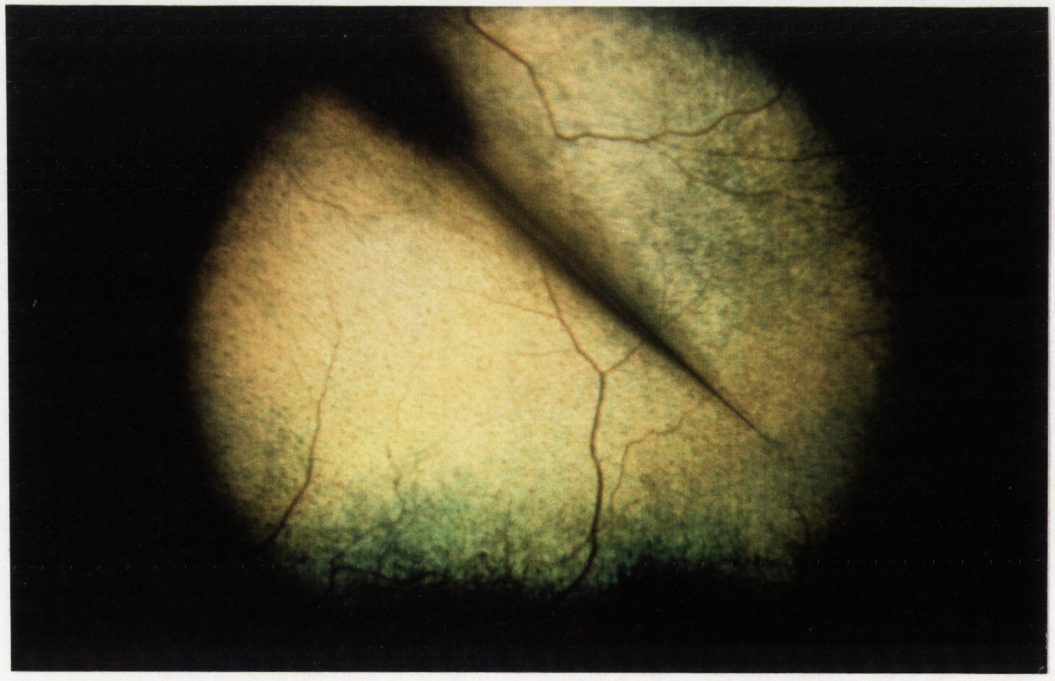

2.3 PLACEMENT OF THE STIMULATING ELECTRODES.

In all but the cats prepared by Professor Burke, shielded bipolar stimulating electrodes composed of glass-insulated sharpened platinum-iridium wire with 1 mm bared tips, mounted 1 mm apart and inserted through a 18 gauge carrier needle (approximate resistance 5-10 Mohms), were lowered through small craniotomies. In some 21 control animals and in all 8 cats with a demyelinated lesion created by the application to the ON of antigalactocerebroside antiserum (anti-GC), the recording electrode was placed in the right eye and the craniotomies were made at H-C surface co-ordinates of 9 anterior and 9 lateral over both the right and left OT (Fig. 2.2a). In the remaining 8 control animals, the optic chiasm (OX) was found by lowering the electrode from the surface co-ordinates of 13.5-13 anterior and 2-1.5 lateral (Fig. 2.2b) and the recording electrode was placed in the left eye. The stimulating electrodes were placed with the orientation of the bipoles perpendicular to the path of fibres.

The final placement of the stimulating electrodes was accomplished by positioning the recording electrode at the OD margin at the 11 or 7 o'clock position (to obtain both ipsi- and contralateral axons) so that the background "swish" of axonal activity (Bishop et al., 1962b) could be heard, but no single axons were isolated. As the stimulating electrode was lowered in millimetre steps, the response to 50 μs pulses of 100 volts in strength and of both polarities was noted on the oscilloscope screen. Field potentials attributable to the classic fast (T1) and slower (T2) conducting fibres (Bishop and McLeod, 1954) appeared as negative waves. The threshold for the stimulation of these conducting groups was measured with each successive lowering of the electrodes. Vertical adjustment of the electrodes was regarded as complete when the threshold voltage fell below 1 volt. When the electrodes were satisfactorily positioned, the craniotomies were sealed with Agar (Difco Laboratories, Detroit, USA, 3% in Ringer solution).

In 3 animals obtained from Professor W. Burke's laboratory at the Sydney University, Sydney, Australia, different stimulating electrodes were placed using a different method in a separate preliminary procedure (Fig. 2.2c). The animals were subsequently studied in the Canberra laboratory using the anaesthesia, recording electrode preparation, electronics and classification of RGC described elsewhere in this chapter.

FIGURE 2.2 Position of the stimulating electrodes.

A Stimulating electrodes were placed in both the contralateral and ipsilateral optic tracts. The recording electrode was located in the right eye. This electrode configuration was used in the majority of normal cats and all the cats lesioned with anti-galactocerebroside.

B Stimulating electrode in the ipsilateral optic chiasm and recording electrode in the left eye. This electrode configuration was used to collect control data for the comparison of conduction properties for stimulation from the optic chiasm.

C Stimulating electrodes in the contralateral optic tract, the optic chiasm and the ipsilateral retrobulbar optic nerve. The recording electrode was in the left eye. This electrode configuration was used for the pressure-lesioned animals and for one control.

POSITION OF STIMULATING ELECTRODES

A

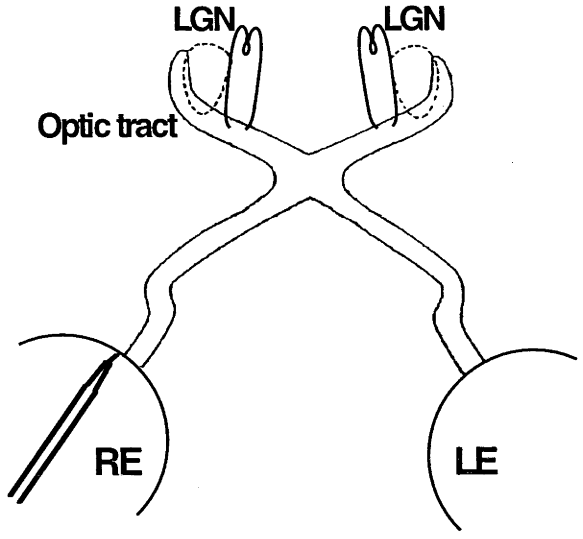

B

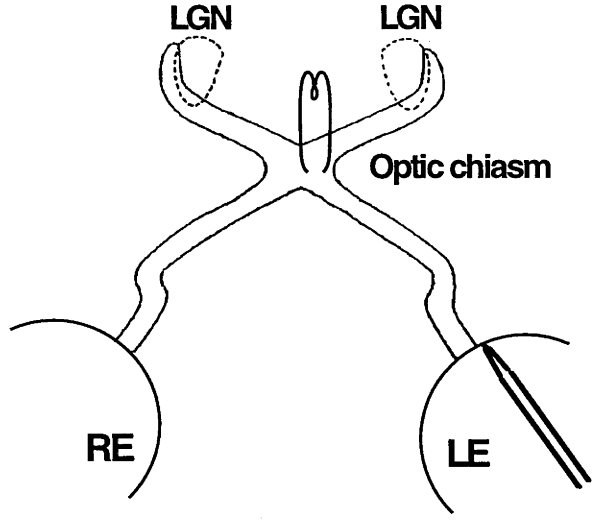

C

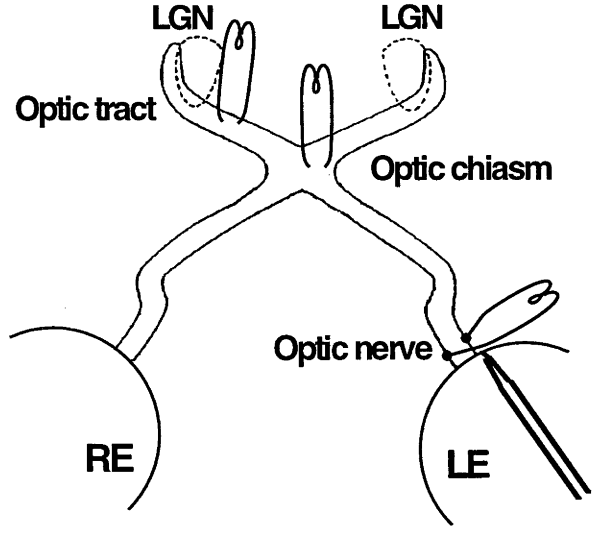

What follows is a short description of Professor Burke's technique (Burke et al., 1986, 1992). Each animal was anaesthetised with sodium pentobarbitone (Nembutal, Boehringer, Ingelheim, initial dose 40 $mg.kg^{-1}$, IP) and surgical anaesthesia maintained with supplementary doses as required. Intramuscular injections of dexamethasone (Decadron, 1-2 mg) and atropine sulphate (Commonwealth Serum Laboratories, 300 μg) were given preoperatively and an antibiotic (Ampicillin, Commonwealth Serum Laboratories, 125 mg) was given on the day of the operation and post-operatively. Reference electrodes (screws) were attached to the skull over the ipsilateral visual cortex (H-C, 0 anterior, 2 lateral) for recording electrical and visually evoked potentials and EEG, and in the contralateral nasal sinus, and in the ipsilateral zygomatic arch for oculographic recording.

Enamelled stainless steel bipolar electrodes with tips separated vertically by 1.1 mm and strengthened by gluing to a Nichrome staff, were placed in one or both of the optic tracts (OT) at H-C co-ordinates of 11 anterior and 7 lateral, through trephined craniotomies. The OX electrode was placed on the side ipsilateral to the recording eye at 15 anterior and 2 lateral (Fig. 2.2c). Vertical placement of the electrodes was assessed by response to a bright flash supplied by a Grass photostimulator. This was judged to be satisfactory when the amplitude of the recorded response approached 1 mV.

In order to place the ON electrode, the ON ipsilateral to the recording electrode was exposed dorsally by removal of the bone above the frontal sinus and the bone over the orbital cavity. To expose the nerve it was necessary to retract the orbital contents covering the nerve and draw the eye slightly forward in the orbit. The electrodes were precoated and sharpened stainless steel wire which were placed on opposite sides of the ON attached to the connective tissue surrounding the ON just behind the eye and secured by tissue adhesive (Ethicon).

The leads from all the electrodes were then gathered and attached to a nine pin plug (Cannon) which was attached to the skull with dental acrylic (Burke et al., 1986; 1990).

Electrode placement was subsequently assessed at the end of experiments in some cats by partial dissection and by examination of 1 mm slices, of the perfused brain. In some instances, pathways were highlighted using a silver myelin stain after the method of Gallyas (1979). Sections (50 um) of ON were cut and mounted on

and 100 ml of acetic anhydride for 30 mins and then washed twice in distilled water for 5 mins each time. The slides were then placed in a ammoniacal silver nitrate solution of pH 7.5 for 1 hour at 20^{0} C. The solution was prepared by dissolving 0.3 grams (g) each of ammonium nitrate and silver nitrate in 300 ml of distilled water to which was added 0.9 ml of 4% sodium hydroxide. They were then washed 3 times for 3 mins in 0.5% acetic acid. The physical developer solution was prepared from 3 solutions.

A) 5% Na_2CO_3

B) 0.6 g ammonium nitrate, 0.6 g silver nitrate, 3 g tungstosilicic acid and 300 ml distilled water.

C) 0.6 g ammonium nitrate, 0.6 g silver nitrate, 3 g tungstosilicic acid, 2.2 ml 35% formol and 300 ml distilled water.

The ratio of the solutions was 150 ml of solution A, 45 ml of B and 105 ml of C. To terminate the staining process, the slides were washed 3 times for 10 mins each in acetic acid. The myelin stained a deep brown and the background a pale yellow.

On occasions, distances along the pathway were measured by placing a thread along the path of the fibres or by application of Pythagoras's theorem in three dimensions to calculate distances in the sliced fixed brain. The distance of the OT stimulating electrode to the back of the eye was an average 30 mm. The average distance to the OX electrode was 21 mm.

2.4 ELECTRONICS.

Signals from the microelectrode were conventionally amplified by a purpose-built high-impedance input amplifier, band-pass filtered (Krohn-Hite, 3500R, 60 Hz to 6 kHz) and displayed on an oscilloscope (Tektronix, 5223) and through a loudspeaker. Stimulus timing was controlled by a Neurolog system (Digitimer, U.K.). Pulses, usually of 50 us duration, were delivered through a stimulus isolation unit (Ortec, Tennessee) with maximum 100 V output, capacity-coupled to the stimulating electrodes. Electrode impedance was estimated to be in the range of 5-10 Kohms. Selected data were also recorded on an audio tape-recorder (Revox A77) at a tape speed of 19 $cm.sec^{-1}$ for subsequent replay, computer digitisation (Hewlett-Packard

21 MX M-series) and output to oscilloscope and chart recorder. In later experiments, the signals were recorded on a VHS video cassette recorder (VCR)(Panasonic, NV-J35) after being converted from analog to digital signals by a VCR adaptor (PCM-2, Medical Systems Corporation, New York) and subsequently replayed on the oscilloscope. The audio channel of the VCR was used to record commentary during the experiment. Records were made of the signals replayed on the oscilloscope screen, using photographs taken with a polaroid camera (Hewlett-Packard, 197B) and Polaroid Land film (107 black and white, 3000 speed).

2.5 LOCALISATION AND CLASSIFICATION OF RETINAL GANGLION CELLS.

The fundus was back-projected (Fernald and Chase, 1971; Pettigrew et al., 1979) onto two tangent screens; one placed 128 cm directly in front and the other at 45^{o} in the temporal visual field at a distance of 114 cm from the nodal point of the cat's eye (Vakkur et al., 1963). The outlines of the OD, vasculature and microelectrode were marked on the screens. The approximate locations of the foot of the perpendiculars from the nodal point of the eye to each screen were also marked. External representation of these landmarks assisted the rapid localisation of receptive fields because of the known trajectories of axons across the retina (Ogawa et al., 1969; Stone and Hollander, 1971). The receptive fields were located and classified with the aid of manually controlled targets, including black and white discs of varying sizes, gratings of differing spatial frequencies and coloured stimuli, generated by placing a blue transmitting (Ilford 622) or yellow transmitting (Ilford 110) filter in front of a light source directed at the screen. The geometric centres of the receptive fields were determined manually and marked on the tangent screens, which had a mean luminance of 12 $cd.m^{-2}$ from diffuse room lighting (incandescent sources). The microelectrode position was observed by ophthalmoscope at the end of each recording run and noted on the screen with reference to the receptive field to which it belonged.

There has been close agreement between authors on the characteristics of responses to visual stimuli by various RGC. Unfortunately in the naming and classification of RGC there exists some disagreement. It is necessary at this juncture to state the scheme of classification used in this study and examine the controversy

surrounding retinal ganglion cell classification. Kuffler (1953) first described the major grouping of cat RGC receptive fields. They were concentric in arrangement, with an "ON" centre which had increased response discharge to increased illumination, or an "OFF" centre with decreased discharge. The receptive fields included an antagonistic annular surround. The organisation of the majority of RGC receptive fields appears to be concentric with an antagonistic surround (review Rodieck, 1979).

In 1966, Enroth-Cugell and Robson suggested that the ON and OFF categories could be further divided into two functional subtypes the "X" or "Y" RGC. The difference between the two classes was characteristically seen when a stationary sinusoidal grating was positioned so that the changes in luminance in one half of the receptive field were the exact inverse of changes in the other half. An X cell did not respond to the introduction or removal of gratings positioned in this manner, while Y cells responded to stimulus transitions regardless of the spatial phase of the grating. Enroth-Cugell and Robson argued that these cells reacted to a summation of the excitatory and inhibitory input from their whole receptive field and based on their test, the summation was linear for X cells and non-linear for Y cells.

Kuffler also observed differences in the duration of response discharge in ON centre receptive fields, some adapted quickly to prolonged illumination ("transient") while others had sustained discharge for the duration of the stimulus. In 1971, Cleland et al. developed this classification, based upon the RGC response to a battery of tests: 1) exposure to a stationary target of appropriate size and contrast, centred on the receptive field, to demonstrate either a sustained or transient response of the discharge of the cell. 2) Fine gratings of decreasing spatial frequency were moved across the receptive field of the cell. The discharge of a sustained RGC continued to modulate around its average discharge rate until the grating was too fine to elicit a response. The transient RGC however went from a modulated to an unmodulated response, but continued to give an increase in the discharge rate as long as movement persisted. 3) The optimum size of an appropriate target and 4) speed of movement of the visual targets was also important in the differentiation of the two classes. For most sustained cells the ideal target was 1^{o} or less. For transient cells, the target was preferably $>1^{o}$ and only the transient cells continued to respond strongly to a large black disc moving rapidly (200^{o}/ sec) across the centre of the receptive field. 5) An unmodulated response to movement of contrast patterns at a considerable distance

from the cell's receptive field (McIlwain, 1964), known as the periphery effect, was present in transient cells only.

Cleland et al. (1971) also determined that the latency of impulses travelling along fibres from the RGC to the target lateral geniculate neurones was longest in fibres from the sustained class of cells. This encouraged them to equate the transient and sustained classes of RGC with the T1 and T2 conduction-groups in the cat ON (Bishop et al. 1953). They also suggested that the sustained and transient classes would be the X and Y types described by Enroth-Cugell and Robson (1966). Stone and Hoffman, in 1972, described two groups of non-concentric RGC. Because of their very slow rate of conduction they designated them W cells and it was thought that these RGC might give rise to the T3 conduction-group of fibres.

Stone and Fukuda (1974) developed a more complex classification of W cells, including in this group many cells with concentrically organised receptive fields, but that had very slow conduction velocity (CV). This created some conflict with the original designation of X and Y cells which had been based on linearity of spatial summation in concentric receptive fields. This new W grouping included cells that previously must have been part of the X and Y groups of cells and accepted as normal variations of that original classification. However the Y, X, W classification of RGC is widely used because of the convenient correlation with the alpha, beta and gamma morphological classification of RGC (Boycott and Wassle, 1974) and therefore with the T1, T2 and T3 CV groups. This was reinforced by the finding (Hoffman, 1973; Fukuda and Stone, 1974) that almost all the slowly conducting fibres terminated in the superior colliculus.

In the same year Cleland and Levick (1974a) reported both transient and sustained RGC that had rather low responsiveness to conventional visual stimuli. These "sluggish" RGC also had longer latencies than those RGC that responded briskly. So further to the transient/sustained dichotomies of ON-centre and OFF-centre concentric receptive fields, they now added brisk and sluggish RGC in both groups, creating a total of eight classes of RGC. They are the brisk transient (BT), brisk sustained (BS), sluggish transient (ST) and sluggish sustained (SS) classes, each of which has equal numbers of representatives in the ON- and OFF-centre classes of RGC. The earlier correlation by these authors of all the sustained and transient cells to the T1 and T2 conduction-groups was revised. The BT receptive fields were linked to the fast conducting T1 fibres and the alpha cells. The BSs to the T2 and

beta cells and the sluggish-concentric units with the slowest, T3 fibres and gamma cells. Cleland and Levick (1974b) and Stone and Fukuda (1974) also described a greater range of non-concentric receptive fields than had been originally described by Stone and Hoffman (1972).

Stone and Fukuda (1974) noted that their W group of RGC was very heterogeneous in physiological properties and it is difficult to justify the inclusion of cells with such widely varying receptive field properties and CVs into one group. The W classification depends largely upon its connection with the conduction groups and cell body morphological description of the alpha, beta and gamma classes. This is not particularly useful when describing the receptive field characteristics and functional roles of cells and axons encountered during the experimental exploration of the retina. It is for these reasons that the descriptions by Cleland and Levick (1974a; 1974b) of RGC receptive field properties have been adopted for this study. It is therefore necessary to be explicit in the description of each class:

2.5.1 On-centre/ off-centre concentric receptive fields:

a) Brisk transient retinal ganglion cells.

A BT RGC response to a stationary contrast stimulus is at first very strong but then the discharge of the RGC usually returns to near the low prestimulus level within a few seconds. Fast moving targets, such as a twirling, black-reverse-side-white disc can drive the discharge rate of the cell in excess of 120 spikes/sec. The BT RGC are characterised by a large receptive field centre and therefore respond to larger targets and as a result have a modulated response to low spatial frequencies only, however they continue to have an unmodulated increase in discharge to moving fine gratings. These cells also have a strong periphery effect unlike other categories of RGC.

b) Brisk sustained retinal ganglion cells.

These RGC have an irregular maintained discharge of around 40 spikes/sec which increases sharply at the appearance of a stimulus and then sags back to a constant level which remains substantially higher than the prestimulus level. They can be optimally excited by a smaller target than a BT and have a well modulated response to high frequency spatial gratings. They demonstrate little periphery effect.

c) Sluggish transient retinal ganglion cells.

ST RGC often have no or only a low level of irregular maintained discharge. They respond only very transiently to the appearance of a stimulus. Unlike BT, they respond best to slow moving (<3^{o}/sec) medium-sized targets (0.5-1^{o}), giving only feeble or no responses to targets moving in excess of 100^{o}/ sec. ST RGC have a relatively weakly modulated response to even fine gratings.

d) Sluggish sustained retinal ganglion cells.

These RGC have a usually low but characteristically regular maintained discharge (<10 spikes/ sec) and response to a stationary stimulus of appropriate contrast is well sustained at an elevated level. The optimal target size is in the range of 1-2^{o} and like ST RGC, they respond best to slower moving targets. They also have a weakly modulated response to quite low spatial frequency gratings. A proportion of this class of RGC shows an unmodulated increase in discharge to fine gratings.

2.5.2 Other, less commonly encountered, receptive field types:

a) Colour-coded retinal ganglion cells.

These RGC have a vigorous maintained discharge and a sustained increase in discharge when activated by blue light and are suppressed by red or yellow light.

b) Local edge detectors.

Also known as excited-by-contrast (Stone and Hoffman, 1972) or on-off phasic RGC (Stone and Fukuda, 1974). These RGC have virtually no maintained discharge and are excited by a small target of either contrast when placed within the receptive field. This RGC has a 'silent' inhibitory surround, that is stimulation of the surround failed to produce an excitatory response but did suppress the excitatory response elicited by stimulation of the centre, as opposed to the classic antagonistic surround of the Kuffler on/off RGC.

c) Direction selective retinal ganglion cells.

These RGC have little or no maintained discharge. They respond moderately to targets passed in a preferred direction across the receptive field but no response is elicited when the target is passed in the opposite or null direction. Responses to targets moved in a direction perpendicular to the preferred direction was weaker and symmetrical. These RGC are excited with an optimally sized target of between 0.5-1^{o}, and are maximally sensitive to targets moving relatively slowly.

d) Uniformity detectors.

Also known as suppressed-by-contrast (Rodieck, 1967) units, these RGC have a brisk maintained discharge that is suppressed or temporarily abolished by all forms of visual stimulation within their receptive field.

e) Edge inhibitory off-centre retinal ganglion cells.

A class of RGC that may be related to uniformity detectors, but appear to be made of three concentric zones. A small inhibitory centre and two antagonistic outer rings which are off and on respectively. These RGC have unusually large receptive fields.

During recording both axons and cell bodies (units) were encountered. The following criteria were used to establish the type of recording. Units with receptive fields that were located close to the recording position were classified as a recording of a cell body, and receptive fields located away from the recording position could be safely classified as axonal recordings. In addition, the waveforms generated by cells and axons can be differentiated. Bishop et al., (1962a) suggested that a cell body spike usually had an inflection on the early portion of the positive phase of the action potential. Recording experience in the retina regularly confirms this. Negative spikes recorded in the retina are thought to originate from the dendrites (Fukuda and Stone, 1974). In addition, the amplitude of the spike elicited from a cell tends to decrease with increased frequency of discharge. On the other hand, recordings from axons exhibit no early inflection of the waveform, and the positive phase is of shorter duration than that recorded from cell bodies. It should be mentioned that it is the neurophysiological convention to display the waveform reversed, that is, with positivity downwards, but all mention made here refers to the actual (not display) direction of the waveform.

The axons in this study were classified primarily by the physiological response of the RGC to a variety of visual stimulation tests, as described above. The RGC were classed as having brisk transient, brisk sustained or sluggish or other uncommon receptive field types, and it is worth re-emphasising that these RGC groupings are thought to be the correlates of the large diameter/fast conducting, intermediate sized/CV, and the small/slow group of optic fibres, respectively. Therefore in this study, where both the visual responses of the RGC and its latency could be ascertained, the RGC were labelled as BT/T1 or BS/T2. The axons with sluggish or other less commonly encountered responses to visual stimulation and slowest latencies were, for the purposes of comparison, considered as a one group of non-brisk/T3 cells.

The axons sampled in this study demonstrate a bias towards the recording of larger diameter axons. BT/T1 RGC represented 80% of the fibres driven from the OT and 77% from the OX and yet are thought to compose only 5% of the total fibre population in the optic pathway (Hughes, 1985, review). Axons with non-brisk responses to visual stimulation represented 3% of the sample from both the OT and OX, but are thought to comprise the majority of optic fibres. The non-brisk RGC with slow CV have axonal diameters in the range of 2 μm or less and therefore may be difficult to record on the basis of their size alone. Non-brisk/T3 axons also proved to be even more difficult to record from for any length of time.

This recording bias has been previously documented (Levick and Thibos, 1983, review) and is supported by the increase in the representation of non-brisk units in the population of recordings from the cell bodies where the larger diameter soma of these small RGC is a more accessible target for the recording electrode than the axon (Chapter 5, Table 1). The bias towards the recording of BT/T1 axons was accentuated by the increased concentration of smaller cells in the area centralis and the tendency of axons from this region of the retina to exit the eye in a narrow sector of the optic disk. By recording from all around the circumference of the ONH, many more axons with peripherally located retinal ganglion cell somas and, by inference, BT/T1 axons (large cells) would have been recorded, than the axons with centrally located somas (possible BS/T2 and non-brisk/T3 axons).

2.6 MEASUREMENT OF CONDUCTION PARAMETERS.

2.6.1 Threshold and latency.

Stimuli of 50 μsec duration were delivered at the rate of 1 Hz. The more favourable polarity at the stimulus bipole was used. If there was no response at a maximum 100 volts, the duration of the stimulus was increased to 150 μsec before the fibre was deemed to be undriveable. The voltage threshold for the eliciting an all-or-none antidromic impulse was determined by adjusting stimulus strength until the impulse was recorded 50% of the time and its latency became consistent. The maintained discharge of the RGC was minimised where necessary by positioning stationary visual stimuli on the receptive field. Stimulus strength was increased to 1.4x threshold and the latency of the antidromic impulse was determined as the time from the onset of the stimulus to the earliest detectable deflection of the recorded impulse from the field potential and baseline noise. The on-line measurement of latency was enhanced by positioning a Neurolog-controlled cursor on the oscilloscope screen. The combination of receptive field classification and location, threshold, polarity and latency and where appropriate the tract from which they were driven, provided a signature with which to identify each cell. Thus re-recordings of axons could be recognised.

2.6.2 Two-stimuli measurements.

The refractory period of transmission (RPT) has been defined as the longest interval between a pair of stimuli, at which the response to the second just fails to appear (McDonald and Sears, 1970, Chapter 1, pp 8-12). In this study, the RPT was operationally assessed by the application of two closely spaced stimuli at a rate of 1 Hz and at a strength > 3.7x threshold. The use of that particular stimulus strength is discussed in Chapter 3. The inter-stimulus interval (ISI) was shortened until the second stimulus just produced a transmitted response approximately 50% of the time. The ISI was then slightly increased to produce a consistent response and the latency of the second response to the second stimulus was measured to provide information about conduction of the second impulse in the refractory wake of the first impulse.

2.6.3 The collision paradigm.

The standard two-stimulus test necessarily determines the RPT of the region of fibre which has the lowest safety factor, but can not resolve the spatial extent of a localised region of physiological vulnerability. At least one moveable electrode or multiple electrodes would be required to obtain further information about the spatial extent of the vulnerable region. In the optic pathway, the numerous RGC fibres are intermingled with dense fibrous bands. This makes identification of individual fibres along the optic pathway impractical with multiple electrodes.

Swadlow (1982) used collision of antidromic impulses with an orthodromic impulse in geniculo-striate fibres to estimate the RPT close to the site of stimulation. Kosugi et al. (1988) have proposed that a collision paradigm could be used to determine a damaged region of fibre. In this study, the paradigm has been extended to determine the RPT along regions of normal and demyelinated optic fibres. By using two closely-spaced impulses in conjunction with collision of the first antidromic impulse with an orthodromic impulse, it is possible to locate a vulnerable region of fibre and to examine the RPT on the stimulus side of the most vulnerable point on the fibre. When collision occurs before the antidromic impulses reach a region of reduced safety factor, then annihilation of the first antidromic impulse relieves the vulnerable portion of the fibre of the burden of carrying closely spaced impulses.

The two-stimuli collision paradigm involved selecting, at intervals of at least 1 s, an orthodromic impulse arising from the normal maintained discharge of the retina. The impulse activated a Schmitt trigger with adjustable threshold. This permitted synchronisation (at an adjustable delay) of two closely spaced stimuli with the orthodromic impulse. For delays set shorter than the antidromic latency, the first antidromic impulse collided with the selected orthodromic impulse, resulting in annihilation of each other (Tasaki, 1949). Only the remaining second antidromic impulse was detected at the recording site. The ISI was then reduced until the second antidromic impulse just failed to transmit 50% of the time. This setting revealed the RPT for that region of fibre between the stimulus site and the collision point (designated the rRPT). The ISI was then increased slightly to permit the timing of the second response to be measured for every pair of stimuli. Collision of action potentials can therefore localise regions of reduced safety factor, demonstrated by an increase in rRPT, to a particular position in time which can then be indirectly referred to a particular point along the fibre.

A convention is used in this thesis to describe the location of lesions, stimulating electrodes and recording electrode relative to each other. Because there is an ambiguity in the use of the terms proximal (towards the cell body or towards the centre) and distal (vice versa) in optic neurons, the terms upstream and downstream have been adopted. Upstream refers to something located towards the LGN and downstream, towards the retina, in reference a physical location such as a stimulating electrode. This also refers to the direction of the passage of an antidromic impulse and this convention is particularly useful in the description of events during the collision paradigm.

2.7 LESIONS OF THE OPTIC NERVE.

As part of the study of conduction vulnerability in optic fibres, lesions of the ON fibres were also examined. Two methods were used to create lesions. Both techniques were performed by collaborators in laboratories elsewhere. Dr W.M. Carroll, Perth, Australia, used antigalactocerebroside antisera (anti-GC) to cause demyelination and Professor W. Burke used pressure applied to the nerve to induce demyelination and some axonal damage. What follows is a brief description of their methods.

2.7.1 Anti-galactocerebroside lesion.

Focal demyelinating lesions were created by micro-injection of high-titre anti-GC into the retrobulbar portion of the right ON, usually 3 mm posterior to the optic nerve's exit from the scleral canal (Carroll et al., 1984; 1985a). The injection of 1-2 µl of anti-GC antisera characteristically results in a localised region of primary demyelination with minimal axonal damage (Carroll et al, 1984; 1985a), occupying 20-50% of the transverse section of the nerve and extending up to 3 mm along the nerve. Cats were subsequently examined over an average period of 2-3 days, commencing recording on different days following the injection of anti-GC. In all, eight adult cats were examined over 4 to 20 days post-injection.

Histological observations were made by Dr Carroll and colleagues, and these are described in detail in the introduction to Chapter 5.

2.7.2 Pressure lesion.

Pressure-induced demyelinating lesions were produced by the inflation of a balloon of silastic tubing pressing the retrobulbar ON on to a small brass side-arm, 1.5 mm in diameter and 3 mm in length. The block was assessed by stimulating the intracranial optic pathway and recording from the ON in front of the block or vice versa (Burke et al., 1985; 1986). Application of pressure initially caused a delay in the latency and a reduction in the amplitude of the T1 waveform of the compound action potential (CAP). Pressure continued to be applied until conduction of the T1 fibres ceased and the T2 waveform was significantly reduced. After the pressure was released, the T2 response tended to rapidly recover. Conduction through the lesion and upstream from the lesion was assessed in the weeks after the application of pressure and the ability of the T1 fibres to conduct between the OX and OT electrodes (ie upstream from the lesion) declined.

This type of procedure caused two forms of damage to the optic fibres. The first was demyelination, caused by a lower pressure block (Ochoa et al., 1972; Clifford-Jones et al., 1980; Burke et al., 1992) which results in a reversible block which recovers over several weeks, possibly with remyelination (Burke et al., 1992). The second, induced by higher pressures, was a severe permanent block caused by severing of the axon cylinder followed by Wallerian degeneration of their central segments, that corresponds to the progressive inability of fibres to conduct impulses between the OX and OT electrodes. In both forms of damage there was a preferential blocking of the larger, T1 optic fibres (Burke et al., 1985; 1986; 1987; 1992).

The pressure lesion was investigated in two adult cats. The first of these, LB73, had a lesser degree of pressure applied, with an initial apparent reduction of 90% of the T1 and 40% of the T2 waveforms in the CAP. The second animal had a greater amount of pressure applied, with 58% of the T2 response initially reduced, as well as the complete absence of the T1 waveform. In the days following the application of pressure, the T1 response upstream from the OX was seen to decline. These animals had conduction parameters examined some 48 days, after the initial operation, in the laboratories in Canberra. The methods of anaesthesia, intraretinal recording and measurement of conduction were as described earlier in this chapter for non-lesioned animals. As a control, an unlesioned animal (LB88), but with the same stimulating electrode placement as previously described for the pressure lesioned animals (Fig. 2.2c), was also examined.

CHAPTER 3
CONDUCTION LATENCY AND REFRACTORINESS IN SINGLE OPTIC AXONS IN THE CAT VISUAL PATHWAY.

3.1 INTRODUCTION

Retinal ganglion cells (RGC) in the cat have been extensively studied (Levick and Thibos, 1983, review) and are thought to form three distinct conduction velocity (CV) groupings known as T1, T2, and T3. It had been generally assumed that the CV of impulses along the myelinated portion of individual optic fibres within these groups remained relatively constant. However, in 1990, Baker and Stryker, reported that in the ferret visual pathway there was an increase in the CV and fibre diameter of both the T1 and T2 fibres in the optic tract (OT) when compared to those in the optic nerve (ON).

Baker and Stryker had used recordings of the response of the whole nerve to measure the changes in the latency of the T1 and T2 peaks of compound action potential's (CAP) stimulated in the OT and chiasm (OX). However, the use of CAP to examine latency in optic fibres is problematical (review, Levick and Thibos, 1983), with considerable variation in the amplitude and separation of the various components of the CAP waveforms, due to the heterogeneous segregation of fibres of different diameters in the cross-section of the optic pathway and the proximity of electrodes to particular groups of fibres. In the present study there was the opportunity to examine data from single fibres of RGC, a situation that permits the latency of a fibre to be unambiguously established.

A comprehensive examination of the refractoriness of single optic axons has also been undertaken to provide information about the conduction properties of normal optic fibres, as a control for a companion investigation of experimentally demyelinated optic fibres (see Chapter 5). Previous studies of refractoriness in the optic pathway have used CAP to determine the minimum interstimulus interval (ISI) for two closely spaced impulses for both T1 and T2 fibres in the optic pathway, and have suggested that there is a small increase in refractoriness for the smaller T2 fibres compared to the larger T1 fibres, in both the cat (Bishop et al., 1953) and the rat (Fox and Ruan, 1989). However, the problems of deciphering the location of the

second T1 waveform when it is embedded in the first T2 wave are considerable. In the present investigation of refractoriness it has been possible to compare the RPT of single axons and the delay in the latency of the second of the two closely spaced impulses.

3.2 METHODS.

Preparations of the animals for experimentation and measurements of latency and RPT were made using the methods described in detail in Chapter 2, pp72-73. The tungsten-in-glass recording electrode was placed within 1/2 a disc diameter of the optic disc margin (see Fig. 2.1a.) so that an approximately constant distance from the stimulating electrode to the recording site could be maintained and to minimise the amount of unmyelinated axon included in the conduction distance. The bipolar stimulating electrodes were placed in the OT of 21 cats, contralateral to the eye from which recordings were made (see Fig. 2.2a). In another 8 animals, the stimulating electrodes were placed in the OX (see Fig. 2.2b). At the conclusion of some experiments, the distance from the stimulating electrode to the back of the eye was measured. From the OT stimulus site, the conduction distance was an average 30 mm and from the OX an average 21 mm.

The axons in this study were classified primarily by the physiological response of the RGC to a variety of visual stimulation tests as described in Chapter 2, pp 68-70. The cells were classed as having brisk transient (BT), brisk sustained (BS) or sluggish or other uncommon receptive field types, and it is worth re-emphasising that these classes of RGC are thought to be the correlates of the largest diameter and fastest conducting (T1), intermediate size and medium speed (T2) and the smallest and slowest (T3) groups of optic fibres, respectively. In this study the axons with sluggish or other less commonly encountered responses to visual stimulation and slowest latencies were, for the purposes of comparison, considered as a one group of non-brisk RGC.

3.3 RESULTS.

3.3.1 Conduction latency in single optic axons.

Because of the delay between stimulus onset and the initiation of an impulse variously known as the set-up time, stimulus-spike time or utilisation time, and possible variations of the distance from the stimulating electrode to the point of initiation of the impulse, no single measurement of latency can reliably give the true CV of an axon. In order to make a comparison of the latencies measured from the OT with those from the OX , the distributions of the ratio of conduction distance to latency measured in mm/ms were considered. While distance/time is a measure of velocity, in this instance the use of the ratio is intentional because in this experimental setup, a number of factors (to be discussed further in this chapter) cause the ratio of conduction distance to latency not to be equivalent to the CV of the myelinated optic fibres.

3.3.1a Comparison of Optic Tract and Nerve Latencies.

Measurements were made of the conduction latency in 256 axons stimulated in the OT, and for 99 axons driven from the OX. The means of the ratio of conduction distance to latency for both the BT/T1 and BS/T2 axons from the OT and OX are shown in Table 3.1.a. and the distributions of the ratios are shown in Fig. 3.1.

If the CVs of BT/T1 and BS/T2 optic axons are constant, then it would be expected that the distribution of the ratio of conduction distance to latency would remain the same when the measurements were made from spatially separated locations along the visual pathway, disregarding the utilisation interval. However, it can be seen that the mean of the ratio of distance to latency increases from the OX to the OT for both BT/T1 (Fig. 3.1d to b) and BS/T2 fibres (Fig. 3.1c to a), in particular the BT/T1 fibres where the mean of the ratio increases by nearly 7 mm/ms in the OT. The distance/latency ratios were significantly different between the OT and ON for both the BT/T1 ($t = 14.66$, $df = 287$, $p < 0.001$) and BS/T2 ($t = 3.10$, $df = 64$, $p < 0.001$) fibres, using Student's t test. Because the ratio of distance/latency measured from the OT to the recording electrode, also includes the latency from the

TABLE 3.1.

A. RATIO OF DISTANCE TO LATENCY.

	BT/T1			BS/T2		
STIMULATION	*MEAN*	*SD*	*N*	*MEAN*	*SD*	*N*
OPTIC CHIASM	21.8	3.0	79	11.9	1.3	20
OPTIC TRACT	28.5	4.4	210	13.7	2.5	46

B. MODIFIED RATIO OF DISTANCE TO LATENCY.

	BT/T1			BS/T2		
STIMULATION	*MEAN*	*SD*	*N*	*MEAN*	*SD*	*N*
OPTIC CHIASM	39.9	5.3	79	20.4	2.2	20
OPTIC TRACT	44.2	7.7	210	20.2	3.9	46

Table 3.1A shows the means of the ratios of the conduction distance to latency of 256 axons stimulated from the OT and 99 from the OX. Values obtained from stimulation in the OT are higher than those obtained with OX stimulation, for both BT/T1 and BS/T2 fibres.

Table 3.1B gives modified ratios of conduction distance to latency, corrected for the slower CV in the unmyelinated axon in the retina, and utilisation time, for the same set of axons. Only the values for the BT/T1 fibres remained higher with OT stimulation than with OX stimulation.

FIGURE 3.1 Conduction distance/ latency ratios.

Conduction distance over latency ratios for BT/T1 and BS/T2 axons, measured from the optic tract (OT) and optic chiasm (OX).

A BS/T2 axons with ratios derived from measurements of latency measured from the OT. The minimum value was 10.3 mm/ms and maximum 21.6 mm/ms.

B BT/T1 axons also stimulated from the OT. The minimum value was 20.0 mm/ms and the maximum was 44.1 mm/ms. Note that the maximum value overlaps the minimum value established for the BS/T2 axons driven from the OT.

C BS/T2 axons with the ratios derived from measurements of latency over the shorter distance from the OX. The ratios measured ranged from 9.3 mm/ms to 13.9 mm/ms.

D BT/T1 axons stimulated from the OX. The minimum value was 15.7 mm/ms and the maximum was 30.0 mm/ms. Note that the ranges of values for the BT/T1 and BS/T2 axons driven from the OX do not overlap.

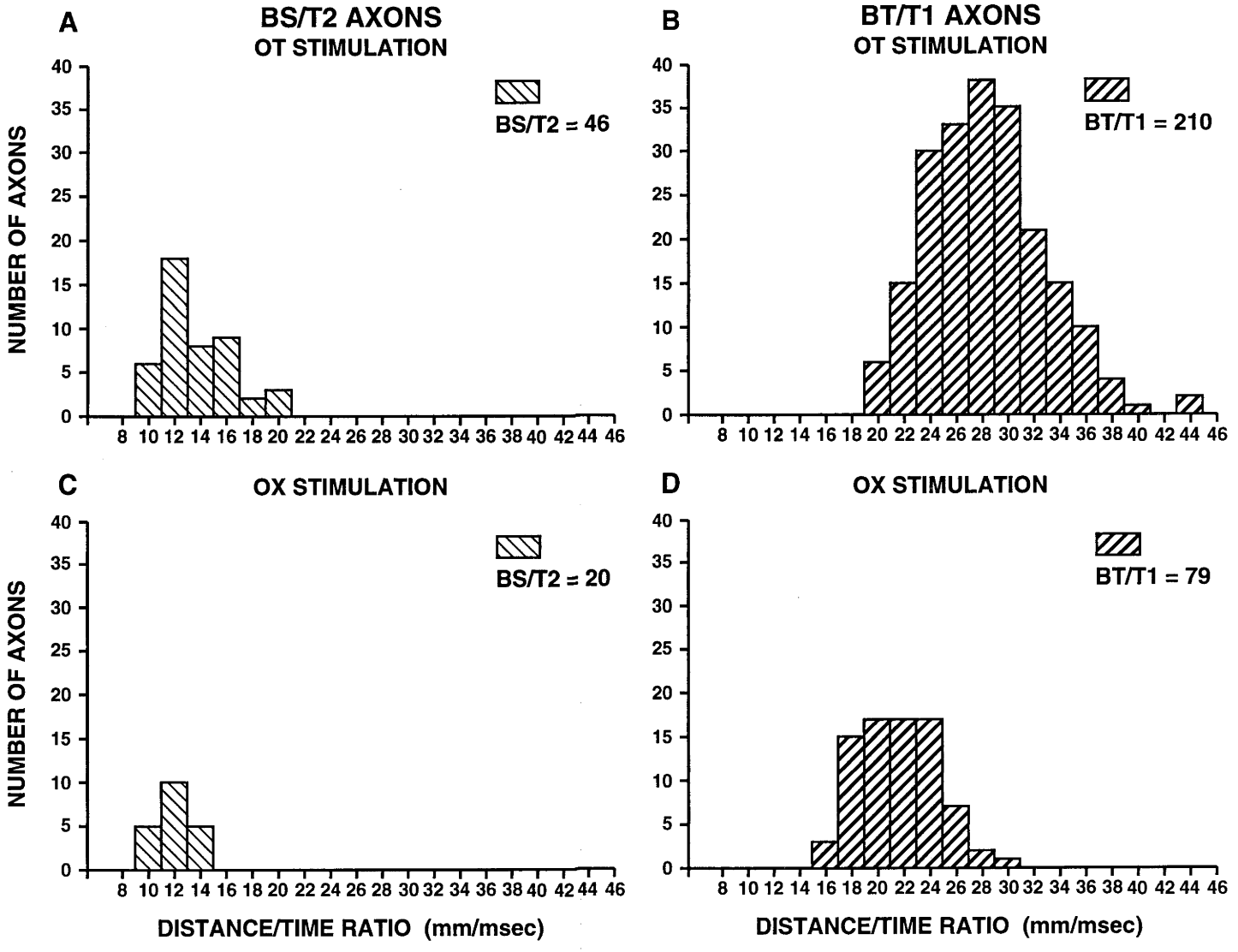
DISTANCE/TIME RATIO
A
BS/T2 AXONS
OT STIMULATION
BS/T2 = 46
B
BT/T1 AXONS
OT STIMULATION
BT/T1 = 210
C
OX STIMULATION
BS/T2 = 20
D
OX STIMULATION
BT/T1 = 79
NUMBER OF AXONS
DISTANCE/TIME RATIO (mm/msec)
0 5 10 15 20 25 30 35 40
8 10 12 14 16 18 20 22 24 26 28 30 32 34 36 38 40 42 44 46

OX, any change in the OT ratio compared to the OX, is likely to be caused by changes in the CV of the axons within the OT itself.

The BT/T1 and BS/T2 populations for those axons stimulated from the OX can be seen to have two non-overlapping distributions (Fig. 3.1c & d). But when the distributions of the ratio for BT/T1 and BS/T2 from the OT are viewed (Fig 3.1a. & b.) it can be seen that these populations overlap. This could be due to the greater chance of revealing the tails of the distribution of the ratios in the larger OT sample of axons.

3.3.1b Comparison of the modified ratio for BT/T1 and BS/T2 fibres.

There are, however, two factors that may contribute to an underestimation of CV inferred from the ratio of conduction distance to latency. These are: 1) the utilisation time, and 2) the length of unmyelinated axon. These factors will have greater impact on estimations of CV for the shorter conduction distance from the OX, than on the time taken to traverse the longer distance from the OT. The utilisation time is difficult to measure directly, but has been estimated to be between 0.1-0.2 ms in myelinated central pathways (Takahashi, 1965, Sumitomo et al., 1969, Stone and Freeman, 1971). In addition, there is some indirect evidence from the collision paradigm (Chapter 4), which supports the probability that utilisation time is somewhat < 0.2 ms in the optic pathway.

The intraretinal unmyelinated length of axon, which is included in the distance from both stimulation sites to the recording site, is known to have CV approximately 8 to 10 times slower than the CV in the myelinated portion of the optic fibres (Motokawa et al., 1957, Ogawa et al., 1969, Stone and Freeman, 1971, Rowe, 1990). It follows that the inclusion of a small region of axon with slower CV will contribute proportionally more to the overall latency measured for shorter conduction distances. The actual length of unmyelinated axon effective in the present experiments can only be indirectly estimated. An adult cat has an OD of an average 0.93 mm in diameter (Bishop et al., 1965) and as the furthest the recording electrode was from the OD margin was in the order of 1/2 a disc diameter, the likely maximum intraretinal distance was in the order of 0.5 mm. The distance beyond the disc to the point of myelination in the cat is not known. However, it has been shown in the rat that this distance is 0.30 mm (Hildebrand et al., 1985) and 1 mm in the human

(Hogan et al., 1971). Blunt et al. (1965) did suggest that unlike other species with a lamina cribrosa, the cat optic fibres commence myelination some distance into the ON, after passing the lamina and that myelination is uniform 1 mm behind the lamina.

Modified distance/ latency ratios were calculated by assuming a utilisation time of 0.1 ms and an unmyelinated length of axon of 1.5 mm with a CV 8 times slower than that in the extraretinal segment (Table 3.1.b.). The modified ratio of conduction distance to latency for BT/T1 axons stimulated in the OT still remained significantly different from that of the fibres driven from the OX ($t = 4.59$, $df = 287$, $p < 0.001$). The values for the BS/T2 population were not significantly different ($t = 0.25$, $df = 64$, $0.8 > p > 0.75$).

3.3.1c Comparison of BT/T1 CV in the optic tract and nerve.

It is possible that not all BT/T1 fibres are increasing their CV at a uniform rate in the OT. In fact, the CV might be decreasing in some fibres while markedly increasing in others. There is confirmation that BT/T1 CV may vary between the nerve and tract from an animal which had stimulating electrodes placed at three sites: the ON, OX and OT (see Fig. 2.1c), enabling calculation of CV for each segment of axon. The average BT/T1 CV for the ON was 54.0 m/s and for the OT alone was 81.5 m/s. While this is an overall increase in CV in the tract, a study of the differences between the OT and ON CVs for 24 individual BT/T1 axons shows that while the majority of BT/T1 axons increase their CV, others slowed down in the OT by up to 22% compared to the CV in the ON (Fig. 3.2). However, the increases in CV in the OT are more marked than the decreases. The number of BS/T2 axons in this experiment were too few for definite conclusions to be drawn, however, indications are that the CV of BS/T2 axons does not alter from the ON to the OT as dramatically as it does for the BT/T1 axons.

3.3.1d Axons with sluggish receptive field characteristics.

A total of 7 other units stimulated in the OT was variously classified as sluggish sustained (6) and sluggish transient. The average ratio of distance to conduction time for these axons was 9.5 mm/ms and ranged from 8.1-10.6 mm/ms. There were also three axons driven from the OX, that had sluggish sustained receptive field

FIGURE 3.2 The difference between optic nerve and tract conduction velocities.

A plot of the difference between the actual conduction velocities in the optic tract (OT) and optic nerve (ON) for 24 individual BT/T1 axons from the one animal LB88. In LB88, stimulating electrodes were placed at 3 sites; in the OT, optic chiasm and ON. Conduction velocities were therefore able to be calculated in the two separate sections of the optic pathway. The ON conduction velocity was then subtracted from the OT conduction velocity.

Note that the conduction velocities of most of the axons increased from the ON to the OT, although a few either decreased or remained essentially unchanged. The magnitudes of the increases were generally greater than those of the decreases.

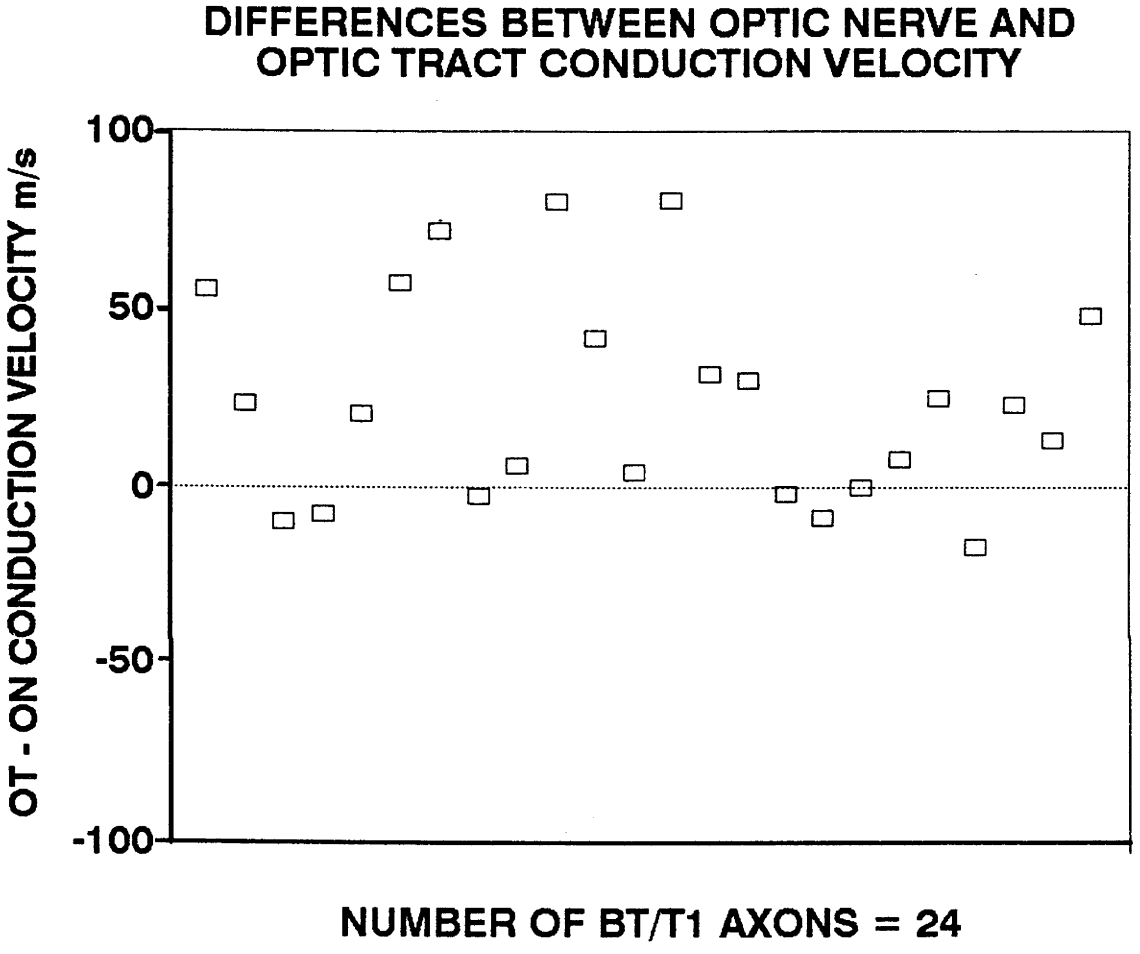
DIFFERENCES BETWEEN OPTIC NERVE AND
OPTIC TRACT CONDUCTION VELOCITY
OT - ON CONDUCTION VELOCITY m/s
100
50
0
-50
-100
NUMBER OF BT/T1 AXONS = 24

characteristics. The ratios obtained from the OX axons ranged from 7.9-8.9 mm/ms, however there are insufficient numbers of these types of RGC to allow any meaningful comparison of data from the two stimulation sites. In addition, the utilisation interval for the non-brisk/T3 axons has not been estimated and the relation between the CV of the myelinated and unmyelinated portions of the T3 optic axons has also not been ascertained.

3.3.2 Refractory period of transmission.

3.3.2a RPT, and stimulus strength relation.

One of the first requirements for testing RPT in optic axons was to ensure that the measurements obtained were the minimum ISI that could be established for each axon, so that values obtained from different axons could be compared, in particular between axons of varying diameters. To this end a number of stimulus strength versus RPT measurements were made to determine if there was a level of stimulus strength, above the threshold for the initiation of a propagating response, that could be used to produce a consistent minimum RPT for each axon. Some 17 axons, 15 BT/T1 and 2 BS/T2, were tested at a variety of stimulus locations using two stimuli of equal strength. Figure 3.3 shows some representative examples of the stimulus strength versus RPT relation.

The commencement of the horizontal line of the graph denotes the ISI where the RPT becomes independent of further increases in stimulus strength. At even greater stimulus intensities, there will be an insufficient fraction of Na^+ channels available for activation to generate a second impulse at a shorter ISI. Therefore the value of the RPT will remain constant, despite the intensity of the stimulus used. These minimum possible ISIs will form a plateau, which is at a level equivalent to the ARP. The start of the plateau was reached in all axons when the stimulus was between 2 to 3.7 times greater than the threshold voltage. The two axons in Fig 3.3 formed a plateau at 3.4 and 2.9 times threshold respectively and there was no correlation between threshold voltage or latency and the stimulus strength above threshold at which axons reached their minimum ISI. It was concluded that a stimulus strength of 3.7 times threshold would establish a definite minimum ISI enabling

FIGURE 3.3 Refractory period of transmission versus stimulus strength.

The refractory period of transmission (RPT) at progressively increasing stimulus strengths. The voltage used is expressed as a proportion of the threshold voltage for that axon, ie as x times the threshold voltage.

A A representative example of a BT/T1 axon with a threshold voltage of 4.03 V. The minimum limiting value of the RPT is reached at approximately 3.4 times the threshold voltage.

B A representative example of a BS/T2 axon with a threshold voltage of 10.3 V. The minimum limiting value of the RPT is reached at approximately 2.9 times the threshold voltage.

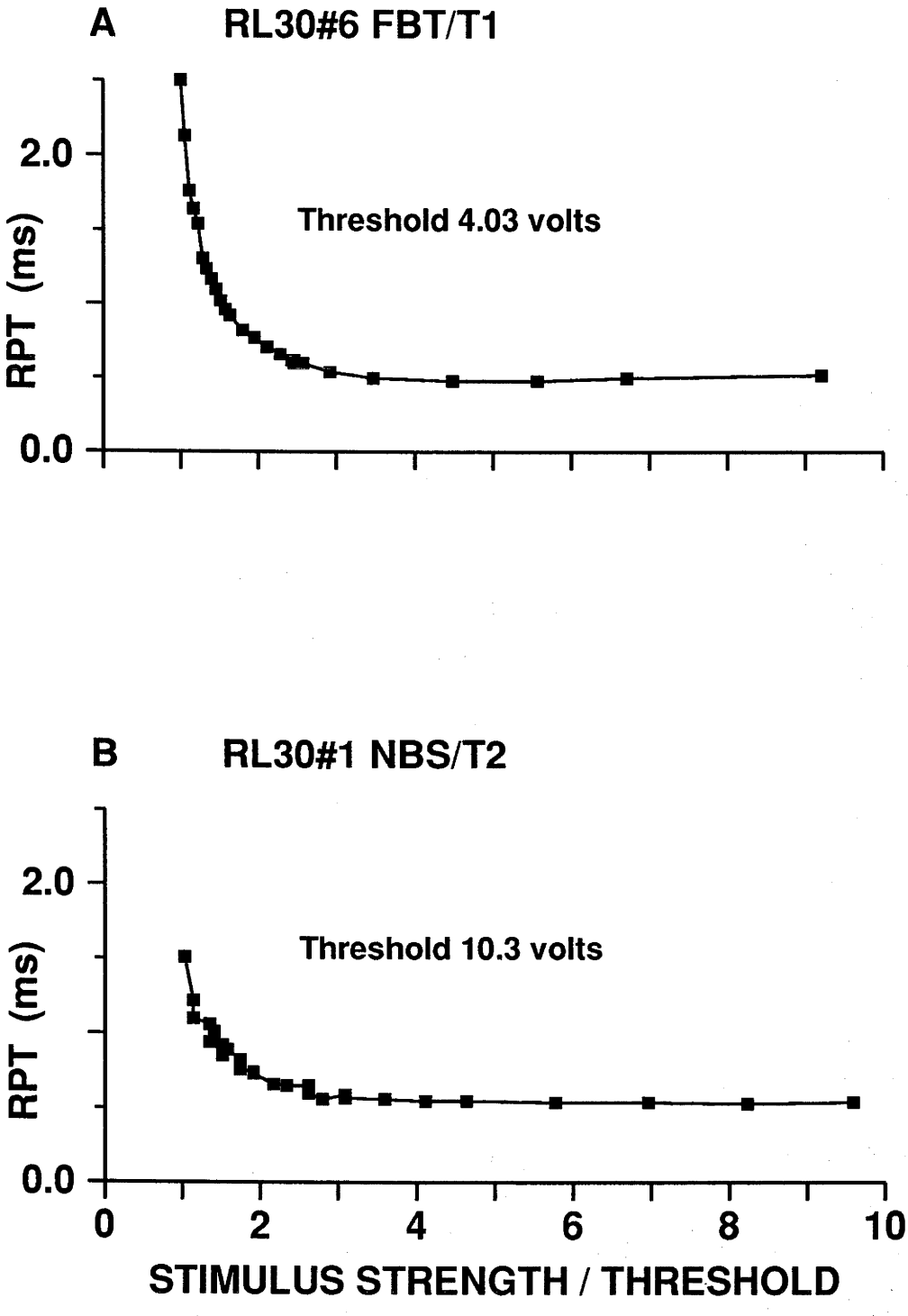
A
RL30#6 FBT/T1
2.0
RPT (ms)
0.0
Threshold 4.03 volts
B
RL30#1 NBS/T2
2.0
RPT (ms)
0.0
Threshold 10.3 volts
0
2
4
6
8
10
STIMULUS STRENGTH / THRESHOLD

comparison of RPT from all BT/T1 and BS/T2 axons in this study. In fact, most fibres in this study had RPT tested above that level.

3.3.2b RPT for BT/T1 and BS/T2 axons.

Measurements of RPT were made in 296 BT/T1 (Fig. 3.4a) and BS/T2 axons (Fig. 3.4b), stimulated in the OT. Of the 241 BT/T1 axons, the average RPT was 0.49 ms, ± 0.05 (range 0.28-0.65). Of the 55 BS/T2 axons tested, the average RPT was 0.50 ms, ± 0.05 (range 0.28-0.58). Using Student's t test, these values were not significantly different ($t = 0.91$, $df = 294$, $0.3>p>0.2$). Thus, BT/T1 and BS/T2 optic axons, which are known to conduct at differing velocities and are thought to have differing axonal diameters, have similar distributions of RPT values. The average RPT for combined BT/T1 and BS/T2 axons was 0.49 ms, ± 0.05, and more importantly the distribution of the combined BT/T1 and BS/T2 RPTs showed no correlation with their latency (Fig. 3.5).

Similarly the RPT of 73 BT/T1 axons stimulated in the OX had an average RPT 0.49 ms, ± 0.05 (range 0.32-0.60). Another 16 BT/T1 axons were stimulated in the ON and had an average RPT of 0.50 ms, ± 0.03 (range 0.45-0.56). This suggests that changing the location of the site of stimulation within the optic pathway does not alter the RPT. Changes in the location of the recording site, to the unmyelinated axon in the peripheral retina or to the perikaryon of the ganglion cell also produced no change in the distribution of RPT measurements.

3.3.2c RPT in non-brisk/T3 axons.

There are insufficient numbers of non-brisk/T3 axons to permit a meaningful comparison with BT/T1 and BS/T2 data. With the inclusion of two units stimulated in the OX it is possible to study the distribution of RPTs for only 6 non-brisk/T3 units. The RPT values ranged from 0.58 to 0.90 ms and the average RPT for this group was 0.69 ms, ± 0.12. On the basis of such a limited sample it is difficult to draw definitive conclusions, however, these units appear to have longer RPTs than the BT/T1 and BS/T2 axons. If this result was confirmed in a larger sample it would reinforce the suggestion that fibres with CV less than 15-20 m/s and therefore

FIGURE 3.4 Distribution of refractory period of transmission

The distribution of the refractory periods of transmission (RPTs) determined by the standard two-stimulus test in 296 axons, stimulated in the optic tract at a minimum of 3.7 times their threshold voltage.

A The distribution of RPT for 241 BT/T1 axons. The mean value for the RPT in these fibres was 0.49 ms and the values ranged from 0.28 ms to 0.65 ms.

B The distribution of RPT for 55 BS/T2 axons. The mean value for the RPT in these fibres was 0.50 ms and the values ranged from 0.28 ms to 0.58 ms.

DISTRIBUTION OF REFRACTORY PERIODS OF TRANSMISSION

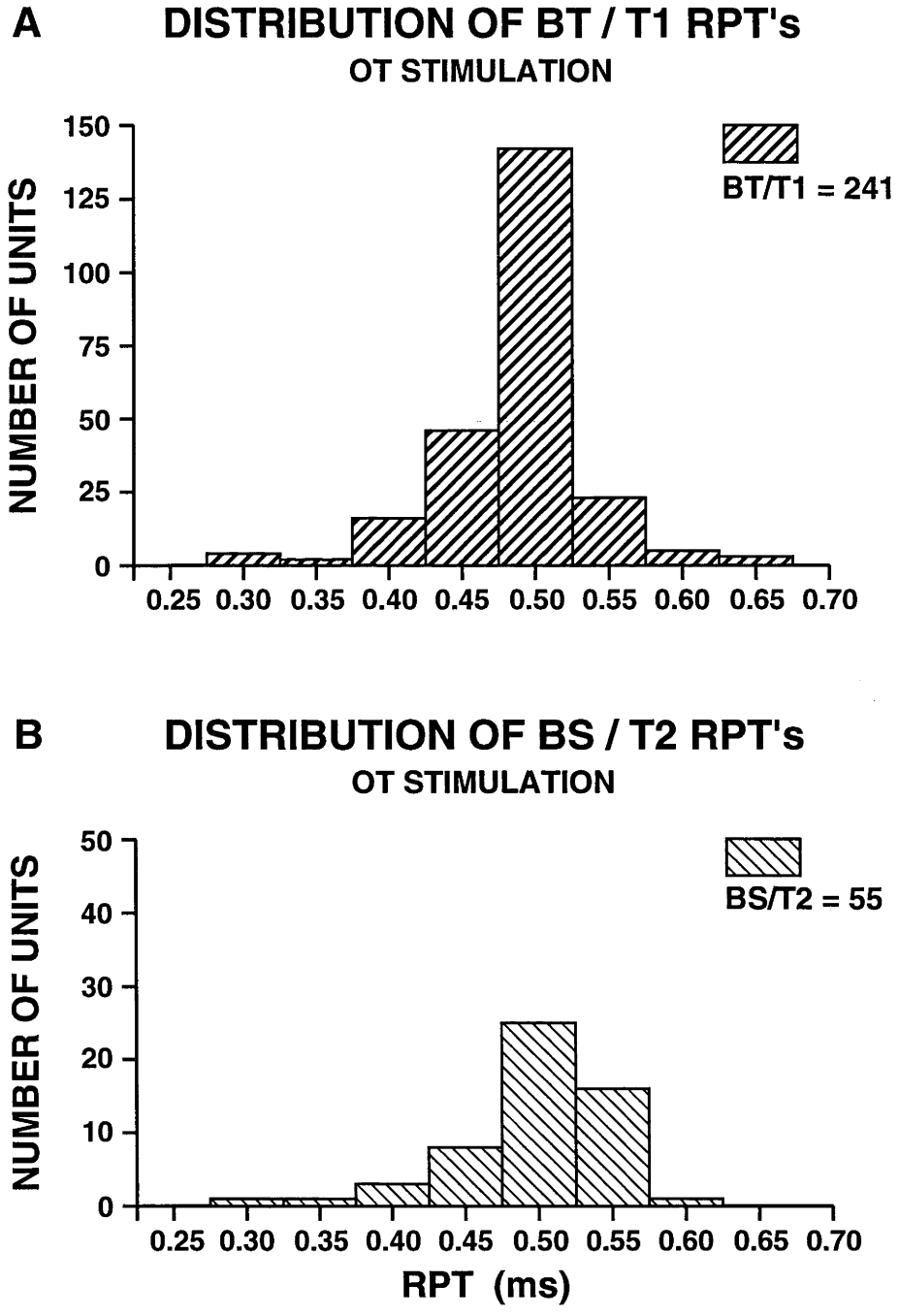

FIGURE 3.5 Latency versus refractory period of transmission, BT/T1 and BS/T2 axons.

Relation of the refractory period of transmission (RPT) to latency in 296 BT/T1 and BS/T2 optic axons. The 241 BT/T1 axons [+] and the 55 BS/T2 axons [o] had latencies measured from the optic tract (OT). These ranged from 0.72 to 2.87 ms. It can be seen that there was no apparent change in the RPT values with the increase in the latency of the optic axons.

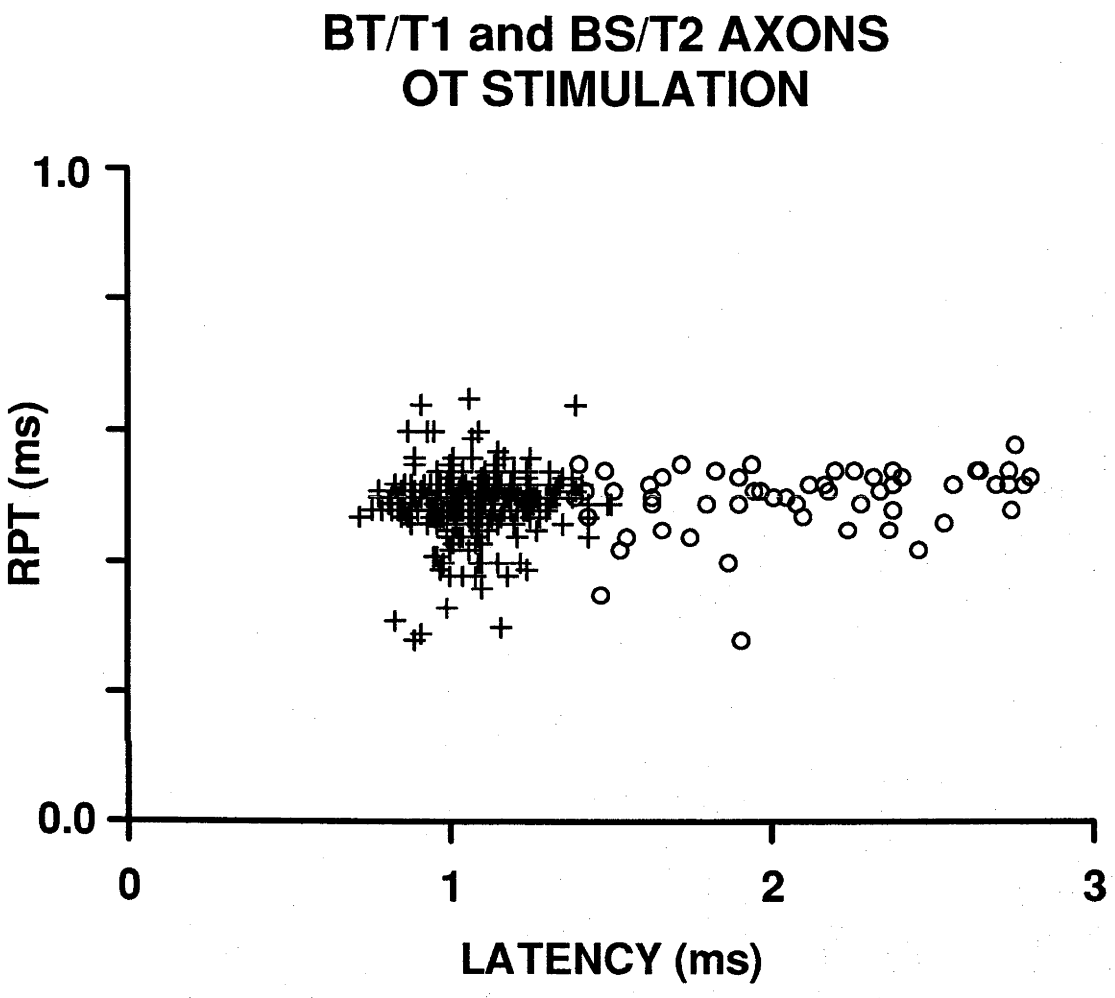
BT/T1 and BS/T2 AXONS
OT STIMULATION
1.0
0.0
RPT (ms)
0
1
2
3
LATENCY (ms)

diameters less than 2-3 μm (Hughes and Wassle, 1976) have a longer RPT than fibres with larger diameters and faster CV.

3.3.3 The latency of the second impulse.

The inter-response interval (IRI) is the interval between the onsets of the two responses at the recording site near the optic disc margin, generated by the application of two stimuli in the OT at the minimum ISI. The IRI for BT/T1 axons (Fig. 3.6a) averaged 1.03 ms, ± 0.07 and for BS/T2 axons was an average 1.25 ms, ± 0.11 (Fig. 3.6b.)

As the average minimum separation of the two stimuli at the stimulation site for BT/T1/T1 axons was an average 0.49 ms and for the BS/T2 it was 0.50 ms, it can be seen that the two responses have increased their spatial separation significantly over approximately 30 mm of fibre. This widening of the IRI is due to an increase in the latency of the second response compared to the latency of the first impulse. In fact the amount that the second impulse is delayed appears to increase with the latency of the first response, that is the longer the latency of the first response, the greater the difference between the first and second responses latency (Fig. 3.7).

As the conduction distance for all fibres is approximately the same and the refractoriness of the BT/T1 and BS/T2 axons is also similar, it is probable that the increase in the latency of the second response with the latency of the first response is a function of the elapsed time that the second impulse has travelled in the wake of the first impulse. It was possible to compare the measurements of some BS/T2 fibres stimulated in the OX with BT/T1 fibres stimulated in the OT, which had similar latencies and RPT, even if very different CVs. These fibres all exhibited a similar degree of delay in the latency of the second response, supporting the suggestion that it is the amount of *time* that a second impulse travels behind the first that determines the amount of delay of the second impulse.

By recording from different locations along the optic pathway (OT, OX and ON) and including both BT/T1 and BS/T2 axons, it is possible to examine the IRI of two impulses applied at a minimum ISI, where the latency of the first impulse ranges from 0.50 ms to 3.00 ms (Fig. 3.8). At 0 latency, the minimum ISI was an average 0.49 ms. The exact timing of the IRI for impulses with latencies <0.50 ms could not be obtained by this experimental set-up.

FIGURE 3.6 The distribution of inter-response intervals.

The distribution of the inter-response interval (IRI) in 278 axons. Two stimuli were applied in the optic tract (OT) at the minimum inter-stimulus interval for each axon, and the responses were recorded at the optic disc margin.

A The distribution of IRI for 227 BT/T1 axons. The mean value for the IRI in these fibres was 1.03 ms and the values ranged from 0.76 ms to 1.24 ms.

B The distribution of IRI for 51 BS/T2 axons. The mean value for the IRI in these fibres was 1.25 ms and the values ranged from 1.05 ms to 1.50 ms.

INTER-RESPONSE INTERVALS

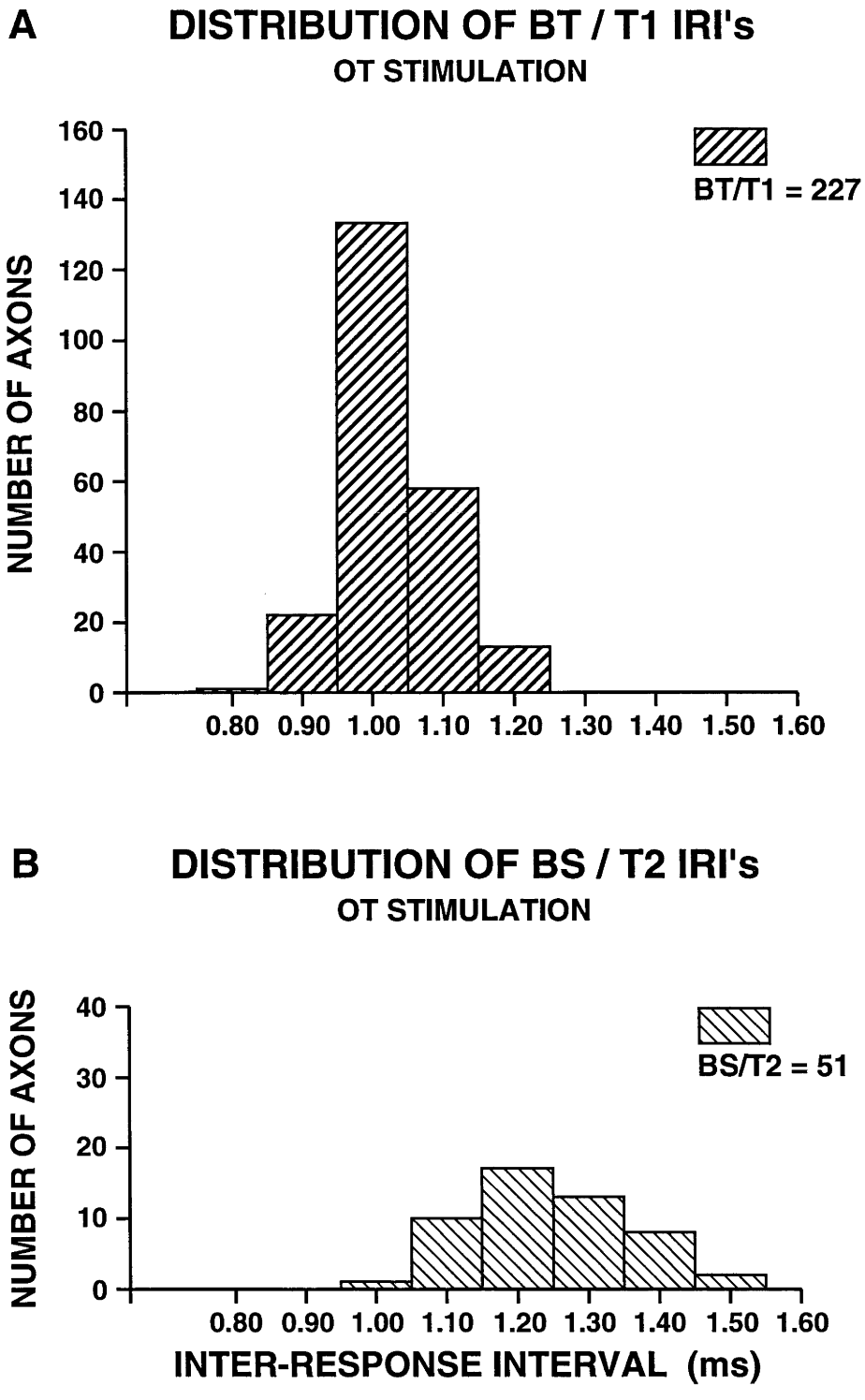

FIGURE 3.7 The increase in the latency of the second impulse versus the latency of the first.

Pairs of antidromic stimuli were applied in the optic tract at the minimum inter-stimulus interval (ISI) for 227 BT/T1 and 51 BS/T2 axons and the responses were recorded close to the optic disc margin. The latency of the first (unconditioned) impulse was subtracted from the latency of the second impulse. The difference between the two latencies was then plotted against the latency of the first impulse. It can be seen that the latency of the second impulse increased, relative to that of the first, with increasing latency of the first impulse.

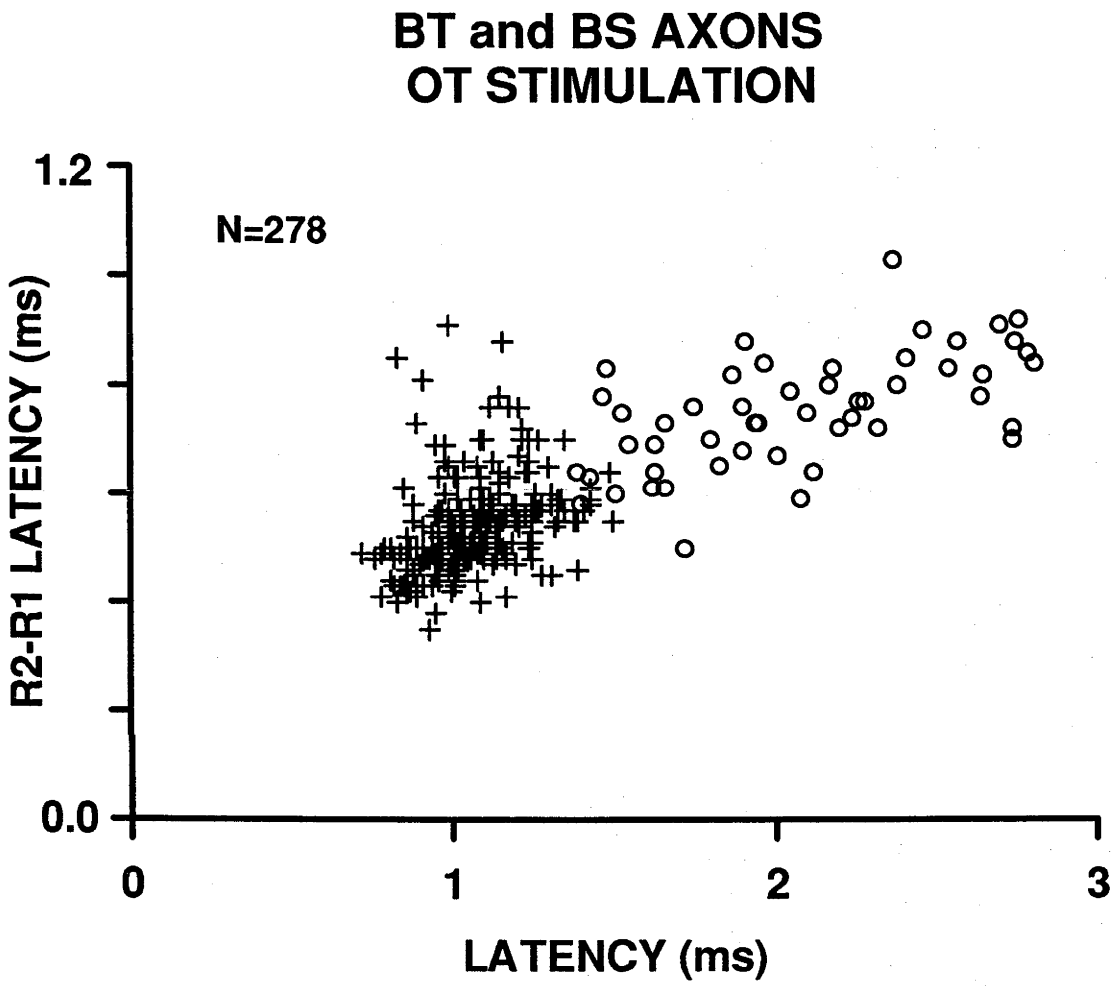
BT and BS AXONS
OT STIMULATION
N=278
1.2
0.0
R2-R1 LATENCY (ms)
0
1
2
3
LATENCY (ms)

From 0.50 ms to 3.00 ms latencies, the IRI continues to increase, but the rate at which the impulses are separating declines. This is caused by the decline in the degree of refractoriness that the second impulse encounters the further it is separated in time from the preceding impulse, allowing the gradual return to normal CV of the second impulse. If the second impulse reaches the same velocity as the first impulse, then the IRI values will be constant and form a plateau. From Fig. 3.8, it can be seen that even by the latency for the first impulse of 3.00 ms and an IRI of approximately 1.4 ms, a constant velocity of the second impulse has not been attained.

In order to estimate the time that the first impulse will have to travel before the IRI has increased sufficiently to allow the second impulse to achieve the velocity of the first impulse, a curve of the form $Y = k\ (1 - e^{-(t-t_0)/tau})$ was fitted, using a Nelder-Mead Simplex algorithm. In fitting a suitable curve it became clear that the IRI values at <0.60 ms produced a significant change to the shape of the curve (Fig. 3.9). Eliminating these points produced constant values for the asymptote, the Y and X intercepts and the time constant. The value of the asymptote for IRI is 1.65 ms.

In a small number of axons (Fig. 3.10), using a different experimental approach, the ISI in each axon was widened to as long as 4.5 ms and the latency of the second response was considered as a percentage of the latency of the first impulse. Consistent with the previous analysis, at an ISI equivalent to the asymptote, the latency of the second response is within 10% of the latency of the first response. In Fig 3.10, for these two representative cases, the second response had reached a latency equivalent to that of the first response, for ISIs >3.50 ms. The latency of the second response never fell below that of a single impulse. There was no evidence of speeding up of the velocity of the second impulse in the BT/T1 or BS/T2 fibre as would occur if the second impulse was initiated during a supernormal phase of the recovery cycle of the axonal membrane.

3.3.4 A third impulse.

In some instances a third stimulus was applied at the minimum interval required to produce a third response at the recording site. The interval between the second and third stimuli was consistently longer than the minimum interval between the first and second stimuli. As with the RPT, there was no demonstrable difference in the minimum ISI between the second and third stimuli for the BT/T1 fibres driven from

FIGURE 3.8 The inter-response interval versus latency.

Inter-response intervals recorded at the optic disc margin for 298 BT/T1 [+] and 63 BS/T2 [o] axons stimulated from either the optic tract, optic chiasm or optic nerve were plotted against their latency. A curve of the form $Y = k\,(1 - e^{-(t-t_0)/tau})$ was fitted to the data using a Nelder-Mead Simplex algorithm for non-linear equations. Seven BT/T1 axons [×] driven from the retrobulbar optic nerve and with very short latencies were not fitted to the curve. Stable values for the asymptote, the Y and X-intercepts, and the time-constant were obtained only after excluding these axons (Fig. 3.9).

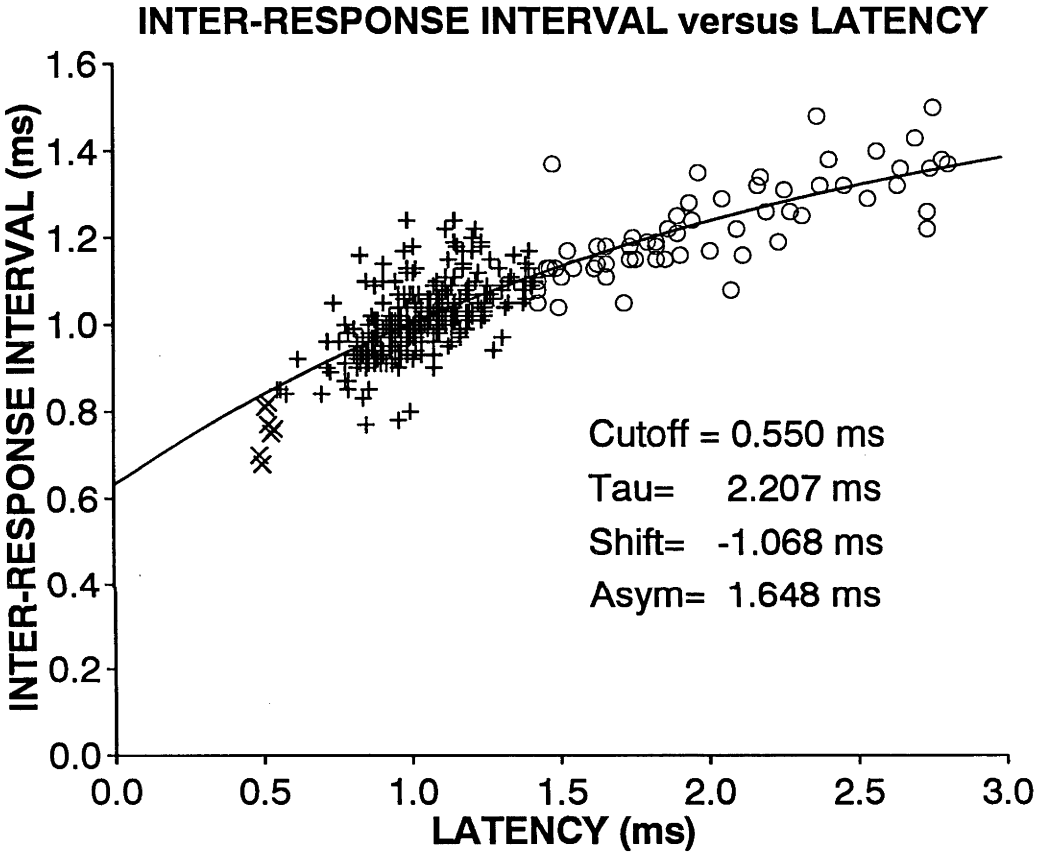
INTER-RESPONSE INTERVAL versus LATENCY
INTER-RESPONSE INTERVAL (ms)
1.6
1.4
1.2
1.0
0.8
0.6
0.4
0.2
0.0
0.0
0.5
1.0
1.5
2.0
2.5
3.0
LATENCY (ms)
Cutoff = 0.550 ms
Tau= 2.207 ms
Shift= -1.068 ms
Asym= 1.648 ms

FIGURE 3.9 The asymptote, the Y intercept, the X intercept and the time constants for the inter-response intervals versus latencies.

Values for the parameters of the equation $Y = k\ (1 - e^{-(t-t_0)/tau})$ fitted to the data in Figure 3.8 for different minimum cut-off latencies, to demonstrate the outlying nature of those data-points less than 0.55 ms. After the exclusion of those BT/T1 axons with latencies less than 0.55 ms, stable values for the parameters were obtained.

(a) The Y-intercept = 0.635 ms ± 0.002

(b) The asymptote = 1.655 ms ± 0.003

(c) The X-intercept = -1.083 ms ± 0.008

(d) Time constant = 2.239 ms ± 0.016

For those BT/T1 axons with latencies less than 0.55 ms, the first antidromic impulse was detected at the recording electrode very close to the time that the second impulse was applied. The factors governing the "IRI" at that point were: the refractory period generated by the first antidromic impulse, and the utilisation time for the second impulse. During this time the velocity of the second impulse was effectively zero.

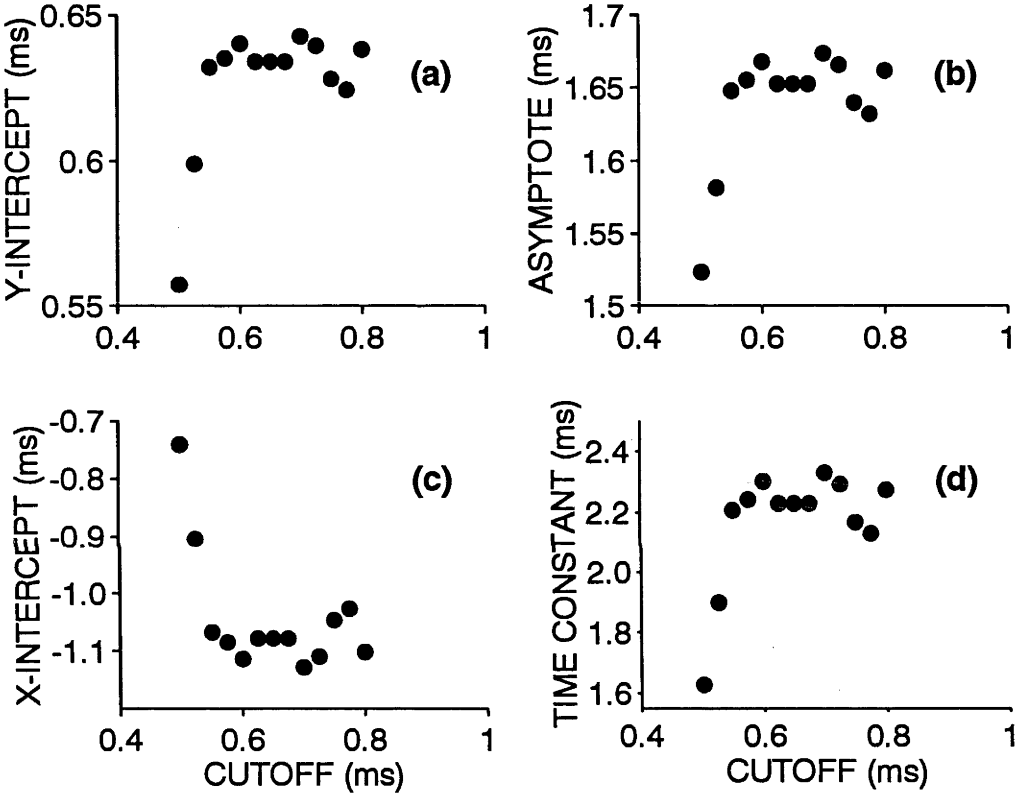
Y-INTERCEPT (ms)
0.65
0.6
0.55
0.4
0.6
0.8
1
(a)
ASYMPTOTE (ms)
1.7
1.65
1.6
1.55
1.5
(b)
X-INTERCEPT (ms)
-0.7
-0.8
-0.9
-1.0
-1.1
(c)
CUTOFF (ms)
TIME CONSTANT (ms)
2.4
2.2
2.0
1.8
1.6
(d)

FIGURE 3.10 The percentage increase in the latency of the second impulse versus the inter-stimulus interval.

Pairs of antidromic stimului were applied in the optic tract at progressively increasing intervals, from the minimum inter-stimulus interval (ISI) for each axon to a separation of 4.0 ms or more. For each ISI, the latency of the first (unconditioned) impulse, measured at the optic disc, was subtracted from that of the second impulse, to determine the increase in the latency of the second response. The increase in the latency of the second response was then plotted as a percentage of the latency of the first impulse against the ISI.

A Representative example of BT/T1 axons. The length of the ISI required for the latency of the second impulse to become the same as that of the first impulse, was 3.75 ms.

B Representative example of BS/T2 axons. The length of the ISI required for the latency of the second impulse to become the same as that of the first impulse, was 3.50 ms.

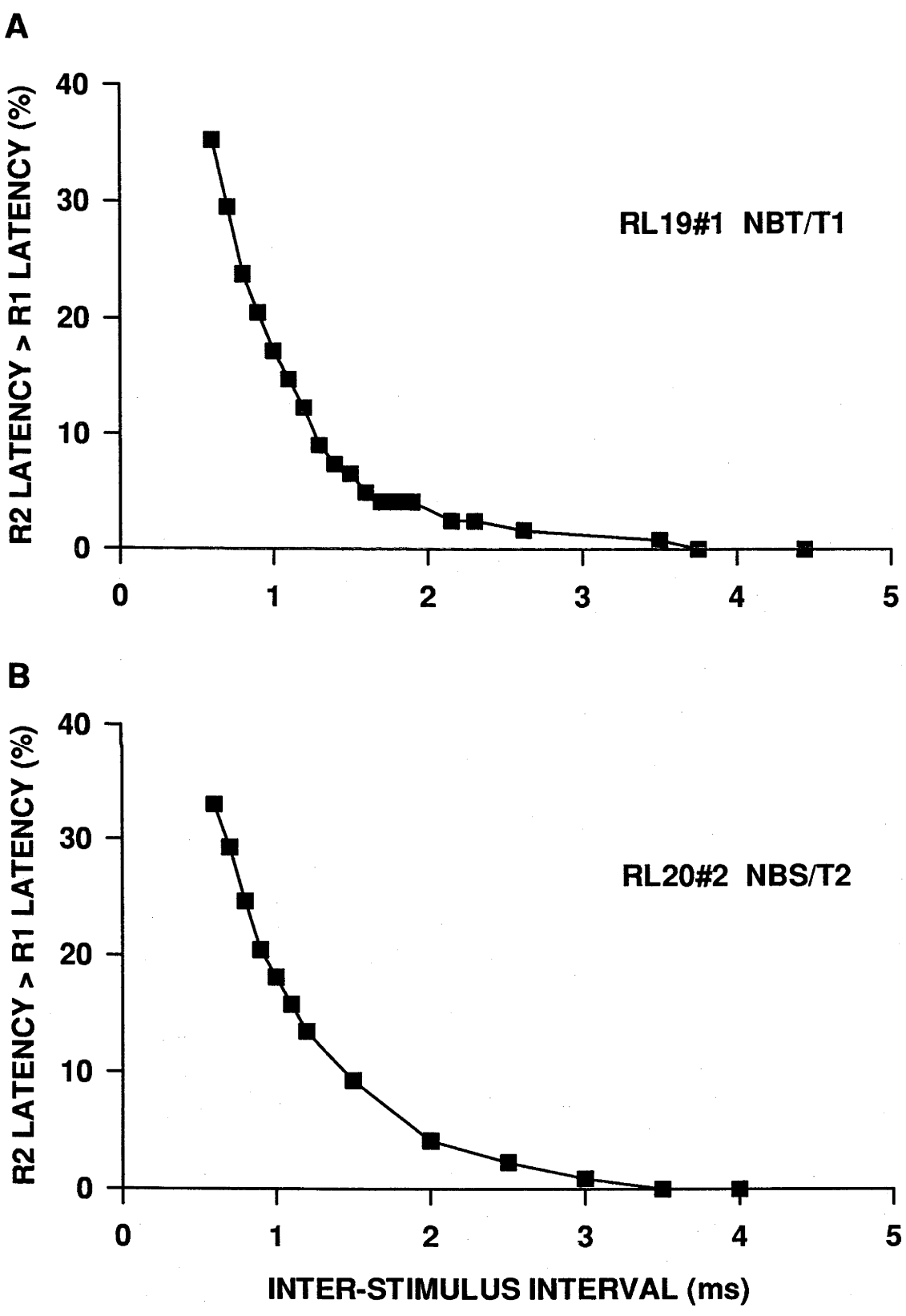
DIFFERENCE IN IMPULSE LATENCY VERSUS ISI
A
R2 LATENCY > R1 LATENCY (%)
40
30
20
10
0
RL19#1 NBT/T1
0
1
2
3
4
5
B
R2 LATENCY > R1 LATENCY (%)
40
30
20
10
0
RL20#2 NBS/T2
0
1
2
3
4
5
INTER-STIMULUS INTERVAL (ms)

either the OT and OX. The average minimum ISI for the 103 BT/T1 axons was 0.65 ms, ± 0.12. The small number of BS/T2 axons (18) had a similar minimum ISI to the third stimulus (0.65 ms, ± 0.06). However, there was a longer average minimum ISI between second and third stimuli when fibres were stimulated at the retrobulbar ON. The average ISI between the second and third stimuli in 14 BT/T1 axons was 0.70 ms, ± 0.13. This is an indication of a possible reduction in safety factor for conduction for the third impulse at the optic nerve heminode.

As previously mentioned in Chapter 1, p 28, the transition from myelinated to unmyelinated axon, as occurs for antidromic impulses in the optic pathway, may be a region of conduction vulnerability, particularly when the safety factor for conduction is further reduced by the passage of closely spaced impulses. However, the standard RPT test, even when initiated in the retrobulbar ON, failed to show any lengthening of the minimum ISI. It is of interest that in 5 fibres stimulated in the retrobulbar ON and recorded eccentric to the optic disc, some 2-2.5 mm from the optic disc margin but distant from their cell body, the average ISI between the second and third stimuli increased to 0.92 ms, ± 0.08. These fibres had RPTs within normal limits. This suggests that it was not just the point of transition from myelinated to unmyelinated axon that has reduced safety factor for conduction but that the length of unmyelinated axon in the retina will result in reduced safety factor for conduction when the fibre is made more refractory by the passage of two preceding impulses.

3.4 DISCUSSION

3.4.1 Refractoriness.

3.4.1a Refractory period and diameter of axons.

A study of ARP in the tract of the cat using CAPs, by Bishop et al., (1953), observed differences in the ARP of the T1 and T2 populations of optic axons that were only very slight. For T1 fibres, the average ARP was 0.47 ms (range 0.35-0.60) and 0.53 ms (range 0.40-0.70) for the T2 group. These observations are in good agreement with the results obtained in this study. The slightly longer average T2 ARP may be attributed to difficulties associated with visualising, at short ISIs, the

remnants of the second T2 response when it is embedded in the first broad T2 waveform. This difficulty does not apply to the narrower T1 waveforms, as can be seen in Fig. 4 of Bishop et al., (1953). In the rat, the ARP of the T1 population of axons averaged 0.40 ms and 0.59 for T2 fibres (Fox and Ruan, 1989). However, Fox and Ruan were unable to use the segregation of small fibres in the upper OT to isolate the T2 response as Bishop and colleagues had, resulting in a very complex picture from which to estimate the ARPs. It is also to be noted that the T2 catagory of rat RGC does not correlate to the BS/T2 class of RGC in the cat.

Paintal (1965) found that ARP varied inversely with the CV of the individual fibres of the vagus and saphenous nerves measured at 20^{o}C. He also noted that the inverse relationship between CV and ARP was insignificant for fibres whose CV exceeded 25-30 m/s. While the T1 fibres have CV in excess of this limit, the CV of T2 fibres is an average 20 m/s (Bishop et al., 1953) which is in agreement with the calculated distance/time ratio in Table 3.1b. Consideration of the idealised curve of the ARP-CV relationship in Fig. 11 Paintal (1966), suggests that, at normal physiological temperatures, the RPT of the BS/T2 axons would be almost double that of the BT/T1 axons. However, this study has established that the two classes of optic axons have the same RPT.

Paintal (1965) also found that in the majority of cases, the interval between the second and third stimuli was greater than the ARP. This coincides with the results obtained in this study. It has been suggested on the basis of computer modelling of impulse-conduction in amphibian myelinated axons (Khodorov and Timmin, 1975), that this occurs if at the time of applying the second impulse the axonal membrane has had insufficient time to return to threshold and as a consequence the rise time of the second impulse will be delayed. This would result in a longer time for the axonal membrane to recover to threshold after the second impulse and increase the minimum ISI before the third stimulus can be successfully applied. As with the measurement of ARP, Paintal also found that the minimum ISI between a second and third stimuli increased with decreasing CV. This was not the case in the BT/T1 and BS/T2 optic axons.

CV and refractory period can be simplistically differentiated. CV is influenced by axonal diameter, internodal length and myelin thickness which are longitudinal properties of the axon. However, the refractory period is determined by the time course of the process of recovery of the axonal membrane from the initiation and

passage of an impulse. Rushton (1951) proposed that axons possessing the same membrane properties, but with different diameters, should have similar refractory periods and the results of this study substantiate his theory. For refractoriness to vary with CV and therefore the diameter of axons, there would have to be appropriate progressive changes in the kinetics of Na^+ channels and/or the effectiveness and type of K^+ channels, which is unlikely in axons of the same type.

Possible changes in ionic channels that may decrease the rate of recovery in myelinated axons could include slowing the rate of recovery from inactivation of Na^+ channels or decreasing the large resting membrane K conductance so that the time constant for Na^+ channel inactivation is increased. Since there is a growing body of evidence to suggest that the resting membrane potential is contributed to by K^+ channels located in the internode of myelinated axons (Baker et al., 1987, Barrett and Barrett, 1982), it may be that alterations in the type and location of K^+ channels could affect the RPT. There are indications that changes in K conductance may occur in myelinated axons of different diameters (Smith and Schauf, 1981b, Fox and Ruan, 1989). The question remains as to whether changes are occurring systematically with reduction in the axonal diameter or if there is a critical limit in diameter beyond which such variations in structure must necessarily occur.

However, the tenet that ARP varies inversely with CV appears to have been widely accepted and it has even been suggested that the refractory period can assist in the electrophysiological identification of axons (Ranck, 1975). While some reports have confirmed the rule (Swadlow and Waxman, 1976, Swadlow et al., 1978, Moyano and Molina, 1980), others have encountered contradictory results (Hopf and Lowitzsch, 1973, Raymond and Lettvin, 1978, Foster et al., 1982, Duron et al., 1984, Horcholle-Bossavit et al., 1987). Early studies of ARP and CV, which have been quoted as supporting this tenet (Paintal, 1973), had in fact noted that the rate of change in ARP with the diameter of fibres, was not consistent across all sized fibres (Erlanger and Gasser, 1937, Hursh, 1939b, Paintal, 1965). A consistent feature does, however, emerge. The vast majority of studies that confirm that ARP is inversely proportional to CV and therefore the diameter of axons, appear to be testing ARP in axons that conduct impulses slowly. Conversely those studies which found that the tenet did not hold were examining fast axons.

So it may be that the inversely proportional relationship of CV to ARP only holds for those axons that conduct impulses at less than 20 to 15 m/sec and therefore

would have a diameter less than 3 μm. This may also provide an explanation for the findings of Fox and Ruan in rat optic axons (1989). The T1 fibres in their study had an average CV of 13.3 m/s and the T2 fibres, 6.2 m/s. However, their calculation of CV did not take into account the utilisation time and because the conduction distance was short, only 8-9 mm, it is possible that the velocities may have been approximately 15.5 m/s for the T1 fibres and 6.6 m/s for the T2 fibres. If this were the case, then their findings in rat optic axons would not be inconsistent with the suggestion that ARP only increases for axons with CV <15-20 m/s.

It has also been suggested that the larger diameter of BT/T1 optic axons may confer upon these axons an increased capacity to carry information because of a reduction in the refractory period which was said to occur with the increasing diameter of axons (Rowe, 1990). But as this study shows, if BT/T1 optic axons had a greater capacity to handle information, this cannot be based upon differences in refractoriness and would have to be attributed to other undetermined factors.

3.4.1b Refractory period and stimulus strength.

The minimum interval between two stimuli of threshold strength that produced two responses represents the end of the RRP for that axon. In reality this measurement was often difficult to make due to the persistent fluctuation of the effective ISI. This is not unexpected, as it has long been known that at threshold strength there is considerable variation in the length of the interval between the application of a stimulus and the appearance of a propagating impulse (Blair and Erlanger, 1933;1936, Hodler et al., 1952). Such variation in the time between the stimulus and the commencement of the first propagating response will cause the interval before a second stimulus can be successfully applied to also fluctuate. At stimulus strengths just above threshold, this fluctuation in RPT subsided. This rapid subsidence of fluctuations may also contribute to the initial rapid change in RPT with only a small increase in stimulus strength.

The smooth curve of the relation primarily reflects the state of the recovery process of the axon following the passage of the first or conditioning stimulus. Hodgkin and Huxley (1952) had found in the giant squid axon that there were two factors responsible for the inability of the axonal membrane to respond to a second stimulus following depolarisation of the membrane during the first action potential.

These were the inactivation of Na^+ channels and the delayed rise of K^+ conductance. In mammalian myelinated axons, however, a voltage dependent K^+ conductance at the node is almost nonexistent (Chiu et al., 1979).

The recovery of the myelinated axonal membrane is primarily due to the ending of the inactivation phase of the excitability cycle of the Na^+ channel and the ability to generate a second impulse is dependent upon a sufficient fraction of Na^+ channels having returned to the resting state. Inactivation is a time-dependent process, so early during recovery, the number of inactivated Na^+ channels is high, and therefore a greater than normal amount of current is required to recruit a high proportion of the few Na^+ channels available for activation. It follows that for a stimulus strength just above threshold, the temporal separation of the two stimuli must be greater than at the higher stimulus strengths, and as the strength of the stimulus is increased, the second stimulus can be applied with effect earlier in the relative refractory phase of the axon.

As previously discussed in Chapter 1, pp8-12, of this thesis, many studies have examined refractoriness in a variety of species and nervous systems. The interpretation of these findings is complicated by the question of the stimulus strength used to test ARP in these studies. Often, stimuli of 1.2 to 2 times threshold were employed (McDonald and Sears, 1970, Swadlow and Waxman, 1976, Duron et al., 1984) or the strength was not stated. The uncertainty in using a stimulus strength below the level that produces a definite minimum RPT is in making judgements about what is a normal or abnormal RPT for any axon, and in comparing RPTs from individual axons. It may be that some axons, in particular unmyelinated axons, but even peripheral myelinated axons or myelinated axons of very small diameter, may have different recovery dynamics to these central myelinated optic axons, and would therefore require a different level of stimulus strength above threshold to establish a minimum RPT. Before testing refractoriness in axons it is necessary to establish the appropriate level of stimulus strength to use. In these CNS myelinated axons of the cat it was established that a stimulus strength 3.7 times greater than the threshold for any BT/T1 or BS/T2 axon, would produce a reliable minimum RPT.

3.4.2 The latency of the second impulse.

It has long been known that a second impulse generated in the refractory period of a preceding impulse will travel more slowly than the first and that the reduction in velocity of the second response is exacerbated when the ISI was shortened (Gotch, 1910, Gasser and Erlanger, 1925). The velocity of the second impulse is not constant but is slowest at the start and gradually quickens as the distance from the stimulation site increases (Gasser and Erlanger, 1925, Tasaki, 1953, 1982). The slower conduction velocity of the second response will result in an increase in the spatial and temporal separation of the two impulses with increased conduction distance. After some distance it is expected that the CV of the second response will reach the normal rate for an unconditioned impulse. Tasaki, (1953) showed in a toad motor axon of 11 μm diameter that after 43 mm conduction distance the second of two impulses initiated 2 ms after the first was still 20% slower than the first impulse. It is therefore unlikely that over the maximum conduction distance of 30 mm in this study, the second impulse, even in the slow BS/T2 axons, would reach a constant velocity.

It has been shown that the delay in the latency of the second impulse as it transmits in close proximity to the first impulse, is a function of both refractoriness and conduction time. There are two implications of this for the BT/T1 and BS/T2 axons which have the same degree of refractoriness but different CV. The first is that in all BT/T1 and BS/T2 axons the second impulse will achieve a constant velocity, equal to that of the first impulse, at the same *conduction time* from the initiation of the first impulse. This is borne out in Fig. 3.10 where the latency of the second impulse, for both the BT/T1 and BS/T2 axons shown, achieves a velocity equal to the unconditioned impulse at an ISI of between 3.50 to 3.75 ms in both cases. This is in good agreement with Paintal's (1965) finding that a fibre with a CV of 84 m/s had the second impulse attain 95% of normal CV some 3 ms after the application of the first impulse. However, it is interesting to note that a fibre with a CV of 11 m/s needed an ISI of 5 ms before the CV of the second impulse was the same as the first, again indicating that axons of slow CV may have different kinetics of recovery to the faster axons. Secondly, because of differing CVs of these two classes of optic axons, the BS/T2 axons will achieve a constant velocity for the second impulse within a shorter *conduction distance* than in the BT/T1 axons.

There is no evidence of an increase in velocity of the second impulse as might be expected if it was travelling in the supernormal phase of the recovery cycle (Kocsis et

al., 1979), although supernormality might have been observed with a different experimental paradigm (Swadlow, 1978). However, it has been suggested that the effects of refractoriness persist for up to 3 ms after a preceding impulse in cat optic axons (George et al., 1984).

3.4.3 Refractoriness through regions of possible physiological vulnerability.

It is well known that an antidromic impulse can be delayed, even blocked at the junction of the axon and the perikaryon, in the region of the initial segment (Coombs et al., 1957a, b). This is due to the increase in the membrane area of the cell body which decreases membrane resistance and the cytoplasmic resistance and increases membrane capacitance. The amount of current generated in the optic axon close to the axon hillock may not be sufficient to excite the increase in area of the axon hillock and cell body when a second impulse attempts to excite a partially refractory perikaryon. In these circumstances it could be anticipated that the RPT recorded in cell bodies may be greater than in the axons, however, this was not the case in RGC driven from the OT.

This, however, can not discount the possibility of conduction vulnerability in the region of the axon hillock of RGC. Frequently when recording from a cell body, the waveform of the second antidromic impulse was observed to be fragmented: increases in the point of inflection during the initial positive phase of the waveform, or the development of a notch in the waveform at that point, and even loss of the later components of the waveform. These distortions of the extracellularly recorded waveform are not dissimilar to those changes observed in the intracellular waveform associated with the antidromic activation of spinal motoneurons (Coombs et al., 1957a) and have been attributed to conduction vulnerability for impulses travelling from the axon hillock into the cell body.

A possible explanation of not eliciting vulnerability with the standard two-stimuli test applied in the OT, lies in the increased spatial and temporal separation of the two impulses as they propagate away from the stimulus site in the OT due to the increased latency of the second impulse. This means that the interval between the two impulses when they reach the initial segment of the RGC may no longer be critical to test any additional refractoriness imposed by the increased area of the cell body.

Similarly, it might be anticipated that the transition of the optic axons from myelinated in the ON to unmyelinated in the retina could also impose a limitation on the transmission of two closely spaced antidromic impulses at the junction of the two segments, as the membrane resistance decreases and capacitance increases in the unmyelinated region. However, the possible reduction in safety factor and therefore increase in refractoriness may not be revealed by impulses generated in either the OT or OX because of the progressive separation of the impulses as they progress away from the stimulation site. By the time the impulses reached the optic disc margin they were separated by a minimum 0.80 ms. This serves to emphasise that in normal relatively homogeneous axons, the RPT is primarily a test for refractoriness at the stimulation site.

Nor was any conduction vulnerability revealed when the RPT was tested from the retrobulbar ON. However, although the number of axons tested from the ON is only small, it is possible that 3 closely spaced impulses generated close to the transition region did demonstrate some minor conduction vulnerability, as revealed by the greater minimum ISI between the second and third impulses when generated in the ON than those initiated in the OT or OX. When the 3 impulses are generated in the OT or OX, again they may not be able to elicit any such minor reduction in safety factor because of the increase in separation of the impulses by the time they reached the transition region of the ON. As previously discussed, because the second impulse is generated during the refractory phase of the first impulse, it may be that the axonal membrane, encountered by any subsequent impulses applied at a minimum ISI, is more refractory than after just one impulse. The question of possible vulnerability for conduction at the optic nerve heminode is addressed again in Chapter 4.

3.4.4 Conduction latency.

There is a strong correlation of BT RGC with the fast latency group T1 and BS RGC with the medium-slow, T2, group, but in this study there was some *overlap* of the latency distributions of the BT/T1 and BS/T2 axons when they are measured from the OT, and this overlap was not evident in the measurements of latency from the OX. Even when factors, which may differentially impact on latency measurements over varying conduction distances were accounted for in the modified distance to latency ratio, the BT/T1 latencies from the OT were still significantly different to those measured from the OX. While these results suggest changes in the

distance/latency ratio measured from the OT and OX, distance/latency ratios cannot give reliable estimates of CV in the myelinated portion of the optic pathway. In particular, it may not be valid to assume that factors which affect the measurement of latency, are consistent between individual optic fibres.

1. Length of unmyelinated axon.

The distance from the stimulation site in the contralateral OT to the back of eye is an average 30 mm. The majority of the axon included in the recording distance is myelinated. However, the axon is unmyelinated from the region of the lamina cribrosa forward to the recording electrode. The unmyelinated intraretinal portion of the optic axons is known to conduct impulses more slowly than the myelinated segment. Obviously variations in the length of unmyelinated axon included will have a comparatively large effect on the latency measured for any particular axon.

There are two possible sources of variation in the length of unmyelinated axon. The first is, that there is not a uniform point at which all optic axons become myelinated, rather they tend to progressively acquire myelin over a 0.5 mm portion of the cat optic nerve, posterior to the lamina cribrosa (Blunt et al., 1965). The second source of variation is the distance from the optic disc margin to the recording electrode. As the maximum distance from the optic disc margin to the recording electrode is estimated to be 0.5 mm, the greatest possible total variation between individual axons in the amount of unmyelinated axon was approximately 1.0 mm. If the slowest intra-retinal CV for a BT/T1 axon is as low as 2.9 m/s (Rowe, 1990) then this would add 0.34 ms to the latency of a BT/T1 axon. This could account for only part of the overlap of the slowest BT/T1 latencies with the fastest BS/T2 latencies. Further, the BT/T1 axons with the longest latencies were not those axons recorded at the maximum distance from the optic disc margin, so some other factors must also variably impact on the conduction time.

2. The utilisation time.

The utilisation time interval will change with the distance of the anode of the stimulating electrode from the nearest node in the axon being tested (Hodler et al., 1952). This may vary at different stimulation sites and even between individual axons driven from the one stimulation site. The significance of this interval, probably between 0.1-0.2 ms in duration (see Chapter 4), in the overall measurement of latency will obviously increase with reduced conduction distance.

3 Axons with far peripheral receptive fields.

Finally it has been observed during the course of this study that axons with very long latencies appear to have a characteristic in common. Of the thirteen BT/T1 axons, stimulated in the OT and with latencies in excess of 1.35 ms, eleven had receptive fields located in what could be designated as the far periphery of the visual field, that is, their receptive fields were located off the tangent screen normally used to record the location of the receptive field. No systematic analysis of this observation was made during the experimental phase of this study and the significance of this observation is unclear.

When the CV in the myelinated portion of the optic pathway could be reliably measured in the one animal with OT, OX and ON stimulating electrodes, then heterogeneous changes in BT/T1 fibre's CV were observed from the ON to the OT. While definite conclusions could not be drawn from the small number BS/T2 fibres observed, the few examples seen suggest that the CV of BS/T2 fibres does not change between the ON and tract. Both these results agree with the observations made for the BT/T1 and BS/T2 axons when the utilisation time and unmyelinated segment were accounted for and the modified ratio of distance to latency was calculated (Table 1.b.). Baker and Stryker (1990) also found the changes in CV in the OT were not as marked for the BS/T2 fibres as for the BT/T1 fibres.

The increases in CV that occur in the BT/T1 fibres in the OT, were of a greater magnitude than the decreases observed. This would explain why whole nerve studies reveal an overall increase in CV in the OT. Bishop et al., (1953) had calculated for the large diameter axons in the cat OT that the ratio of CV (m/s) to axonal diameter (μm) was 8.2. The fastest BT/T1 CV in the OT in this study was 139 m/s which theoretically would require an axon 17 μm in diameter to transmit impulses at that velocity. While the majority of studies of the diameter of optic fibres have been performed in the ON, where the maximum diameter is in the region of 10-12 μm, fibres of larger diameter (15μm) have been reported in the OT (Freeman, 1978) and BT/T1 fibres with CV in excess of 120 m/s have also been previously reported (Fig. 9.b, Cleland and Levick, 1974a).

The observations of different CVs for BT/T1 fibres between the OT and ON made in this study of the cat confirm Baker and Stryker's finding of changes of CV in the OT of the ferret. By examining single axons, it is possible to suggest that there

are both increases and decreases of CV in the OT compared to the ON. These observations require further experiments to determine the pattern of CV changes for T2 fibres and to determine if there is any systematic change in optic tract CV consistent perhaps with the location of the RGC cell body within the retina. It may be that these heterogeneous changes of CV in the OT are providing some temporal compensation for differences in the lengths of the RGC axons across the retina.

3.4.5 Summary

1) The RPTs of BT/T1 and BS/T2 optic fibres in the cat appear to be the same, while the CV of BT/T1 fibres is approximately double that of the BS/T2 fibres. This does not fit with the widely held view (Paintal, 1965, 1966) that the ARP increases in proportion to the CV of a fibre.

2) An examination of the literature, and data from the non-brisk/T3 fibres in this study, suggests that an increase in refractoriness may occur for fibres whose CV is less than 15-20 m/s.

3) The CVs of BT/T1 optic fibres may vary between the optic nerve and the tract, with increases in CV in the tract predominating.

4) The slowing of the second of two closely spaced impulses is determined by the length of time that the second impulse has travelled in the wake of the preceding impulse, and not directly by the distance travelled.

5) Conduction vulnerability at the optic nerve heminode could only be demonstrated by the application of three closely spaced impulses, stimulated from the retrobulbar ON.

CHAPTER 4
FURTHER INVESTIGATIONS OF REFRACTORINESS IN NORMAL OPTIC AXONS: THE COLLISION PARADIGM.

4.1 INTRODUCTION.

In a homogeneous axon, security of conduction is ensured by a five-fold margin of safety factor for conduction (Tasaki, 1953, p 44, 1955). However, heterogeneity in axonal structure can cause changes in axonal cable properties. This may then result in changes in the conduction properties of the axon and reduction in the safety factor for conduction. Points of physiological conduction vulnerability may occur where an axon experiences an increase in membrane area such as at the branching of an axon (Dun, 1955, Krnjevic and Miledi, 1959) or when an antidromic impulse attempts to propagate into the axon hillock-soma region (Coombs et al., 1957a & b).

Another site of possible conduction vulnerability is the transition of an axon from being myelinated to unmyelinated, such as occurs in the preterminal region of motor nerve fibres (Katz and Miledi, 1965). The reduction in safety factor for conduction is due to impedance mismatch caused largely by the increased membrane capacitance and conductance of the increased membrane area or of the unmyelinated segment. Mammalian optic axons are myelinated extraocularly but are usually unmyelinated in the retina. The transition zone for myelination is located behind the lamina cribrosa in the retrobulbar ON and the junction of the myelinated and unmyelinated portions of the axon forms the ON heminode. For antidromic impulses, the ON heminode may be a region of conduction vulnerability, particularly if the margin of safety factor is further reduced by a closely preceding impulse.

While the standard two stimuli RPT test is arguably the single most effective means of assessing the security of conduction of multiple impulses along a length of nerve or axon (Smith et al, 1981) it cannot ascertain the spatial location of a region of heterogeneity. In particular, it is not possible to determine whether the axon between some region of conduction vulnerability and the stimulus site has normal conduction properties.

By utilising the collision of an orthodromic and the first of two antidromic impulses, it is possible to limit the length of axon that will be tested by the conduction of the two closely spaced antidromic impulses. If a region of conduction vulnerability is revealed by an increase in the standard RPT, then when collision is timed to occur before the antidromic impulses reach the region of reduced safety factor, a shortened RPT measure will indicate that the axon upstream from the region of conduction vulnerability has normal conduction properties.

This chapter introduces the collision paradigm as a technique for examining the spatial location of a region of conduction vulnerability. Previously, collision tests have been used to confirm antidromic activation (Bishop et al., 1962b) and branching of axons. Swadlow (1982) has used the technique to measure the refractory period close to the site of electrical stimulation. In this study, collision of impulses has been used to investigate the heminode in the cat ON as a possible region of reduced safety factor for conduction, while obviating the invasive insertion of multiple or moveable electrodes in a pathway not amenable to such methods. In Chapter 6 this paradigm is used to examine focal demyelinating and pressure lesions in the retrobulbar ON.

4.2 METHOD.

The paradigm as used in these experiments is described in detail in Chapter 2, pp 73-74. At a variable delay (D1) after a spontaneously occurring orthodromic impulse (O) is detected at the recording site in the retina, two electrically generated stimuli (S1 and S2) are applied to the optic pathway. If the D1 interval is less than the conduction time from the stimulus to the recording site, the first antidromic response and the orthodromic impulse will collide and each will be abolished. If the interval between the two antidromic stimuli (D2) exceeds the maximum RPT of the axon up to and including the location of the collision, the second antidromic impulse will then be transmitted beyond the collision point and be detected at the recording site. When the D1 interval is zero (application of first antidromic stimulus coinciding with detection of the orthodromic impulse), the two impulses will collide at the mid-time point for conduction (MTP). Increasing D1 will progressively shift the collision location towards the stimulus site. The minimum inter-stimulus interval (ISI), or D2 measurement, is established for each D1

interval, which generates a graph which can be interpreted as the regional RPT (rRPT) over progressively shorter regions of the axon, from the MTP back towards the stimulus site.

4.3 RESULTS.

4.3.1 The space time diagram.

To explain the complex interplay of the orthodromic and antidromic impulses in the D2 versus D1 graphs, space-time diagrams (Fig. 4.2) have been introduced to illustrate events in the collision paradigms (Fig. 4.1). The Y axis is the spatial axis (mm) and represents the distance along the axon from the stimulus electrode located at the origin to the recording electrode, at the top of the axis. The X axis is the temporal axis and represents elapsed time (ms), with zero denoting the time at which the orthodromic impulse is detected at the recording electrode, as it spontaneously arises from the maintained discharge of the RGC. The timing of subsequent events at the stimulus site, such as application of electrical stimuli and arrival of orthodromic impulses, are marked out along this axis.

The linear trajectory of the orthodromic impulse (ORTHO) descends to the right from the top of the Y axis and would, in the absence of collision with an antidromic impulse, intersect the X axis at a point equivalent to the orthodromic conduction latency. The trajectory of the first antidromic impulse (S1) ascends to the right from a point on the X axis that marks the time at which the stimulus was applied (A1). The area to the right of the trajectories of ORTHO and S1, bordered by the dashed line, represents the refractoriness associated with each impulse. During this time, a second impulse (A2) cannot be launched or travel due to the refractory nature of the axolemma.

It can be seen that if A1 is applied at the same time that the orthodromic impulse is detected, the orthodromic and antidromic impulses will necessarily collide at the MTP (Fig 4.2a). The second impulse (S2), which has been successfully applied the end of the refractory period associated with S1, will continue to propagate past the collision site.

FIGURE 4.1 D2 versus D1 graphs

Three representative collision paradigms from normal BT/T1 axons (A, B, C). The graphs are a plot of the D1 interval (the time elapsed from the detection of the orthodromic impulse to the application of the first antidromic stimulus) versus the D2 interval (the minimum inter-stimulus interval or regional refractory period of transmission). The horizontal dashed line corresponds to the value of the standard refractory period of transmission (RPT). The vertical dotted line represents the D1 interval at which the antidromic impulse no longer collides with the orthodromic impulse, ie the orthodromic impulse has passed the stimulus site and its associated refractoriness has subsided, allowing the successful transmission of both antidromic impulses. For longer D1 intervals the antidromic impulses remained collision-free. The oblique dotted line is the idealised ramp with a slope of -1. The intersection of the horizontal plateau with the ordinate axis (D1 = 0) identifies the mid-time point for collision along the axon.

A D2 versus D1 graph with a ramp of a slope = -1.

B D2 versus D1 graph with a decelerating ramp.

C D2 versus D1 graph with an accelerating ramp.

D Shows the characteristic features of the D2 versus D1 graphs: the plateau, ramp, the collision-free D1 interval and the post-collision-free plateau.

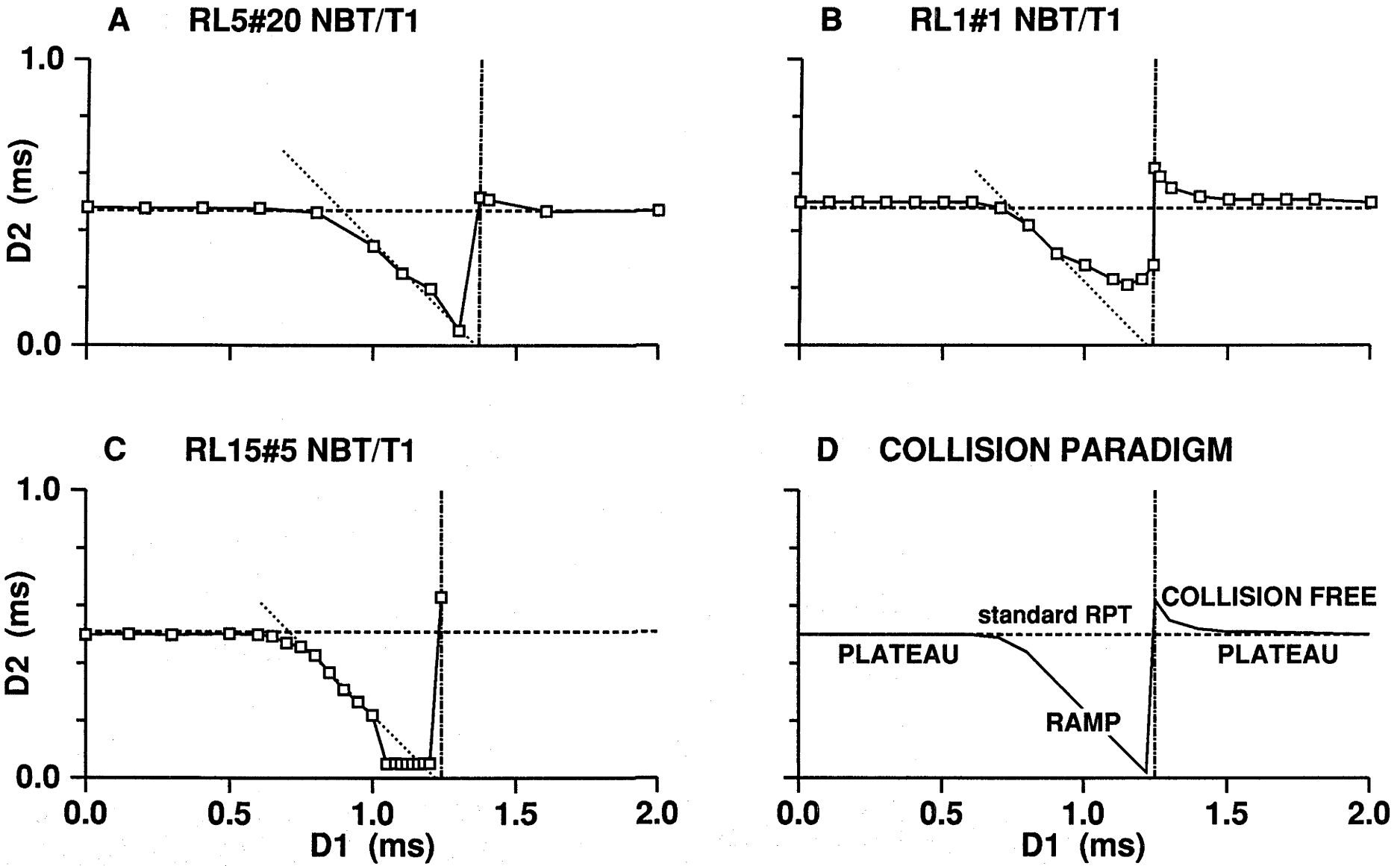
A RL5#20 NBT/T1
B RL1#1 NBT/T1
C RL15#5 NBT/T1
D COLLISION PARADIGM
1.0
0.0
D2 (ms)
0.0
0.5
1.0
1.5
2.0
D1 (ms)
standard RPT
COLLISION FREE
PLATEAU
PLATEAU
RAMP

From there on it will encounter axon in a progressively lessening refractory state, and will proceed through any potential regions of conduction vulnerability, unhindered by any increased refractoriness that would have existed if S1 were still preceding S2. The arrival time of the second impulse at the recording site (R2), is shown on the second horizontal axis at the top of the diagram which is used to indicate timing of events at the recording site.

The space-time representation of, provides a useful framework for the interpretation of the various features of the D2 versus D1 graph. The use of straight line approximations of impulse trajectory leads to a simple geometric understanding of events and gives a convenient representation of the collision of impulses. It also has the advantages of showing refractoriness in space as well as time and providing a simple rule for the successful transmission of A2.

Representing impulse trajectories by straight lines, assumes that CV is constant and equal for both the orthodromic and antidromic impulses. It is acknowledged that this clearly ignores some known factors that can cause variations in orthodromic and antidromic conduction times. These include utilisation time (Fuller and Schlag, 1976), acceleration of impulses approaching collision (Tasaki, 1949), possible delay of the antidromic impulse at the ON heminode and that caused by the positioning of the Schmitt trigger level above the noise level on the initial phase of the orthodromic impulse, to enable consistent timing between it and the application of the antidromic stimuli. Similarly, changes in CV which may cause the MTP of conduction not to coincide with the mid-distance, such as possible alterations in CV within the OT (Baker and Stryker, 1990, Table 3.1, p79) and the effect of slowed CV in the unmyelinated segment at the beginning of the conduction time of the orthodromic impulse, are also disregarded as of little relevance for recordings made at the OD margin, though the latter factor has greater relevance to recordings made in the peripheral retina. Finally, the slowing of the second antidromic impulse in the relative refractory wake of the first impulse is not accounted for in this simplified description of events. Despite these caveats, the space-time diagrams are a useful tool for the understanding the complexities of the collision paradigm.

FIGURE 4.2 The space-time diagrams.

The construction of the space-time diagrams for the analysis of the D2 versus D1 graphs is described in detail in the text. Each diagram explains the main features of the graphs as shown in figure 4.1d, p 110. The values used, such as latency and refractory period of transmission, are representative of a BT/T1 axon stimulated by an optic tract electrode.

A D1 = 0, the plateau. Collision between the orthodromic (ortho) and first antidromic (A1) impulses occurs at the mid-time point. The limiting boundary for the passage of second antidromic impulse (A2) is the refractoriness generated by A1 up to the point of collision.

B D1 intervals between 1.0 and 1.4 ms, the ramp. When the first stimulus is applied after the arrival of the orthodromic impulse at the stimulus site and while refractoriness associated with O persists at the stimulus site, then A1 can not be launched. The limiting boundary for the transmission of A2 is the ending of the refractoriness, associated with the passage of the orthodromic impulse past the stimulus site.

C D1 = 1.5 ms, the elevated D2 value at the collision-free D1. It can be seen that when A1 can first be launched after the ending of refractoriness at the stimulus site, A1 is in effect the second impulse in close sequence. The timing for A2 is therefore limited by the greater refractoriness between a second and third impulse.

D D1 interval = 1.7 ms, the post-collision plateau. When the time between the orthodromic and A1 impulses is sufficient for the RPT of A1 to be unaffected, the limiting boundary will be the refractoriness generated by A1.

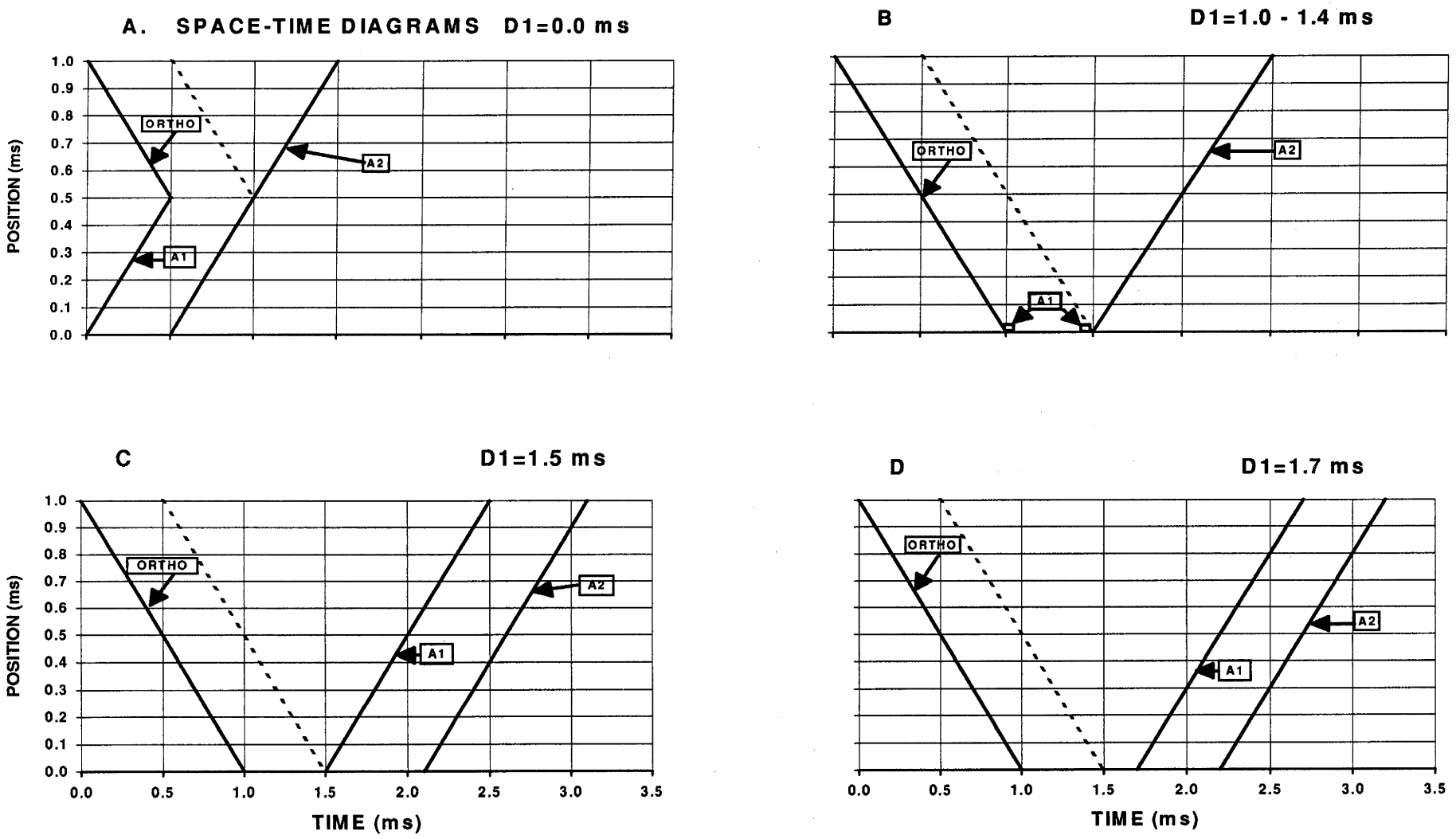
A. SPACE-TIME DIAGRAMS D1=0.0 ms
B
D1=1.0 - 1.4 ms
C
D1=1.5 ms
D
D1=1.7 ms
POSITION (ms)
TIME (ms)
ORTHO
A1
A2
0.0
0.1
0.2
0.3
0.4
0.5
0.6
0.7
0.8
0.9
1.0
0.5
1.0
1.5
2.0
2.5
3.0
3.5

4.3.2 Regional RPT in axons recorded at the optic disc.

Fig. 4.1 shows three representative D2 versus D1 graphs. Fig. 4.1d describes the four characteristic features of these graphs: the plateau, the ramp, the elevated collision-free D2 value and the post-collision plateau.

I The plateau.

In the D2 vs D1 graphs, the plateau is formed by constant D2 values for settings of D1 delays from zero to a D1 value approximately equal to the orthodromic conduction latency. This horizontal plateau was a consistent feature of all 42 BT/T1 and BS/T2 optic fibres tested from the OT. The difference between the height of the horizontal plateau and the standard RPT was on average 0.00, ± 0.02 ms and the maximum difference in any axon was 0.06 ms (Fig. 4.3).

It can be seen from the space-time diagram (Fig 4.2a) that the successful launch of S2 is dependent upon the ending of the refractory period generated by S1. In these circumstances, the D2 interval is independent of the timing of D1, if there are no points of conduction vulnerability between the MTP and the stimulus site. That is, the D2 measures remain constant for collisions as they approach the stimulus site. This forms the horizontal plateau.

In those rRPT graphs where sufficient data points were collected, the end of the plateau (designated the "shoulder") appeared rounded (see Discussion in this chapter). In these circumstances, the shoulder was defined as the intersection of a line corresponding to the average plateau height and a line of slope -1, which was fitted by eye to the upper portion of the ramps (Fig. 4.1a-c).

The shoulder was thought to commence when the orthodromic impulse reached the stimulus site (see next section for further explanation). The duration of the plateau should therefore be equivalent to the conduction time, from the recording electrode to the stimulus site, for the orthodromic impulse. The duration of the plateau was always shorter than the measured antidromic latency for each axon (Fig. 4.4). The straight line of best fit through the points on the graph (latency = 0.97 x the time to shoulder + 0.29

FIGURE 4.3 The differences between the standard refractory period of transmission and the height of the plateau in the D2 versus D1 graphs.

The height of the horizontal plateau measured from the D2 versus D1 graphs was subtracted from the standard two-stimulus test for the refractory period of transmission (RPT) in 41 BT/T1 and BS/T2 axons. The difference between the two measures is plotted for each axon.

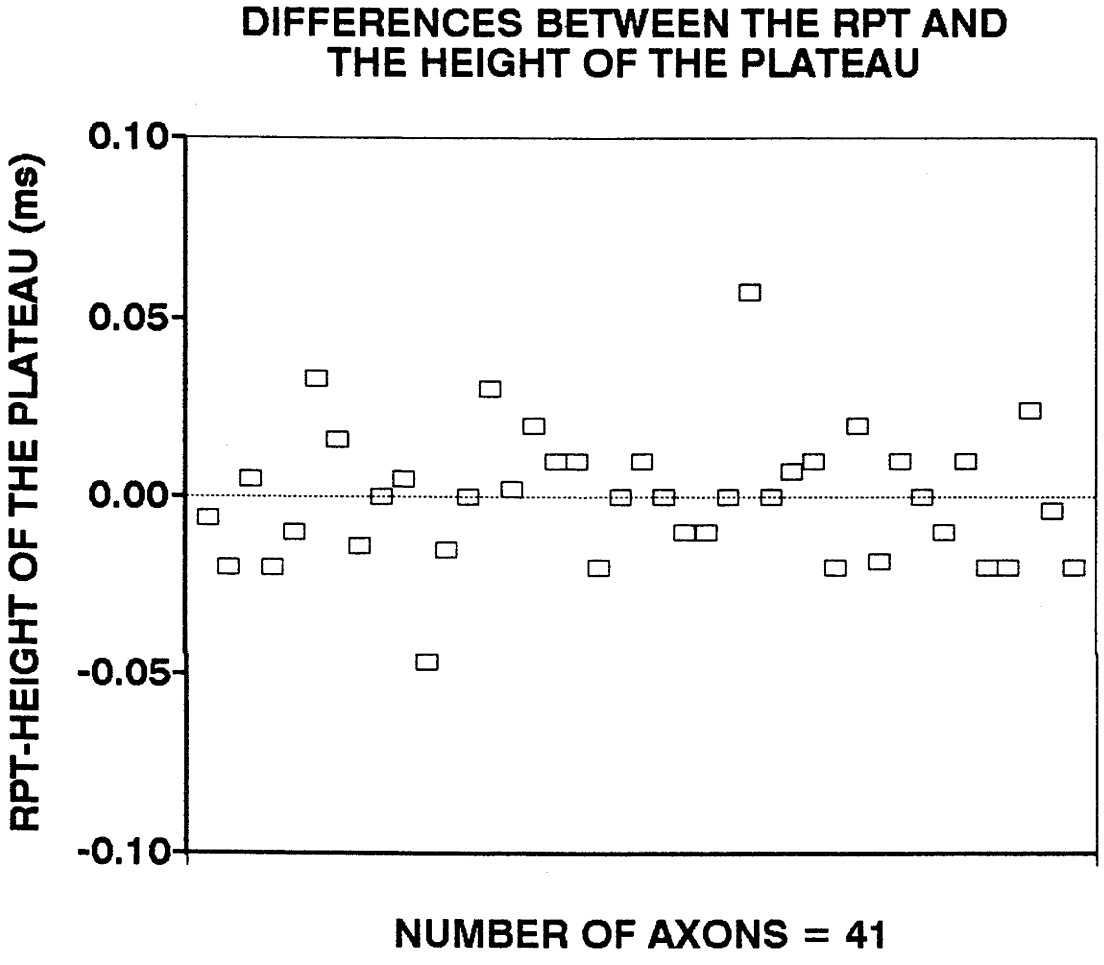
DIFFERENCES BETWEEN THE RPT AND
THE HEIGHT OF THE PLATEAU
RPT-HEIGHT OF THE PLATEAU (ms)
0.10
0.05
0.00
-0.05
-0.10
NUMBER OF AXONS = 41

FIGURE 4.4 Latency versus the D1 interval to the shoulder of the D2 versus D1 graph.

The latency of each axon, stimulated in the optic tract and recorded at the optic disc margin was plotted against the D1 interval that coincided with the shoulder, ie the end of the plateau and the commencement of the ramp, in the D2 versus D1 graphs. A straight line of best fit was drawn through the data-points. The Y intercept was 0.29 ms..

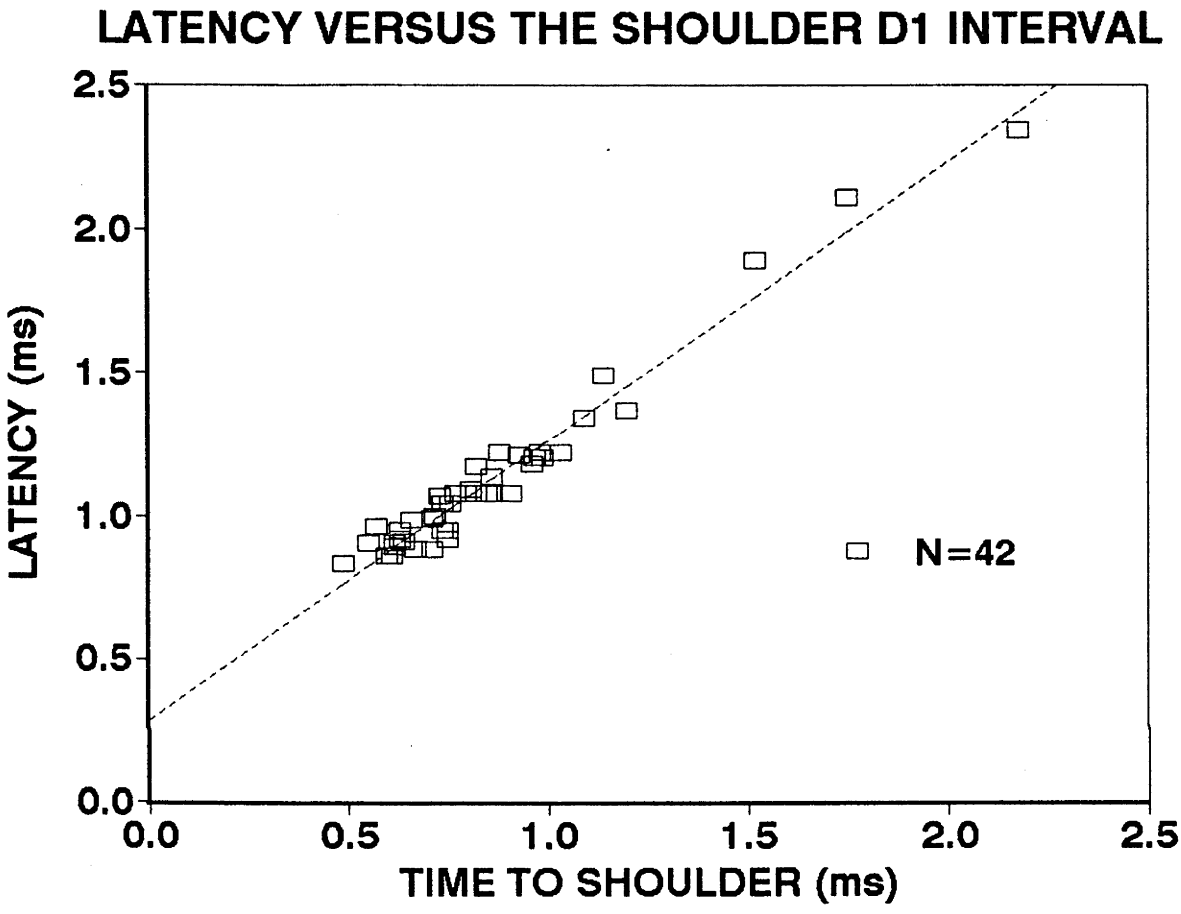
LATENCY VERSUS THE SHOULDER D1 INTERVAL
LATENCY (ms)
2.5
2.0
1.5
1.0
0.5
0.0
0.0
0.5
1.0
1.5
2.0
2.5
TIME TO SHOULDER (ms)
N=42

ms) intersects the Y axis at 0.29 ms which is nearly equal to the average of the difference between the antidromic latency and the D1 value at the shoulder for each axon (0.27 ms, ± 0.06).

II The ramp.

The next feature is the descending ramp of D2 values. It was observed that the upper portion of the ramp appeared to fit a slope of -1. The width of the ramp was in good agreement with both the standard antidromic RPT and the height of the first plateau, varying from both these values by a maximum of only 0.10 ms (average 0.03 ms).

Using the space-time diagram (Fig. 4.2b.) it can be seen that if S1 is applied at a D1 interval that coincides with the arrival of the orthodromic impulse at the stimulus site, A1 will not be generated. However, A2 will be successfully launched at the end of the refractory period of the orthodromic impulse at the stimulus site. As the D1 interval is increased, A1 is still unsuccessful in generating an impulse and the timing of the successful launch of A2 will continue to be determined by the ending of refractoriness of the orthodromic impulse. Because all timing is referenced to the detection of the orthodromic impulse at the recording site, the end of the orthodromic refractory period at the stimulus site will also occur at a constant position on the space-time diagram. It follows that the launch of a successful A2 must also be at a constant position and in these circumstances, the time to the launching of A2 will remain a constant (D1 + D2) and the expected profile of the ramp would be a slope of -1, as was seen in the experimental data.

That the profile of the upper ramp was being determined by events associated with the passage of the orthodromic impulse was confirmed experimentally by disconnecting the circuit which generates S1. The D2 values, without S1 in place, closely match the placement and slope of the upper portion of the ramp (Fig. 4.5.). Because this part of the ramp occurs at D1 values approximately equal to and greater than the antidromic latency and because of the explanations given and experimentally confirmed for the slope of the upper part of the ramp, it is reasonable to infer that the D2 measurements in this region are associated with refractoriness at the stimulus site, generated by the orthodromic

FIGURE 4.5 D2 versus D1 graphs. Various ramp profiles.

The ramps of the D2 versus D1 graphs were observed to have a variety of profiles in addition to a ramp with a slope of -1. To confirm the explanations for these differing ramp profiles, the D2 interval was measured both with (S1 on) and without (S1 off) the first stimulus connected.

A A ramp with a decelerating slope. When S1 was disconnected, the D2 values formed a ramp with a slope of -1. As was occasionally observed in decelerating ramps, there are two separate D2 values measured just before the collision-free D1 interval.

B A ramp with an accelerating slope. In this example the D2 values abruptly descended to 0.05 ms and persisted at that level for some 0.20 ms. When S1 was disconnected, the D2 values again formed a ramp with a slope of -1.

C Less frequently a D2 versus D1 graph was seen with a decelerating ramp of D2 values and a series of separate very short D2 values. When S1 was disconnected, these short D2 values can be seen to coincide with the D2 values obtained when S1 is absent.

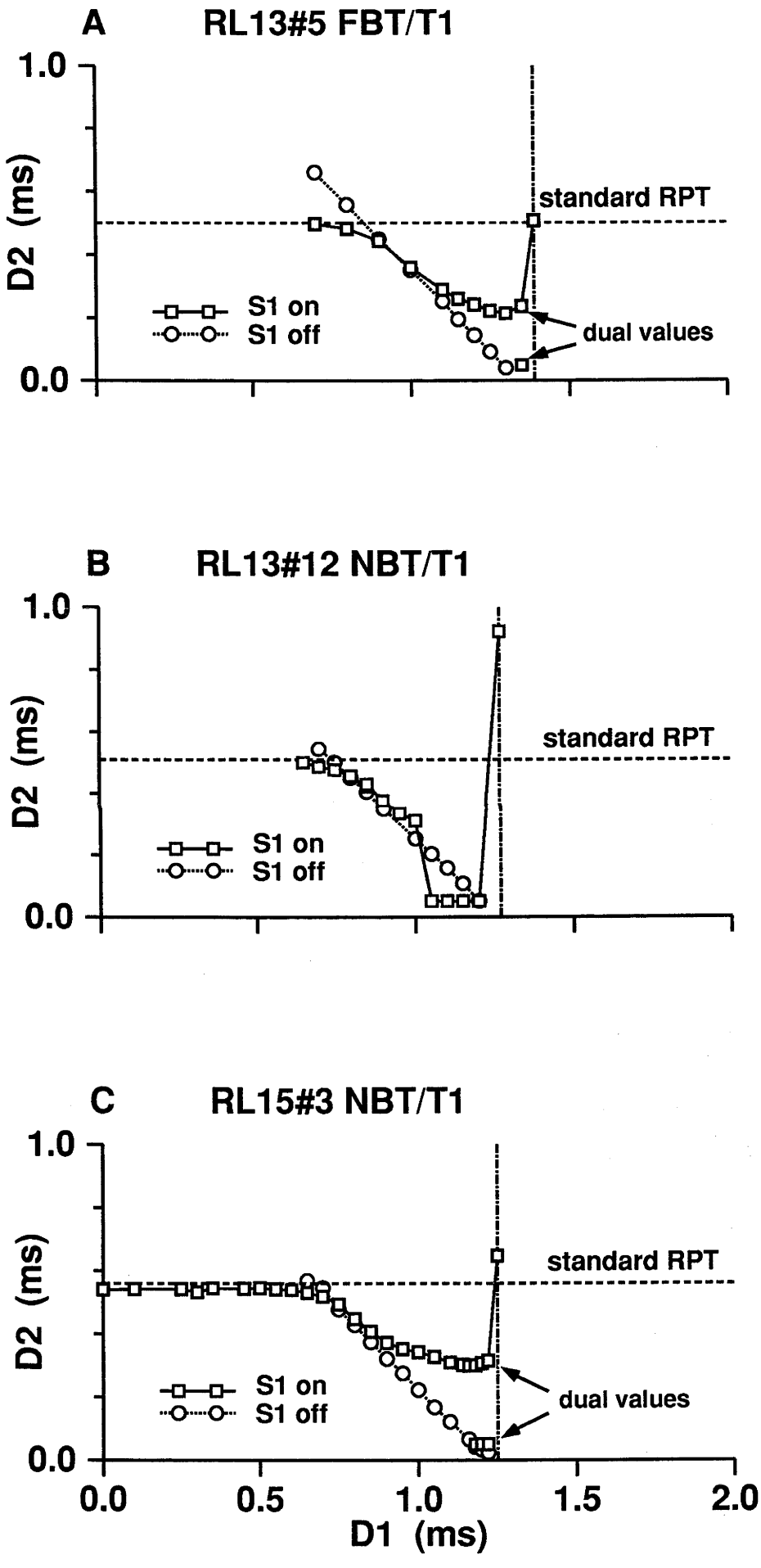
A
RL13#5 FBT/T1
1.0
0.0
D2 (ms)
standard RPT
S1 on
S1 off
dual values
B
RL13#12 NBT/T1
1.0
0.0
D2 (ms)
standard RPT
S1 on
S1 off
C
RL15#3 NBT/T1
1.0
0.0
D2 (ms)
standard RPT
S1 on
S1 off
dual values
0.0
0.5
1.0
1.5
2.0
D1 (ms)

impulse. The shoulder D1 value, being the earliest D1 value on the idealised ramp, therefore corresponds with the arrival of the orthodromic impulse at the stimulus site. From this D1 value, the orthodromic conduction latency can be inferred.

The ramp commences when the orthodromic impulse reaches the stimulus site. The ramp terminates when the D1 interval is sufficiently lengthened so that A1 is applied at a time beyond the sum of the orthodromic latency and the associated refractoriness at the stimulus site. A1 will then be able to generate a propagating impulse (Fig 4.2c). The D2 interval will then again be determined by refractoriness associated with S1. From the space-time diagram, it can be seen that the width of the ramp should be equivalent to the duration of the refractory period of the orthodromic impulse at the stimulus site. Because the mechanism which generates refractoriness is determined by the kinetics of ion channels and axonal structure, at any point along the axon, the refractory phase following an impulse should be of the same duration, irrespective of the direction the impulse was travelling in. As the standard RPT, in a normal axon, is primarily determined by refractoriness at the stimulus site, it can be anticipated that the standard RPT would be equivalent to the width of the ramp, as it indeed was.

The profile of the lower part of the ramps varied. A straight ramp, with D2 measurements gradually shortening to very small values, and with a constant slope of -1 occurred in 13 of the 42 units examined (Fig. 4.1b). In another 24 units, the lower D2 values remained longer, creating a more positive slope, so that the ramp appears to be decelerating (Fig. 4.1b). Some of these decelerating ramps also had a brief period just before the end of the ramp when the D2 value plunged below 0.10 ms and frequently two D2 values could be found for the one D1 interval (Fig. 4.5a &,c). In the remaining 5 cases the slope was more negative and the ramp appears to accelerate and then form a short plateau of D2 values between 0.02 to 0.10 ms (Fig. 4.1c, 4.5b). This originally appeared to suggest that a second region of lower rRPT had been detected. But D2 values of less than 0.1 ms are difficult to reconcile with the known kinetics of the recovery processes of normal axonal membrane. A more likely explanation of these variations is made in the Discussion.

III The post-collision D2.

The ramp is terminated with the appearance at the recording site of two impulses. The recording of R1, establishes that A1 is no longer colliding with O. At this time there is also a sharp increase in the D2 measure. This can only occur when the stimuli are applied at a sufficiently long delay after the detection of the orthodromic impulse, so that the orthodromic impulse and its refractory period have passed the stimulus site before the antidromic responses are launched. The first post-collision D2 value was often greater than the original plateau height, being an average 0.12 ms, ± 0.11 more than the height of the first plateau. This period of elevated D2 values was short-lived, with a rapid (within 0.30 ms) and progressive return to D2 values approaching those of the standard RPT.

IV The second horizontal plateau.

In the final phase of the graph, the D2 values return to a level approximately equal to those on the first horizontal plateau, the difference between the first and second plateau being an average 0.00 ms, ± 0.02. The second plateau was not investigated for a D1 interval greater than 3.0 ms beyond the collision-free interval.

4.3.3 Regional RPT in eccentrically recorded axons.

By moving the recording electrode out into the peripheral retina, the orthodromic impulse must traverse a greater length of unmyelinated axon, which as previously discussed in Chapter 1, p 50, has considerably slower CV than the myelinated segment of the axon. The effect of including this length of unmyelinated axon is to move the MTP for collision out into the retina, if the distance from the OD margin to the recording electrode was sufficient to allow the intraretinal conduction time to equal or exceed the extraretinal conduction time.

A small number of axons, 8 BT/T1 and 1 BS/T2 axons, fulfilled this criterion and had complete rRPT graphs. These graphs displayed the all the same features as those previously described for axons recorded at the OD margin (Fig. 4.6a.). They all had a level plateau and the difference between standard RPT and height of plateau was very

FIGURE 4.6 D2 versus D1 graphs from peripheral and cell body recordings.

A Representative example of the 9 D2 versus D1 graphs made from axons stimulated in the optic tract and recorded in the peripheral retina. This graph displays features that are consistent with the collision paradigms from recordings made at the optic disc margin.

B Representative example of the 14 D2 versus D1 graphs recorded from the cell body of the retinal ganglion cell. Again the features of the graph are similar to those recorded both at the optic disc margin and in the peripheral retina.

A PERIPHERAL RECORDING

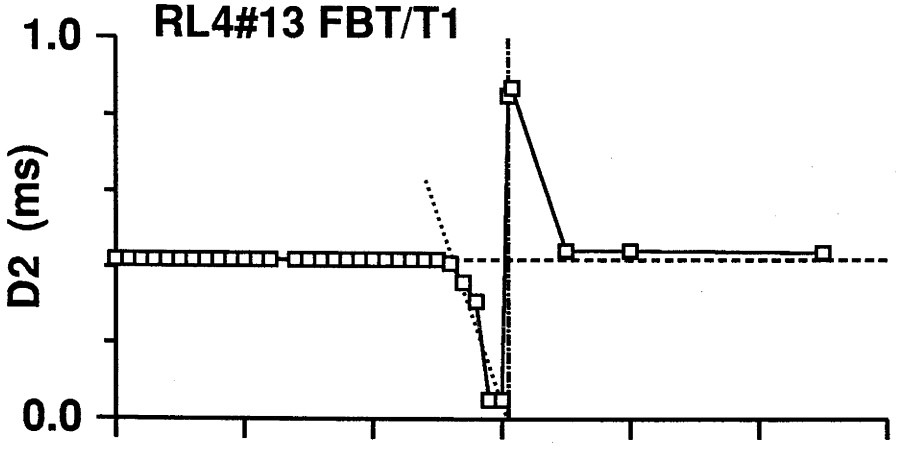

B CELL RECORDING

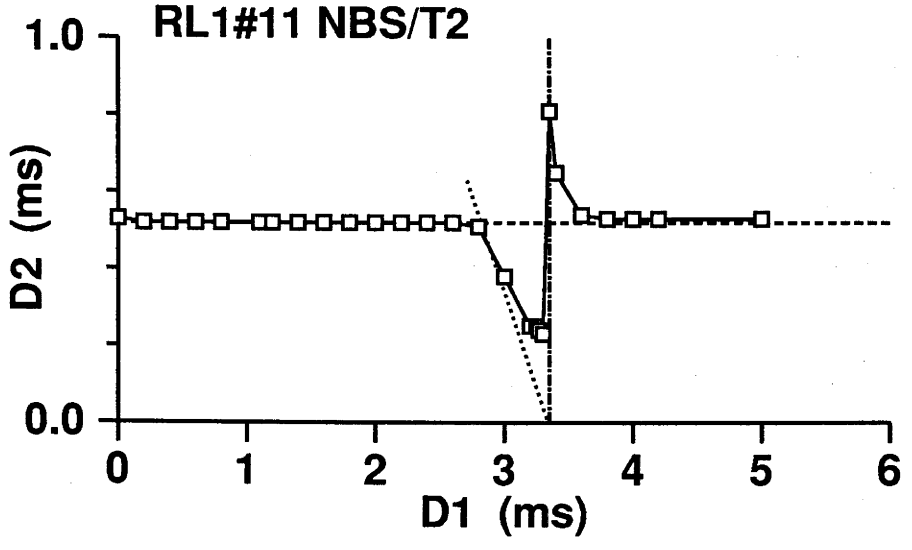

small (mean difference 0.01 ms ± 0.01). This was similar to the axons recorded at the OD despite the ON heminode being within the range of collision of impulses and despite the addition of up to 8 mm of unmyelinated axon. All three forms of ramp were found and the difference between the antidromic latency and the D1 interval to the shoulder was an average 0.27 ms ± 0.03, as it was in the axons recorded at the OD margin.

4.3.4 Regional RPT in cell bodies.

Recordings were made from 10 BT/T1 and 4 BS/T2 cell bodies located in the peripheral retina. Again the rRPT graphs displayed all the features described for the recordings from axons (Fig. 4.6b.). However, the antidromic latency was now an average 0.46 ms ± 0.10 longer than the D1 interval to the shoulder, which was an increase of 0.19 ms compared to the average difference for axons recorded both at the OD margin and peripherally.

4.3.5 Regional RPT in axons stimulated from the ON. The ON heminode.

There were 6 BT/T1 axons that were driven from a stimulating electrode located 2.5 mm behind the eye on the ON (Fig. 2.1c.). These axons were recorded by an electrode placed in the peripheral nasal retina between approximately 1.85 mm to 2.5 mm away from the optic disc margin. All axons had receptive fields located in the temporal visual field. Four of the axons had rRPT graphs that displayed similar characteristics to the graphs of axons driven from the OT. In the other 2 axons there are unexpected additional features. These features are secondary ramps and in one case an additional plateau.

In the first graph (Fig. 4.7a.) there is an upper plateau at a height (0.60 ms) similar to the standard RPT measure (0.62 ms) that ends at a D1 value of 0.66 ms in a short ramp which levels again to form a short second plateau at a height of 0.46 ms and then falls in an accelerating ramp. The post collision D2 values gradually return to a value approximately equal to the standard RPT measure.

FIGURE 4.7 D2 versus D1 graphs, stimulated from the optic nerve electrode.

In the one control animal, LB88, with a stimulating electrode located in the retrobulbar optic nerve (ON) it was possible to perform the collision paradigm in 6 axons, with the stimulus site close to the ON heminode. Of these, 4 displayed all the features of the D2 and D1 graphs seen thus far. However, two of the graphs had additional features.

A The D2 versus D1 graph for this axon had a plateau at the level of the value of the standard RPT, but as the D1 interval was increased, the D2 values descended in a short ramp before forming a second, lower plateau. This plateau then ended in a second, lower descending ramp. The collision-free D2 value and post-collision plateau are as seen previously.

B In this D2 versus D1 graph, there is a short ramp, commencing at D1 = 0 and ending in a plateau which is below the value of the standard refractory period of transmission measured for this axon. The rest of the features of the graph, such as the low ramp, collision-free D2 value and the post-collision plateau are similar to those observed in other axons.

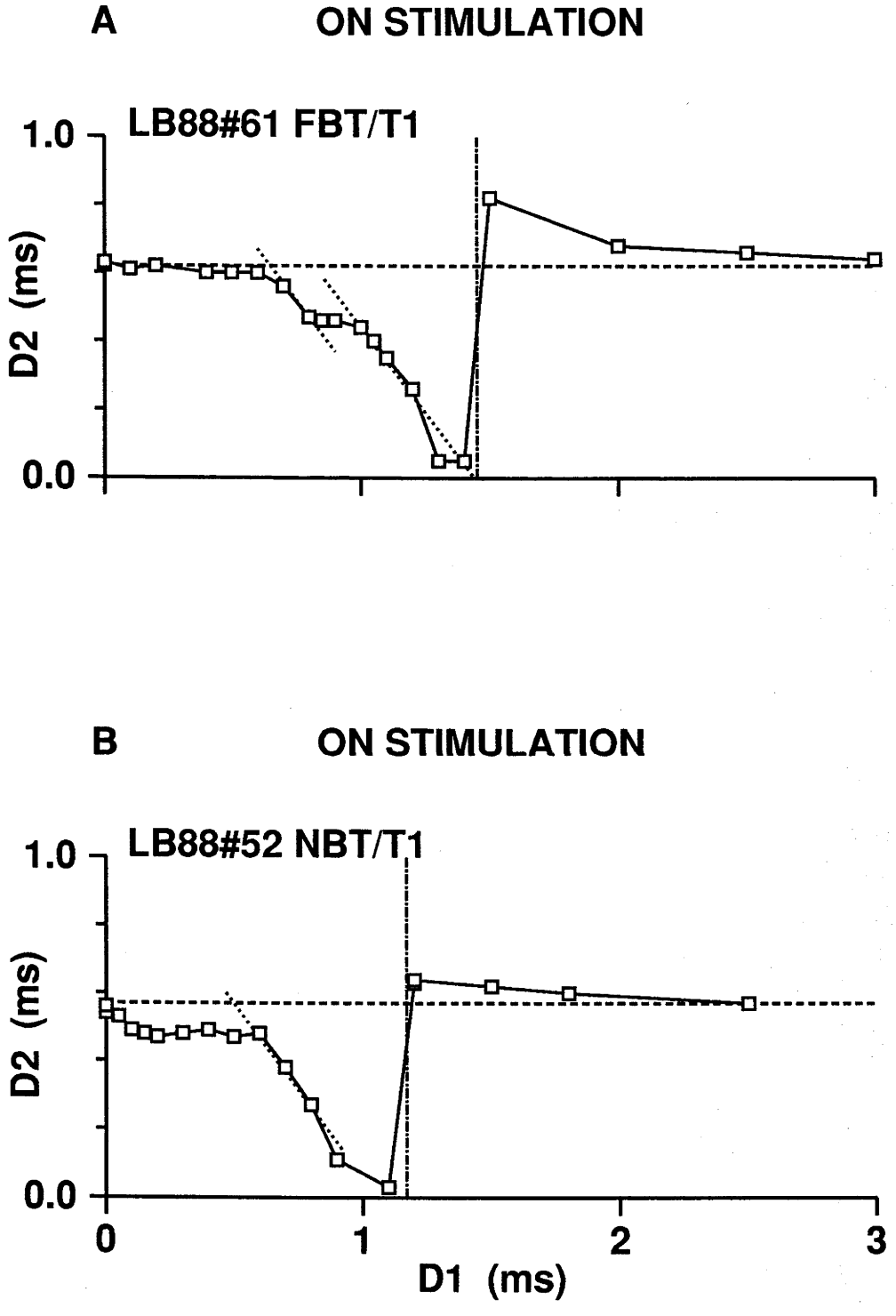
A
ON STIMULATION
LB88#61 FBT/T1
1.0
0.0
D2 (ms)
B
ON STIMULATION
LB88#52 NBT/T1
1.0
0.0
D2 (ms)
0
1
2
3
D1 (ms)

In the second rRPT graph (Fig. 4.7b.) the D2 values descend from 0.56 ms at D1 = 0 in a short ramp, before forming a plateau at a height of 0.48 ms, some 0.09 ms lower than the standard RPT of 0.57 ms. At the end of the plateau the D2 values again descend in a second ramp until the antidromic and orthodromic impulses become collision-free. The post-collision-free D2 returns to 0.60 ms at a D1 value equal to 2.5 ms.

4.4 DISCUSSION.

4.4.1 The D2 versus D1 graph

The collision paradigm allows examination of RPT measures over spatially limited regions of axon from the MTP to the stimulus site. In all fibres and cells driven from the OT, there was a plateau of consistent D2 values measured from the MTP to the stimulus site. The height of the plateau was approximately equal to the standard RPT in each case. In interpreting the D2 versus D1 graph, the space-time diagram is an important tool for clarifying the complex events involved in the collision paradigm. The space-time diagram shows that a plateau of consistent D2 values would occur if there were no localised regions of conduction vulnerability between the MTP and the stimulus site. If such a hypothetical region existed and set an elevated standard RPT value, it would be demonstrated by a fall in D2 values along the plateau towards the stimulation site, indicating that normal conduction properties exist upstream from the region with reduced safety factor. Similarly, a discrepancy between the standard RPT and height of the plateau, would suggest a region of elevated RPT between the MTP and the recording electrode, as the standard RPT tests the entire length of axon.

Consistent with the interpretation of events described in Fig. 4.2, the duration of the ramp, from the shoulder to the collision-free D1 value, was determined by the refractory period associated with the orthodromic impulse at the stimulus site. The duration of the ramp is in good agreement with the standard RPT and the height of the plateau. The upper portion of the ramp with a slope of -1 was explained in terms of the ending of the refractory phase associated with the passage of the orthodromic impulse past the

stimulus site. Furthermore, deviations from the idealised D2 versus D1 ramp can be explained.

4.4.1a Variations in the profile of the ramp.

The interpretation of the ramp that has a constant slope is readily illustrated by the space-time diagram (Fig. 4.2b). However, the majority of rRPT graphs had a ramp that either decelerated or accelerated away from the slope of -1 (Figs. 4.1c,d and 4.5b,c). In those cases where S1 was removed from the collision paradigm in the region of the decelerating or accelerating ramp, the timing for D2 reverted to forming a slope of -1 (Fig. 4.5). The obvious conclusion is that in both the decelerating or accelerating form of ramp, when S1 was included the timing for the successful launch of A2 was being determined by the application of S1, in addition to the effect of the passage of the orthodromic impulse through the stimulus site.

These variations in the shape of the ramp appear to occur towards the supposed end of the refractory period associated with the passage of the orthodromic impulse at the stimulus site (Fig. 4.2). This suggests that the lengthening or shortening of the minimum D2 interval, in this region of the ramp, is likely to arise from the interaction of S1 with the partially refractory axonal membrane at the stimulus site. It appears that S1 is modifying the state of the axonal membrane, without giving rise to a propagating response.

The decelerating ramp shows D2 values at first lying on the constant slope of -1, then deviating upwards and to the right of the constant slope (Figs. 4.1c. and 4.5a.). The simplest explanation of how the application of S1 may lengthen D2 is based on the concept of a stimulus that is delivered during the refractory phase of a preceding impulse giving rise to an impulse that is non-propagating but that still generates a local response, together with the refractoriness which it induces at the point of stimulation. This phenomenon is known as an 'abortive spike' (Paintal, 1966, see also Chapter 1, p 11). The additional refractoriness will delay the moment before A2 can be successfully generated and transmitted.

The accelerating form of the ramp is characterised by D2 values less than 0.10 ms

that again are occurring towards the end of the supposed refractory phase of the orthodromic impulse at the stimulus site and cause the ramp to deviate down and to the left of the constant slope. The explanation of such short D2 values is likely to lie in the phenomenon of latent addition (Tasaki, 1982), where there is summation of two very closely spaced subthreshold stimuli resulting in one response. While the two stimuli delivered here are not normally subthreshold, during the refractory phase when a large number of Na+ channels are still unable to be activated, the effective threshold of the axonal membrane may rise. In these circumstances the first stimulus can be subthreshold. The charge deposited on the membrane capacitance by the brief stimulus pulse will outlast the stimulus duration of 50 μs. If a second stimulus is delivered before the effect of the first stimulus has dissipated, then the charge associated with the second stimulus will combine with the first and the combined stimuli will be of greater strength than a single stimulus alone. The combined stimuli will then result in a single propagating action potential. The period of latent addition in the large fibres of the cat optic nerve has been measured at 0.13 ms or less (Bishop et al., 1953), so latent addition is likely to occur when D2 is less than this.

In Fig. 4.1d, S2 was able to generate a response 0.24 ms after the arrival of the orthodromic impulse at the stimulus site, 0.27 ms less than the standard RPT for this axon. In all cases of accelerating ramps with D2 values less than 0.13 ms, S2 (in combination with S1), was able to generate an action potential earlier in the refractory phase than a single suprathreshold stimulus was able to (see Fig. 4.3b). This cannot be the result of a summed stimulus alone. An examination of Fig 3.4, will show that above 3.7 x threshold the RPT does not vary significantly with increased stimulus strength. This suggests that something other than the mere summation of stimuli is occurring.

One possibility may lie in the symmetrical distribution of refractoriness around the stimulus site after applying an electrical stimulus compared to the spatial extent of the refractory phase of the orthodromic impulse as it progresses past the stimulus site. Because the orthodromic impulse is propagating in one direction, the cycles of refractoriness on the two sides of the stimulus site will be out of phase with each other. This may allow the excitation of a node located on the recording side of the stimulus site, which is further recovered from the passage of the orthodromic impulse than the node

closest to the stimulating electrode. The summation of S1 and S2 may provide sufficient current density at the next node to generate a propagating impulse.

It is not immediately clear why some D2 vs D1 graphs have demonstrated latent addition and others an abortive impulse when a normally suprathreshold stimulus (ie > 3.7 x threshold) is applied to axonal membrane in a state of partial recovery from the passage of an action potential. One factor is the size of the interval between the two electrical stimuli. In a number of cases of apparently decelerating ramps, just before the D1 interval placed S1 and the orthodromic impulse out of the range of collision, two independent D2 values could be obtained at the same D1 interval (Fig. 4.3a,b). The first of the dual values was below 0.1 ms implying latent addition, and the second separate D2 value was at the level of the decelerating ramp. This suggests that the mechanism for generating latent addition or an abortive impulse can apply in the one axon using the same stimulus regime and can be switched between simply by widening or narrowing the ISI.

If S2 is applied close enough to S1, there is the opportunity for the two stimuli to summate but that when the ISI is widened the opportunity is lost. In these circumstances S1 can no longer combine with S2 to generate a single propagating impulse but S1 may still result in an abortive impulse. The second of the dual values will arise when the ISI is widened to the point where S2 can be successfully launched after the conclusion of the refractoriness produced by the S1 generated abortive spike. Dual values were, however, not detected in all cases. So some additional factor must predispose for the occurrence of latent addition versus an abortive impulse.

A likely source of difference between axons would be the proximity of the effective stimulating electrode to the closest node of Ranvier of the axon being tested. It is well established that electrical properties of axons such as threshold for electrical pulses of brief duration, chronaxie and rheobase, vary with the distance from and the orientation of, the stimulating electrode to the node of Ranvier, both in peripheral (Hodler et al. 1952) and central myelinated axons (Ranck, 1975, review). The increase in threshold can be as great as approximately 30-fold, as the distance from the electrode to node widens from 25 to 300 μm (Roberts and Smith, 1973, Fig. 4). Such substantial variation in electrical sensitivity may be reflected in the differing shapes of the ramps of the rRPT

graphs seen in this study. Tasaki (1982, pp 100-102) has observed that the effects of a stimulus delivered directly to a node will rise and decay more rapidly than if the stimulus is applied more remotely. A remote stimulus will have to charge a greater length of membrane capacitance delaying the rise in current at the node, therefore possibly extending the period for latent addition.

4.4.1b The rounding of the shoulder.

At the end of the plateau, the rounding of the shoulder may result from the local circuit currents of the orthodromic impulse facilitating the setting up of the first antidromic impulse, thereby reducing the time it would normally take the stimulus to drive the 'at rest' membrane to threshold. As D2 is measured from the application of S1 to the successful application of S2, any reduction in the utilisation time of the first impulse will be reflected in an overall reduction of the D2 value. That facilitation of the setting up of the antidromic impulse could occur, is suggested by Tasaki (1949) in his paper on the behaviour of colliding impulses. He observed that the time to excitation of the node in between two approaching impulses was considerably shortened due to strong local circuit currents driving the intermediate node very readily to threshold. When this occurs at the stimulus site, the first antidromic impulse will be generated in reduced time, but will very shortly collide with the orthodromic impulse.

The progressive nature of the minor decreases in D2 measure at the shoulder, may be a factor of the timing of the application of S1 in relation to the impending arrival of the orthodromic impulse at the stimulus site and the degree to which the associated local circuit current has raised the excitability of the axonal membrane towards threshold. The facilitating effect of the local circuit current of the orthodromic impulse on the setting up of the antidromic impulse is maximal just before the orthodromic impulse proper invades the stimulus site and the axonal membrane at the stimulus site subsequently becomes absolutely refractory. Until this occurs, refractoriness at the stimulus site will be generated by A1. This interpretation is reinforced by the rRPT graphs shown in Fig. 4.3. With S1 removed, the D2 values at the shoulder were increased, because the delay before S2 could be successfully applied was determined solely by the time taken for the

orthodromic impulse to pass through the stimulus site and refractoriness there to subside. With S1 returned to the collision paradigm, the timing for D2 shortened. This demonstrates that A1 must be determining the timing for D2 but that the interaction with the local circuit currents of the orthodromic impulse as it approaches the stimulus site is facilitating a slightly shorter D2.

While the source of the variations from the idealised D2 versus D1 graphs are not readily apparent from the space-time diagrams, they can be explained by the known behaviour of action potentials when interacting with various states of the axonal membrane, induced by prior impulses.

4.4.1c The post-collision elevated D2 value.

The rapid increase in D2 to a value above the normal plateau height seen immediately post collision, can be explained in terms of the number and frequency of impulses at the stimulus site at that time in the paradigm. As previously shown (Chapter 3, pp 92-96), when three stimuli are applied to an axon, the minimum ISI between the second and third stimuli is longer than that between the first and second. At the collision-free D1 values, the axon at the stimulus site will have experienced three impulses in close succession; the orthodromic closely followed by the two electrically evoked stimuli at minimum ISI. In effect the post collision D2 value here reflects the minimum ISI between the second and third of three impulses at the stimulus site. This situation rapidly subsides as the D1 interval is further lengthened, allowing the orthodromic impulse to move further away from the stimulus site and the axonal membrane at the stimulus site to recover further before the first antidromic stimulus is applied. The D2 value will progressively return to a level that reflects the minimum ISI between just two stimuli.

4.4.2 Orthodromic versus antidromic conduction time.

According to the analysis in the space-time diagram it can be inferred that the D1 interval that coincides with the shoulder, is equivalent to the arrival of the orthodromic impulse at the stimulus site. Comparison of the orthodromic conduction time ascertained

in this manner and the antidromic latency, showed that the orthodromic latency was always less than the antidromic (Fig 4.4). The reduction in orthodromic conduction time relative to that of the antidromic impulse can be caused by a number of factors. A small factor is the placement the Schmitt trigger above the noise level on the initial phase of the orthodromic impulse. This means that the orthodromic impulse has already commenced at the recording electrode and that its local circuit currents have extended beyond the recording site before the antidromic impulse has been triggered. An upper limit of 0.05 ms for the interval from the arrival of the orthodromic impulse at the recording site to the level of the Schmitt trigger can be given, but the advantage to the orthodromic latency of the extension of the local circuit currents beyond the recording site is not quantifiable.

A primary factor is the utilisation time necessary for the generation of the electrically evoked antidromic impulse (Fuller and Schlag, 1976), that is, the time from the application of the stimulus to the launch of a propagating impulse. The measurement of the difference between antidromic versus orthodromic latency in recordings from fibres, with the 0.05 ms subtracted for the height of the Schmitt trigger, was on average 0.22 ms, which was in good agreement with previous estimations of 0.10-0.25 ms for utilisation time in the CNS (Takahashi, 1965, Sumitomo et. al., 1969, Stone and Freeman, 1971).

However, there is one other possible factor in the delay of the antidromic latency compared to the orthodromic. It cannot be revealed in the present paradigm whether the antidromic impulse in travelling from the myelinated to unmyelinated axon, may experience a short delay in latency at the junction zone, as has been suggested to occur when impulses propagate from myelinated axon into the unmyelinated amphibian motor nerve terminals (Katz and Miledi, 1965, Braun and Schmidt, 1966). Rough calculations, from Fig. 2 in Braun and Schmidt (1966), suggest that a delay in the order of 0.10 ms may occur at the commencement of the unmyelinated portion of the motor nerve terminal. If the axonal structure of the site of discontinuity of myelin in the motor nerve terminal and the ON are similar, a delay of a similar magnitude might be expected. This would further reduce the estimated utilisation interval to an average of 0.12 ms, which would still be within the range of previous estimates.

In the recordings from cell bodies, the difference between the D1 interval to the shoulder and the antidromic latency increased in comparison to the difference found in axons either recorded at the OD margin or in the peripheral retina. It is unlikely that recording from a cell body would alter the events, already mentioned, for antidromic impulses initiated some distance from the cell body. So here it is possible that the conduction time for impulses is longer in the antidromic direction than in the orthodromic. A possible cause of a delay in antidromic latency would be the well-known (Coombs et al., 1957a) slowing of an antidromic impulse at the junction of the axon hillock-soma region in motoneurons. A second possibility occurs because the possible site of initiation of an orthodromic impulse is the initial segment of the axon (Coombs et al., 1957a). This is the section of narrowed axon which joins the axon hillock to the axon proper, and which has a high density of Na+ channels (Wollner and Catterall, 1986). After the action potential is generated here, the impulse moves in two directions, both into the axon and the cell body. Presumably the orthodromic impulse is already underway as the other impulse is recorded in the cell body. This will also decrease the orthodromic conduction time relative to the antidromic latency.

4.4.3 The position of the mid-time point.

While utilisation time, the placement of the Schmitt trigger and possible delay in the antidromic latency in the region of the ON heminode, will move the MTP collision back towards the stimulus site by between 0.16- 0.39 ms, there are two other considerations to be made when determining the possible location of the MTP in the optic pathway. The most prominent will be the portion of unmyelinated axon that must be traversed by the orthodromic impulse between the recording electrode and the junction of the unmyelinated and myelinated segments in the ON. CVs of impulses in the unmyelinated portion of the optic axons is at least 10x slower that of the myelinated segment (Stone and Freeman, 1971, Chapters 1 and 3 of this thesis) and the amount of slowing of the latency of the orthodromic impulse will be dependent upon the electrode recording position in relation to the OD margin. In the case of the axons recorded near the OD the length of unmyelinated axon is minimal (2-3 mm). By placing the recording electrode in

the peripheral retina, this feature of the optic pathway was used to substantially move the MTP out into the retina so that the ON heminode could be traversed by the collision paradigm.

There is a further variable in the position of the MTP collision. This is the CV of impulses in the OT compared to the ON. As already discussed in Chapter 3, pp 103-106, there is now evidence that the CV of impulses in the OT is faster than in the ON of the ferret (Baker and Stryker, 1990). In addition evidence from the experiments discussed in Chapter 3 of this thesis, indicates that changes in the CVs of impulses in the ON and OT of the cat may not be homogeneous, particularly for the BT/T1 fibres. Obviously the effect of faster CV in the OT would be to shift the position of the MTP collision towards the retina, while slower OT CV would move the MTP towards the stimulating electrode.

4.4.4 Conduction at the optic disc heminode.

Even when the recording electrode was placed in the peripheral retina, so that the MTP for collision occurred downstream from the ON heminode, the degree of vulnerability that could be tested by stimulating electrodes in the OT was limited. As discussed in the previous chapter, the increasing separation of paired responses with increased conduction time, would render S1 and S2 "non-critical" for testing small degrees (approximately less than 0.90 ms from Fig. 3.8) of conduction vulnerability at the optic heminode. The use of a retrobulbar stimulating electrode substantially reduces the conduction distance between the stimulating electrode and the ON heminode (to approximately 3 mm of myelinated axon) and therefore shortens the conduction time.

Of the six axons tested with the collision paradigm using the retrobulbar ON stimulation site and an eccentrically located recording electrode, two had D2 versus D1 graphs that markedly departed from the form of graph so far illustrated and explained. In the first of these D2 versus D1 graphs (Fig 4.5a) there was an upper plateau at the height of the standard RPT of 0.61 ms. Both the height of the plateau and the RPT were within normal limits, but at the upper end of the normal range. The shoulder is located at a D1 of 0.65 ms and then the ramp descends to a second plateau for a short distance at an

average of 0.46 ms, which is close to the average RPT value.

The second graph (Fig 4.5b) does not have a an upper plateau, but has an upper ramp which commences at D1 = 0 and descends from the level of the standard RPT at 0.57 ms, to a plateau with a height of 0.48 ms. Again the standard RPT was within normal limits, but in both cases the discrepancy between the standard RPT and the lower plateau with a shorter rRPT, indicates a region of vulnerability along the axon. A more complete explanation of the form of the abnormal rRPT graph and their associated space-time diagrams is proposed in Chapter 6.

In determining whether the unusual features of these D2 versus D1 graphs could be related to events at the ON heminode, it is important to establish either the site of the MTP for collision or the edge of the region of vulnerability. Simple spatio-temporal considerations indicate that for any increase in the D1 interval, the orthodromic impulse will travel along the axon for a time equivalent to half the increment in D1. Similarly, the antidromic impulse will travel for less far along the axon before collision, that is a lesser conduction time also equivalent to D1/2.

In Fig .4.5a, the ending of the upper plateau represents the temporal extent of the region of vulnerability on the stimulus side of the lesion. The ending of the lower plateau gives the D1 value that represents the time at which the orthodromic impulse has reached the stimulus site. The additional delay can therefore be calculated by $D1_{LS}$- $D1_{US}$. The resulting equation is for LB88#61 (Fig .4.5a) is 1.05-0.65 = 0.40 ms. Half of this increment in the D1 interval. that is ($D1_{LS}$- $D1_{US}$)/2, gives the additional time travelled by the orthodromic impulse from the edge of the lesion to the stimulus site, that is 0.20 ms. The distance that could be traversed in this time can be calculated as the CV in the ON for this axon was known to be 46.1 m/s, so the distance is in the order of 9.2 mm. As the stimulating electrode was located 2.5 mm behind the eye, it is unlikely that the high plateau is a demonstration of conduction vulnerability at the ON heminode.

In the second abnormal rRPT graph (Fig. 4.5b) an initial high plateau was not detected but the highest D1 value on the upper ramp was nearly the same as the standard RPT. This implies that the edge of the region of vulnerability was just beyond or at the MTP. For LB88#52, the additional time needed for the orthodromic impulse to conduct

from the edge of the lesion to the stimulus site can therefore be estimated as 0.60/2 = 0.30 ms. The CV in the ON was not measured for this axon, but if an average BT/T1 CV of 30-60 m/s is assumed, the distance to the MTP is in the order of 9 to 18 mm. The later estimate is obviously an impossible distance, however, some 3 mm from the ON stimulating electrode the optic fibres become unmyelinated with a corresponding decrease in CV. It is likely that the regions of vulnerability in both LB88#61 and #52 were located within the retina.

These two D2 versus D1 graphs are demonstrating that a region of conduction vulnerability exists, but raise the question of the source of that vulnerability. As the exact distance from the ON stimulating electrode to the junction of the myelinated and unmyelinated segments is not known for each axon, it can not be excluded that it is in fact the ON heminode, particularly if there is a delay in latency for an impulse conducting from the myelinated to unmyelinated segment of the axon. There is also the possibility of damage either to axons directly or their extracellular environment, by prior recordings of axons that had been made close to the OD margin. In this type of experiment, the order in which retinal regions are explored with the recording electrode is important. If the recording electrode is located near the OD margin, one must be aware of the potential for inadvertent damage to fibres of passage, if the need arises to move the recording electrode into the peripheral retina.

Overall, the inability to demonstrate marked evidence of conduction vulnerability at the junction of myelinated and unmyelinated optic axons, at normal physiological temperature (35.7^{o}C), both by the collision paradigm and the results in Chapter 3, pp 102-103, is somewhat surprising. It has been predicted from models of conduction into segments of axon devoid of myelin that impulses would be blocked at the site of demyelination (Waxman, 1977, Stephanova, 1988). This was predicted despite the presence of Na+ channels in the bared axon, and was thought to be due to impedance mismatch between the myelinated and unmyelinated segments caused by the increase in exposed area of the demyelinated segment.

Given that, under most circumstances, conduction vulnerability is not seen at the ON heminode, the question then arises as to the mechanisms by which conduction may be made secure in this region. Examination of the question of facilitation of conduction

into demyelinated regions of axon by computer simulation studies showed that impedance mismatch could be alleviated by a variety of changes to axonal structure and membrane properties. Waxman and Wood (1984) found that an increase in Na+ channel density or a more substantial decrease in the K+ conductance at the transition region of the myelinated to demyelinated axon or even reduced K+ channel density in nodes of the myelinated region to levels approaching that of mammalian physiology, facilitated conduction into the demyelinated zone.

Waxman and Brill (1978), using a model of a myelinated fibre with axonal diameter of 10 μm, calculated that the presence of at least two shortened internodes less than 600 μm placed proximal to the demyelinated zone would restore conduction. When the length of the internode was increased beyond 1,000 μm, conduction failed. It is reasonable to assume that in the smaller optic axons, a similar reduction in the ratio of length of the internode to axonal diameter prior to the ON heminode would considerably increase the amount of current available at the heminode to charge the increased capacitance of the unmyelinated axon, allowing transmission of impulses to be restored. Such shortened internodes would increase the security of conduction but may minimally delay the impulse at the transition zone.

These theoretical examinations of the possible increases in security of conduction by alterations in axonal properties in the region of transition from myelinated to axon devoid of myelin, have been supported by freeze fracture and electromicroscopic studies of the retina-optic nerve junction of the adult rat. Both node-like structures in the unmyelinated axon and short internodes in the area of acquisition of myelin have been observed (Black et al., 1982, 1985, Hildebrand et al., 1985).

In their mathematical model of conduction into the unmyelinated terminal of motor nerve fibres, Khodorov and Timin (1975) noted that conduction was most readily secured by two morphological mechanisms, the shortening of the internodal distance in the preterminal area and most effectively by the reduction in diameter of the terminal compared to the myelinated preterminal axon. A step reduction of axonal diameter has been suggested to cause both increased CV and reduced refractoriness as the impulse approaches the region of diameter reduction (Goldstein, 1978). Recent indirect evidence from the cat indicates that intraretinal axons, in particular those of small and medium

diameter, may decrease in size in the retina in comparison to their diameters in the ON and OT (Fitzgibbon and Funke, 1994). There is also some morphological evidence that rat optic axons have larger diameters in the optic nerve than in the retina (Hildebrand et al., 1985), but no direct evidence of a rapid or step-like decrease in axonal diameter at the ON heminode in individual axons.

If any of these modifications of normal axonal morphology exist in the cat optic axons in the region of the ON heminode, then it is difficult to imagine that they would be regulated by a need to increase security of conduction as the normal orthodromic direction of impulses is from the unmyelinated segment to the myelinated extraretinal axon. Impulses travelling from unmyelinated to myelinated axon, would be expected to rapidly establish normal myelinated CV (Waxman and Brill, 1978). Where shortened internodes (Waxman and Melker, 1971) and other changes in axonal morphology have been observed in the CNS, it has been suggested that such variations may serve a functional role in the processing of neural information (Waxman, 1972).

However, if these axonal specialisations are not functionally necessary in the region of the termination of myelin in the ON, they may occur as a consequence of the sequence of the progressive myelination of optic axons during development. The glial progenitors of oligodendrocytes (Raff et al., 1983), migrate from the optic chiasm and proliferate and differentiate in the nerve (Small et al., 1987). As a consequence, the number of available oligodendrocytes, as the lamina cribrosa is approached, may be limited. This may have two consequences; first it may restrict the number of axons that can be enveloped by myelin and second, because the capacity of the oligodendrocytes is being stretched, less myelin may be available for each wrap therefore creating shortened internodes.

4.4.5 Summary.

1) An experimental paradigm utilising the collision of impulses has been adapted to examine the rRPT of spatially limited regions of single optic axons. Reduction in safety factor for conduction in normal axons was not demonstrated in any of the rRPT measures, when using the OT stimulating electrodes.

2) The evidence presented here and in Chapter 3 indicates that conduction vulnerability for antidromic impulses at the junction of the myelinated and unmyelinated segments of optic axons is minimal

3) The space-time diagram is an important device for explaining the interaction of impulses, as collision is progressively moved from the MTP towards the stimulus site. The use of a simple geometric representation of events allows simple interpretations of the rules governing the successful transmission of antidromic impulses. This method of interpretation is crucial when applied to the even more complex situation of understanding collisions through regions of reduced safety factor for conduction created by pathological lesions of the optic pathway, such as are discussed in Chapter 6.

CHAPTER 5.
CONDUCTION IN DEMYELINATED AND PRESSURE-LESIONED AXONS.

5.1 INTRODUCTION

Pathologically, loss of myelin in optic axons can result from auto-immune demyelinating diseases, such as multiple sclerosis (MS), or from pressure on the optic pathway caused by tumours or trauma. Experimental demyelination has been produced by a variety of means (see Chapter 1, p 29). The immunological anti-galactocerebroside (anti-GC) technique of demyelination has the advantage of directly affecting myelin only, without damaging the axon (Saida et al., 1979). Injection of serum containing anti-GC antibodies directly into the optic nerve (ON) causes selective destruction of the oligodendrocytes and creates a focal demyelinating lesion in the CNS (Sergott et al., 1984, Carroll et al., 1984). Despite the complete disappearance of oligodendrocytes, remyelination by oligodendrocytes occurs after 14 days (Carroll et al., 1985). Remyelination in mammalian CNS has been observed in neuropathological and experimentally induced demyelination, though it is slower and less complete than that seen in the PNS (Ludwin, 1988).

Carroll et al. (1990 and personal communication) have described the morphological changes in the ON from 2-24 days following the injection of anti-GC. These occur in 4 main time periods.

1) From 2-3 days post-injection, there was damage to myelin sheaths, as they became wrinkled and splits appeared between groups of lamellae, leading to vesiculation. The periaxonal space between the innermost myelin lamella and the axolemma became greatly enlarged. This was followed by complete loss of oligodendrocytes presumably by intense scavenging by macrophages, leaving axons bare of myelin. The only remaining glial cells were large astrocytes.

2) By days 4-6 post-injection, all extracellular myelin debris was removed and the number of glial cells increased until by day 6 they had almost doubled and were

composed of two distinct types, large and small glial cells.

3) From days 7-13, named by Carroll and colleagues the "premyelination phase", the glial cells specialised and matured, culminating in new oligodendrocytes starting to form myelin. They concluded that the most likely origin of the oligodendrocytes, was the small glial cells.

4) From day 14 on the number of axons with myelin and the number of lamellae steadily increased, until by day 24, 95% of axons were remyelinated by several wraps of the oligodendrocytes. Remyelination at 14 days following demyelination by injection of anti-GC into the spinal cord of rats, has been associated with functional recovery (Kaji et al., 1988).

While pressure applied experimentally to nerves is also known to cause demyelination, the lesion produced is more complex. The effects of pressure on the axons varies with both the degree of pressure applied and the length of nerve over which the pressure is exerted. Low levels of pressure result in a rapidly reversing conduction block, while it appears that intermediate levels of pressure cause demyelination of axons (Denny-Brown and Brenner, 1944, Ochoa et al., 1972, Powell and Myers, 1986). Remyelination also occurs, but would appear to be slower to initiate than in fibres demyelinated by anti-GC, taking up to 5-6 weeks for the axons to be covered by a thin layer of myelin (Clifford-Jones et al., 1980, Ge et al., 1982). Degeneration of neuronal cells has been observed in rat axons subject to higher pressures (at least 80 mmHg; Powell and Myers, 1986), probably because severe pressure is thought to distort, sever or rupture the axon.

The greater susceptibility of the larger diameter axons in a nerve to conduction block when pressure is applied, has long been known (Gasser and Erlanger, 1929). It has been suggested that this greater susceptibility is due to distension of the axonal membrane by accumulation of displaced axoplasm at the edges of the cuff, rather than compression under the cuff itself (MacGregor et al., 1975). Because the volume of the axoplasm increases in proportion to the square of the axonal diameter, while the surface area increases in direct proportion to the diameter, the net effect is that the stresses on axolemma at the edge of the cuff, would be greater in larger diameter axons. In addition, there is evidence that larger myelinated axons with their high neurofilament content may

suffer faster and greater declines in axonal structure and conduction properties, following neuronal injury (Titmus and Faber, 1990).

Conversely, it has been suggested that very high pressure (of at least 750 mmHg, Fern and Harrison, 1991) or pressure applied by a narrow ligature (Batista and Alban, 1983) can cause the selective conduction block of small diameter axons. However, the regime used to compress fibres in this study would appear to preferentially block the large diameter (T1/BT) fibres (Burke at al., 1985, 1986).

Demyelination of the optic axons can block conduction of impulses, and in less severe cases, increase conduction latency and lengthen the refractory period of transmission (RPT). Optic axons can normally transmit impulses up to 800 Hz (Kuffler, 1953) and increased RPT will adversely affect the fidelity of transmission of high frequency trains of impulses. These deficits of conduction can affect higher levels of visual processing, as can be demonstrated by the Pulfrich phenomenon (Frisen et al., 1973) in cases of minor involvement of one ON only. Despite the differences in the two methods of attaining a demyelinating lesion, each provides an excellent opportunity to study the conduction properties of single demyelinated and remyelinating optic axons.

5.2 METHODS

The two methods used to create demyelinating lesions have been described in detail in Chapter 2, pp 75-76. Electrophysiological measurements of latency and RPT were also as previously described in Chapter 2, pp 72-73. However, unlike the latency data discussed in Chapter 3, the data presented in this chapter includes measurements of latency of axons from both the left and right optic tract (OT) (Fig 2.1a).

Retinal ganglion cells (RGC) were classified into the brisk-transient (BT/T1) or brisk-sustained (BS/T2) or rarely encountered non-brisk classes, by their responses to stimuli presented in their visual receptive field. This classification was confirmed, where possible, by the measurement of conduction latency. In the case of blocked RGC, this confirmation could not be obtained.

5.3 RESULTS

5.3.1 Encounter rates. A method of detecting possible ganglion cell degeneration.

If, due to injury, RGC have degenerated, then they would obviously not be detected by either visual or electrical stimulation. It is important to determine whether one class of RGC is more affected than others, in particular in the pressure lesion where the BT/T1 fibres are thought to be more profoundly damaged than other classes of RGC. Comparison of the proportion of the various classes of RGC encountered by the recording electrode in normal cats, to that in the animals with the experimentally induced ON lesions (Table 5.1), may reveal a decline in the percentage of a particular class of RGC, indicative of degeneration.

The least encountered targets were the axons of the non-brisk class of RGC. The second row of Table 5.1 includes the encounter rates for the cell bodies of the different classes of RGC in normal cats. The cell bodies obviously provide a larger target for the recording electrode than their thinner axons and the rate at which the cell bodies of the different classes of RGC were encountered alters significantly in favour of the more morphologically prevalent beta/BS and gamma/non-brisk classes (Hughes, 1985). Because of these increases in the frequency of encounter of particular classes of RGC when recording from cell bodies and the small numbers of cells encountered in the pressure-lesioned animals, only recordings from axons are considered in the comparisons of lesioned and normal animals.

The rate at which the various classes of RGC axons were encountered in the animals injected with anti-GC, when compared to the encounter rate for axons in the normal animals, shows a reduction in the percentage of BT/T1 axons and a compensatory rise in the percentages of BS/T2 and non-brisk axons recorded. This suggests that a portion of the BT/T1 population of axons has degenerated as a result of the anti-GC injection.

The animal with the mild pressure lesion of the ON (LB73), had percentages of the different classes of RGC encountered that closely resembled the anti-GC population. There was a similar small decline in the BT/T1 axons recorded, down from 77.0% in

TABLE 5.1 RECORDING ENCOUNTER RATE OF DIFFERENT CLASSES OF RETINAL GANGLION CELLS.

	RECORDING	*BT/T1*	*BS/T2*	*non-BRISK*	*N*
CONTROL	CELL BODY	38.8%	38.8%	23.4%	81
	AXON	77.0%	20.7%	2.3%	557
ANTI-GC	AXON	65.3%	27.2%	7.5%	710
PRESSURE					
MILD, LB73	AXON	68.8%	27.5%	3.7%	80
SEVERE, LB85	AXON	5.2%	45.2%	49.6%	115

Table 5.1 shows the rates at which the various classes of RGC were encountered by the recording electrode in the retina. The percentage encounter rate in the normal cats was compared with the animals in which the optic nerve was lesioned, either by injection of anti-GC or by pressure. The two pressure lesioned animals are considered separately. The RGC were classified by their responses to visual stimuli and where possible this classification was confirmed by latency measurements.

normal cats, to 68.8% in LB73, and to 65.3% in the anti-GC animals. This result could be anticipated in LB73 because of the well-known susceptibility of the larger diameter fibres to damage by pressure. There is, however, a difference in the proportions of non-brisk axons encountered, with 7.5% of all axons recorded from the anti-GC animals being of that class of RGC, while in the normal animals and LB73 they formed 2.3% and 3.7% respectively.

The susceptibility of large diameter fibres to the effects of pressure was more obvious in LB85, where the ON was subjected to a greater degree of pressure. The percentage of BT/T1 RGC was reduced to only 5.2% of the total number of axons encountered. In addition to the marked decline in the BT/T1 population, LB85 also shows an apparent marked increase in the percentage of non-brisk axons that were recorded.

A close examination of this class of RGC from LB85, reveals that their responses to visual stimulation mostly resembled the responses of sluggish-transient units in the normal control animals. Common to all transient RGC, they had either ON or OFF responses to illumination of the centre of their receptive field, but their discharge was particularly transient. However, in contrast to most normal RGC of the ST class, they only responded to very large targets and coarse gratings ($> 15^{o}$) and it was sometimes difficult to determine if the receptive field was concentric. Often the classification was queried during the experiment and the possibility that these might be "sick BT" RGC was raised. Unlike regular BT/T1 RGC, they had little or no maintained discharge, their response to visual targets was sluggish and no periphery effect could be elicited. A retrospective examination of comments noted during the experiments on the anti-GC animals, also highlighted atypical reactions to visual stimulation by a number of RGC that were classified as non-brisk on the basis of their sluggish responses to receptive field stimulation.

In LB85, classification could not be confirmed by latency measurements from either the OT and OX, as all these axons were blocked from those stimulus sites. However, 22 of the 54 non-brisk axons could be driven from the ON stimulus site and the latencies measured to the OD recording electrode ranged from 0.53 to 3.41 ms. In the one normal cat (LB88), which had a retrobulbar ON stimulating electrode placed in the same manner

as in the pressure-lesioned animals, the range of latencies for 24 BT/T1 axons was 0.47 to 0.70 ms and for 3 BS/T2 axons was 0.75 to 0.92 ms. Because the number of axons sampled was small and the course of optic fibres as they exit the eye is variable, these latency distributions are only indicative of normal conduction latency in this region of the optic pathway. Four of the axons recorded from LB85 at the OD margin conducted impulses from the retrobulbar ON electrode at latencies (0.53 to 0.70 ms) suggestive of T1 conduction rates and another 2 took <0.90 ms. In view of these short latencies, these 6 axons could not belong to the T3/non-brisk class of RGC, despite their sluggish responses to visual stimulation. It is also very likely that some other sluggish RGC are "sick BT" RGC with abnormal conduction latencies.

There were other indications of axonal injury. The four units with the longest latencies from the ON (2.19 to 3.41 ms) had substantial reductions in their latency measurements (0.78 to 1.67 ms) when the stimulus strength was increased. This phenomenon was not seen during any other instances of stimulating from the ON. At OT and OX stimulation sites in normal animals, the maximum decrease in latency with an increase in stimulus strength from 1.4 up to 9 times threshold was only 0.12 ms and from the ON was 0.10 ms.

In two LB85 units where this was examined in more detail, the increases in latency occurred at progressive increments in stimulus strength. Indications from the RPT and rRPT measures in both these axons suggests that the axon at the ON stimulus site was abnormal. It may be that the utilisation interval is long when setting up an impulse in demyelinated axon and that it takes a greater than "slightly above threshold" stimulus strength (Holder et al., 1952) to achieve a consistent measure of latency in these circumstances. It is certain that all these axons with unusual receptive field characteristics had been affected by the pressure lesion, as they were all undrivable from the stimulating electrodes in the OT and OX.

5.3.2 Conduction block.

In examining conduction block in single RGC it is worthwhile noting that not all fibres are able to be activated with the particular arrangement of stimulating electrodes in the central pathways, even in normal control animals and using maximum stimulus

strength with a pulse duration of up to 150 μs. Because the viability of the ON portion of the axon is unrelated to the recording location, recordings from both cell bodies and axons, whether at the OD margin or in peripheral retina, are included. The percentage of each class of normal RGC that can not be driven increases with decreasing axonal diameter (Table 5.2) and was as high as 9.4% of all the non-brisk class of RGC. This was an anticipated result as it is accepted that the threshold for excitation of small diameter fibres is higher than that of fibres of larger diameter (Chapter 1, p 4). Because current density (current flow per unit cross-sectional area) will decrease with distance from the source of current, a proportion of optic axons, of any given diameter, may lie outside the region where the current density is sufficient to excite them. This will occur for the smallest diameter axons first.

Table 5.2 shows that in the anti-GC animals, approximately half of all the non-brisk class of RGC could not be driven from the OT stimulating electrode. By comparison, the percentages of BT/T1 and BS/T2 RGC suffering from conduction block were relatively low. The high percentage of blocked non-brisk RGC could be due in part, to the inclusion of "sick BT" RGC in this category. The large number of BT/T1 and BS/T2 RGC that still conduct in the presence of a demyelinating lesion is probably the result of two factors. The first is the limited spread of the lesion in the ON and the second is that a number of the animals were examined during the recovery phase of the anti-GC lesion. These factors will be examined in greater detail later in this chapter.

In the mild pressure lesion (LB73), approximately a quarter of all BT/T1 fibres were blocked, while in the severe pressure lesion (LB85) only one BT/T1 axon could be driven. When the data in Table 5.1 is considered in conjunction with the proportion of fibres blocked in both LB73 and LB85 (Table 5.2), it confirms the vulnerability of large diameter optic axons to damage by pressure. It also shows that the greater the pressure applied, the more severe the degree of damage to the large (BT/T1) optic axons. By comparison, in both the mild and severe pressure lesions just over 20% of the BS/T2 fibres were blocked, suggesting that while the effects of pressure on the ON were not restricted to the large diameter fibres, increased pressure did not alter the percentage of BS/T2 fibres damaged. In LB85, no non-brisk fibres could be driven, leaving the BS/T2 fibres as the only class of RGC still conducting impulses in any numbers.

TABLE 5.2 THE PERCENTAGE OF BLOCKED FIBRES IN EACH CLASS OF RETINAL GANGLION CELLS.

	BT/T1	*BS/T2*	*non-BRISK*
CONTROL	0.4% (n=460)	3.4% (n=146)	9.4% (n=32)
ANTI-GC	11.9% (n=488)	16.8% (n=214)	50.8% (n=36)
PRESSURE			
MILD, LB73	26.8% (n=56)	21.7% (n=23)	0.0% (n=3)
SEVERE, LB85	75.0% (n=4)	21.7% (n=46)	100.0% (n=54)

The percentage of each of the different classes of RGC that was blocked in both the normal and lesioned optic pathways. Maximum stimulus strength (100 V) and a pulse duration of 150 μs were used in each case to ascertain that a fibre could not be driven. The numbers of fibres include RGCs recorded either from the axon or cell body, and stimulated from either the optic chiasm or tract.

5.3.3 Conduction latency and refractory period of transmission.

5.3.3a Anti-GC Lesion.

Of the 765 RGC recorded from the 8 animals injected with anti-GC, 430 RGC (320 BT/T1 and 128 BS) were recorded as axons at the OD margin and had both latency and standard two stimuli RPT measurements taken. To determine whether these conduction parameters were within normal limits, comparison was made with the companion study of normal cats. In examining the RPT measure, the BT/T1 and BS/T2 populations of RGC can be grouped together because of similar distributions, as discussed in Chapter 3, p 86. The maximum RPT recorded in the normal animals was 0.65 ms and so, any RPT measurement greater than this was deemed abnormal. It is to be noted that there may be some axons in the anti-GC population which normally had RPT at the lower end of the distribution of the RPT of normal cats and which in the presence of the anti-GC lesion increase their RPT, but only to a level that was still within the normal distribution.

The histogram of RPTs for the anti-GC animals (Fig. 5.1.b) shows that the majority of axons (79.5%) have RPT within the normal range of 0.28 to 0.65 ms (Fig 5.1.a). The minimum RPT was 0.30 ms and the mean RPT for those axons with RPT less than 0.65 ms, was 0.50 ms, similar to the mean RPT (0.49 ms) in normal animals. This would suggest that the anti-GC RPT population was unlikely to contain a large proportion of abnormal fibres with RPTs at the upper end of the normal range. The tail of abnormal RPT values extends to 4.90 ms. There appears to be a small, but potentially significant difference in the percentage of BT/T1 (22.2%) and BS/T2 (16.4%) axons with abnormal RPT.

A plot of the RPT values against their latencies for the BT/T1 (Fig. 5.2.a) and BS/T2 (Fig. 5.2.b) fibres again shows that most RGC have latencies and RPT values that lie within the normal ranges for these conduction parameters, as shown by the clustering of points in the lower left-hand quadrant. Some 26.2% of BT/T1 and 23.4% of BS/T2 axons had either abnormal latency (lower right) or RPT (upper left) or both (upper right). There was no clear correlation between the degree of abnormality in RPT and latency values. The four BT/T1 RGC with extremely abnormal RPT (Fig. 5.2a) will be discussed as a special category of abnormal axons in Chapter 6.

FIGURE 5.1 Distribution of refractory periods of transmission in demyelinated and normal optic axons.

The distribution of the refractory periods of transmission (RPTs) determined by the standard two-stimulus test in 296 axons normal axons compared to the distribution of RPT in 430 axons from the animals which had a micro-injection of anti-galactocerebroside in the optic nerve. The impulses were generated in the optic tract (OT) for both the lesioned and control animals.

A The distribution of RPT for 241 BT/T1 axons and 55 BS/T2 axons from the normal animals. The mean value for the RPT in these fibres was 0.50 ms and the values ranged from 0.28 ms to 0.65 ms.

B The distribution of RPT for 302 BT/T1 and 128 BS/T2 axons from the animals with the anti-galactocerebroside demyelinating lesion. The mean value for the RPT in these fibres was 0.63 ms and the values ranged from 0.30 ms to 4.90 ms. A large percentage of fibres had RPT values that were within normal limits.

DISTRIBUTION OF REFRACTORY PERIODS OF TRANSMISSION

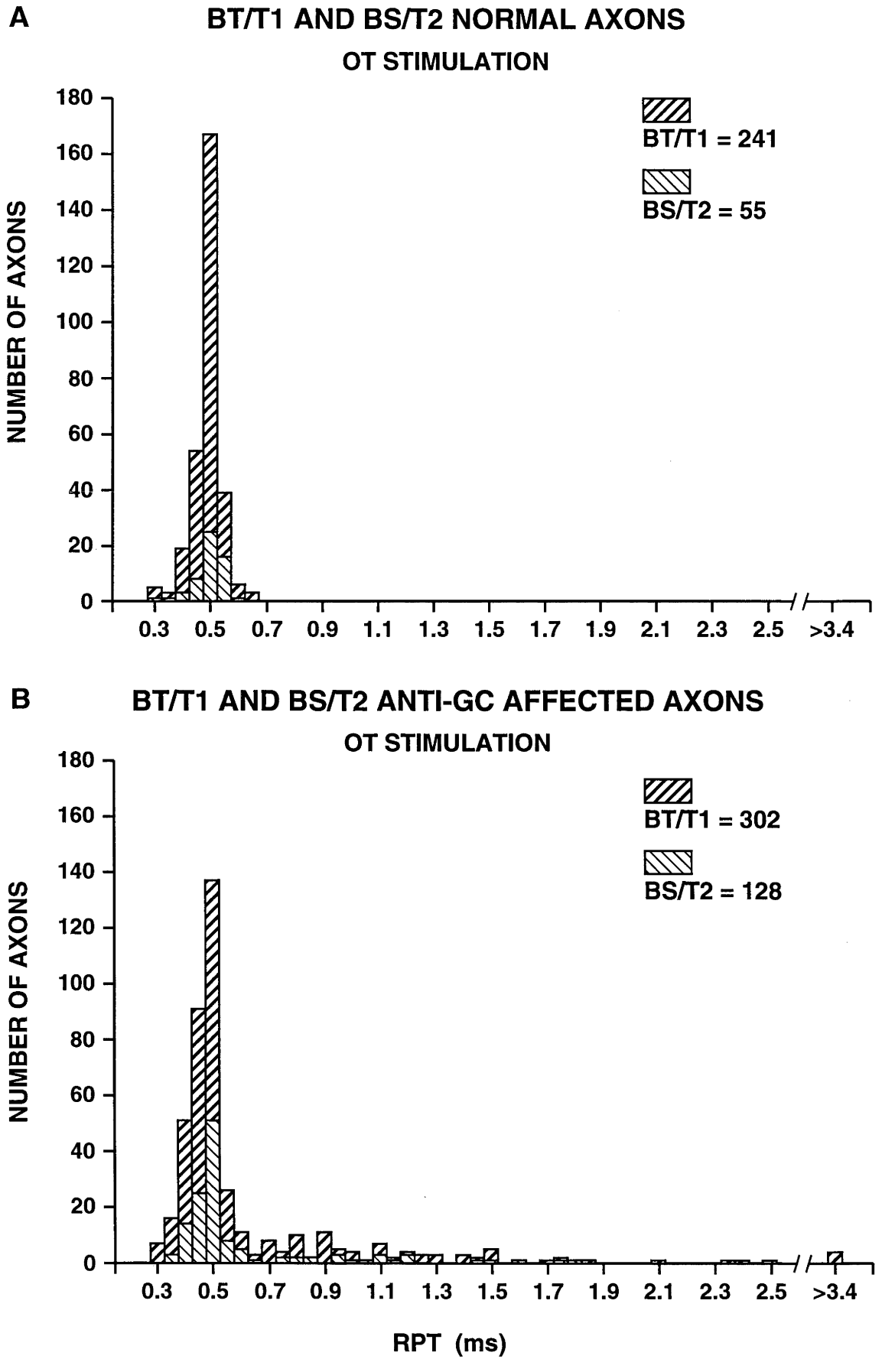

FIGURE 5.2 Refractory period of transmission versus latency.

Relation of the refractory period of transmission (RPT) to latency in 302 BT/T1 and 128 BS/T2 optic axons. The axons had latencies measured from the optic tract (OT) and recorded at the optic disc margin. The vertical dashed lines represent the maximum latency values measureed for the normal ipsilateral (light dash) and contralateral (heavy dash) optic fibres. The horizontal dashed lines mark the maximum RPT measurements made in the control population.

A BT/T1 axons with latency and RPT measures. Of the 302 axons 11.9 % had both abnormal latency and RPT, 4.0 % abnormal RPT but normal latency and 10.3 % had abnormal latency only. Note 4 axons with RPT measurements greater than 3.0 ms. These four axons are referred to in Chapter 6.

B BS/T2 axons with latency and RPT measures. Of the 128 axons 8.6 % had both abnormal latency and RPT, 7.0 % abnormal RPT but normal latency and 7.8 % had abnormal latency only.

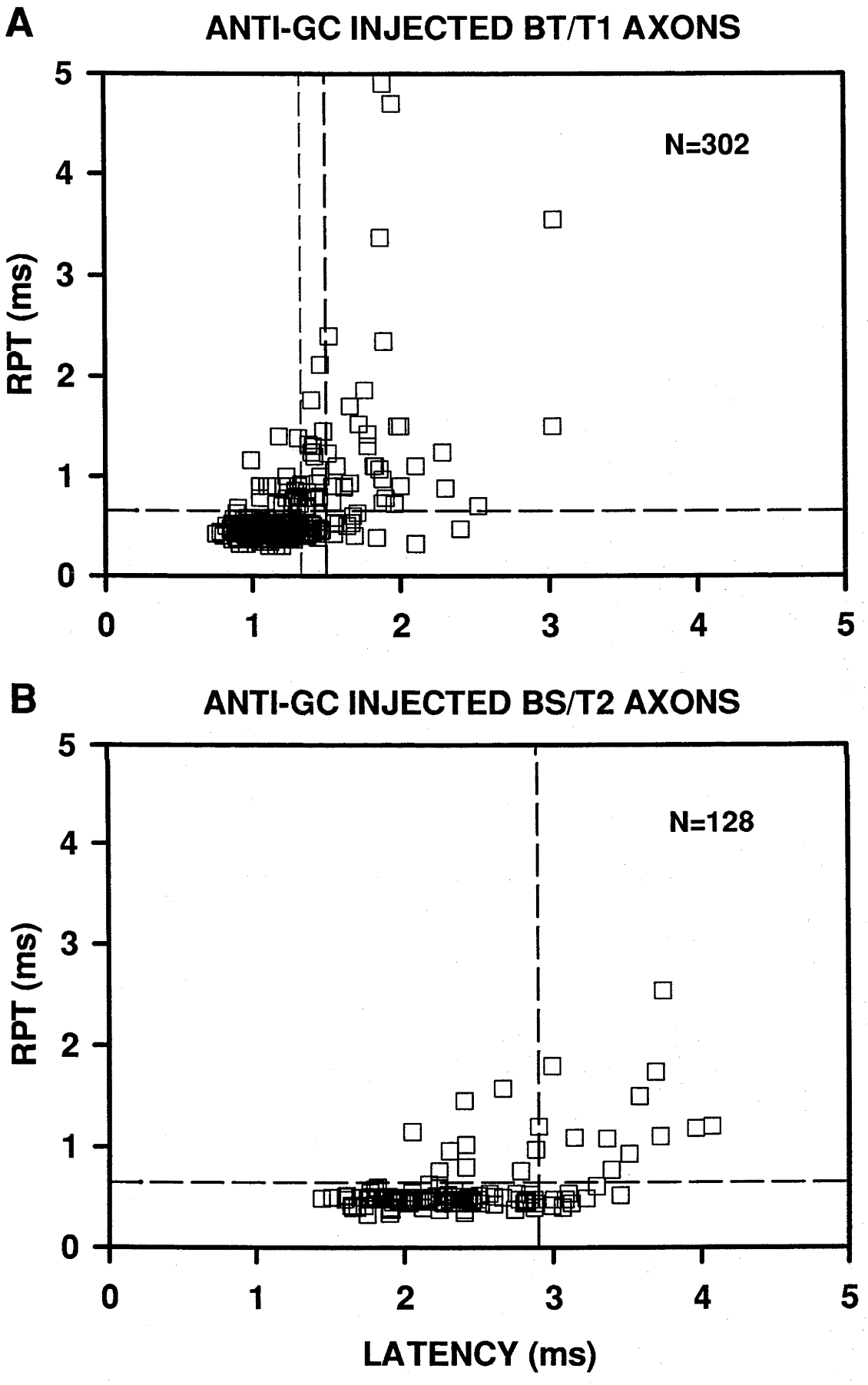
A
ANTI-GC INJECTED BT/T1 AXONS
N=302
RPT (ms)
0
1
2
3
4
5
B
ANTI-GC INJECTED BS/T2 AXONS
N=128
RPT (ms)
LATENCY (ms)

Comparison of latencies is more complex than comparing the RPT values. Firstly, both the BT/T1 and BS/T2 axons must be considered separately, due to their very different latencies. In addition, fibres that come from the OT either ipsilateral or contralateral to the recording eye, must also be segregated, because of known differences in the CV of crossed and uncrossed fibres (Bishop et al., 1953) which is confirmed here (Fig. 5.3.a and c, Fig. 5.4.a and c). When this is taken into consideration, the numbers of axons from the anti-GC animals become rather small for some categories of RGC, so an additional 127 axons recorded at the OD margin and with latency but not RPT values, have been added to the original 430 axons, for comparison with the normal animals. Again it is evident that in the animals lesioned with anti-GC, a large percentage (83%) of all the BT/T1 axons (Fig. 5.3c and d) and BS/T2 axons (Fig. 5.4c and d) have normal latency. There was no difference in the proportion of BT/T1 (17.04%) versus BS/T2 (17.09%) axons suffering detrimental effects of the demyelinating lesion on latency.

The high proportion of normal axons in the presence of the anti-GC lesion, as already mentioned, can be attributed to the focal nature of the anti-GC lesion and to recording during the recovery phase. The micro-injection of anti-GC was made into only one point, of the ONs. The lesions were observed to occupy between 10-70% of the transverse sections of the ON (Carroll et al., 1990). As the injection was made within 3 mm of the exit of the ON from the eye, there was topographical continuity of the demyelinated optic axons in the nerve with their location intra-ocularly, particularly when they were recorded close to the OD margin. As a probable consequence of the small volume of the injection (2 µl) and its limited spread in the ON, it was found that the majority of axons with abnormal conduction parameters tended to be recorded from only one or two quadrants of the retina.

An example from one animal, CL57, is presented here to illustrate the localisation of the lesion (Fig. 5.5). Recordings from the right eye of this animal were made between days 12 to 13 post-injection. The recording site was noted as a position on a clock, placed around the OD margin. This is a convention normally used to locate retinal lesions. The 12 o'clock position is at the most superior point of the OD rim and 3 o'clock, in the right eye, is located on the nasal side. The primary location of abnormal conduction parameters in CL57 was centred around the 11 o'clock position on the OD margin with a second sector located at 5 o'clock. As the syringe was introduced from

FIGURE 5.3 Latency in normal and anti-galactocerebroside affected BT/T1 axons.

Latencies measured from both the contralateral and ipsilateral optic tracts (OT) to the left eye in 273 normal BT/T1 axons and in 389 BT/T1 axons from the animals with the left optic nerve injected with anti-galactocerebroside (anti-GC).

A Stimulated from the contralateral OT, latencies measured in 208 normal axons ranging from 0.76 ms to 1.50 ms.

B Stimulated from the ipsilateral OT, latencies measured in 65 normal axons ranging from 0.72 ms to 1.33 ms.

C Stimulated from the contralateral OT, 334 axons affected by the injection of anti-GC with latencies ranging from 0.75 ms to 3.27 ms.

D Stimulated from the ipsilateral OT, 55 axons affected by the injection of anti-GC with latencies ranging from 0.86 ms to 1.92 ms. The range of latencies is not as great as those from the contralateral OT, probably because of the smaller population size.

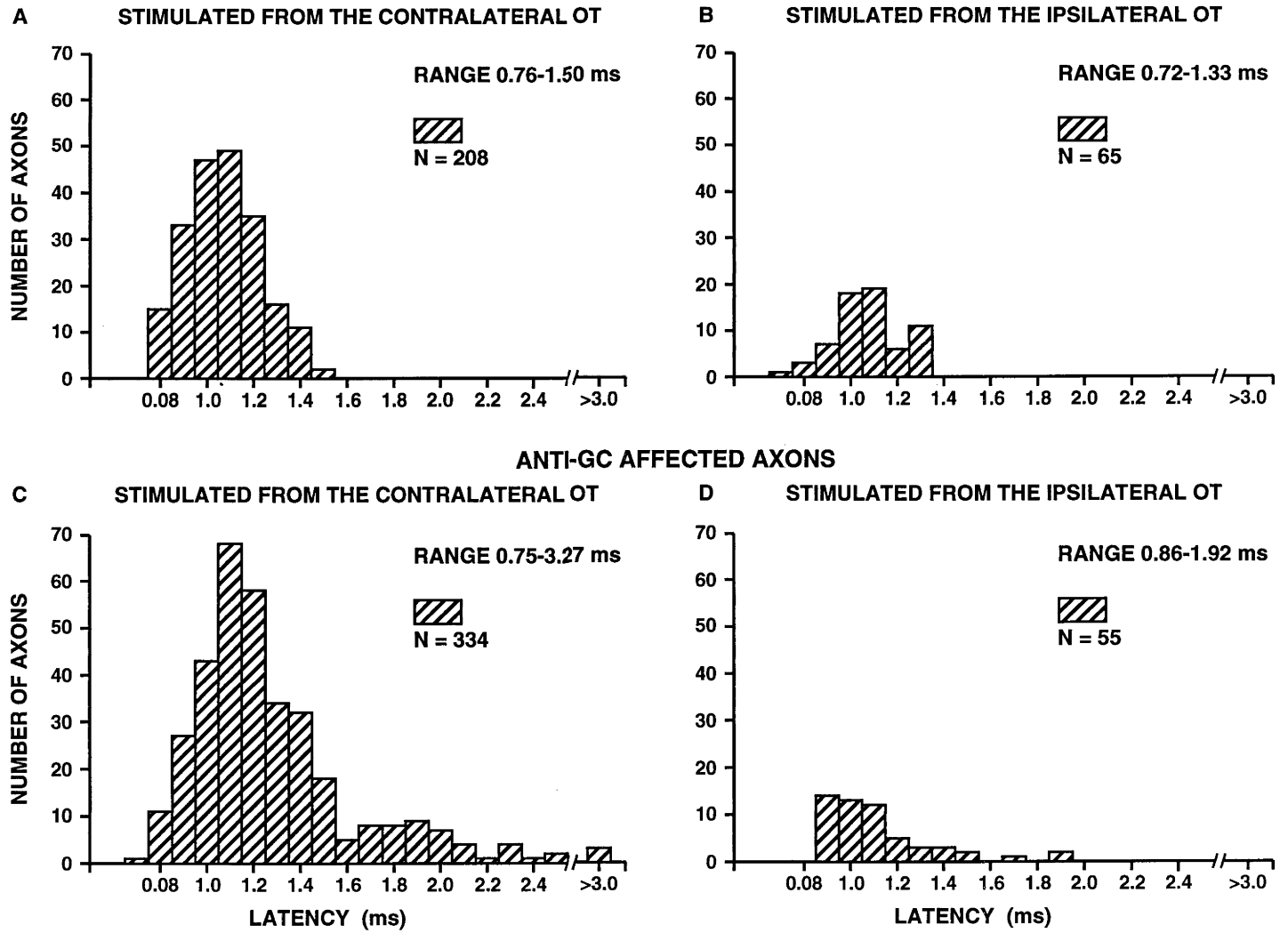
LATENCY IN BT/T1 AXONS
NORMAL AXONS
A
STIMULATED FROM THE CONTRALATERAL OT
RANGE 0.76-1.50 ms
N = 208
B
STIMULATED FROM THE IPSILATERAL OT
RANGE 0.72-1.33 ms
N = 65
ANTI-GC AFFECTED AXONS
C
STIMULATED FROM THE CONTRALATERAL OT
RANGE 0.75-3.27 ms
N = 334
D
STIMULATED FROM THE IPSILATERAL OT
RANGE 0.86-1.92 ms
N = 55
NUMBER OF AXONS
0
10
20
30
40
50
60
70
0.08 1.0 1.2 1.4 1.6 1.8 2.0 2.2 2.4 >3.0
LATENCY (ms)

FIGURE 5.4 Latency in normal and anti-galactocerebroside affected BS/T2 axons.

Latencies measured from both the contralateral and ipsilateral optic tracts (OT) to the left eye in 75 normal BS/T2 axons and in 158 BS/T2 axons from the animals with the optic nerves injected with anti-galactocerebroside (anti-GC).

A Stimulated from the contralateral OT, latencies measured in 46 normal axons ranging from 1.50 ms to 2.91 ms.

B Stimulated from the ipsilateral OT, latencies measured in 29 normal axons ranging from 1.39 ms to 2.88 ms.

C Stimulated from the contralateral OT, 100 axons affected by the injection of anti-GC with latencies ranging from 1.63 ms to 3.96 ms.

D Stimulated from the ipsilateral OT, 58 axons affected by the injection of anti-GC with latencies ranging from 1.44 ms to 4.53 ms.

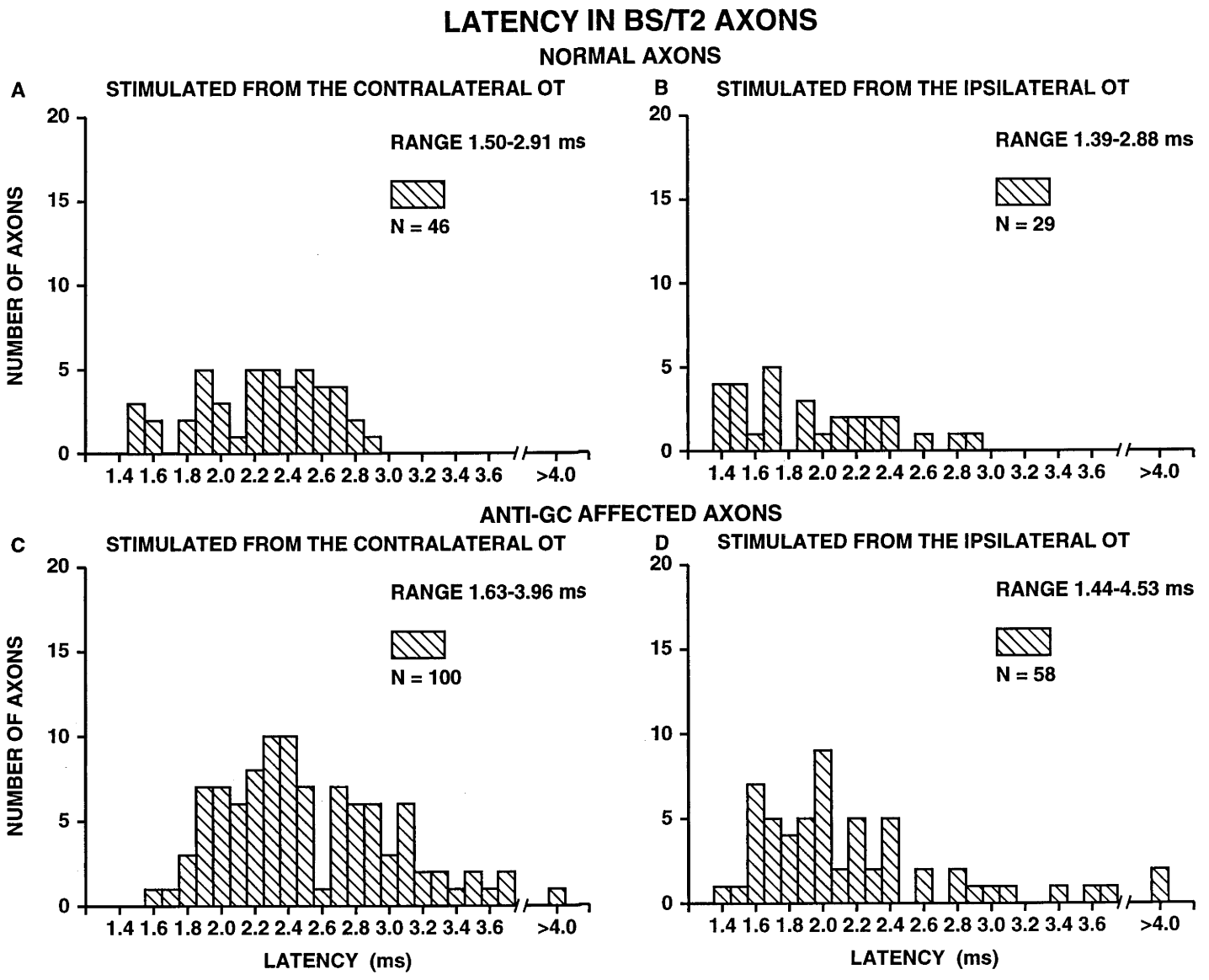
LATENCY IN BS/T2 AXONS
NORMAL AXONS
A
STIMULATED FROM THE CONTRALATERAL OT
RANGE 1.50-2.91 ms
N = 46
B
STIMULATED FROM THE IPSILATERAL OT
RANGE 1.39-2.88 ms
N = 29
ANTI-GC AFFECTED AXONS
C
STIMULATED FROM THE CONTRALATERAL OT
RANGE 1.63-3.96 ms
N = 100
D
STIMULATED FROM THE IPSILATERAL OT
RANGE 1.44-4.53 ms
N = 58
NUMBER OF AXONS
0
5
10
15
20
1.4 1.6 1.8 2.0 2.2 2.4 2.6 2.8 3.0 3.2 3.4 3.6 >4.0
LATENCY (ms)

FIGURE 5.5 Distribution of normal and abnormal fibres around the optic disc.

From a representative animal, CL57, the incidence of axons that are either blocked, have abnormal refractory periods of transmission (RPT) or have normal conduction properties and their recording location around the optic disc. The recording site was noted as a position on a clock face, ie recordings made at the most superior border of the optic disc were located at 12 o'clock (see accompanying diagram of optic disc). The majority of abnormal axons were located in the supratemporal sector of the retina, and to a lesser extent in the infratemporal sector. This would correspond to a probable injection site in the dorsolateral optic nerve, 3 mm behind the eye.

CL57 UNITS BY RECORDING POSITION

BT/T1 AND BS/T2 UNITS, OT STIMULATION

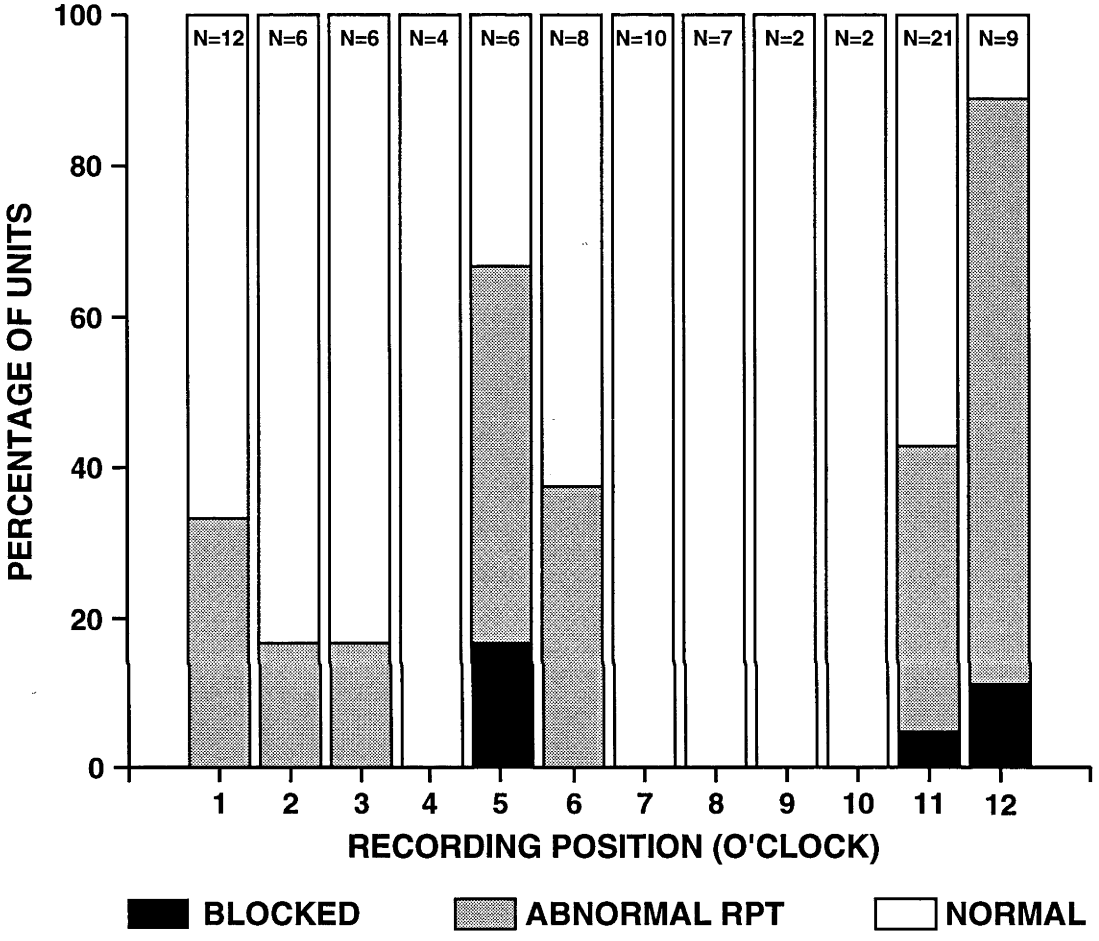

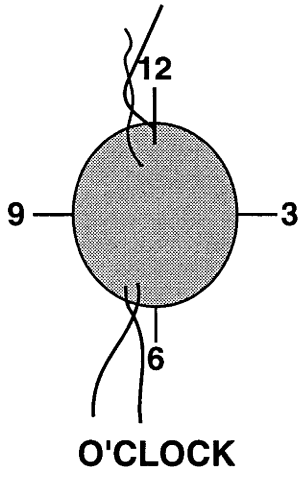

above and to the lateral side of the retrobulbar ON and the injection was made within the ON, the pattern of the distribution of affected fibres is not surprising. All other animals showed similar clustering of conduction abnormalities at specific recording locations around the OD. While this demonstrates the focal nature of the lesion, it also means that recordings made from axons passing through the unaffected regions of the ON increase the proportion of normal fibres detected.

5.3.3b The pressure lesion.

By considering RPT data from RGC recorded as axons or cell bodies and stimulated in either the OT or OX, it was possible to study the distribution of RPT for 37 RGC from LB73, the mild pressure lesion and for 23 from LB85, the severe pressure lesion. While the number of RGC sampled was small, some trends are evident. In the mild pressure lesion (Fig. 5.6.a), the range of RPT values was 0.27 to 3.04 ms. While the distribution of RPT for LB73 appeared to superficially resemble the anti-GC distribution (Fig. 5.1.b), over half the fibres had abnormal RPT. Nearly 70% of the BT/T1 axons had abnormal RPT, while only 2 of the 11 BS/T2 axons were abnormal by this test.

In the severe pressure-lesioned animal, LB85, the BT/T1 class of RGC were even more seriously affected (Fig. 5.6.b). Only one genuine BT/T1 axon was able to transmit across the lesion, and its RPT was grossly increased beyond the normal range (2.09 ms), which was the maximum RPT recorded in this animal. Of the 22 BS/T2 units, nine had abnormal RPT and the remaining 13 with RPT <0.65 ms, had a mean RPT of 0.57 ms. Even though the sample is small, the average RPT and minimum RPT value suggest a shift towards the upper end of the normal distribution of the RPT of the BS/T2 class of RGC with RPT <0.65 ms, implying the presence of abnormal RGC with RPT still in the normal range. This also shows that while the BT/T1 axons were probably almost all damaged by the application of heavy pressure to the nerve, the medium diameter BS/T2 axons had also suffered some detriment to their ability to conduct closely spaced impulses.

A total of 16 BT/T1 axons from LB73 had latencies ranging from 1.33 to 1.90 ms and only 5 of these had a latency less than 1.50 ms, the upper limit of normal latency from the contralateral OT (Fig. 5.3a). The 17 BS/T2 axons from LB85 had latencies

FIGURE 5.6 Distribution of refractory period of transmission in the pressure -lesioned optic nerves.

The distribution of the refractory periods of transmission (RPTs) measred by the standard two-stimulus test in 37 BT/T1 and BS/T2 axons from the animal LB73 with the milder pressure lesion of the optic nerve compared to the distribution of RPT in 23 axons from the animal LB85 with the more severe pressure lesion. The impulses were generated in either the optic tract (OT) or optic chiasm (OX). Refer to figure 5.1a for the distribution of RPTs in a population of normal animals.

A The distribution of RPT for 25 BT/T1 axons and 12 BS/T2 axons from LB73. The RPT values ranged from 0.27 ms to 3.04 ms. The majority of the BS/T2 axons had normal RPTs, ie < 0.65 ms, but only eight of the BT/T1 axons had normal RPT.

B The distribution of RPT for 1 BT/T1 axon and 22 BS/T2 axons from LB85. The RPT values ranged from 0.40 ms to 2.09 ms. This maximum value belongs to the only BT/T1 axon.

DISTRIBUTION OF REFRACTORY PERIODS OF TRANSMISSION PRESSURE – LESIONED OPTIC NERVE

A BT / T1 AND BS/T2 UNITS FROM LB73, MILD LESION
OT AND OX STIMULATION

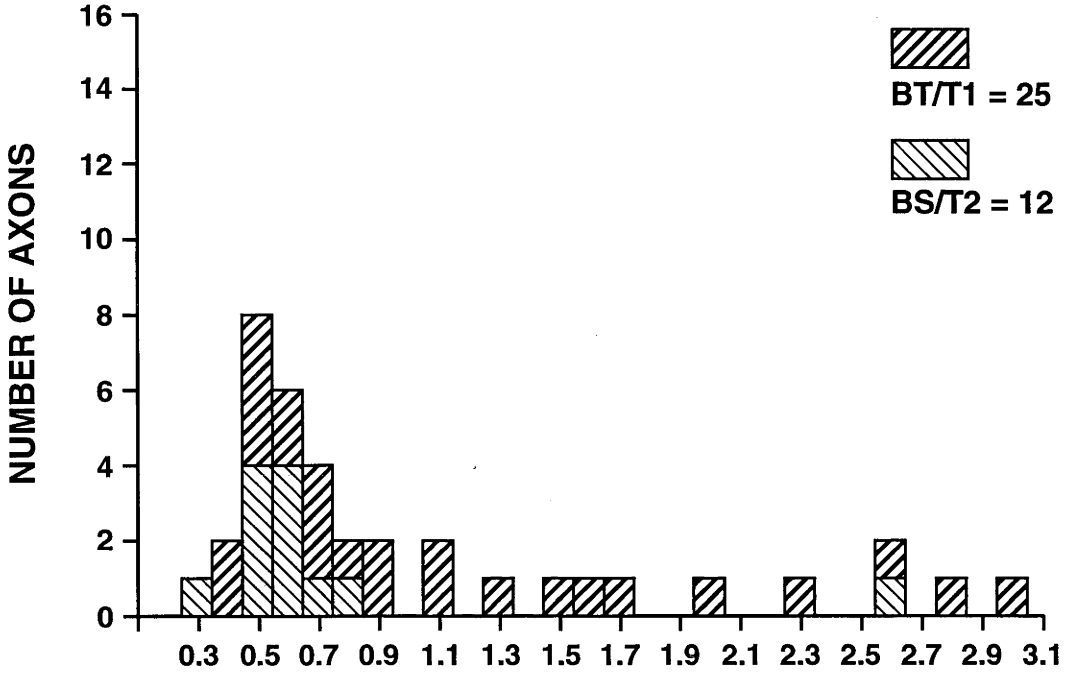

B BT/T1 AND BS/T2 UNITS FROM LB85, SEVERE LESION
OT AND OX STIMULATION

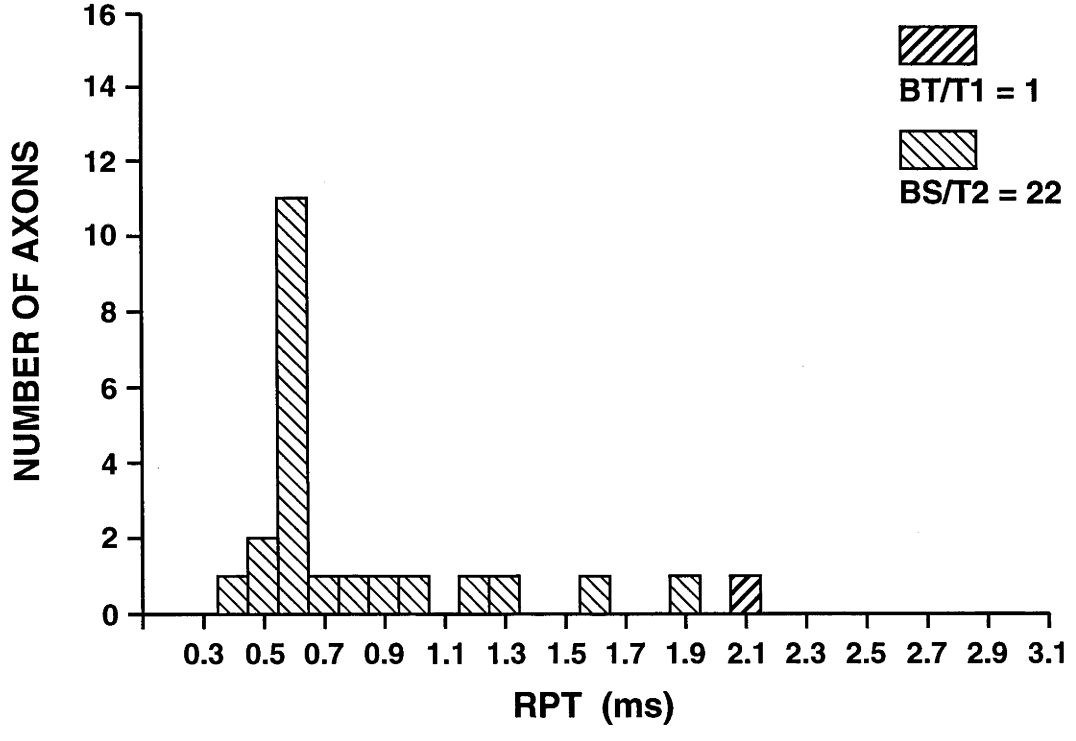

ranging from 2.48 to 3.55 ms, 8 had latencies greater than 2.91 ms, which is the upper limit for BS/T2 axons from the contralateral OT in normal cats (Fig. 5.4a). The significance of these differences is not clear since the placement of electrodes in the pressure-lesioned animals may have been slightly different to the placement in the normal cats.

5.3.4 Recovery from demyelination caused by anti-galactocerebroside.

Eight animals were examined over a period of 2-4 days each. Experiments commenced on different days following the injection of anti-GC and recordings were made between 4-20 days post-injection. This meant that recordings from different animals sometimes overlapped days. No recordings were made for days 14-15 post-injection. The RPT values include recordings made from both axons and cell bodies whether located at the margin of the OD or eccentric to it. However, all measures of latency were only made from axons recorded within 1/2 a disc diameter of the OD margin as, unlike RPT, latency will vary with recording location. Even though the criteria for inclusion in the latency series was more restrictive than the RPT, more RGC had latency than RPT measured, so the latency population is larger (N = 638) than the RPT (N = 563). Finally, the days post-injection are grouped to provide sufficient numbers to show trends.

The progressive recovery of conduction, and improvement of latency and RPT (Fig 5.7.a & b) was evident, until by day 18 there were no blocked BT/T1 and BS/T2 units and only 3.6% of axons had abnormal latency and 10.4% had abnormal RPT. If axons originating in sectors of the ON unaffected by the anti-GC injection dominated the recordings made, for example, on 16-20 days post-injection, this may bias the data towards apparent normality on those days. To demonstrate that recovery was not an artefact of recording from around the whole OD margin including sectors of predominantly normal axons, a separate graph is presented, of recordings made from the most affected quadrant of the OD in each animal (Fig. 5.8), such as between the 11 to 1 o'clock recording location in CL57 (Fig. 5.5). This additional graph clearly shows that recovery of RPT was occurring after day 7, even in the most affected regions of the demyelinated ON, with the percentage of abnormal or blocked RGC dropping from 95%

FIGURE 5.7 Recovery of conduction from demyelination.

The distribution of proportions of BT/T1 and BS/T2 optic fibres observed to have either conduction block, abnormal conduction parameters or normal conduction on the days following the micro-injection of anti galactocerebroside into the optic nerve. No data was obtained for days 14-15 post-injection. The stimulating electrode was located in the optic tract (OT) and recordings were made from axons at the optic disc margin.

A The percentages of fibres recorded at the optic disc, which were blocked and those that had abnormal or normal RPT on the different days post-injection.

B The percentages of fibres which were blocked and those that had abnormal or normal latency on the different days post-injection.

Note that the recovery of normal latency measurements was greater on days 16-20 post-injection, than the recovery in RPT.

RECOVERY OF CONDUCTION FROM DEMYELINATION BY ANTI-GC

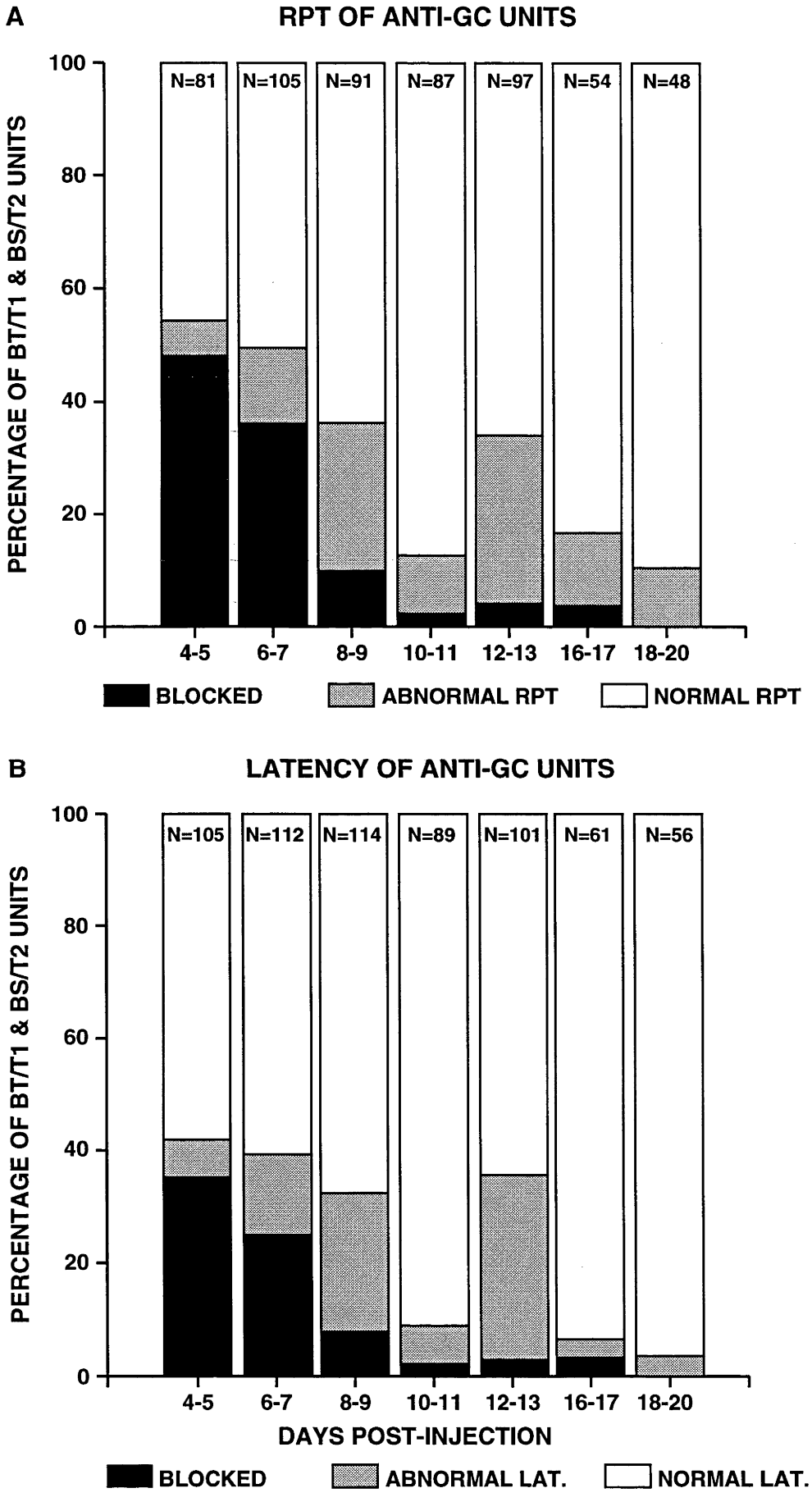

FIGURE 5.8 Recovery of conduction from demyelination in the most affected quadrants of the retina.

To ascertain whether the apparent recovery of optic fibres from conduction block and abnormal refractory period of transmission could be contributed to by the inclusion of the high percentage of normal fibres due to the focal nature of the lesion, only axons from the most affected quadrants around the optic disc margin (see Fig. 5.4, p 152) were included in this analysis. It can be seen that the trend observed in figure 5.7, towards recovery from conduction block and the later recovery of RPT, is maintained.

RECOVERY FROM ANTI-GC INJECTIONS
UNITS FROM THE MOST AFFECTED QUADRANTS

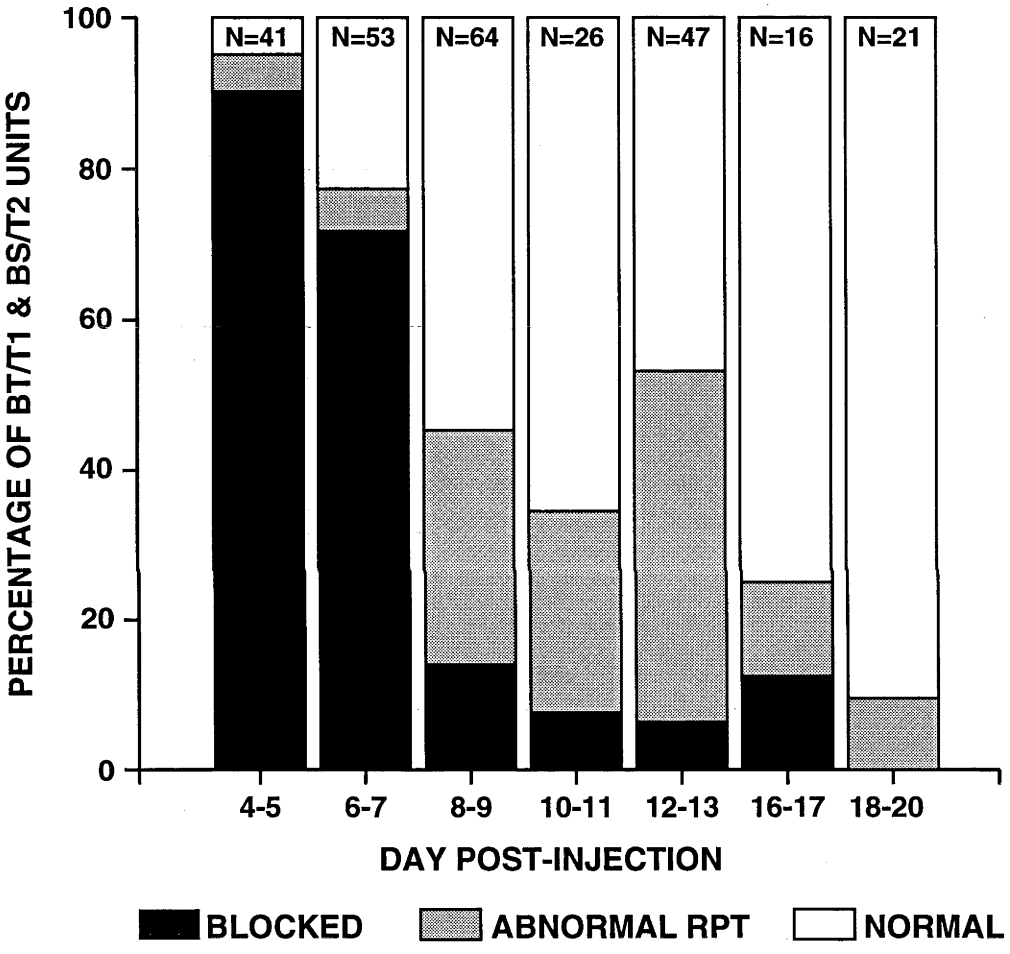

on days 4-5 post-injection to less than 10% by days 18-20.

The effect of recording on different days from sectors of the OD margin which contain predominantly either normal or abnormal axons does, however, account for some of the fluctuations in the progressive recovery of RPT and latency. On days 10-11 post-injection (Fig 5.7.a & b), recordings were made of axons from the predominantly unaffected sectors of the ON, as is evidenced by the marked increase in the proportion of RGC with abnormal RPT on days 10-11, when recordings from the most affected quadrant only are considered (Fig. 5.8).

By re-grouping the data into the appropriate days post-injection, 4-6, 7-13 and 16-20 (Carroll et al., 1985, 1990), it becomes even clearer that the conduction properties were undergoing recovery before remyelination, that is before day 14. This approach also gives sufficient numbers of the BT/T1 and BS/T2 classes of RGC in each time-frame, for the different classes to be considered separately.

One feature of the all the post-injection graphs of latency and RPT for BT/T1 and BS/T2 units (Fig. 5.9), is the marked increase in the number of RGC conducting abnormally after day 6, coupled with a dramatic decrease in the number of blocked RGC. It appears that BT/T1 and BS/T2 units that may have been previously blocked have recovered sufficiently to conduct impulses but with slowed CV and lengthened RPT. In addition, an examination of the distribution of abnormal RPTs (ie. RPT >0.65 ms) for all the days post-lesion (Fig. 5.10) clearly shows that the most severely affected RPT measurements in BT/T1 and BS/T2 units were encountered on days 7-13 post-lesion. While the mean abnormal RPT did not vary considerably from days 7-13, where it was 1.33 ms (± 0.90), to days 4-6 (average 1.27 ms, ± 0.25) and days 16-20 (average 1.12 ms, ± 0.41), the standard deviation measurements show an obvious increase in the degree of abnormal RPT found during the middle period of recovery and the maximum RPT of 4.90 ms was recorded on day 12.

There appear to only be minor differences in the degree and rate of recovery of latency and RPT for the BT/T1 versus BS/T2 units, the main difference occurring in the rate of recovery of RPT in BT/T1 units over days 16-20 post-injection (Fig. 5.9a). The percentage of BT/T1 RGC with abnormal RPT on days 16-20 was 17.5%, while the rate for BS/T2 RGC, was less than 4%. However, the rate of abnormal latency in both BT/T1

FIGURE 5.9 Recovery of conduction from demyelination.

The proportions of BT/T1 and BS/T2 retinal ganglion cells (RGC) that have either conduction block, abnormal conduction parameters or normal conduction are grouped by days 4-6, 7-13 and 16-20 post-injection, paralleling the time frame for significant changes in the lesion that were observed histologically (p 137, this chapter, Carroll et al., 1990).

A The percentages of 382 BT/T1 RGC observed to be either blocked, or to have abnormal or normal RPT over the days 4-20 post-injection.

B Observations of 179 BS/T2 RGC from days 4-20 post-injection, with conduction block and where possible, the RPT measured.

The RPT in these units appeared to take longer to recover than the BS/T2 units, as the percentage of units with abnormal RPT still remains above 10 % for days 16-20 post-injection.

C Conduction block determined and latency measured where possible in 451 BT/T1 optic fibres from days 4-20 post-injection. Unlike the RPT neasurements, latencies were recorded only from axons at the optic disc margin.

D Conduction block, and latency assessed in 187 BS/T2 optic fibres over days 4-20 post-injection.

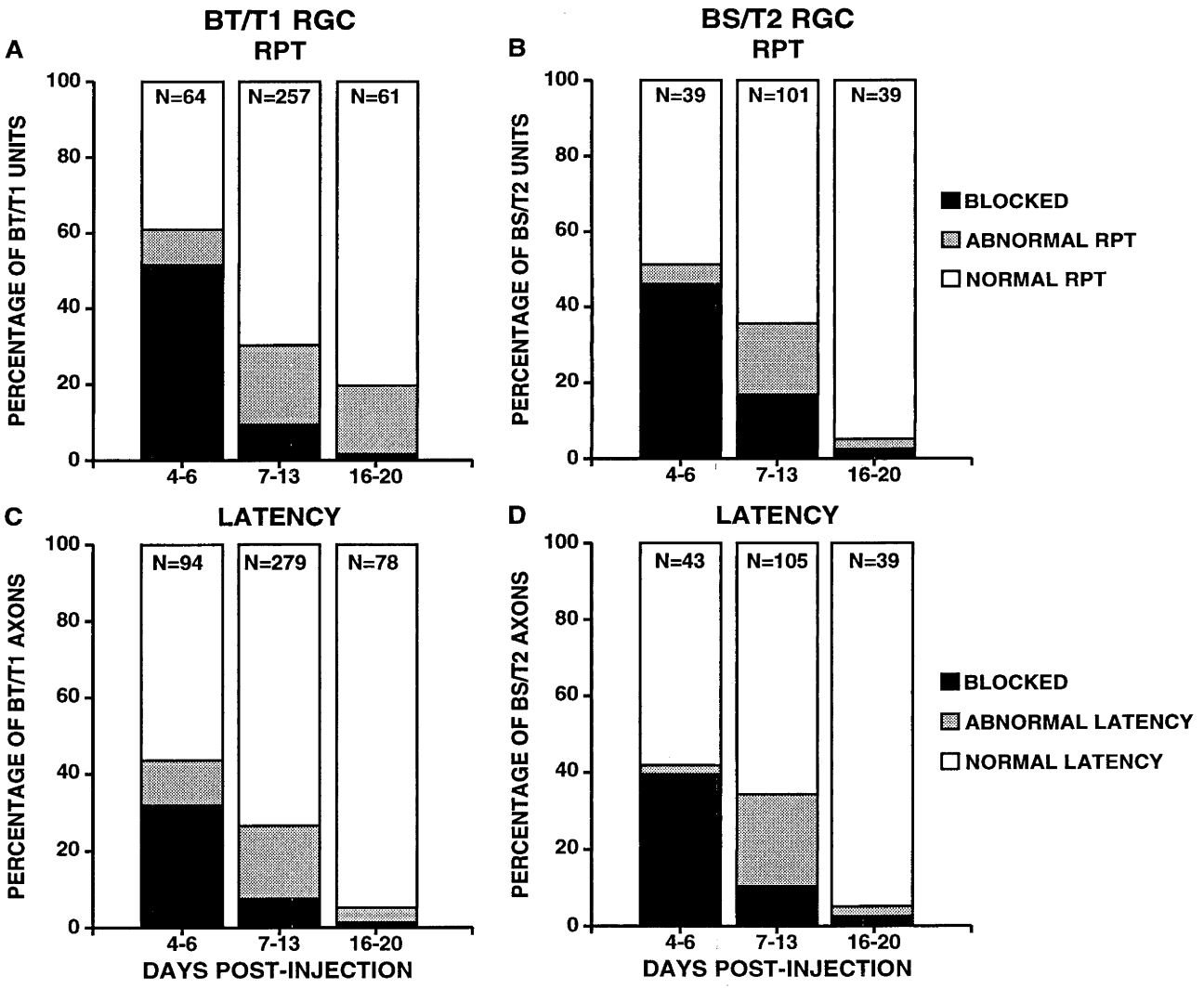
RECOVERY OF CONDUCTION FROM ANTI-GC INJECTIONS
DATA GROUPED FOR COMPARISON WITH MORPHOLOGICAL CHANGES
A
BT/T1 RGC
RPT
PERCENTAGE OF BT/T1 UNITS
N=64
N=257
N=61
B
BS/T2 RGC
RPT
PERCENTAGE OF BS/T2 UNITS
N=39
N=101
N=39
BLOCKED
ABNORMAL RPT
NORMAL RPT
C
LATENCY
PERCENTAGE OF BT/T1 AXONS
N=94
N=279
N=78
D
LATENCY
PERCENTAGE OF BS/T2 AXONS
N=43
N=105
N=39
BLOCKED
ABNORMAL LATENCY
NORMAL LATENCY
0
20
40
60
80
100
4-6
7-13
16-20
DAYS POST-INJECTION

FIGURE 5.10 Abnormal refractory period of transmission in the anti-galactocerebroside affected axons by days post-injection.

To further illustrate the possible two phases of recovery of BT/T1 and BS/T2 axons, the refractory period of transmission (RPT) of 93 axons with RPT > 0.65 ms are plotted against the time post-injection that they were recorded. It can be seen that between days 4-6, when the majority of abnormal axons were blocked, the values of the abnormal RPTs were only moderately elevated. However, between days 7-13 post-injection, there were a number of axons with very abnormal RPT values. Only one very long RPT value was evident for days 16 to 20 post-injection.

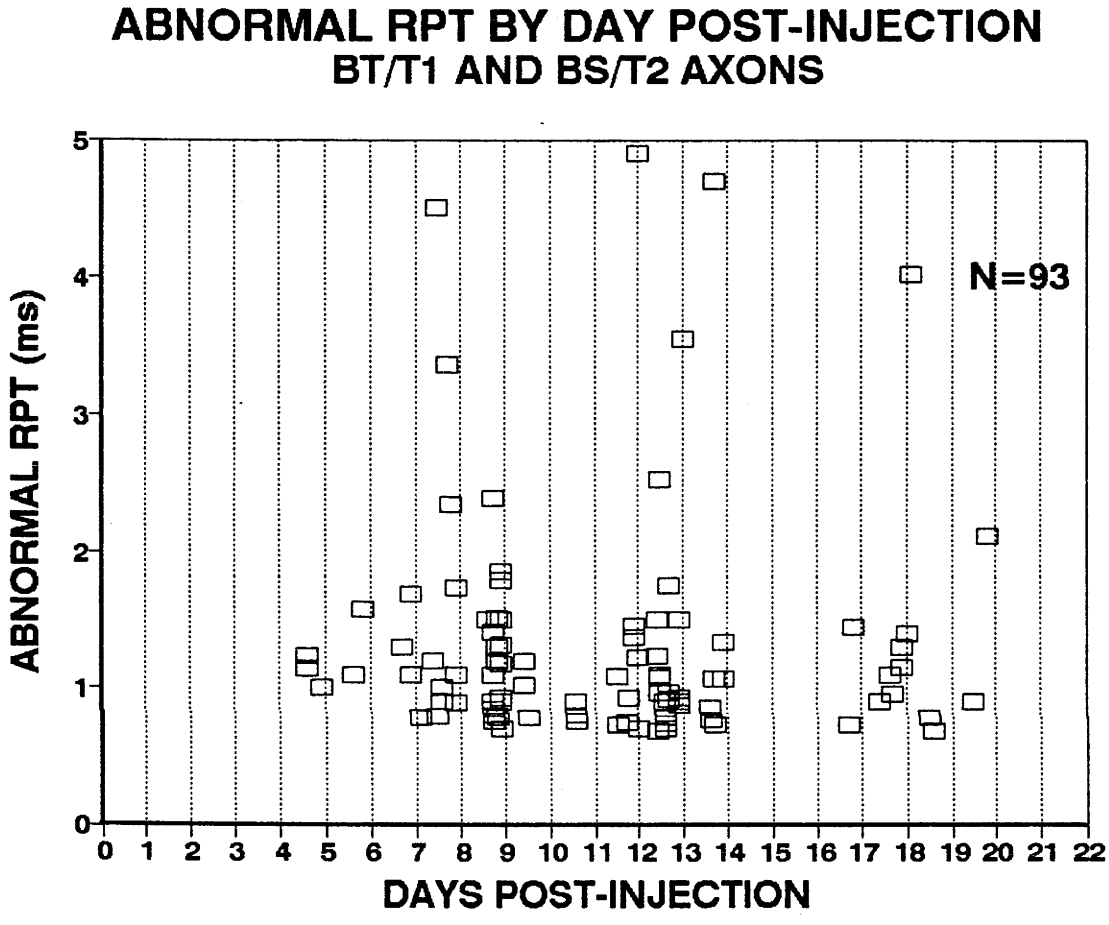
ABNORMAL RPT BY DAY POST-INJECTION
BT/T1 AND BS/T2 AXONS
ABNORMAL RPT (ms)
DAYS POST-INJECTION
N=93
0
1
2
3
4
5
0 1 2 3 4 5 6 7 8 9 10 11 12 13 14 15 16 17 18 19 20 21 22

FIGURE 5.11 Recovery from demyelination of non-brisk units.

Recovery from conduction block in retinal ganglion cells (RGC) classified as having non-brisk responses to visual stimulation. Normally RGC of this classification are considered to be the correlates of the slowly conducting T3 fibres, but because many were blocked, classification could not be confirmed by latency measurements. Because there is little control data for the conduction properties of T3 fibres, this graph only considers whether these RGC were blocked or not. Unlike the BT/T1 and BS/T2 RGCs, recovery from conduction block was delayed until days 16-20 post-injection.

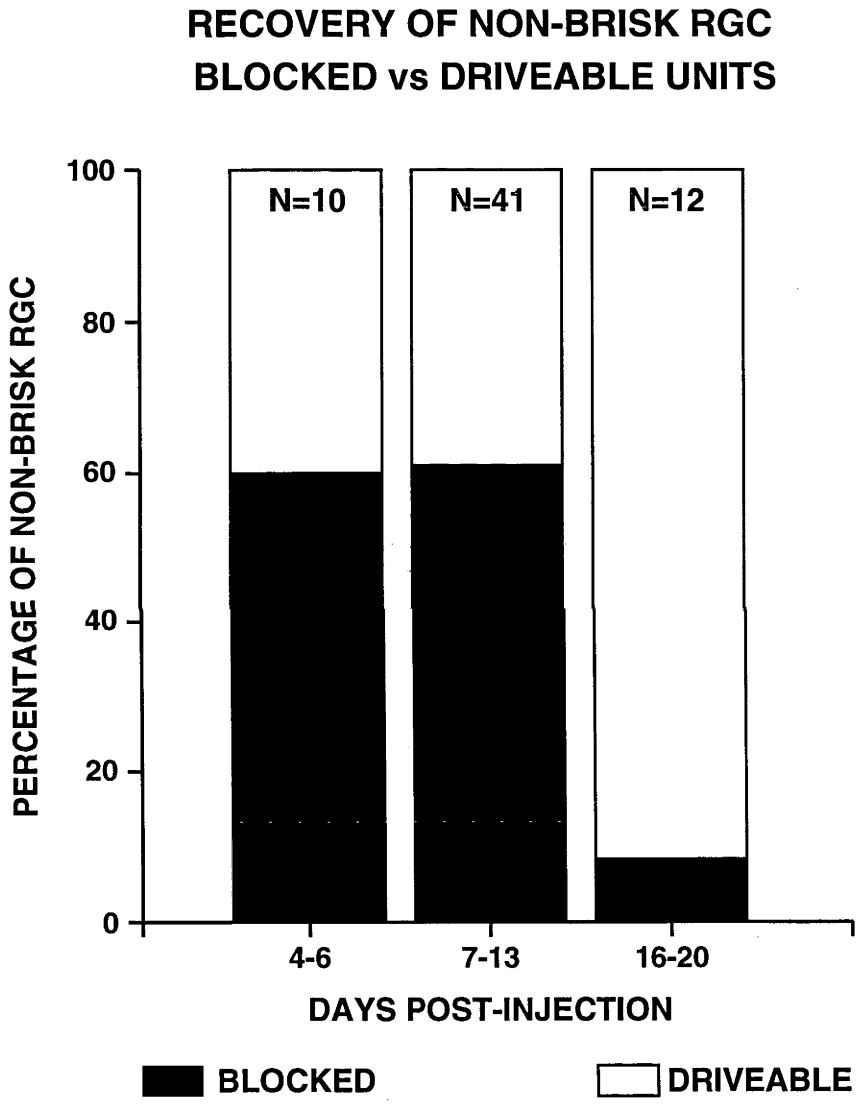
RECOVERY OF NON-BRISK RGC
BLOCKED vs DRIVEABLE UNITS
PERCENTAGE OF NON-BRISK RGC
100
80
60
40
20
0
N=10
N=41
N=12
4-6
7-13
16-20
DAYS POST-INJECTION
BLOCKED
DRIVEABLE

and BS/T2 axons was also below 4%.

The final graph (Fig. 5.11) of 63 RGC with non-brisk type of responses to visual stimulation (which could include some "sick BT"), shows an interesting departure from the pattern of recovery observed so far. Because the range of normal RPT and latency for these classes of RGC has not been established, only whether they are blocked or can conduct impulses, can be assessed. Here the number of blocked axons remains high, approximately 60%, up to day 13 post-injection. Then there is a dramatic return of conduction by day 16, when the percentage of units blocked falls below 10%.

5.4 DISCUSSION

5.4.1 Conduction parameters and demyelination.

Both RPT and latency are indicators of axonal integrity and it is apparent from the data that they can vary independently. In the 430 axons from the anti-GC animals with both latency and RPT values, 10.9% had both abnormal RPT and latency, but a further 14.4% of axons had either abnormal RPT or abnormal latency. There was no consistent correlation between the amount latency was slowed and the degree to which RPT was lengthened (Fig. 5.2). Similarly, the pressure lesioned animals showed instances of RGC with abnormal RPT and normal latency, and vice versa. It has been suggested that RPT may be a more reliable indicator of the clinical deficit caused by demyelination (Smith and Hall, 1980, Shefner and Dawson, 1990), however, this study would suggest that they are equally sensitive but, at least, partially dissociated measures of axonal function.

The speed with which an impulse can propagate depends upon the rate at which local circuit currents can depolarise the next inactive node, ahead of the impulse, whereas the RPT is more dependent on the kinetics of recovery from activation/inactivation. This suggests that RPT and latency are measuring two separate aspects of transmission. Differences in the degree to which they are altered by demyelination will also arise because RPT is a measure of the handicap at the most severely demyelinated point on the axon, whereas latency measures the functionality of a length of fibre. It could be that paranodal demyelination versus general thinning of

myelin, or the demyelination of one internode versus a length of axon encompassing many internodes, will differentially contribute to the slowing of an impulse or to the minimum interval before a second impulse can propagate successfully. The collision paradigm discussed in Chapter 6, provides some evidence to support the contention that variations in the lesion itself may affect RPT and latency to different degrees. It also introduces an explanation of the axons that have very long RPT with relatively unaffected latency (see Fig. 5.2).

5.4.2 The anti-galactocerebroside lesion and remyelination of fibres.

In this study the conduction parameters of single optic fibres have been examined during recovery from antibody-mediated demyelination caused by intraneural injection of anti-GC. This model has the advantage of paralleling the human CNS multifocal demyelinating neuropathies, such as MS. The most significant observation of this study is that conduction returns before remyelination.

Following the intraneural injection of anti-GC, there is progressive recovery from conduction block and gradual improvement of both latency and RPT in BT/T1 and BS/T2 RGC over the 20-day post-injection period (Fig. 5.7). The initial and greatest degree of recovery of conduction, in particular from conduction block, occurs between days 7-13 post-injection, coinciding with the complete removal of myelin and preceding remyelination (Carroll et al., 1990). There have been other reports of return of conduction prior to remyelination, both in the PNS and CNS (Smith and Hall, 1980, Bostock et al., 1980, Smith et al., 1982, Kaji et al., 1988).

Since demyelination is typically thought to cause conduction block in the first instance, it would seem to be logical that restoration of myelin would be necessary to return function. However, as this study shows that remyelination is not necessary for the recovery of function, the question arises as to what else may occur to the demyelinated and blocked axon to cause it to regain the ability to conduct impulses.

It has been suggested that an aggregation and redistribution of Na^+ channels in the demyelinated axolemma, at shorter than normal internodal spacing, may assist the restoration of conduction (Smith et al., 1982), prior to remyelination. If such

aggregations of Na^+ channels occur, then their primary effect would be to increase the security of conduction, rather than to speed up the transmission of impulses.

Such new aggregations of Na^+ channels, named "phi nodes" have been detected electrophysiologically, at shorter than normal internodal spacing, following experimental demyelination in the PNS (Bostock et al., 1980, Smith et al., 1982). There is also much morphological evidence, ranging from freeze-fracture studies to immunocytochemistry (see Chapter 1, p 40) which add weight to the body of evidence that Na^+ channels are reorganised in the internodal axolemma prior to remyelination. The reduced internodal spacing would be critical for these new or "phi nodes" to have a beneficial effect on safety factor for conduction (Waxman and Brill, 1978) and they may sustain conduction, even if the density of Na^+ channels is low (Waxman et al., 1989). However, that demyelinated axons form "phi nodes" prior to remyelination has recently been disputed by Dugandzija-Novakovic et al. (1995).

Another mechanism by which demyelinated axons could restore function is a reduction in axonal diameter in the region of demyelination. Reduction in axonal diameter has been observed within MS plaques (Prineas and Connell, 1978) and also seen to occur shortly after the application of anti-GC (Saida et al., 1980). While this may be theoretically expected to improve the safety margin for conduction (Goldstein, 1978), reduction of axonal diameter was not associated with return of conduction in the axons demyelinated with anti-GC (Saida et al., 1980).

Because of the infrequency of parallel electrophysiological and morphological studies of demyelination and remyelination, in particular using the new opportunities provided by the visualisation of Na^+ channels using polyclonal antibodies, it is difficult to draw conclusions as to the exact nature of the structural changes in the axon that might facilitate conduction and their dependence upon association with myelinating cells or other glial cells such as astrocytes. Studies of both CNS and PNS fibres using a variety of demyelinating agents that permit the remyelination of axons, such as anti-GC in the CNS, are needed to clarify the present uncertainty that surrounds these questions.

After day 14 post-injection, there was a substantial reduction of the percentage of fibres both blocked and with abnormal conduction parameters (Fig. 5.7). This further recovery may be associated with remyelination, since, after day 14, significant

remyelination was observed (Carroll et al., 1990). Even though the remyelinated axon usually has thinner than normal myelin and shorter than normal internodal lengths, both in the CNS (Gledhill et al., 1973; Blakemore and Murray, 1981; Smith et al., 1981) and PNS (Saida et al., 1980;) such remyelinated axons have been shown to conduct impulses at rates near normal (Smith et al., 1981). Paralleling the morphological observation of 95% of axons remyelinated 24 days after injection with anti-GC (Carroll et al., 1990), in this electrophysiological examination, between days 18-20 post-injection, over 90% of BT/T1 and BS/T2 units were conducting normally.

5.4.2b Two phases of recovery of conduction.

Those results also suggest that recovery of conduction occurs in two phases. Certainly, the graphs of recovery demonstrate a gradual decline in the percentage of axons blocked, but the progression of recovery from abnormal conduction was not smooth. The percentage of BT/T1 and BS/T2 units with abnormal latency and RPT (Fig. 5.9) more than doubled on days 7-13 post-injection. This suggests that RGC which may have been previously blocked, had recovered sufficiently to conduct impulses but were doing so abnormally. This is reinforced by the increase of very abnormal RPT measurements over days 7-13 (Fig. 5.10) and the reduction in the range of abnormal RPTs again by days 16-20 post-injection. It appears that at least some axons advance from being blocked to conducting impulses very abnormally, and then to partial improvement of conduction parameters progressing to complete recovery. These stages may coincide with initial demyelination, followed by structural alterations of the axolemma and finally gradual acquisition of myelin which progressively thickens.

5.4.2b Recovery of the non-brisk units.

In Figure 5.11, the recovery of conduction of the non-brisk RGC occurs after the commencement of remyelination, and later than for the BT/T1 and BS/T2 RGC. It needs to be stressed that the statement that non-brisk RGC recover more slowly from demyelination than larger diameter axons, cannot be made with any certainty. Firstly, the numbers were small. Secondly, it is possible that many of these RGC were in fact "sick

BTs". It would be expected that axons that have been so badly damaged as to cause major disruption of the responses of the RGC to visual stimuli, may take longer to recover than axons that have been demyelinated but retain their normal responses.

This hypothesis could be taken further. It may be that axons which are demyelinated but which retain intact axon cylinders have the capacity to synthesise and/or reorganise Na^+ channels in the demyelinating axolemma. However, those axons in which the internal axonal transport mechanism is disrupted may lose this capacity due to the loss of supply of necessary components and/or re-routing of metabolism towards attempted regeneration. They therefore may have to wait until continuity is restored, and then undergo delayed structural alteration or remyelination before being able to conduct impulses again. This, however, does imply that the axonal disruption was less severe than axotomy, as axotomised mammalian CNS fibres have a poor capacity for functional regeneration.

The delay in recovery of the "sick BT" fibres may also partially account for the increased percentage of BT/T1 units with lengthened RPT at days 16-20 post-injection (Fig. 5.9a). If severely affected "sick BTs" were recovering by day 16 and their pattern of recovery was gradual, as has been suggested for other RGC, then it would be anticipated that by days 16-20 post-injection, they would be conducting impulses, albeit abnormally. This does not explain the difference between the proportions of abnormal latency and RPT for BT/T1 units on those days. Perhaps that lies in the way in which these particular axons were injured (such as a small but severely damaged segment of axon) and the way in which such an injury would differentially affect latency versus RPT. This is explored further in Chapter 6.

There is a further factor which needs to be considered. The external application of anti-GC has been found to block more rapidly those peripheral nerve fibres conducting at less than 30 m/s (Lafontaine et al., 1982). The susceptibility of slowly conducting fibres to the external application of anti-GC may be due to a less effective seal between the axon and myelin at the paranode by the myelin microvilli in small diameter fibres (Landon and Hall, 1976, Berthold, 1978). While this initially allows greater access by external agents to the paranodal axolemma, it does not, however, suggest a reason for the greater resistance of the small diameter axons to remyelination.

5.4.3 Are there "sick BTs."?

Failure to encounter BT/T1 axons in the same proportions as in the normal population implies the absence of their axons at the recording sites apparently due to axonal degeneration, possibly caused by axotomy. In LB85, the animal with the heavier pressure lesion, if the missing BT/T1 axons (71.8%) have completely degenerated, then the proportions of the remaining BS/T2 and non-brisk neurons should be 9 BS/T2 axons to every non-brisk axon, as seen in the normal population (Table 5.1). Instead, the BS/T2 and non-brisk axons are encountered in approximately equal proportions.

This can be explained in two ways. First, in addition to the degeneration of the BT/T1 axons, a proportion of the BS/T2 axons could also have degenerated. In LB85, if no BS/T2 axons had degenerated, then the percentage of BS/T2 axons encountered would have been 85.3%. As the actual percentage was 45.2% (Table 5.1), it would suggest that some 40% of the BS/T2 class of RGC would have also degenerated. This would not be expected, as it has previously been reported that it is predominantly the large diameter axons that were affected by the application of pressure to the optic nerve (Burke et al., 1985, 1986). Furthermore, in LB73, with a reduction of only 8.2% in BT/T1 axons encountered, the actual rate at which BS/T2 axons were recorded (Table 5.1) was close to the anticipated rate of 28.1%. If severe pressure destroys BS/T2 fibres to a greater extent than mild amounts of pressure, then it would also be expected that the proportion of blocked BS/T2 units in LB85 would significantly exceed the percentage blocked in LB73. They were in fact the same (Table 5.2).

A second explanation of the increased encounter rate for blocked non-brisk axons in LB85, could be the misidentification of some of the BT/T1 RGC into the non-brisk class, because of reliance on the receptive field properties of the parent ganglion cell. It is possible that the visual receptive field properties might in fact be severely altered by some functional interruption of the cell's axon at a distant location. If this was the case, the affected BT/T1 RGC would not have degenerated, as their cell bodies were still responding, albeit with markedly different response properties. As already noted, the responses to visual stimulation of a number of the non-brisk RGC from LB85 was atypical, and in some cases their classification as non-brisk/T3 axons was not supported by their conduction latency from the ON stimulus site, which is situated downstream

from the lesion.

Some of the axons included in the non-brisk class of RGC from the anti-GC affected animals also had atypical visual responses and the encounter rate for non-brisk axons was also 4% greater than would be anticipated by a decline of 11.7% in the percentage of BT/T1 axons and 9:1 ratio between axons of the BS/T2 and non-brisk classes of RGC. It is possible that some of the large diameter fibres in the ON of the animals injected with anti-GC may have been directly injured or indirectly subjected to a transitory rise in pressure within the ON associated with the injection. There is morphological evidence of a small number of degenerating axons after intraneural injection with anti-GC, consistent with severe damage to some axons by the injection (Sergott et al., 1984, Carroll et al., 1984).

The possibility that neurons which suffer severe axonal injury, in addition to becoming blocked, may have had the behaviour of their cell body altered, is not a new idea. In this case, it implies that injury remote to the RGC cell body can change the manner in which the RGC responds to visual stimuli. Then the question arises as to what may be occurring to the neuron to change its behaviour.

The receptive field of a RGC is that region of the visual field in which the application of a visual stimulus will alter the ongoing discharge of the RGC. The different characteristics of the receptive fields of the various classes of RGC (Chapter 2, pp 68-70) appear to be mediated by the complex connections of the structural elements within the retina (Chapter 1, p 47).

Contacts made by the RGC with other retinal cells are vital for the formation of its characteristic receptive field. Any loss of these contacts would have profound consequences for the RGC responses to visual stimuli. Marked changes in the morphology of neurons following axotomy are well known (Liebermann, 1971; Barron, 1975) but in the severe pressure lesion, while a small proportion of fibres may have been severed, it is probable that many have been sufficiently injured to cause complete degeneration, or partial degeneration (ie degeneration which has obliterated only part of an axon, but which may progress to complete degeneration).

Retraction of the dendritic tree of hypoglossal neurons following the blockage of neuromuscular transmission due to interference with the mechanism for release of

acetylcholine caused by injection of botulinus toxin into the tongue of rats (Sumner and Watson, 1971), and more specifically, decreases in the number of synaptic boutons per dendrite (Sumner, 1977) have been reported. This would appear to suggest that failure of normal synaptic activity can cause degenerative changes in dendritic structure and loss of synaptic inputs to those dendrites.

5.4.3a A role for neurotrophic factors.

It has also been shown that neuronal electrical activity may regulate the rate of release of neurotrophic factors from the targets of neurons (Black, 1993). Neurotrophic factors can originate from the innervated post-synaptic cell and pass into the terminal synapses of the innervating neuron and hence to the perikaryon of the cell by retrograde axonal transport (Hendry et al., 1974). There is a substantial body of evidence to suggest that a variety of these molecules regulates the survival of cells during development (Purves and Lichtman, 1985). Neurotrophic factors are also thought to determine regeneration after injury and in some cases, the viability of adult neurons (Ruit et al., 1990). The target of a neuron also appears to regulate the spread and pattern of dendrites of the cell and its synaptic connections (Purves et al., 1988).

Interrupting retrograde axonal transport by the application of colchicine produces a decline in the number of presynaptic terminals that innervate the affected neuron and transmission of antidromic action potentials into the soma of the cell tends to fail. These changes are similar to those seen following axotomy. (Purves, 1976). These changes can be partially prevented by the local supply to the cell body of axotomised neurons, of exogenous nerve growth factor, a well-known neurotrophic factor (Nja and Purves, 1978).

It is possible that the supply of some critical neurotrophic factor to the RGC has been interrupted, either by the failure for several weeks of orthodromic electrical activity along the axon (implied by the failure of antidromic activation) or by actual physical interruption of the axonal transport mechanisms at the site of pressure application. Because not all signs of the receptive field have disappeared, it can be assumed that some synaptic contacts with other retinal cells are retained. Continued, but altered synaptic transmission has been observed even with considerably reduced synaptic contacts

following axotomy (Eugene and Taxi, 1991).

5.4.3b A role for cell coupling?

While changes to the structure of the injured BT/T1 axon may hinder the RGC's ability to retain synaptic contacts with other retinal cells, it is possible that the degeneration of a proportion of the BT/T1 cells in the retina may also affect the behaviour of the remaining BT/T1 RGC. Even if all non-brisk RGC encountered in LB85 were "sick BTs" then it still would not account for nearly 22% of the normal BT/T1 population. Even though RGC are known to be strongly resistant to degeneration (Leinfelder, 1938, Stone, 1966, Maffei and Fiorentini, 1981), it would be reasonable to assume that at least this percentage of the BT/T1 class of RGC had completely degenerated several weeks after the application of pressure.

There is some evidence that BT/T1(Y) RGC may be linked to other BT/T1 RGC that have the same centre response characteristics. Mastronarde (1983) demonstrated that the antidromic activation of single BT/T1 RGC would increase the firing rate of a neighbouring BT/T1 RGC with the same centre response. Because the delay between the interactions was short, Mastronarde suggested that they were mediated by a specialised electrical junction, either from ganglion cell to cell, or indirectly via interneurons.

More recently, by using the tracer neurobiotin, alpha cells, the morphological correlates of BT/T1(Y) RGC (Chapter 1, p 49), have been shown to be coupled to several other alpha cells of the same centre response-type that are regularly arranged around the dendritic margin of the injected RGC (Vaney, 1991). Interestingly the beta (BS, X) cells did not show tracer coupling. This suggests that there are connections between BT/T1 ganglion cells that may be important for their normal behaviour. While the diameter of the receptive field of a BT/T1 RGC does not encompass the dendritic spread of a BT/T1 RGC and its surrounding linked cells, Vaney (1994) has suggested that the coupling of alpha cells may enhance their response profile, without significantly enlarging the receptive field size, but this remains to be established. If this were the case, when neighbouring BT/T1 cells have degenerated, this may alter the responses of the remaining BT/T1 cell.

While it was not possible within the scope of this study to determine which of the mechanisms outlined above leads to changes in the receptive field behaviour of RGC, it seems clear that there were some cells within the retina of the animals with injured axons, that had atypical responses to visual stimulation and were unable to transmit impulses through the region of the lesion. They were more prevalent in the pressure lesion and their frequency increased with the severity of the lesion. It is suggested that these are BT/T1 RGC which have lost vital synaptic contacts with retinal interneurons such as amacrine cells or have lost input from surrounding BT/T1 RGC that have degenerated.

5.4.4 Comments on the pressure lesion

The use of a cuff to apply pressure to the ON has been used to selectively block the BT/T1 class of RGC and thereby reveal the physiological role of BT/T1 axons in vision by examining the effects of their absence on the receptive fields of visual cortical neurones (Burke et al., 1985, 1987, 1992). The efficacy of the BT/T1 block has in the past been assessed by monitoring the elimination of the T1 component of the compound action potential (CAP) generated by electrical stimulation of the optic pathway (Burke et al, 1985). A study of individual optic axons provides a much more detailed appraisal of the effects of the lesion, and gives access to the receptive field characteristics and the opportunity to confirm the identification of the class of RGC, even if the latency had been altered by the lesion.

The present study has shown that the pressure lesion has a substantial impact on the ability of BT/T1 fibres to conduct impulses. The detriment to BT/T1 fibres was particularly noticeable in the severe pressure lesion (LB85) where only one BT/T1 axon was found to conduct impulses across the lesion. This represents <2% of what would have been LB85's proportion of BT/T1 RGC prior to creating the lesion. The milder degree of pressure applied to the ON of LB73, obviously had a less detrimental effect on the BT/T1 population, with 65% of BT/T1 units still being able to conduct impulses across the lesion.

Burke and colleagues (1990) have studied electron micrographs of cross-sections of ON, both upstream and downstream from a pressure lesion. Some 2 to 3 years after the

crush, they observed that there was an average loss of 90% of axons >5 μm in diameter, upstream from the crush site and only 33% downstream towards the cell body. This implies that a considerable percentage of large optic axons had degenerated from the crush site towards the LGN and remained intact below, ie. towards the retina.

Examination of the retina also demonstrated a reduction of approximately 57% of cell bodies with soma diameters greater >25 μm (alpha/BT RGC). Because of the difference in the percentage of degenerated large axons in the ON downstream from the lesion and the loss of RGC bodies with large soma from the retina, it was suggested that some of the large RGC bodies may have shrunk in diameter. Even though these morphological observations were made some time after the crush of the ON, it seems to fit well with the picture emerging from this study, of some disappearance of BT/T1 fibres, a large proportion of undriveable fibres (presumably with intact but altered soma structure) and some unaffected BT/T1 RGC.

Both in the mild and severe pressure lesions, 21.7% of BS/T2 units were blocked. That some damage might be caused to the medium diameter fibres is not unexpected. Gasser and Erlanger (1929) had shown that slower conducting fibres were also susceptible to pressure but to a much lesser extent than the fastest conducting fibres. In an earlier morphological study of the ON lesion (Burke at al., 1986), it was found that only 2% of medium diameter fibres had shown signs of degeneration, although the electrophysiological evidence suggested a higher proportion of damaged BS/T2 fibres in some animals. In explaining the discrepancy between the percentage of degenerating BS/T2 fibres observed morphologically and the percentage of blocked BS/T2 fibres (21.7%) in this study, it is important to note that axons with blocked conduction are not necessarily degenerating. They may just be sufficiently demyelinated to halt conduction of impulses but still retain axonal continuity. Therefore in the pressure-lesioned animals where there was a mix of completely and partially degenerated fibres and demyelinated axons, the number of blocked fibres will exceed the number of partially degenerated fibres.

It may be that, while the BT/T1 axons themselves are more susceptible to direct damage by pressure and therefore more likely to degenerate, the BS/T2 medium diameter fibres are primarily affected by demyelination or mild axonal damage, which

causes them to become blocked but not necessarily to degenerate.

The percentages of blocked BS/T2 fibres in the mild and severe pressure lesioned animals appear not to be related to the magnitude and duration of the pressure applied. This observation must be made with some caution, as a sample of only two animals can only be indicative. However, the situation alters somewhat when the proportions of units that were either blocked or abnormally conducting impulses are considered. In the mild pressure lesion (LB73), 96.0% of the BT/T1 and 39.9% of the BS/T2 units had their ability to conduct impulses either blocked or partially impaired. In LB85, the one BT/T1 RGC detected had abnormal conduction and 62.6% of the BS/T2 units were blocked or had abnormal RPT. These numbers do represent an increase in conduction detriment associated with the magnitude of pressure applied, for both BT/T1 and BS/T2 fibres.

Where there were sufficient latency measurements available, the data confirmed this trend towards an increase in conduction detriment associated with the magnitude of pressure applied. In LB73, 68.8% of the remaining BT/T1 axons had latencies that lay outside the normal range for crossed BT/T1 fibres (Fig. 5.3a). In fact all of these abnormal BT/T1 fibres had latencies that were similar to the normal range for contralateral BS/T2 fibres (Fig. 5.4a), barring any differences in electrode placement. This shift of latencies has implications for those studies using CAPs to assess the degree of damage caused by pressure applied to the ON. Attention should be paid to changes in the breadth and amplitude of the T2 waveform when delayed T1 latencies blend with the T2s, as similarly noted by Gasser and Erlanger (1929, Fig. 1.) when they studied the alpha and beta waveforms of pressure-affected bullfrog peripheral nerve.

The ON pressure lesion has been primarily used to assess the impact of the various classes of RGC on higher visual processing and it can be concluded from this study that it does preferentially block T1/BT (Y) fibres. If attempting to remove all input from the BT/T1 fibres, it is obvious that the degree of block of BT/T1 fibres is directly associated with the magnitude of pressure applied. In addition, in the mild pressure lesion, using latency measures as the sole classification criteria will lead to damaged T1 fibres with slowed CV being included in the T2 category. To achieve the ideal circumstance of all BT/T1 fibres unambiguously blocked and retention of a large proportion of BS/T2 fibres, it would appear to be necessary to apply the more severe lesion. The lesser detriment

suffered by the BS/T2 fibres appears to be approximately 1 in every 50 BS/T2 RGC that are either blocked or degenerated. This is a significant proportion of connected BS/T2 fibres remaining, probably more than sufficient to ensure that the responses of cortical neurons are unchanged.

5.4.5 Summary

1) Recovery of conduction in optic axons demyelinated by micro-injection of anti-GC, occurs prior to remyelination.

2) Recovery of conduction appears to occur in two stages; firstly, in axons that were initially unable to conduct impulses the ability to conduct impulses returns but conduction parameters remain abnormal, and then later, latency and RPT measurements attain normal values.

3) Some RGC demonstrated sluggish but atypical non-brisk responses to visual stimulation. The majority of these RGCs were unable to transmit impulses. A few were able to conduct impulses downstream from the lesion at conduction latencies that were consistent with T1 latencies. It is suggested that these RGC are in fact "sick BTs", that is BT/T1 RGC whose visual responses have been altered by retrograde changes to the cell body and dendrites.

CHAPTER 6.
THE COLLISION PARADIGM IN PATHOLOGICALLY DAMAGED OPTIC AXONS.

6.1 INTRODUCTION

Conduction in damaged axons has usually been studied by measurements of latency and the standard two-stimuli test of refractory period of transmission (RPT). The standard RPT of an axon will be determined by the point on the axon with the lowest safety factor for conduction, while latency is more a measure of the integrity of the whole length of the axon between the stimulating and recording electrodes. However, whether normal conduction is preserved upstream from the injured region of a nerve (ie. towards the stimulating electrode) is not answered by measurements of latency or RPT. The unlesioned region of the nerve is not normally accessible for examination without additional recording electrodes being placed between the stimulus site and the region of damage. The optic pathway is not amenable to such a technique, both because of the surgery required to access the nerve and because of difficulties in recording at multiple sites from individual optic fibres caused by their tortuous course along the optic pathway. By using a collision technique it is possible to determine the conduction parameters in single optic axons, on the stimulus side of a lesion, without exposing the nerve.

The creation of a focal demyelinated lesion by micro-injection of antigalactocerebroside antiserum (anti-GC) into the optic nerve (ON) (Carroll et al., 1984; 1985) or by localised pressure on the ON (Burke et al., 1992), provides an excellent opportunity to study the pathophysiology of single demyelinated optic axons. Focal demyelination and focal pressure occur in various disease states such as multiple sclerosis (MS) and orbital tumours. The symptoms that people suffer as a consequence are due to disturbances in the transmission of impulses along nerve fibres. Transmission of impulses underlies almost every function of the brain. It is therefore valuable to have a detailed knowledge of the effects of demyelination and pressure lesions on the transmission of impulses, with a view to assessing the mechanisms underlying disturbed

transmission. The collision technique has an important advantage over existing methods because it is capable of yielding a much more detailed picture of the nature of the disturbed transmission along the length of the axon, including the segment on the far side of the lesion

6.2 METHODS

The method of performing the collision paradigm has been explained both in Chapters 2 and 4. The D2 versus D1 graph in normal axons has been shown in Fig. 4.1, p 110, and the reasons for its shape, and variations to its profile, have also been described in detail. The space-time diagram was introduced in Chapter 4, pp 109-112 and will be extensively used in this chapter, to assist in the understanding of results obtained.

Axons were selected for analysis by the collision paradigm if measurements of conduction parameters indicated that they were affected by a lesion. These were: 1) if their standard RPT measurement was in excess of the upper limit of the distribution of the standard RPT for normal cats (0.65 ms, Table 6.1 and Fig. 3.4), and/or 2) they had latencies which exceeded the maximum values for latencies in normal BT/T1 and BS/T2 axons (Table 6.2 and Figs 5.3 and 4). A further 2 axons were included because of a significant difference (> 3 standard deviations from the mean) between their standard RPTs (which were >0.62 ms) and the height of the upper plateau of D2 values (see below) in the D2 versus D1 graph.

6.3 RESULTS

6.3.1 The anti-GC lesion.

Three of the 8 animals injected with anti-GC were investigated using the collision paradigm. These 3 animals were examined between days 7-13 post-injection, which coincides with the early phase of conduction recovery (Chapter 5, pp137-138). Of the

TABLE 6.1. STANDARD REFRACTORY PERIOD OF TRANSMISSION.

BT/T1 AXONS

	MEAN	*MIN*	*MAX*	*N*
CONTROL	0.49	0.28	0.65	241
ANTI-GC	1.41	0.62	4.90	32
MILD PRESSURE	1.40	0.75	3.04	7
SEVERE PRESSURE	–	–	–	0

BS/T2 AXONS

	MEAN	*MIN*	*MAX*	*N*
CONTROL	0.50	0.28	0.58	55
ANTI-GC	1.20	0.61	2.54	13
MILD PRESSURE	2.64	–	–	1
SEVERE PRESSURE	1.20	0.82	1.72	6

Means and ranges of the standard two-stimulus test for RPT of 396 optic axons from normal animals, 45 axons affected by injection with anti-GC (1 excluded, see text) and 14 axons from the animals with a pressure-lesioned optic nerve. The RGC have been classified according to their responses to visual stimulation (BT, BS) and in the normal axons, also their latency (T1, T2). All the normal axons and those injected with anti-GC were stimulated from the optic tract only. Seven of the pressure-lesioned axons were stimulated from the optic chiasm, the other eight from the tract.

TABLE 6.2. ANTIDROMIC CONDUCTION LATENCIES.

BT/T1 AXONS

	MEAN	*MIN*	*MAX*	*N*
CONTROL	1.08	0.76	1.50	210
ANTI-GC	1.70	1.05	3.03	32
MILD PRESSURE	1.54	1.33	1.64	4
SEVERE PRESSURE	–	–	–	0

BS/T2 AXONS

	MEAN	*MIN*	*MAX*	*N*
CONTROL	2.25	1.50	2.91	46
ANTI-GC	3.20	2.16	4.53	13
MILD PRESSURE	3.50	–	–	1
SEVERE PRESSURE	3.10	2.68	3.73	3

Means and ranges of antidromic latencies measured by stimulation from the optic tract only, in 256 axons from a control population of normal animals, 45 axons from animals that had an injection of anti-GC into the ON (1 excluded, see text) and 8 axons that had been affected by a pressure-induced lesion. The RGC were classified on the basis of their responses to visual stimulation and in the normal axons, classification was confirmed by latency measurements.

314 optic axons encountered in these animals, 46 were studied in sufficient detail to give comprehensive D2 versus D1 graphs. Of these, 32 belonged to the BT/T1 class of retinal ganglion cells (RGC). Another 13 were of the BS/T2 class, and the classification of 1 axon was not ascertained because its receptive field was located so far in the periphery of the visual field, that it was interrupted by some of the experimental equipment. The data from this axon is excluded from any analysis of latency (as in Table 6.2). All units were driven from OT stimulating electrodes.

6.3.2 The pressure lesion.

A total of 195 axons were encountered in the two animals with the mild (LB73) and severe (LB85) pressure lesions. Of these, 14 axons driven from either the OT or OX, were investigated in detail, using the collision paradigm. Seven of the axons were of the BT/T1 class of RGC, and the others from the BS/T2 class. One of the BS/T2 axons had collision paradigms performed using 3 stimulus sites, the OT, OX and ON. This axon is discussed in greater detail later in this chapter, but when making comparisons with other D2 versus D1 graphs, only the data from the OT stimulating electrode is included.

Another 3 axons were examined from the ON stimulus site only, as they were undrivable from the other stimulus sites. These were of special interest, as they were classified as non-brisk RGC but queried as possible "sick BTs" (Chapter 5, pp 167-169). All these axons came from LB85, the severe pressure lesion, and had RPTs ranging from 0.86 to 2.32 ms, which are abnormal. These 3 axons were recorded within 1/2 disc diameter of the optic disc (OD) margin. Two had latencies (1.30-3.41 ms), that would not normally be considered as coming from T1 RGC, but the third latency measurement of 0.89 ms from the ON, is more suggestive of a T1 latency (Chapter 5, p 143). The D2 versus D1 graphs for these axons are considered below and the implications for the phenomenon of "sick BT" axons are discussed later in this chapter.

6.3.3 The D2 versus D1 graphs.

The rRPT graphs could be categorised into 5 main groups, designated A-E, on the

basis of the profile of the graph. Each type of rRPT graph was found in both the anti-GC and pressure-lesioned animals. Representative examples of each type of graph are shown in Figures 6.1-6.9 and the conduction parameters for each group are shown in Tables 6.1 and 6.2. The graphs within these groups had a number of distinctive features while also displaying features similar to control D2 versus D1 graphs from the normal animals, such as; the plateau, the ramp, the elevated D2 value at the first collision-free D1 interval and the post-collision plateau (Fig 4.1, p 110).

As the A-E groups represent progressively increasing departures from the normal D2 versus D1 graph, it may be useful to reiterate understanding of the basic features of the normal D2 versus D1 graph. The horizontal plateau is formed at the level of the standard RPT, by values of D2 for collisions between the orthodromic and antidromic impulses along the axon from the mid-time point (MTP) up to the stimulus site. The ramp is caused when the refractoriness, generated by the orthodromic impulse at the stimulus site, determines the time at which the second antidromic impulse can be successfully initiated and transmitted to the recording site. The antidromic and orthodromic impulses become collision free when the orthodromic impulse has passed the stimulus site and its associated refractoriness has subsided before the first antidromic impulse is applied. Then both the antidromic impulses can be transmitted to the recording site. The D2 values will then rapidly return to those equivalent to the standard RPT for that axon, forming the post-collision plateau.

6.3.3a Group A.

For the group A D2 versus D1 graphs, the most notable departure from the normal graph is that the horizontal plateau is at a level that is below that of the abnormally high standard RPT and the equivalent post-collision plateau. In the 14 anti-GC and 2 pressure-lesioned axons that comprised the group A graphs, the D2 values that formed the low plateau were always less than the standard RPT measured for each axon. A representative example is shown in Fig. 6.1. This group contains the four axons with standard RPT

FIGURE 6.1 D2 versus D1 graph, type A.

Representative collision paradigm from the 16 type A, D2 versus D1 graphs. The graph is a plot of the D1 interval (the time elapsed from the detection of the orthodromic impulse to the application of the first antidromic stimulus) versus the D2 interval (the minimum inter-stimulus interval or regional refractory period of transmission). The horizontal dashed line corresponds to the value of the standard refractory period of transmission (RPT), 0.80 ms in this case. The vertical dotted line represents the D1 interval at which the antidromic impulse no longer collides with the orthodromic impulse, ie the orthodromic impulse has passed the stimulus site and its associated refractoriness has subsided, allowing the successful transmission of both antidromic impulses. For greater D1 intervals the antidromic impulses remained collision-free. The oblique dotted line is the idealised ramp with a slope of -1.

In type A graphs, from D1 = 0 the horizontal plateau of D2 values remained level until ending in a single descending ramp of D2 values. The height of this plateau (0.40 ms) was below both the standard RPT and the post-collision plateau. (Refer to Figure 4.1, p 110, for a more comprehensive description of the various components of the D2 versus D1 graph).

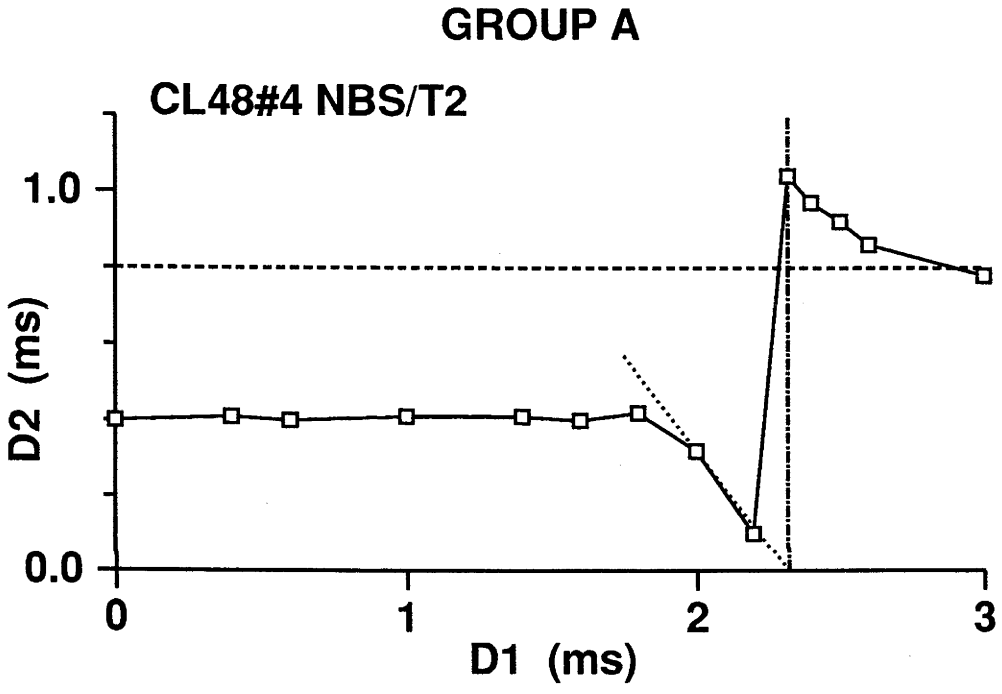
GROUP A
CL48#4 NBS/T2
1.0
0.0
D2 (ms)
0
1
2
3
D1 (ms)

FIGURE 6.2 D2 versus D1 graph, type B.

Representative example of the 15 axons with D2 versus D1 graphs classified as type B. In this group there was a single horizontal plateau of D2 values at a level (0.45 ms) which was below the standard refractory period of transmission (RPT) (1.46 ms in this case). However, at D1 = 0, the D2 value (1.30 ms) was much closer to the standard RPT measurement and from there the D2 values descended in a ramp, the upper portion of which lay on a slope of -1, as shown by the oblique dotted line. The lower portion descended more rapidly, a phenomenon seen in some B type graphs and in D type graphs (p 158), where it is explained in greater detail. The plateau ended towards the collision-free D1 in a lower descending ramp of the decelerating type (see Chapter 4, p 124). The post-collision D2 values progressively approached those of the standard RPT.

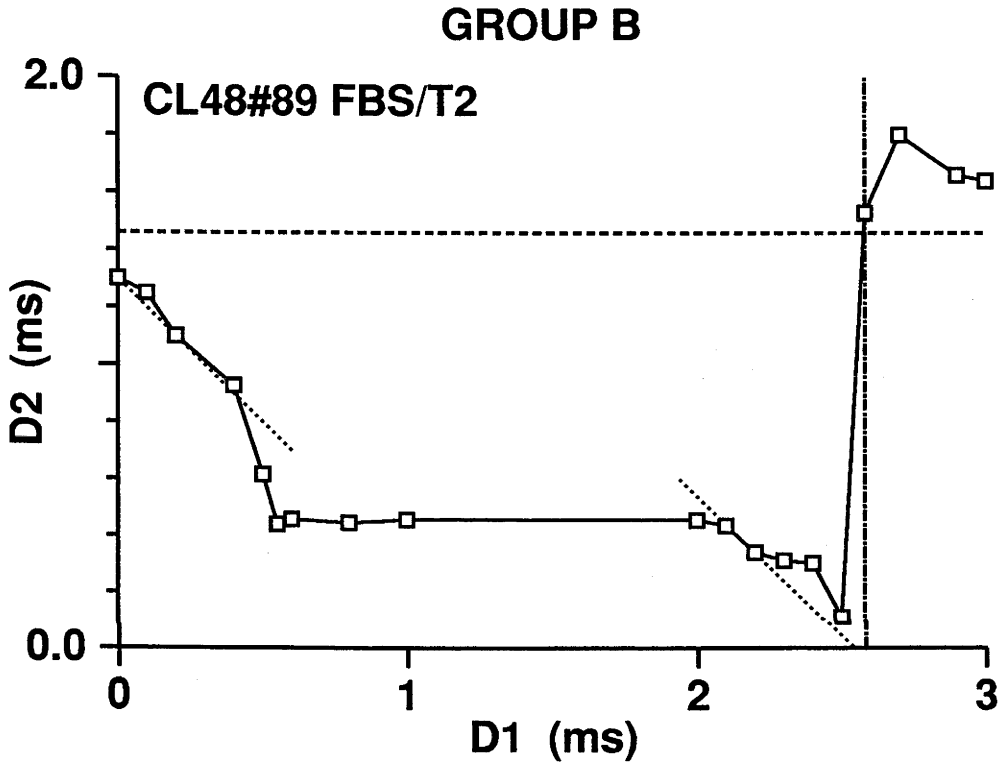
GROUP B
CL48#89 FBS/T2
2.0
0.0
D2 (ms)
0
1
2
3
D1 (ms)

values <0.65 ms but the heights of the lower plateau were between 0.15-0.24 ms less than the standard RPT measured in each case. This difference is well in excess of differences between plateau height and standard RPT found in normal axons (see Fig. 4.3, p 114).

6.3.3b Group B.

As in group A, the group B D2 versus D1 graphs had a plateau of D2 measures l than the value of the standard RPT and the height of the post-collision plateau. A new component of these graphs occurred towards the lower abscissa values where a progressive increase in the D2 values form an upper ramp (Fig. 6.2). The D2 value at = 0 is closer to the elevated standard RPT value than the height of the low plateau. There was a total of 15 axons placed in this group, 11 from the anti-GC animals and 4 from the pressure-lesioned animals.

6.3.3c Group C.

In group C, a further feature was an upper plateau (Fig. 6.3). The 15 anti-GC an pressure-lesioned axons in this group had a low plateau and ramp towards the collisio free D1 and a upper ramp and plateau formed by greater D2 values at low abscissa values. The height of the upper plateau closely coincided with the standard RPT in ea case.

In these first 3 groups of D2 versus D1 graphs, all 50 axons demonstrated a low plateau of rRPT values that were within the range of both the distribution of control measures of the standard RPT test, and the height of the plateau in the D2 versus D1 graphs for normal cats (Fig. 6.4). This demonstrates that there was a region of axon w lower rRPT values on the upstream side of the lesion and that this segment of axon w able to transmit two impulses at normal minimum inter-stimulus intervals (ISI), unaffected by the presence of a lesion along part of its length.

FIGURE 6.3 D2 versus D1 graph, type C.

A representative example of the 19 type C D2 versus D1 graphs. The feature of these graphs was the presence of both an upper and lower plateau of D2 values. The height of the upper plateaux, in all cases, was close to the standard refractory period of transmisssion (RPT) measurement. In this case, at D1 = 0 the D2 value was 0.97 ms, just above the level of the RPT at 0.93 ms. A short plateau extended to the right and then the D2 values descended in an upper ramp (slope of -1) to the lower plateau which was at a height of 0.47 ms. The lower plateau terminated in a second, lower ramp of the decelerating type. After the collision-free D1 at 1.96 ms, the D2 values gradually approached the standard RPT measurement.

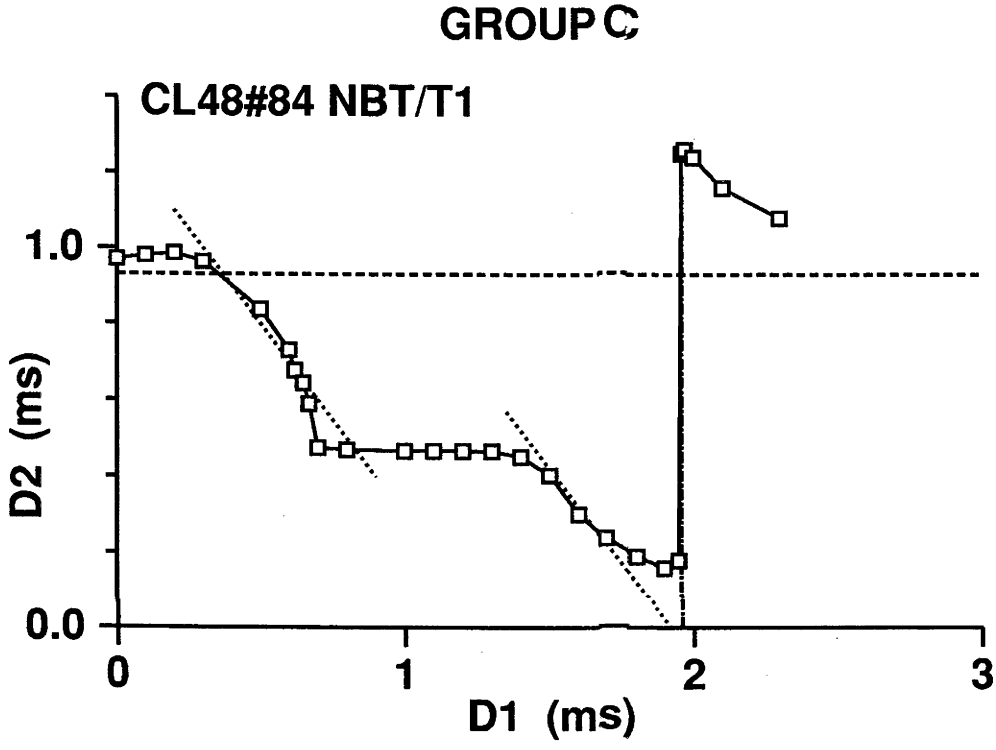
GROUP C
CL48#84 NBT/T1
1.0
0.0
D2 (ms)
0
1
2
3
D1 (ms)

FIGURE 6.4 A comparison of the height of the lower plateau with RPT measures from normal axons.

The height of the lower plateau from abnormal D2 versus D1 graphs was compared with two measures from normal axons; the height of the horizontal plateau from normal D2 versus D1 graphs and the standard two-stimuli refractory period of transmission (RPT) values for normal axons.

A The distribution of the height of the low plateau in 50 BT/T1 and BS/T2 axons from the animals with an optic nerve lesion and a resultant abnormal D2 versus D1 graph categorised into either the A, B or C groups. The mean of the heights of the low plateaux was 0.46 ms and the value ranged from 0.37 to 0.55 ms.

B The distribution of the height of the plateau in the D2 versus D1 graphs from 41 normal BT/T1 or BS/T2 axons. The mean value was 0.50 ms and the heights of these plateaux ranged from 0.37 to 0.58 ms.

C The distribution of the RPTs measured by the standard two-stimulus test performed on 296 normal BT/T1 and BS/T2 axons. The average RPT was 0.50 ms and the range of RPT values was from 0.28 to 0.65 ms.

A HEIGHT OF LOW PLATEAUX IN A, B, C GRAPHS

OT AND OX STIMULATION

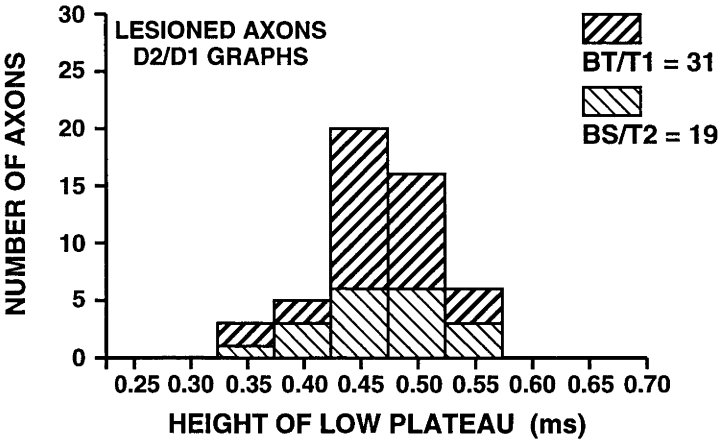

B HEIGHT OF PLATEAUX

OT STIMULATION

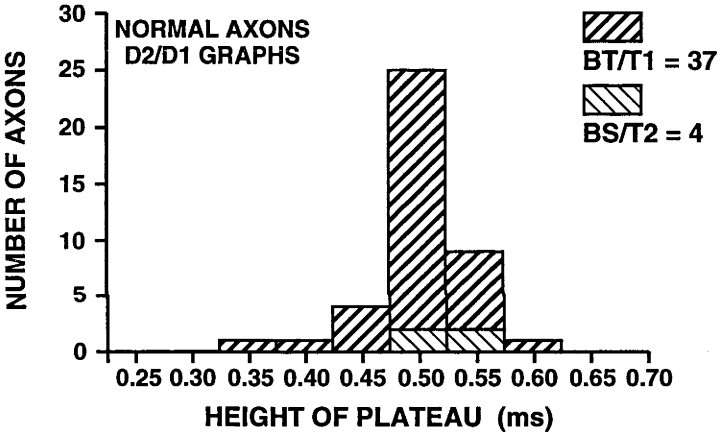

C STANDARD RPT VALUES

OT STIMULATION

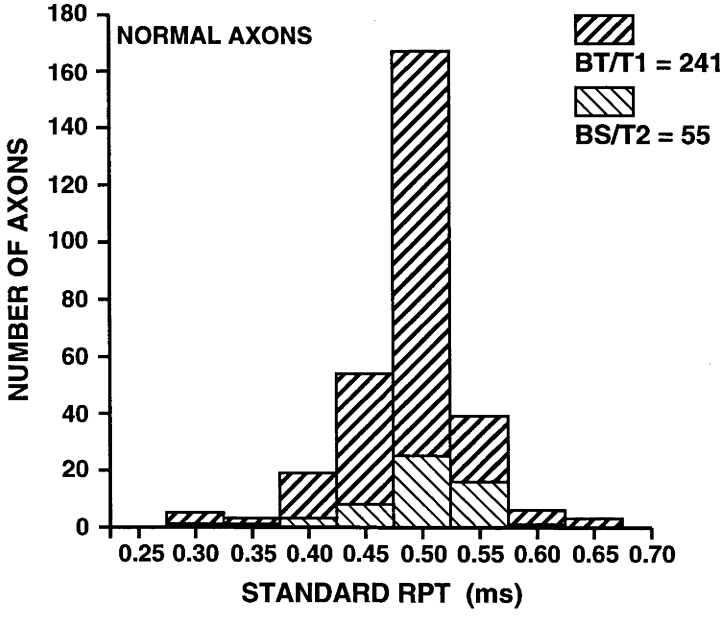

Graphs of type C contain elements of both the A and B type graphs and the determining factor between the types of graphs is the proximity of the MTP to the lesion (see discussion). For the C type graphs, the MTP could occur within the lesion or on the recording side of the lesion. As the stimulating and recording electrodes were similarly placed in each animal and the different types of graphs were seen in each animal, movement of the location of the MTP is likely to be due to variation in the conduction time through the lesion itself. If the conduction within the lesion were infinitely slow, then the closest that the MTP could be located to the recording position would be the midpoint of the lesion. The slower the CV of the orthodromic impulse through the region of demyelination, the more likely the MTP is to be located within the lesion. Consistent with this idea, the figures 6.5a and b of RPT versus latency for BT/T1 and BS/T2 axons, shows that there was a general trend for the C group to have longer antidromic latencies than the axons in A-B groups.

6.3.3d An additional (or intermediate) plateau.

On four occasions in the pressure-lesioned animals, a variation on each of the A, B, C graphs was seen. In these cases there was an additional plateau at D2 values intermediate between those of the low plateau, which lie in the normal range of the RPT values, and that of the elevated standard RPT measured in each axon. In one C-like example there was an upper plateau (Fig. 6.6) and in the 3 remaining cases there was an intermediate plateau at D2 values that were less than the standard RPT and higher than that of the lower plateau. However, in the two B-like cases there was no upper plateau at the height of the standard RPT, but a short ramp extended upwards from the intermediate plateau towards the level of the standard RPT. In the one A-like example, both the upper plateau and ramp were absent. The presence of an intermediate plateau and/or ramp appeared to be confined to the pressure lesion.

In these four axons, stimulated from the optic tract and chiasm, the rRPT of the lowest plateau was between 0.37-0.56 ms. The average of D2 values that formed the intermediate plateau were at least 0.22 ms higher than the lower plateau and lower than

FIGURE 6.5 Refractory period of transmission versus latency.

A plot of refractory period of transmission (RPT) values against individual latency measurements from axons with abnormal D2 versus D1 graphs.

A 29 BT/T1 axons from the D2 versus D1 graphs that were classified as A [□], B [▲] or C [○] groups.

B 14 BS/T2 axons similarly grouped for the D2 versus D1 graphs.

It can be seen that some general trends emerge for these axons. Those belonging to the group B had the longer RPTs, while the C group generally had the longest latencies. The A group of axons tended to have the shortest latencies and RPTs.

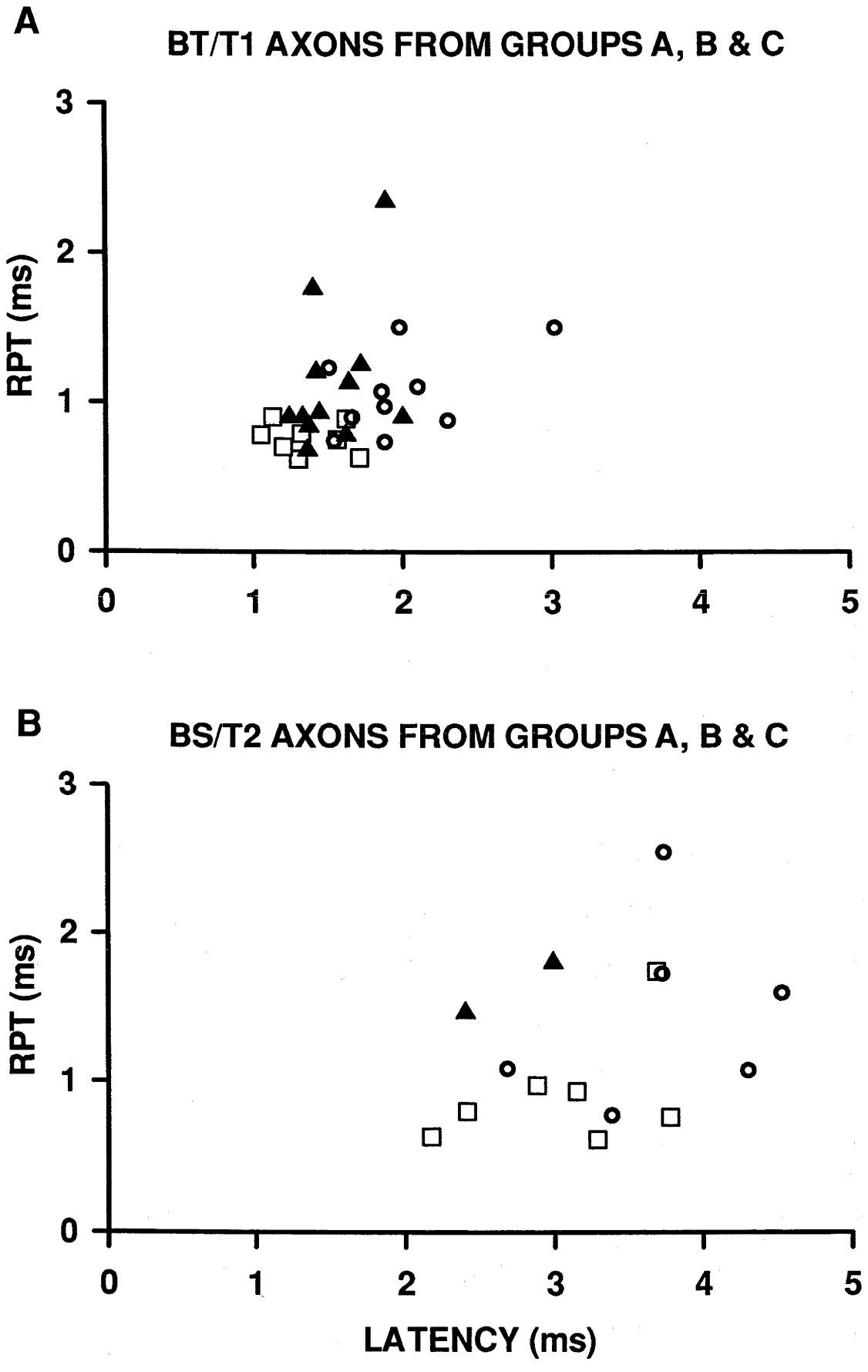
A
BT/T1 AXONS FROM GROUPS A, B & C
RPT (ms)
0
1
2
3
0
1
2
3
4
5
B
BS/T2 AXONS FROM GROUPS A, B & C
RPT (ms)
0
1
2
3
0
1
2
3
4
5
LATENCY (ms)

FIGURE 6.6 An intermediate plateau.

Two examples of the 4 D2 versus D1 graphs, from the animals with the pressure-lesion, that indicated the presence of an intermediate plateau. In three examples, the upper plateau was not evident (**B**), but plateaux at heights between the low plateaux (0.80 ms) and the standard refractory period of transmission (1.25 ms) were evident, and three ramps were observed in two other examples. In **A**, all three plateaux and ramps are evident. The height of the upper plateau (1.72 ms) was close to the standard RPT measurement (1.73 ms). The D2 values descended in an upper ramp (slope of -1) to a short intermediate plateau which was at a height of 1.21 ms. The intermediate plateau terminated in a ramp which descended (again with a slope of -1) towards a low plateau (0.51 ms). This plateau terminated in a third, low ramp.

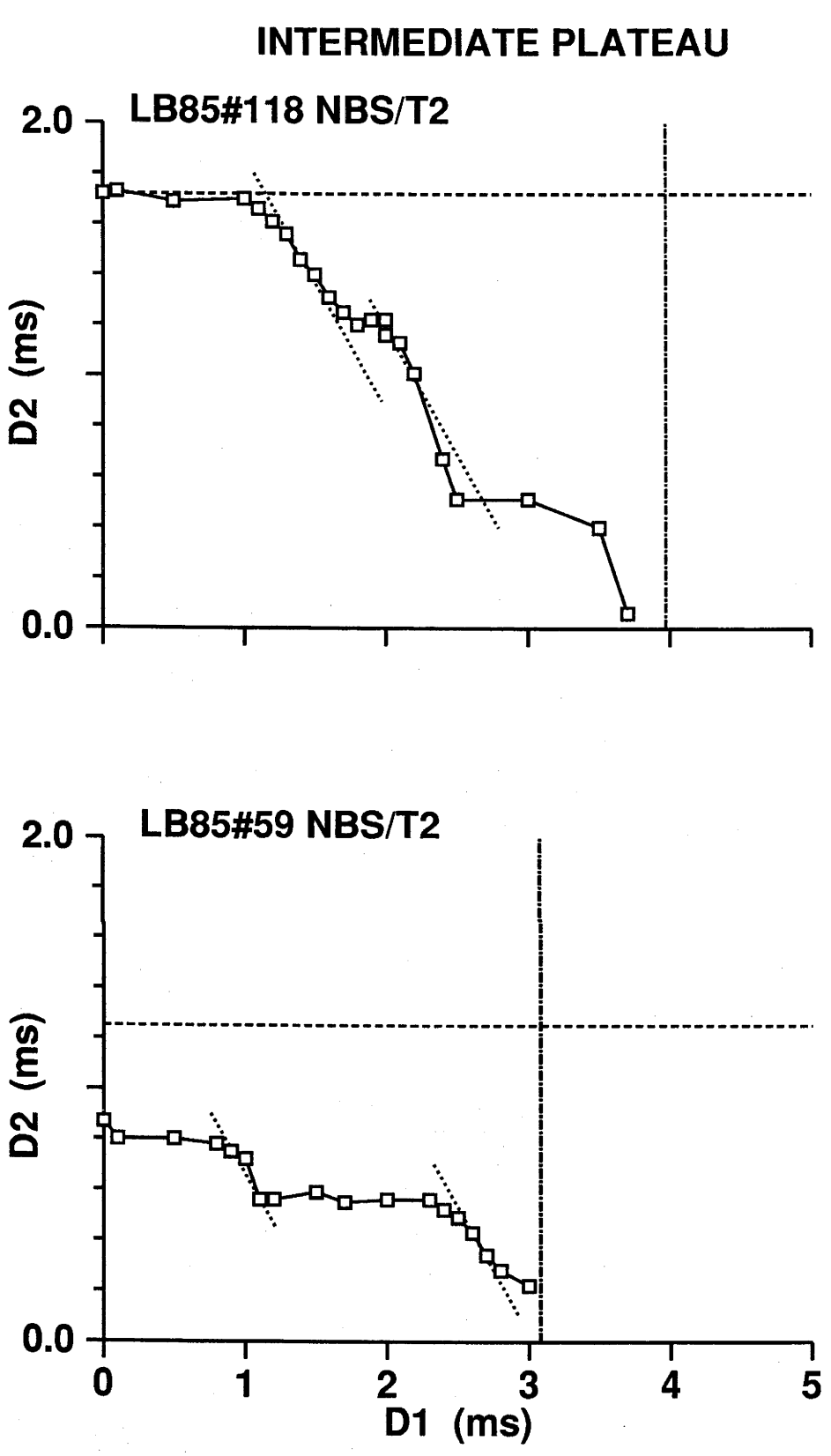
INTERMEDIATE PLATEAU
LB85#118 NBS/T2
2.0
0.0
D2 (ms)
LB85#59 NBS/T2
2.0
0.0
D2 (ms)
0
1
2
3
4
5
D1 (ms)

the standard RPT. In Fig 6.6 (LB85#118), the low plateau was at an average D2 value of 0.51 ms, the intermediate plateau at 1.21 ms and the upper plateau was at 1.71 which was consistent with the standard RPT (1.72 ms) for this axon. As the rRPT of the intermediate plateau was always >0.65 ms and the standard RPT even longer again, this suggests that in these instances the stimulus side of the pressure lesion had a progressive step-like reduction in transmission vulnerability. In other words, antidromic impulses are encountering regions of progressively greater transmission vulnerability on their passage through the lesion in the direction of the recording site. The rRPT of the low plateau was within normal limits, suggesting that the segment of axon towards the stimulus site had normal conduction properties.

6.3.3e Group D.

The first notable feature of the 6 BT/T1 and 1 BS/T2 axons that form this group was their long standard RPT measurements (2.46-4.90 ms), especially compared to their only moderately affected latencies. In the 4 anti-GC axons that had graphs of this type, the trend towards high RPT coupled with moderately lengthened latency was evident in Fig 5.2a, as the 4 BT/T1 axons that had the longest RPT (> 3.0 ms). The D2 versus D1 graphs for the 4 anti-GC and 3 pressure-lesioned axons also displayed a number of features not previously described for groups A, B, C.

The graphs commenced at D1 = 0 with a descending ramp of slope of -1, as seen in the representative D1 vs D2 graphs shown here (Fig. 6.7a, CL48#98 and b, LB73#56). There was no upper plateau evident at small abscissa values in any of the D type graphs. The ramp often terminated by a more or less abrupt downward step, and the subsequent D2 values formed a lower plateau, the height of which, in all but two cases, was significantly above the upper limit of the standard RPT (0.65 ms).

It is at the end of the plateau that the most obvious new feature occurs, the rise in rRPT before the collision free zone and the therefore inevitable absence of a descending ramp towards the collision free D1. The absence of a lower ramp towards the collision free D1, was the main feature that characterised this group of D2 versus D1 graphs.

FIGURE 6.7 D2 versus D1 graph, type D.

Two representative examples of the 7 D type D2 versus D1 graphs. The determining features of these graphs were; at D1 = 0 the D2 value was below the level of the standard RPT and the D2 values immediately descended in a ramp with slope -1. This feature is reminiscent of the B type D2 versus D1 graphs. The ramp terminated in a rapid drop to the low plateau, which was of variable height and length. Finally there was an abrupt rise in D2 values towards the collision-free D1 interval and the subsequent formation of a short plateau of a height that was between the lower plateau and the value for the standard RPT. After the collision-free D1, the D2 values gradually approached the standard RPT value.

A A representative example of the D type graphs from the anti-galactocerebroside injected animals. At D1 = 0, the D2 value was 4.59 ms, just below the value for the standard RPT (4.90 ms). The height of the low plateau was an average D2 value of 1.88 ms. At the D1 interval of 4.00 ms, the D2 values increased rapidly and a short intermediate plateau at a height of around 4.00 ms was formed, before the collision-free D1 interval was reached at 4.72 ms.

B A representative example of the D type graphs from the pressure-lesioned animals. At D1 = 0, the D2 value was 2.36 ms, which was below the value for the standard RPT (3.04 ms). The height of the low plateau was an average D2 value of 0.81 ms and this low plateau was much shorter than the example displayed above, lasting for only 0.40 ms. At the D1 interval of 1.65 ms, the D2 values rapidly increased and formed an intermediate plateau at a height of 2.13 ms. The S1 stimulus was disconnected [■] at D1 intervals close to the collision-free D1 interval at 2.50 ms, corresponding to the rise in D2 values. The D2 value then fell to a level that approximated a continuation of the slope of -1 from the upper ramp.

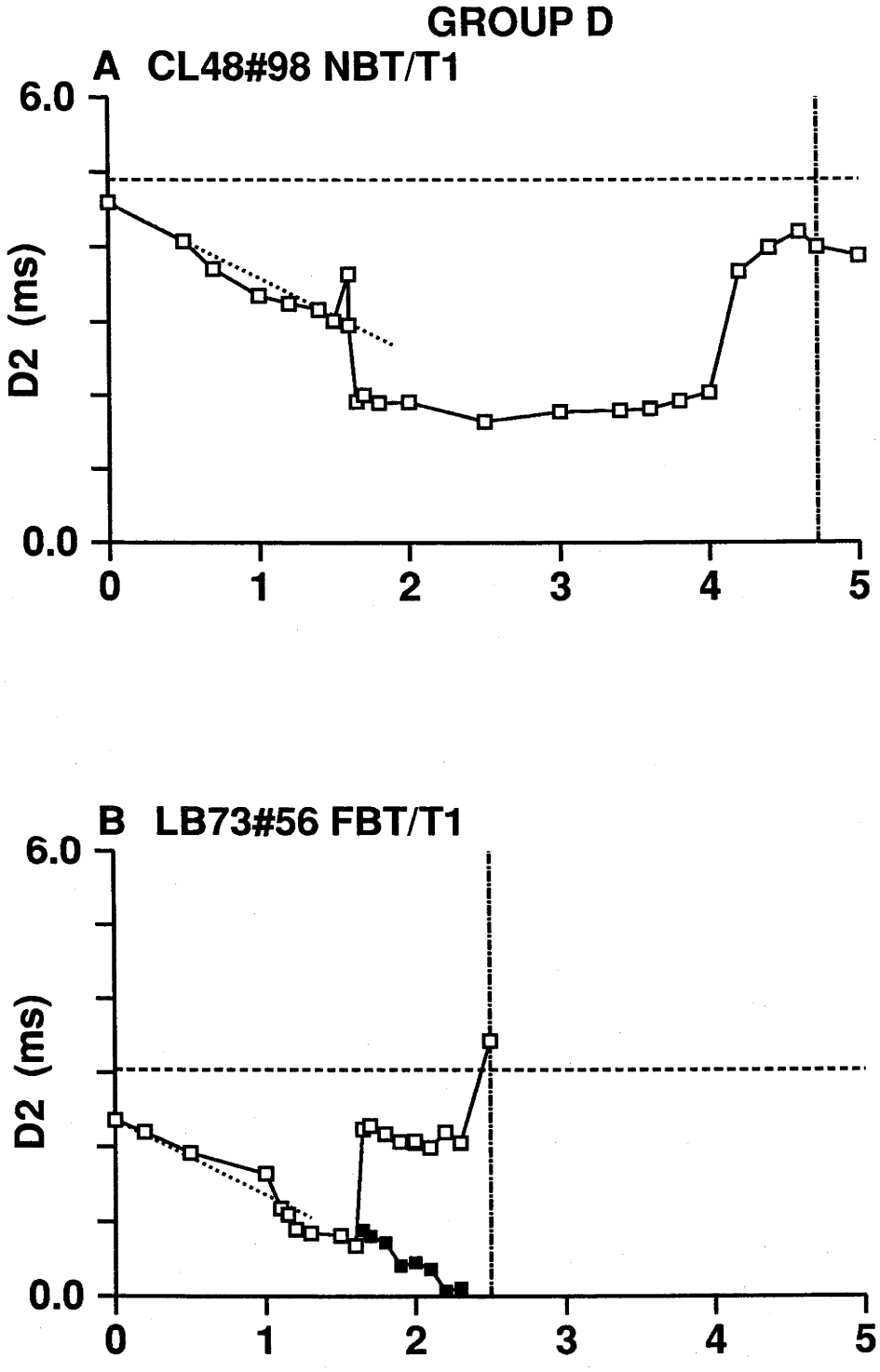
GROUP D
A CL48#98 NBT/T1
6.0
0.0
D2 (ms)
0
1
2
3
4
5
B LB73#56 FBT/T1
6.0
0.0
D2 (ms)
0
1
2
3
4
5

6.3.3f Group E.

In 3 axons, 1 BS/T2 axon from the pressure-lesioned animals and another 2 BT/T1 axons from the anti-GC animals, the D2 versus D1 graphs differed from the groups A-D graphs, while superficially resembling the normal graph. The key feature was the elevated D2 plateau, matching the abnormal standard RPT within 0.10 ms, for all the collisions back to the OT stimulus site (Fig. 6.8). There was no evidence of a segment of axon with normal refractoriness upstream from the lesion. However, in these 3 cases there was also no indication of a diffuse injury to the RGC, as latencies were within normal limits, the receptive fields were readily located and the responses of the RGC were readily identifiable as belonging to each particular class.

6.3.4 "Sick BTs".

In a number of RGC from the pressure-lesioned animals, the responses of the RGC to visual stimulation were atypical and the axons of these RGC could not be driven from either the OT or OX stimulating electrodes. These RGC were thought to be of the BT/T1 class and designated 'sick' (Chapter 5, pp 167-169) because of their atypical receptive field characteristics and their inability to conduct impulses. A small number could, however, be driven from the ON stimulating electrode (Chapter 5, p 142). The collision paradigm was performed in 3 such axons from LB85, the animal with the severe pressure lesion. The resulting D2 versus D1 graphs are presented in Fig. 6.9.

The D2 versus D1 graph for LB85#43(Fig. 6.9c), can be classed as a type E graph. There is an elevated plateau, consistent with the abnormal standard RPT, but no evidence of a lower plateau of normal (< 0.65 ms) height.

The other two graphs (Fig. 6.9a and b), appear to belong to groups A and B respectively. However, there is an important departure from the typical characteristics of those groups, namely the rRPT of the lower plateau is not of a value that falls within the range of normal RPTs (0.28-0.65 ms). In LB85#38, the height of the lower plateau is

FIGURE 6.8 D2 versus D1 graph, type E.

Representative of the 3 axons with type E D2 versus D1 graphs. The determining feature of these graphs was the presence of a single plateau coinciding with the elevated standard refractory period of transmission (RPT). In this example the standard RPT was 0.72 ms and the average D2 value along the plateau was also 0.72 ms. The D2 values in the ramp lay along a slope of -1 and the ramp was of the accelerating type. There was a region, immediately before the collision-free D1 interval where the D2 values persisted at < 0.1 ms for a period of some 0.20 ms.

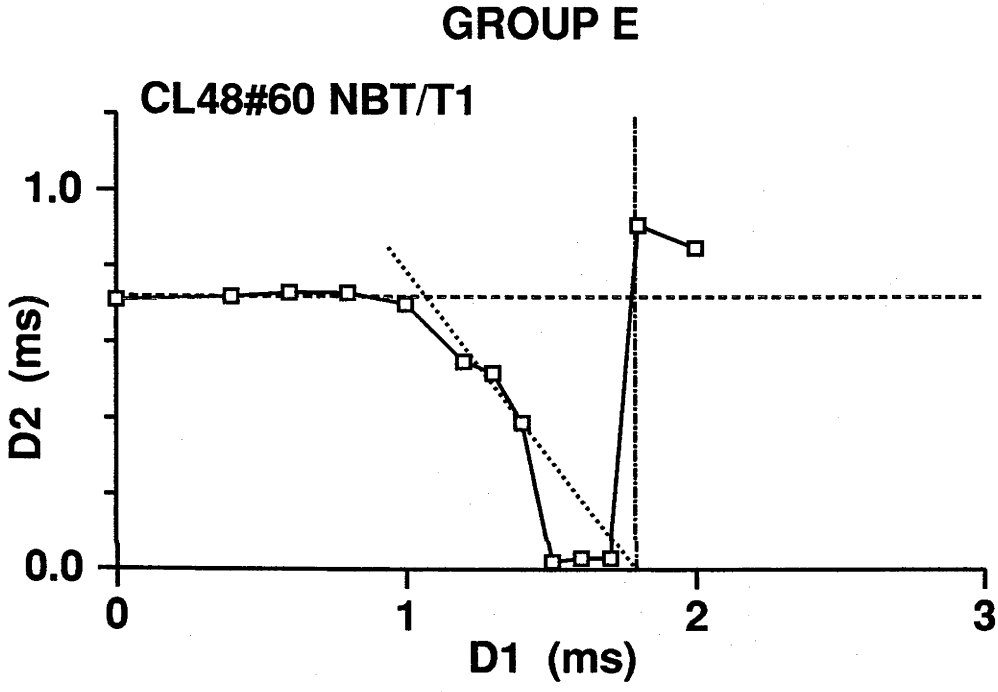
GROUP E
CL48#60 NBT/T1
1.0
0.0
D2 (ms)
0
1
2
3
D1 (ms)

FIGURE 6.9 D2 versus D1 graphs, "sick BTs".

A small number of axons with atypical responses to visual stimulation could be driven from the retrobulbar stimulating electrode, despite being blocked from both the optic tract and optic chiasm electrodes. Two of the 3 axons present further variations of the D2 versus D1 graph.

A LB85#38 had a standard RPT of 2.32 ms and the single horizontal plateau was at an average D2 value of 1.33 ms. The discrepancy between this graph and the A type graph lies in the elevated D2 values of the lower plateau.

B At D1 = 0, the D2 value of 1.12 ms was just below that of the standard RPT measurement (1.21 ms). The D2 values then descended to a plateau at a new height of 0.75 ms. Despite the superficial resemblance to B type graphs, the lower plateau still remained above the upper limit for normal axons, which excludes this axon from being included in the type B graphs.

C LB85#43 appeared to be a typical E type of graph. The height of the plateau (0.85 ms) and the standard RPT (0.86 ms) are essentially the same but are greater than the upper limit for RPT in normal axons.

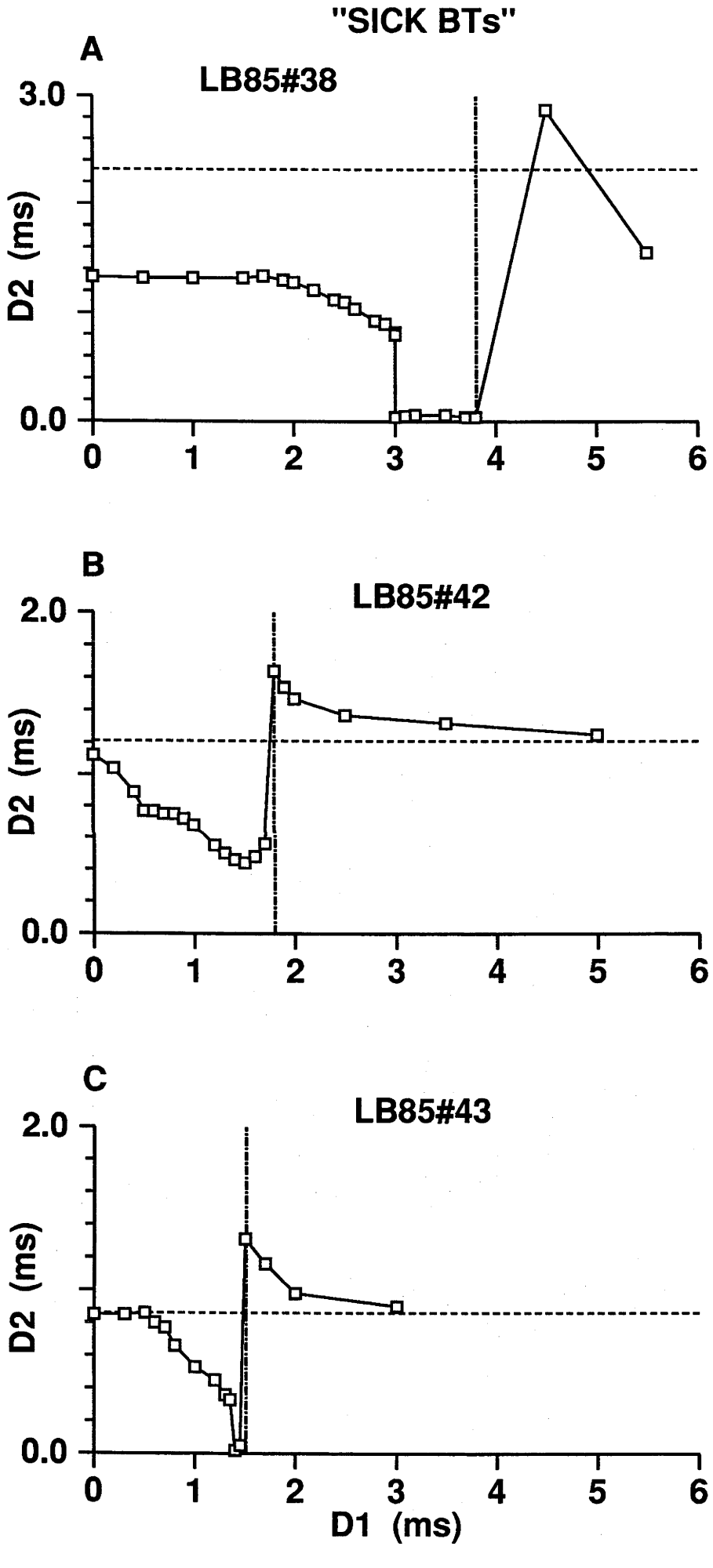
"SICK BTs"
A
LB85#38
3.0
0.0
D2 (ms)
0
1
2
3
4
5
6
B
LB85#42
2.0
0.0
D2 (ms)
0
1
2
3
4
5
6
C
LB85#43
2.0
0.0
D2 (ms)
0
1
2
3
4
5
6
D1 (ms)

1.33 ms, which is substantially in excess of 0.65 ms and still approximately 1.00 ms less than the standard RPT in this axon. In LB85#42, the standard RPT was 1.21 ms and the height of the lower plateau was 0.75 ms.

6.3.5 Interpretation of graphs using the space-time diagrams.

To effectively interpret events along the axon that cause the various features of the different groups of D2 versus D1 graphs, it is useful to again refer to space-time diagrams. The space-time diagram was introduced in Chapter 4 to interpret the rRPTs of normal axons. The purpose of the diagrams is to illustrate the interaction of the orthodromic and two antidromic impulses in the collision paradigm. The diagrams merely depict the events associated with the D2 versus D1 graphs in an easily understood manner.

The method of constructing the diagrams, is explained in detail in Chapter 4 (pp 109-112). It is important to note that the passage of an impulse between its point of initiation or detection and the collision site is represented by a straight line, despite variations in CV in different regions of the axon. The vertical scale is locally transformed so that the length of axon has been translated into the latency of an impulse to reach the corresponding region of the axon. This is achieved by dividing the distance by the CV of an impulse within each region. This has particular relevance for the axons with a focal lesion, where CV within the lesion is slower than other segments of the axon.

In the space-time diagram, the latency of the impulse is linked to the physical distance by dashed lines from the vertical axis to the diagram of the optic pathway on its left. It has been assumed that the position of the lesion is centred around 3 mm behind the eye, as both the micro-injection of anti-GC and the placement of the pressure cuff were located at approximately this point. For the majority of cases, the lesion's effect on transmission of impulses is assumed to be uniform within the lesion. The edge of the lesion is also assumed to be sharp. These assumptions are modified only in those D2 versus D1 graphs that indicate the presence of an intermediate plateau. These axons are assumed to have step-like changes in refractoriness from one sub-region to another. Between each step the degree of refractoriness is constant.

All the separate features of the D2 versus D1 graphs are best illustrated by the C type graph and the space-time diagram associated with it. It is apparent that the extent of the upper plateau indicates the temporal extent of a region of conduction vulnerability, suggested by the increased rRPT. The lower plateau, with normal or reduced rRPT, indicates the refractoriness of the axon upstream from the lesion, towards the stimulus site.

6.3.5a The C type graph.

The space-time diagrams illustrate 6 key events in the C type D2 versus D1 graphs (Fig. 6.3).

1). The upper plateau.

For the launch of A1 at a D1 = 0 ms, the trajectory of A1 will commence at the origin of the space-time diagram (Fig. 6.10a) and ascend to the right. The orthodromic impulse descends from the upper left to the right and will collide with A1 at the MTP, located within the lesion.

The transmission of the A2 impulse to the recording electrode, is dependent upon its ascending trajectory not passing through any refractory regions indicated on the space-time diagram. It can be seen that the limiting boundary for the successful passage of A2 is the refractoriness associated with A1, as it enters the lesion prior to the collision point. The orthodromic impulse will have no limiting effect on the passage of A2 at this time. The rRPT for this region, as indicated by the height of the upper plateau, should therefore be the same as the standard RPT measurement.

As the time between the detection of the orthodromic impulse and the application of S1 (the D1 interval) is increased, the launch of A1 will move to the right on the horizontal axis of the space-time diagram. The trajectories of A1 and associated refractoriness are similarly moved to the right. The shift of A1 will postpone the moment at which A2 can be successfully launched, by the same amount of time as the increment

FIGURE 6.10 Space-time diagrams for the C type D2 versus D1 graphs.

A space-time diagram constructed for the key points in the C type D2 versus D1 graphs. The construction of the diagrams is explained in detail in Chapter 4, pp 109-112. The parameters of this diagram are representative of all C type graphs and are based on the data from Figure 6.3, the conduction properties of BT/T1 and BS/T2 axons, the probable size and extent of the lesion and the likely conduction properties of the lesion itself.

A D1 = 0.0 ms, formation of the upper plateau. Collision of the orthodromic (O) and first antidromic (A1) impulses occurs within the lesion. The limiting boundary of refractoriness along the axon (the dotted line) for the transmission of the second antidromic impulse (A2) is the refractoriness generated by A1 within the lesion.

B D1 = 0.33 ms, the shoulder. Collision at the stimulus edge of the lesion creates the shoulder D2 value. At this point the limiting boundary for the transmission of A2 to the recording site switches to being the refractoriness generated by O in the lesion.

C D1 = 0.50 ms, the upper ramp. Collision in axon just on the stimulus side of the lesion causes no change in the boundary for the successful transmission of A2. Despite the increase in the D2 interval, it remains the refractoriness generated by O within the lesion.

D D1 = 1.00 ms, the lower plateau. Collisions closer to the stimulus site start to extend the refractoriness caused by A1 to the right and beyond the edge of the lesion. A1 then sets the boundary for the transmission of A2.

E D = 1.86 ms, the lower ramp. The arrival of O at the stimulus site means that when S1 is applied it is not effective. The limiting boundary for A2 becomes the ending of the refractoriness that is generated by the passage of O through the stimulus site.

F D1 = 2.13 ms, the collision-free D1. A1 is now able to be transmitted to the stimulus site. The limiting boundary for the transmission of A2 is generated by the passage of A1 through the lesion.

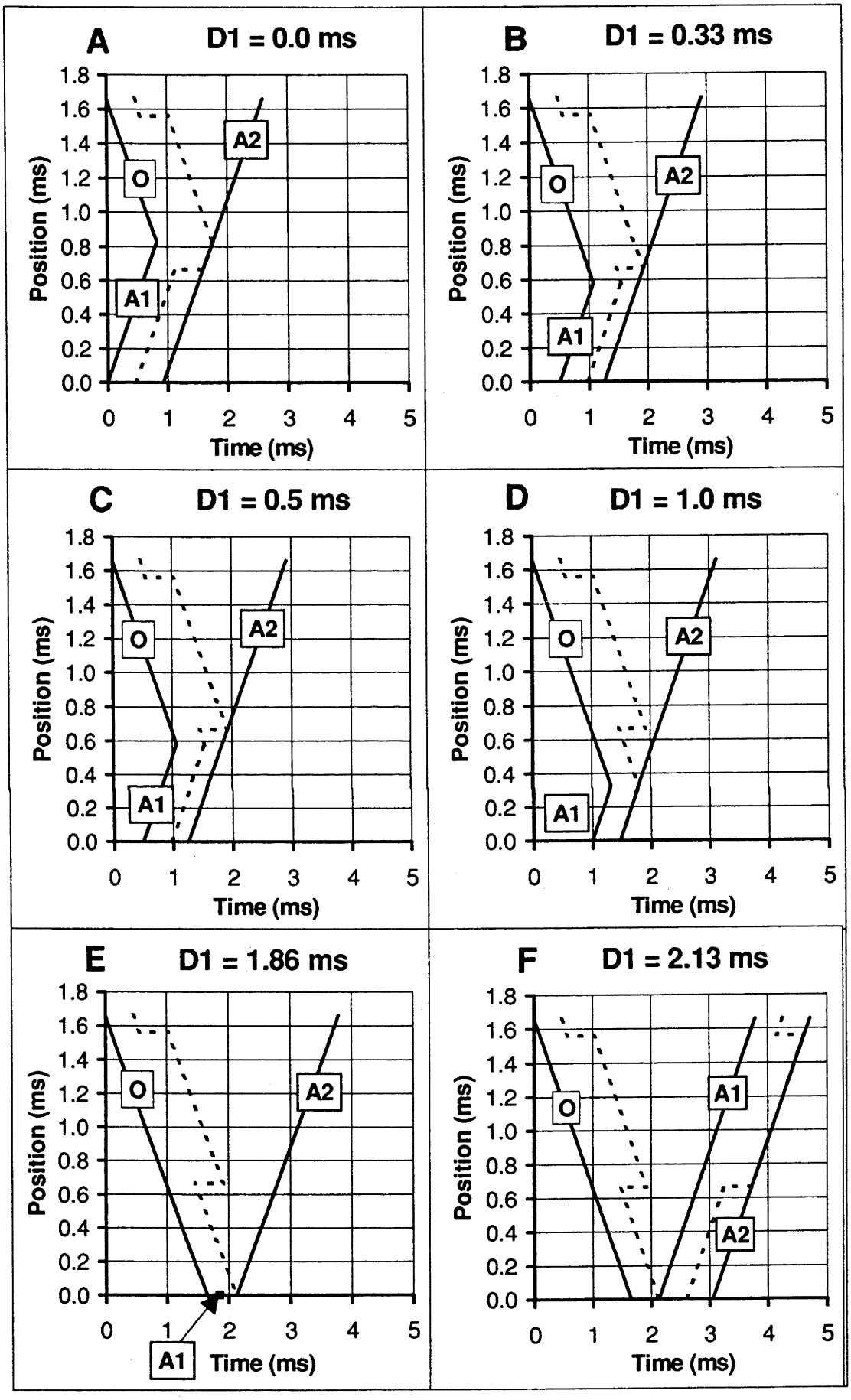
A
D1 = 0.0 ms
B
D1 = 0.33 ms
C
D1 = 0.5 ms
D
D1 = 1.0 ms
E
D1 = 1.86 ms
F
D1 = 2.13 ms
Position (ms)
Time (ms)
O
A1
A2
0.0
0.2
0.4
0.6
0.8
1.0
1.2
1.4
1.6
1.8
0
1
2
3
4
5

in the D1 interval. In other words, the minimum interval between the application of S1 and S2 (the D2 interval) that results in the generation of two antidromic impulses, will remain the same. The consistency of the D2 measurement forms the upper plateau of the D2 versus D1 graph.

2). The upper shoulder.

This situation remains until collision occurs at the edge of the lesion (Fig 6.10 b). As the D1 interval is slightly increased and the trajectory of A1 moves to the right, the refractoriness generated by A1 is now less than the refractoriness within the lesion. At this time the limiting boundary can be seen to switch from refractoriness associated with A1, to the residual refractoriness caused by the passage of the orthodromic impulse through the edge of the lesion.

3). The upper ramp.

When the D1 interval is sufficiently extended, the orthodromic impulse has time to pass beyond the edge of the lesion on the side of the stimulus, before colliding with A1 (Fig. 6.10c). As with the lower ramp of D2 values in the normal axons (Chapter 4, pp 116-118), the earliest time for the uninterrupted passage of the A2 impulse to the recording site is now being determined by the timing of the orthodromic impulse.

The linking of the launch of A2 to the timing of the orthodromic impulse means that the successful application of S2 will occur at a fixed time after the detection of the orthodromic impulse at the recording site. In terms of the D1 and D2 measurements, for every increment of D1 there is a corresponding decrease in the D2 interval, so that the time to the launch of A2 remains the sum of the D1 + D2 intervals. The constant time for the launch of A2, will ideally form a ramp with a slope of -1. Variations in the slope of the ramp have been discussed in Chapter 4, pp 124-127, and will be further examined at the end of this chapter.

4). The low plateau.

As the D1 interval is increased, the next change in the shape of the graph occurs as the limiting event for determining the D2 interval reverts to the launch of A1. In the space-time diagram, as the collision point approaches the stimulus site, the refractoriness generated by the passage of A1 to the collision site, will extend to the right beyond the residual refractoriness associated with the orthodromic impulse at the edge of the lesion

(Fig. 6.10d). The critical moment for the launch of A2 is now linked to the timing of A1 and the D2 interval will be constant, reflecting the rRPT of the segment of axon beyond the lesion. As in the graphs of normal axons, the constant D2 measurements form a low plateau, until the orthodromic impulse reaches the stimulus site.

5). The low ramp.

As in the normal D2 versus D1 graphs, when the orthodromic impulse reaches the stimulus site, the application of S1 is ineffective for eliciting the successful launch of A1. The timing of the successful application of S2 is now dependent upon the end of the refractory phase at the stimulus site, generated by the orthodromic impulse (Fig. 6.10e).

6). The post-collision D2.

When the D1 interval is increased so that S1 is able to generate an impulse that propagates after refractoriness at the stimulus site subsides, then the transmission of A2 to the recording site will be determined by the refractoriness generated by the passage of A1 through the lesion (Fig. 6.10f). The D2 measurement should therefore approximate both the height of the upper plateau and the standard RPT.

6.3.5b The B type graphs.

The space-time diagrams for the B type graphs are shown in Figure 6.11 and are illustrative of the D2 versus D1 graph in Figure 6.2. It can be seen that the B type graphs have elements of the C type graph (Fig. 6.3). The major difference appears to lie in the location of the MTP relative to the lesion. The D2 measurement at D1 = 0 approaches the level of the standard RPT measurement but for increases in the D1 interval, the D2 value progressively decreases, forming an upper ramp. The immediate appearance of the ramp and the absence of an upper plateau suggests that the MTP for collision between the orthodromic impulse and A1 occurs on the upstream side of the lesion. In these circumstances, as suggested above, the limit for the successful transmission of A2 is the end of refractoriness at the edge of the lesion, generated by the passage of the orthodromic impulse through the lesion.

FIGURE 6.11 Space-time diagrams for the B type D2 versus D1 graphs.

A space-time diagram constructed for the key point in the B type D2 versus D1 graphs. The parameters of this diagram are representative of all B type graphs and are based on the data from Figure 6.2. The diagram is constructed for the time D1 = 0 when the orthodromic (O) and first antidromic (A1) are colliding at the mid-time point for collision (MTP). It can be seen that the MTP occurs just upstream from the stimulus edge of the lesion. The limiting boundary is the refractoriness generated by the passage of O through the lesion. All subsequent features of the B group of graphs are as described for parts D, E and F in Figure 6.10.

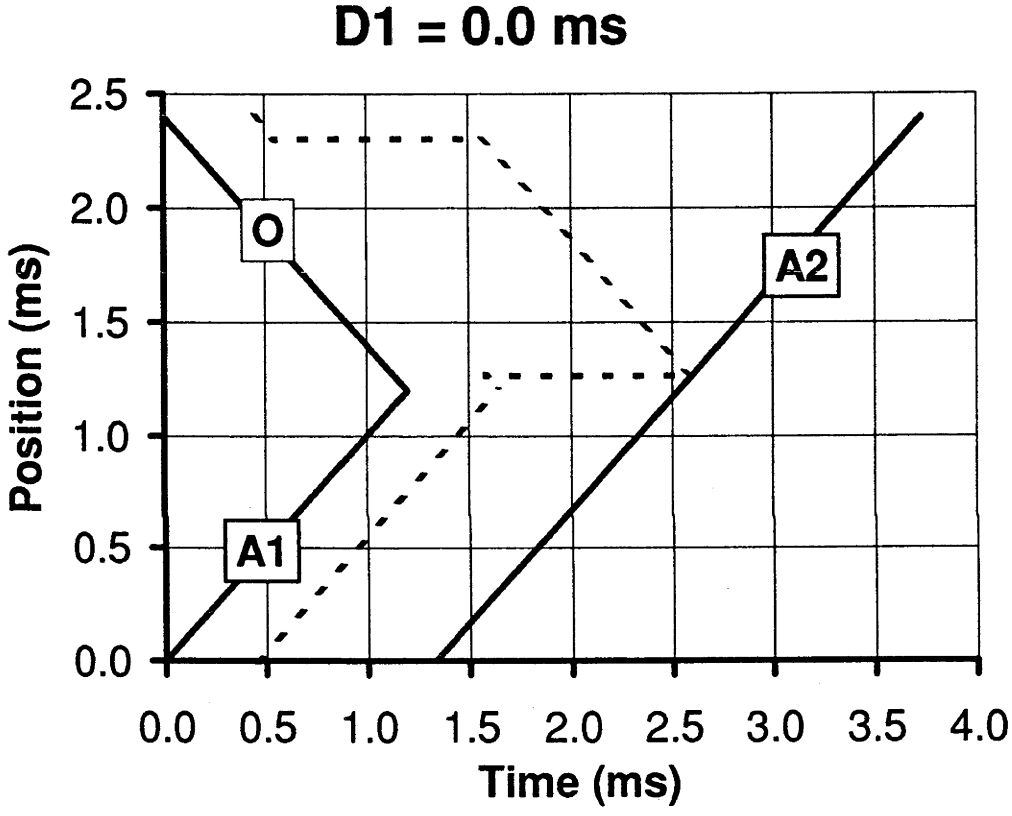
D1 = 0.0 ms
Position (ms)
2.5
2.0
1.5
1.0
0.5
0.0
O
A1
A2
0.0 0.5 1.0 1.5 2.0 2.5 3.0 3.5 4.0
Time (ms)

The lower plateau and ramp are features shared with the C type graphs and the events causing these features are the same as described in the C type space-time diagrams (Fig. 6 10c-e).

6.3.5c The A type graphs.

The A type space-time diagrams (Fig. 6.12) indicate that the MTP for collision occurs even closer to the stimulus site than in the B-C graphs, probably due to a faster conduction time through the lesion. Consequently, the collision for D1 = 0 corresponds to the lower plateau and is similar to the D2 versus D1 graphs for normal axons. The key determinant of abnormality in these graphs is the discrepancy between the height of the plateau and the standard RPT measurement. The other features of this type of graph, the lower ramp and the post-collision D2 measurements, are as described above and in Chapter 4 for normal axons.

6.3.5d The intermediate plateau.

The phenomenon of an intermediate plateau can be interpreted in the same manner as the upper plateau and ramp of the C type graphs. The space-time diagrams (Fig. 6.13a, b, c) reveal that the axon must have three regions of differing refractoriness, that decrease step-wise, to form the 3 plateaux and ramps evident in this D2 versus D1 graph (Fig. 6.4). At D1 = 0, the collision will occur within the most severely affected region of the axon. The upper ramp and plateau are formed in the manner previously described.

At a longer D1 interval, collision occurs in a second region of less conduction vulnerability and an intermediate plateau is formed as the transmission of A1 again sets the temporal limit for the passage of A2. The low plateau is finally achieved as the result of a normal span of refractoriness that is generated by A1 in an unaffected region of axon, close to the stimulus site. The post-collision rRPT will be determined by the passage of A1 through the most vulnerable of these regions and therefore the D2 measurements will return to the height of the upper plateau and the standard RPT.

FIGURE 6.12 Space-time diagrams for the A type D2 versus D1 graphs.

A space-time diagram constructed for the key points in the A type D2 versus D1 graphs. The parameters of this diagram are representative of all A type graphs and are based on the data from Figure 6.1. This diagram is constructed for D1 =0. The midtime point for collision is occurring towards the stimulus site and some distance upstream from the lesion. While the presence of the lesion can be detected by the standard RPT, here A2 is limited only by the refractoriness generated by A1 in the normal portion of the axon and this is removed after A1 collides with O.

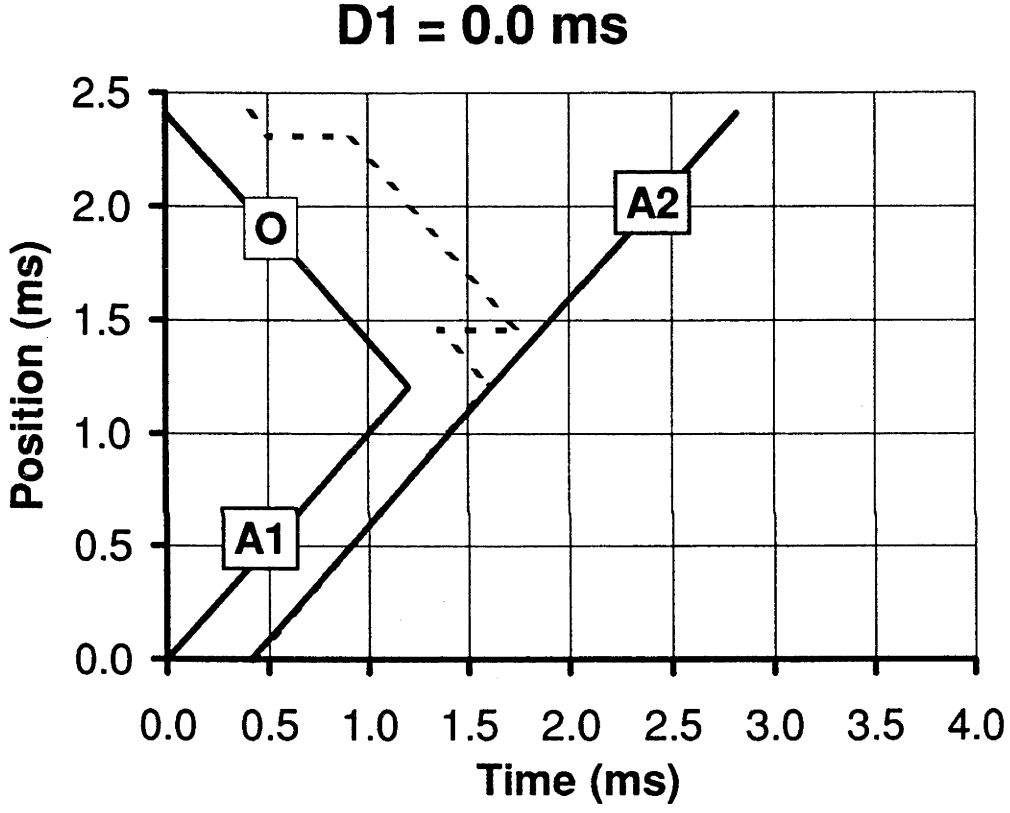
D1 = 0.0 ms
Position (ms)
2.5
2.0
1.5
1.0
0.5
0.0
O
A1
A2
0.0
0.5
1.0
1.5
2.0
2.5
3.0
3.5
4.0
Time (ms)

FIGURE 6.13 Space-time diagrams for D2 versus D1 graphs with an intermediate plateau.

A space-time diagram constructed for the key points in the D2 versus D1 graphs that demonstrate an intermediate plateau. The parameters of this diagram are based on the data from Figure 6.6.

A D1 = 0, the upper plateau. The mid-time point for collision occurs within the region of longest refractoriness along the axon and the refractoriness generated by A1 in this region is the limiting boundary for the passage of A2 to the recording site.

B D1 = 1.80 ms, the intermediate plateau. The collision now occurs within the region along the axon that has a less severe conduction deficit than the region closer to the recording electrode, but the rRPT is still abnormal. Refractoriness generated by A1 within this region is the limiting boundary for the transmission of A2.

C D1 = 2.90 ms, the lower plateau. Collision now occurs in axon with normal conduction parameters and the limiting boundary for the passage of A2 is set by the refractoriness in the normal axon caused with A1 up to the point of collision.

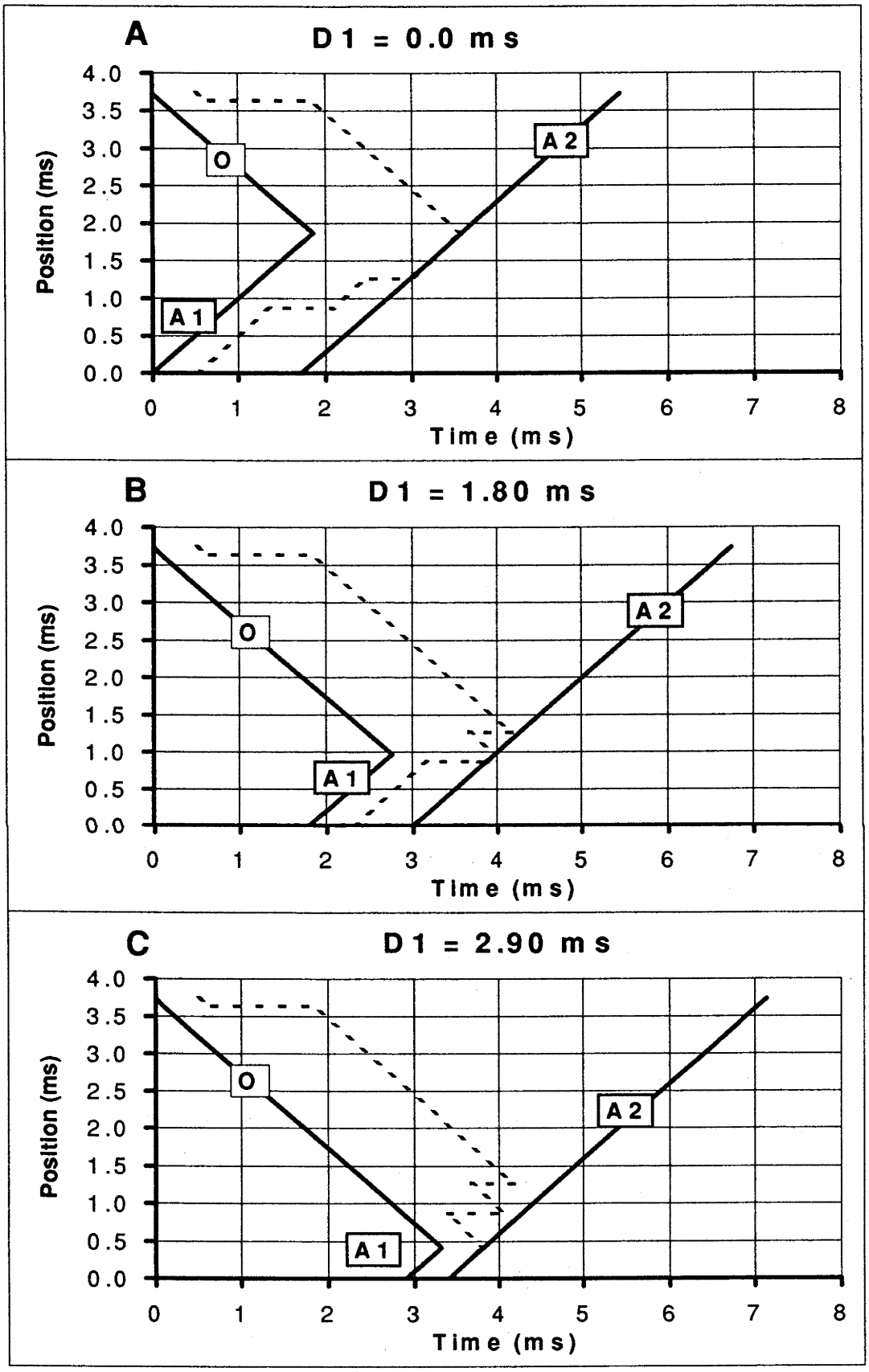
A
D1 = 0.0 ms
Position (ms)
Time (ms)
O
A1
A2
B
D1 = 1.80 ms
Position (ms)
Time (ms)
O
A1
A2
C
D1 = 2.90 ms
Position (ms)
Time (ms)
O
A1
A2

6.3.5e The D type graph.

Because of the unusual features displayed in the D type graphs (Fig 6.7a & b) and the limited number of examples of this type of D2 versus D1 graph, the space-time diagram constructed from CL48#98 should be regarded as in part speculative. From the understanding gained from the space-time analysis of the B group of graphs, the absence of an upper plateau and the commencement of a descending ramp at D1 = 0, would imply that the MTP for collision would be located on the stimulus side of the lesion. This agrees with the only moderately increased latencies in this group and more severely affected RPTs, as seen in the B type graphs. During a ramp feature, the limiting factor for the transmission of A2 was refractoriness generated by the orthodromic impulse within the lesion, when collisions are occurring on the stimulus side of the most affected region of the axon (Fig 6.14a).

Previous analysis suggests that a lower plateau would occur when there is a region of axon towards the stimulus site with refractoriness less than the region of most elevated RPT. The height of the plateau would be determined by the passage of A1 through the region of lesser refractoriness. The plateau should then end with the arrival of the orthodromic impulse at the stimulus site. There are, however, a number of features of D graphs that do not coincide with this analysis.

First and foremost, the low plateau should end in a descending ramp, not a sharp rise to a new elevated plateau of D2 values. Secondly, the probable orthodromic latency is not in agreement with the D1 value at the end of the low plateau. In normal axons, the orthodromic latency (derived from the D1 interval to the shoulder of the ramp) ranged from being 0.16-0.39 ms shorter than the antidromic latency (Chapter 4, pp 128-130). For CL48#98 the orthodromic latency (by subtraction from the measured antidromic latency) would therefore be between 1.50-1.73 ms and for LB73 #56, 0.89-1.12 ms. This can be seen to fall well short of the end of the low plateau in both cases (Fig. 6.7) and coincide more with the commencement of the low plateau.

FIGURE 6.14 Space-time diagrams for the D type D2 versus D1 graphs.

A space-time diagram constructed for the key points in the D type of the D2 versus D1 graphs. The parameters of this diagram are representative of all D type graphs (Figure 6.7).

A D1 = 0, the upper ramp. The MTP for collision of the orthodromic (O) and first antidromic (A1) was located within the second region of refractoriness (R#2), however, the limiting boundary for the passage of second antidromic impulse (A2) was the refractoriness generated by O in the third (R#3) and most severely affected region along the axon.

B D1 = 1.96 ms, the low plateau. When S1 was applied after the effects of the passage of O through the stimulus site have subsided A1 is launched and passes through the region of mild conduction deficit (R#1), but fails to transmit to the recording site when it encounters further refractoriness towards the recording site. The new limiting boundary for the transmission of A2 then becomes the ending of the refractoriness generated by A1 in the R#1 region of axon.

C D1 = 2.54 ms, the rise in the D2 values towards the collision-free D1. When the A1 is launched at a time that is long enough to allow it to just progress past both R#1 and R#2 regions, it will be unable to progress into region R#3. The refractoriness generated by A1 in the R#2 region will then be the limiting event for the transmission of A2.

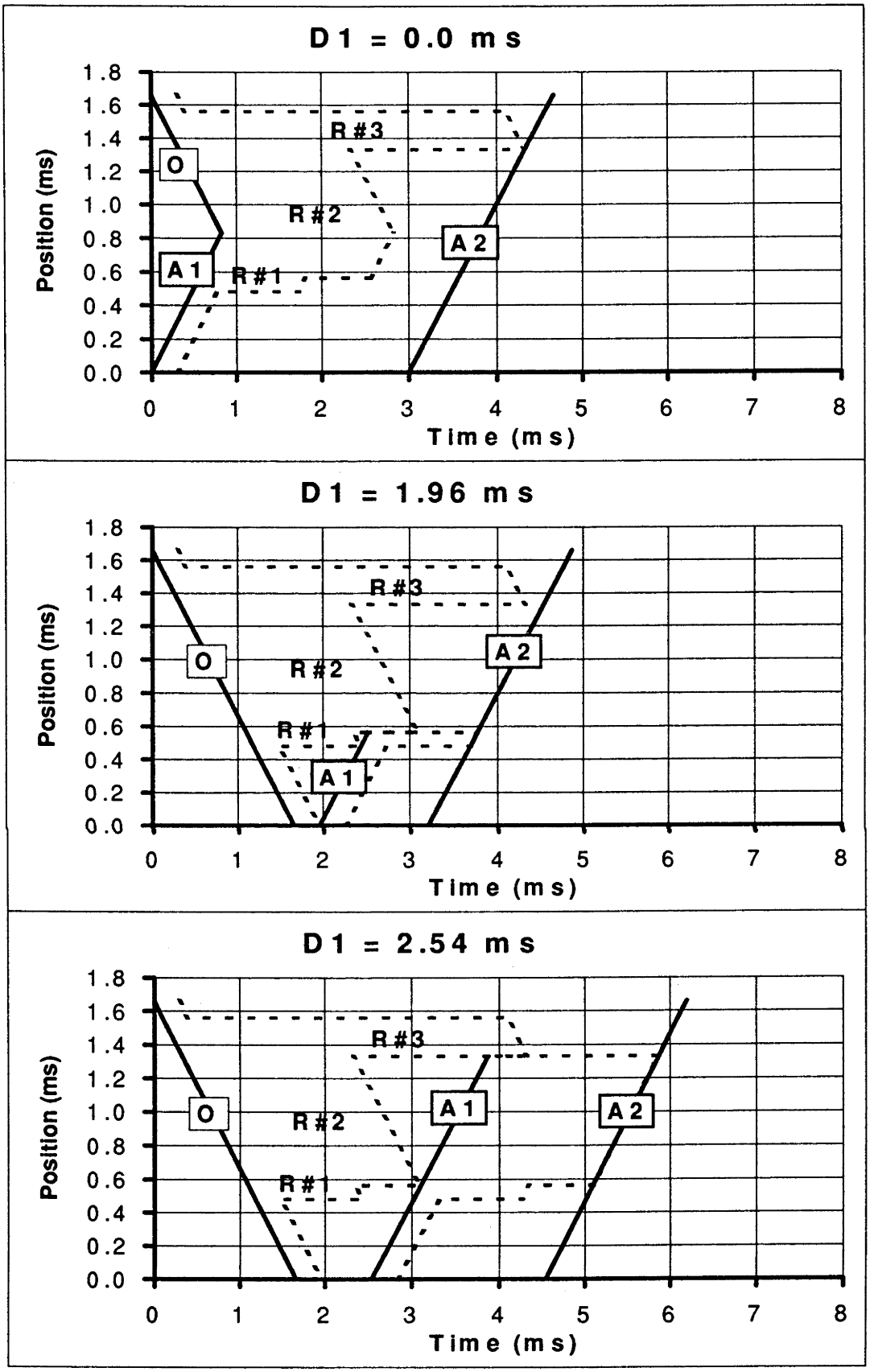
D1 = 0.0 ms
Position (ms)
Time (ms)
O
A1
A2
R#1
R#2
R#3
D1 = 1.96 ms
Position (ms)
Time (ms)
O
A1
A2
R#1
R#2
R#3
D1 = 2.54 ms
Position (ms)
Time (ms)
O
A1
A2
R#1
R#2
R#3

Furthermore, in normal axons, the critical value of D1 for launching a non-colliding A1 ('collision-free D1') is equal to the sum of the orthodromic latency (D1 value at the junction of lower plateau and lower ramp - ie. at the lower shoulder) plus the refractoriness at the stimulus site (ie. height of the lower plateau). With the two axons now under consideration, the sums of orthodromic latency and the average rRPT value of the low plateau were 3.38-3.61 ms for CL48#98 and 1.70-1.93 ms for LB73#56 and the measured intervals were 4.72 and 2.50 ms respectively.

It is suggested that the solution to these discrepancies may lie in lesions with regions of differing refractoriness. These clearly occurred in the D2 versus D1 graphs with an intermediate plateau. In order to generate the D type graphs, these multiple regions of refractoriness must be organised to produce particular limiting boundaries for the partial propagation of A1 at various D1 intervals which have differing consequences for the timing of the propagation of A2 to the recording site. While the borders of these regions cannot be clearly delineated, with the present paradigm, the space-time analysis shows that a lesion with multiple regions of refractoriness, could produce the features observed in D type graphs.

In Fig. 6.14a, the collision at the MTP occurs on the stimulus side of the region of greatest refractoriness and the passage of the orthodromic impulse through this most severely affected region (3) of the axon, sets the limiting boundary for the successful transmission of A2. Because the end of this refractoriness is fixed in time from the detection of the orthodromic impulse at the recording site, further increments in the D1 interval cause the D2 interval to decrease by a similar amount, thereby forming the upper ramp.

This situation is maintained until the increase in the D1 interval causes A1 to be generated after the passage of the orthodromic impulse though the stimulus site and the subsidence of any associated refractoriness at the stimulus site (Fig. 6.14b). A1 will proceed past the first region of refractoriness, only to fail to transmit through the second region. The refractoriness generated by A1 in the first region of the lesion will then become the limiting boundary for the passage of A2. This boundary is, however, far enough to the right of the edge of lingering refractoriness associated with the passage of the orthodromic impulse in the most severely affected region of the axon, that A2 can

proceed unhindered to the recording site. Further increments in the D1 interval will cause a similar increment in the D2 value, so that they form the lower plateau.

It is suggested that the rise in D2 values at the end of the low plateau, will occur when A1 can be transmitted past the end of refractoriness generated by the orthodromic impulse in region 2 of the lesion. When A1 encounters the still refractory edge of the segment of axon with the greatest conduction deficit, the impulse fails to transmit to the recording site. The passage of A1 through region 2 creates a new refractory boundary for the transmission of A2. A2, having been shifted again further to the right will proceed unhindered to the recording location (Fig. 6.14c). This will create a new horizontal plateau, in the D2 versus D1 graph, but the level of this plateau will reflect the refractoriness associated with region 2, not that of the most severely affected segment of axon.

During the pressure-lesion experiments, it was possible to seek some confirmation of this understanding of the formation of a rise in D2 values, by disconnecting the first stimulus and comparing the D2 values obtained with those when S1 was in place (Fig. 6.7b, LB73#56). When S1 was disconnected, the D2 values fell to a level that was consistent with the launch of A2 at a fixed time after the detection of the orthodromic impulse (slope -1). When S1 was reconnected, the D2 value rose, clearly demonstrating that the A1 impulse was determining the time to the launch of A2, in this section of the D2 versus D1 graph.

Again, when A1 could finally pass the refractoriness generated by the orthodromic impulse in all parts of the axon, both antidromic impulses are detected at the recording site. The D2 interval would, in these circumstances be determined by the refractoriness generated by the first antidromic impulse in the severely affected region of the axon.

6.3.5f The E type graphs.

The elevated plateau and its coincidence with the standard RPT measurement implies that these axons had abnormal refractoriness extending back to the stimulus site (Fig. 6.15). In these circumstances the limiting refractoriness for the transmission of A2

will remain the same until the orthodromic impulse reaches the stimulus site. The ramp of D2 values will then be generated in the manner already described above.

6.3.6 The stimulus-side edge of the lesion.

As explained in Chapter 4, p 132, it is possible to calculate the time from the stimulus site to the edge of the lesion. In the temporal domain, any increase in the D1 interval represents an increase in the travelling time of the orthodromic impulse that is half the increment in D1. Where there is an upper plateau, such as in C type graphs, the shoulder of the upper plateau is thought to coincide with collision at the edge of the vulnerable region closest to the stimulus site. The shoulder at the end of the lower plateau is thought to coincide with the arrival of the orthodromic impulse at the stimulus site. The time it will take the orthodromic impulse to travel from the edge of the lesion to the stimulus site, is therefore $(D1_{LS}-D1_{US})/2$. To translate the time that it takes for the orthodromic impulse to travel from the edge of the lesion to the stimulus site into the spatial domain, it is necessary to know the CV of the impulse in the putatively normal upstream segment of the axon. Then distance (mm) to the edge of the lesion = $[(D1_{LS}-D1_{US})/2] \times CV$.

In one example (#21) from the animal LB85, the latency and collision paradigms were measured from all 3 stimulation sites, the OT, OX and ON (Fig 6.16a, b, c). The distance between each of the stimulating electrodes was also measured at the conclusion of the electrophysiological experiment. It was 21 mm from the ON to OX electrode and 9 mm from the OX to the OT stimulating electrodes. The D2 versus D1 graphs from the OT and OX (Fig 6.16a, b), are both C type graphs with upper plateaux, and lower plateaux at a height that is within the range of standard RPT in normal cats.

FIGURE 6.15 Space-time diagrams for the E type D2 versus D1 graphs.

A space-time diagram constructed for the key points in the E type D2 versus D1 graphs. The parameters of this diagram are representative of all E type graphs and are based on the data from Figure 6.8. This diagram is constructed for D1 =0. The presence of a focal lesion was not detected by the collision paradigm but both the elevated standard RPT and the height of the plateau, indicate that the axon had been affected. A2 is limited by the refractoriness generated by A1 in the segment of the axon from the mid-time point to the stimulus site.

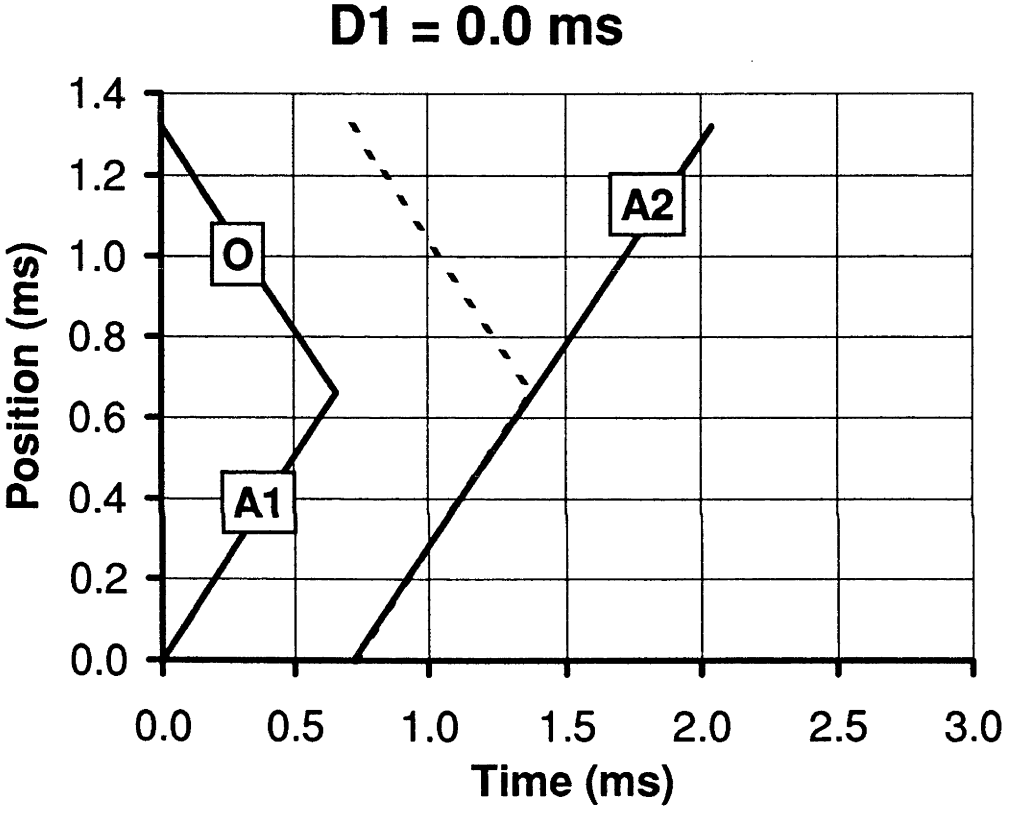
D1 = 0.0 ms
Position (ms)
1.4
1.2
1.0
0.8
0.6
0.4
0.2
0.0
O
A1
A2
0.0
0.5
1.0
1.5
2.0
2.5
3.0
Time (ms)

FIGURE 6.16 D2 versus D1 graphs for an axon driven from all three stimulation sites

A series of D2 versus D1 graphs based on data obtained from one BS/T2 axon LB85#21, and measured from three stimulation sites along the optic pathway.

A Stimulating electrode located in the optic tract (OT). The latency of the axon when measured from the OT stimulation site was 2.68 ms and the RPT was 1.08 ms. The D2 versus D1 graph belonged to group C.

B Stimulating electrode located in the optic chiasm (OX). The latency of the axon had shortened to 2.22 ms and the RPT was 1.17 ms. The D2 versus D1 graph still was a C type.

C Stimulating electrode located in the optic nerve (ON), below the lesion site. The latency of the axon had considerably shortened to 0.78 ms and the RPT was 0.62 ms. The D2 versus D1 graph was now a normal graph type, with no indication of conduction vulnerability.

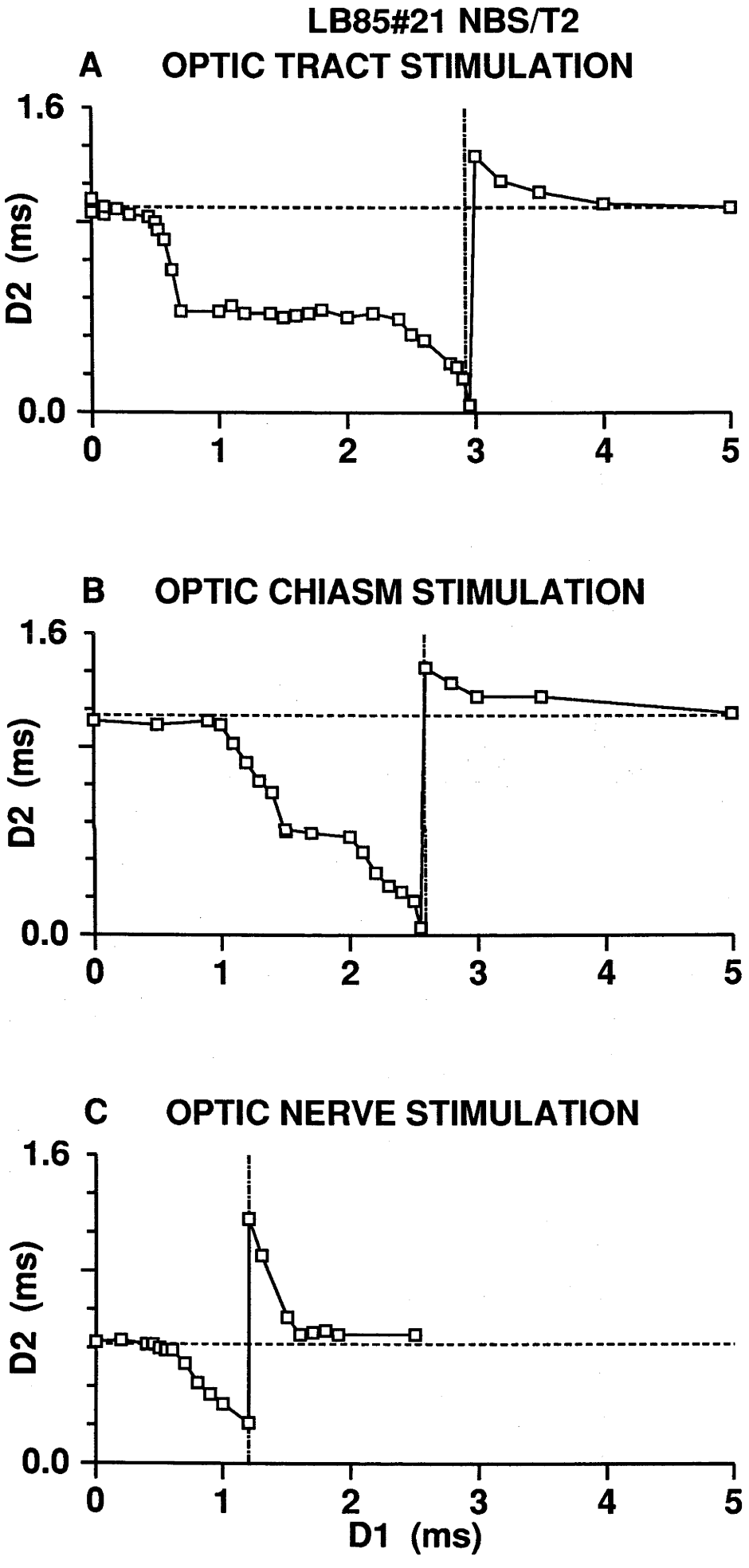
LB85#21 NBS/T2
A OPTIC TRACT STIMULATION
1.6
D2 (ms)
0.0
0
1
2
3
4
5
B OPTIC CHIASM STIMULATION
1.6
D2 (ms)
0.0
0
1
2
3
4
5
C OPTIC NERVE STIMULATION
1.6
D2 (ms)
0.0
0
1
2
3
4
5
D1 (ms)

The shoulder of the upper plateau in the graph from the OT (Fig. 6.16a) is at a D1 of 0.46 ms and the D1 at the end of the lower shoulder is 2.40 ms. The time for the orthodromic impulse to travel from the lesion to the stimulus site is therefore (2.40-0.46)/2 = 0.97 ms. The CV (distance between the stimulus sites divided by the difference in antidromic latencies) from the OT to OX stimulating electrodes was 19.6 m/s. As the lesion was located in the ON, this is likely to be the CV in the normal segment of axon. In addition, this CV is within the range for contralateral T2 axons as measured by Bishop, Jeremy and Lance (1953) and as measured for normal axons (Table 3.1, p 79). The distance from the edge of the lesion to the OT stimulating electrode is therefore 19.0 mm. While variations in the CV between OT and ON would affect the present calculation, it was noted that little such variation occurred for the BS/T2 fibres (Table 3.1, p 79).

Similar calculations can be performed on the data obtained from the collision paradigm driven from the OX electrode (Fig. 6.11b). The time from the edge of the lesion to the stimulus site is (2.05-1.00)/2 = 0.53 ms. Therefore the distance from the edge of the lesion to the OX stimulating electrode is 10.4 mm. As the distance from the OX to OT electrodes was 9 mm, it can be seen that these two separate estimates of distance to the edge of the lesion, in the one axon, give consistent results.

The third graph (Fig. 6.11c) from the ON stimulating electrodes is, however, a normal D2 versus D1 graph, with no evidence of an upper plateau or elevated standard RPT. This indicates that the axon downstream from the ON electrode is unaffected by the pressure lesion.

6.4 DISCUSSION

6.4.1 Collision paradigm.

The present method of using the collision paradigm to study conduction vulnerability in focal lesions of single axons of the optic nerve, has a number of advantages. The paradigm has, most importantly, allowed the examination *in vivo* of regional security of conduction in mammalian CNS. It has demonstrated the likely

regional security of conduction in mammalian CNS. It has demonstrated the likely localisation of regional conduction vulnerability to the physical lesion. It has also detected the presence of a segment of axon upstream from a focal lesion with conduction within normal limits. It allows comparisons with other CNS studies that have used more invasive methods. Finally, the development of the space-time analysis, permits greater visualisation of the electrophysiological events that occur along the axon.

There are some restrictions associated with the present method, that need to be clarified. Of relevance to the limit of refractoriness that can be ascertained by the paradigm is the slowing of the CV of a second impulse when it is generated during the refractory period of a preceding impulse (Gotch, 1910, Gasser and Erlanger, 1925). As previously discussed in Chapters 3 and 4, when a retrobulbar region of conduction vulnerability lies some distance from the stimulus site (approximately 30 mm from the OT and 21 mm from OX stimulating electrodes), the increasing separation of paired impulses with long conduction time, may cause mild conduction vulnerability to be undetected by the collision paradigm. Data derived from normal cats, suggests that RPTs of between 0.9-1.1 ms for BT/T1-BS/T2 driven from the OT and 0.8-1.0 ms in BT/T1-BS/T2 axons from the OX, may not be revealed.

A further restriction is that the collision paradigm is confined to examining a length of axon from the MTP to the stimulus site. In the present experiments, with an OT or OX stimulating electrode, a recording electrode at the OD margin and the use of the normal maintained discharge, as it passed the recording electrode, as the source of the orthodromic impulse, the retrobulbar lesion was not always reached by a collision at the MTP. Alteration of the conduction distance by locating either the recording electrode out into the peripheral retina or the stimulating electrode towards the ON, would move the MTP within the lesion. This also occurs with increased conduction time within the lesion itself, which is what occurred in those axons which had an upper plateau consistent with the standard RPT. Because the MTP varied in each axon, the length of axon over which the rRPT could be measured also varied.

Further, moving the MTP to the retinal side of the lesion does not permit examination of the RPT of the axon on that side of the lesion. The greater refractoriness within the lesion will always conceal the possibly shorter RPT of the normal axon on the

other side of the lesion. The collision paradigm with the present electrode configuration can therefore not establish the spatial extent of a lesion in its entirety. However, a lesion could be experimentally probed from the opposite direction by a stimulus site in the retina with a recording electrode in the OT and a further stimulating electrode further back in the pathway (to generate the colliding single impulse). It would also be possible to obtain a more extensive picture by using a stimulating electrode positioned at the site of the lesion.

6.4.2 Space-time analysis.

The advantages of using the space-time analysis to interpret the features of the D2 versus D1 graphs were numerous. By presenting the trajectories of the impulses in two dimensional space, and ultimately, through the transformation of the Y axis, as straight lines, it was possible to visualise their intersection (collision) and the effects of their associated refractoriness on the transmission of subsequent impulses. Most usefully, the space-time diagrams allowed the plateau and ramp features of the graphs to be readily related to the switch between when the first antidromic impulse (plateau) to when the orthodromic impulse (ramp) generated the limiting boundary of refractoriness.

In the D group axons, the interpretation of the ramp and plateau became critical to establishing that the initial ramp was associated with events set up by the orthodromic impulse and that the plateau and more importantly that the rise in D2 values at the end of the plateau were associated with the first antidromic impulse. In the other lesioned axons, it also enabled features such as upper plateaux and ramps to be linked to the spatio-temporal location of the lesion.

6.4.3 The spatial distribution of conduction vulnerability.

The spatial extent of the lesion can, in part, be obtained from the data derived from the collision paradigm. The key limitation is not being able to ascertain the temporal location of the retinal edge of the lesion. As mentioned at the start of the discussion, the collision paradigm is only able to reveal the rRPT from the MTP to the stimulus site. A

lower rRPT on the downstream side of the lesion will always be masked by the higher rRPT upstream within the lesion. Even with these restrictions, a lot of information about the spatial extent of the lesion can be acquired.

In the experimental paradigm employed, the distance between the OT stimulating electrode and the OD recording electrode measured 30 mm. In axons without any lesion, the MTP of collision would occur 15 mm from the OT stimulating electrode, barring any consideration of variations in CV such as slower CV through the short unmyelinated segment, the utilisation time associated with the electrical generation of the antidromic impulse and differing CV within the OT and ON (Chapter 3, p 104). In the axons demyelinated by anti-GC, the lesion was thought to be centred 3 mm behind the eye and to extend over some 3 mm. For collision to occur at the stimulus-side edge of the lesion, the orthodromic impulse would have to travel 1.5 mm of normal axon and 3 mm of demyelinated axon in the time that the antidromic impulse travelled 25.5 mm. A simple consideration of the equation, time = distance/ velocity, reveals that an 8-fold decrease of CV within the lesion is necessary to bring the MTP to the stimulus edge of the lesion.

This decrease to 12.5% of normal CV through the lesion is a reasonable estimate of slowing of CV in a demyelinating lesion. The intraretinal CV in unmyelinated optic axons has been calculated to be 10% of the CV in the myelinated portion of the optic axons (Stone and Freeman, 1971), although Bostock and Sears (1978) estimated that CV through a PNS demyelinating lesion (diphtheria toxin), had slowed to a lower 5% of normal CV.

Variation in the intra-lesion conduction time would obviously alter the point on the axon where the MTP for collision would occur and account for the formation of either an A, B or C type D2 versus D1 graph, the C graph obviously having the slower intra-lesion CV. Increasing the conduction distance between the recording site and the lesion would have a similar effect. Recordings from the peripheral retina were, however, not routinely used, as it was observed that affected axons could be readily located by recordings from around the OD margin, particularly in the anti-GC lesioned animals, whereas they could only be located with difficulty in the peripheral retina.

In the pressure-lesioned axons, the longitudinal extent of the lesion is not as

possible to establish that the stimulus edge of the lesion was approximately 10 mm from the OX stimulating electrode. As the CV in the unaffected OT was known (19.6 m/s), it can be calculated that if the lesion extended close to the ON electrode, a distance of 11 mm, the time taken to travel the unaffected portion of axon would be 0.51 ms. The latency from the ON electrode to the OX stimulus site was 1.44 ms, so the time to traverse the lesion would be 0.93 ms, which translates to a CV of 11.8 m/s, around 60% of the normal CV.

If, however, the lesion was only 1 mm in extent, the time to traverse the lesion would be 0.42 ms. This gives a intra-lesion CV of 2.38 m/s, around 12.1 % of the normal CV. While the extent of the lesion on the retinal side cannot be established, the latter percentage reduction of normal CV is very similar to that obtained in the anti-GC-induced lesion.

The spatial extent of the lesion in the D group of axons was difficult to establish, because of uncertainties in the exact interplay of possible events along the axon. Any variations in the lesion of those axons with E types of graphs could not be ascertained, because there were no regions along the axon that had greater RPT than at the stimulus site.

6.4.4 Functional aspects of the lesion

The collision paradigm has demonstrated that single demyelinated optic axons can transmit two impulses upstream from the lesion, at a minimum interval which reflects the RPT for normal axons. This supports the classic neuropathological observation of Charcot (1877), that the distal segments of axons demyelinated in MS, retain their integrity. It also concurs with the neurophysiological observations of McDonald and Sears, (1970) and Smith et al., (1981), that normal CV occurs in segments of axons that are located outside the portions of spinal cord that have been demyelinated by diphtheria toxin and lysophosphatidyl choline respectively.

All 49 axons from both the anti-GC injected and pressure-lesioned animals, with D2

versus D1 graphs classified as A, B, or C, had lower plateaux of a height that was within the range of the standard RPT for normal axons, proving that despite the presence of a lesion, these axons continued to have normal conduction parameters upstream from the lesion. The increment in the standard RPT over the height of the lower plateau, in these individual axons, ranged from a 1.3-5.5 fold increase. In the D group axons, where the RPT of the axon upstream from the lesion could not be ascertained, the increase in the standard RPT over the mean normal RPT (0.50 ms) was as great as tenfold.

This is in good agreement with an eightfold increase in the standard RPT measure in single demyelinated dorsal column axons (McDonald and Sears, 1970). Their reported normal RPT for spinal axons was 0.85 ms, somewhat higher than the normal RPT in optic axons, possibly due to the low stimulus intensity used by McDonald and Sears (1.2 x threshold), compared to the minimum stimulus strength used in this present study (3.7 x threshold, Fig 3.3, p 85). Smith et al., (1981) using CAPs, obtained RPT measurements prior to demyelination of between 0.60-0.80 ms, and observed an increase in the range of measured RPT (0.80-4.0 ms) after the application of lysophosphatidyl choline.

6.4.5 The D group of graphs.

The D type graphs were the most complex to interpret. A construction of the space-time diagram revealed that the rise in the D2 values towards the collision free D1, could only be attributed to refractoriness generated by the first antidromic impulse. This was confirmed in the pressure-lesion experiments, (LB73 #56, Fig 6.7b) where the disconnection of the first stimulus during this phase of the collision paradigm, caused the D2 value to fall in a short ramp with a slope of approximately -1. The space-time analysis also revealed that the initial ramp was associated with the passage of the orthodromic impulse through the most severely affected region of the axon and that the MTP for collision was on the stimulus side of the edge of the lesion.

However, not all features of the D group of axons could be established with certainty. This is primarily because the nature of the axon towards the stimulus site is not known. Space-time analysis had lead to the understanding that the critical limiting event

for the formation of a plateau must be the refractoriness generated by the first antidromic impulse.

Formation of the low plateau and variations in its length (compare Figs 6.7a and 7b) may be brought about by changes in the timing of the ending of the various regions of refractoriness in relation to each other and their spatial extent. One possibility that appears to meet the data obtained in the D2 versus D1 graphs is, the further the refractoriness associated with region 2 of the lesion extends to the right, then the more extended will be the time over which the low plateau should persist.

The multiple regions of refractoriness and the rapid changes between the D1 interval at which an A1 impulse is blocked and then can pass to the next region, will also account for the rapid changes in D2 values, seen at the commencement and the endings of the low plateau.

The exact dimensions and numbers of regions of differing refractoriness towards the stimulus site, cannot be determined by the collision paradigm in its present form. These may be further determined by the addition of a third antidromic impulse in the collision paradigm, the use of additional stimulating electrodes and the disconnection of the first impulse at other times to confirm which impulse, the antidromic or orthodromic, is determining the value of D2 at any juncture. This does, however, require very good stability in the recording over a long period of time.

6.4.6 The intermediate plateau.

While there is some indirect evidence of possible multiple regions of different refractoriness in the D type graphs, direct evidence of an intermediate plateau, indicating at least three zones of differing refractoriness, was found only in the pressure-lesioned animals. There are two aspects of the pressure lesion that may predispose this form of axonal injury to creating regions of varying conduction deficit. It has been observed that preceding demyelination in pressure-lesioned axons, there is some displacement of the nodes of Ranvier located at the edges of the cuff used to apply pressure to the nerve. This is then followed by paranodal demyelination around the affected nodes with relative

sparing of the portion of the axons under the pressure cuff (Ochoa et al., 1972). Unlike the injection of anti-GC which causes an apparently uniform and focal lesion (Carroll et al., 198x), applying pressure to a nerve appears to damage both the portion of the axon located under the cuff and to severely distort the structure of the axon at the edges of the cuff.

A second factor may lie in the severity of the pressure lesion compared to that observed in the animals with optic axons demyelinated by anti-GC. Evidence presented in Chapter 5, indicates that the percentage of blocked and abnormally conducting axons was much higher, both in the mild and severe pressure lesions, than in the anti-GC animals. Some of the cause of the increased percentages of blocked axons may lie in the longitudinal extent of the pressure induced lesions. Coupled with evidence of secondary zones of conduction deficit remote to the primary lesion (see below), it is possible that such an axonal injury may cause zones of different conduction deficit along the axon.

6.4.7 "Sick BTs"

The possibility that a number of severely damaged axons may have their responses to visual stimulation altered, has already been raised in this thesis. It has been suggested that in addition to axonal damage sufficient to block conduction, secondary changes may also be occurring towards the cell body of the neuron, causing possible retraction of the dendritic structure of the RGC, amongst other effects (Chapter 5, pp 168-169).

The three RGC with atypical visual responses, able to be driven from the ON electrode alone and which had rRPT measured by using the collision paradigm, revealed that the segment of axon close to the ON electrode had abnormal rRPT. It is important to note that all these axons were unable to transmit impulses from either the OT or OX stimulating electrodes, suggesting that upstream from the ON electrode, there were regions of severe damage. In the two axons (LB85#38, LB85#42) that have a plateaux of rRPT lower than the standard RPT measured, it would suggest that there is a region downstream from the MTP (towards the retina), that has a moderate to severe conduction deficit, more severe than that detected between the MTP to the ON stimulus site. In the third axon (LB85#43), the region downstream from the ON electrode does

not appear to have any region of more severe conduction deficit than at the stimulus site.

It is not possible to estimate the position of the region of axon with more severe damage in either LB85#38 or LB85#42, as it is located beyond the reach of the MTP and the CV in the region with the lesser rRPT, is unknown. The possibility that the region of elevated rRPT downstream from the ON electrode may be associated with physiological conduction vulnerability at the ON heminode can largely be discounted on the basis of results discussed in Chapter 4, p 131-135. In only two of six axons from normal animals tested from an ON electrode, was a region of vulnerability indicated and in marked contrast to the three rRPT graphs from the pressure-lesioned animal, the rRPTs of the upper and lower plateaux in the unlesioned animals, were within the range of standard RPT for normal animals.

The site of the pressure lesion was above the ON electrode and in the cases of RGC with normal visual responses, the collision paradigm from the ON electrode revealed a normal D2 versus D1 graph, such as in LB85#21 (Fig. 6.16). In these three RGC, it is apparent that the segment of axon downstream from the ON stimulation site was abnormal. In the two examples where the rRPT rose towards the MTP, it would appear that a further site of conduction vulnerability occurred towards the retina, secondary to the damage caused directly by the pressure device to the axon upstream from the ON electrode. This secondary loss of security of conduction may be associated with changes in the cell body linked to the damage of the axon of the RGC, at some distance to the cell body (see Chapter 5, pp 168-171).

6.4.8 Summary.

1) The application of the collision paradigm to axons with lesions that cause increases in RPT, produce D2 versus D1 graphs with multiple plateaux and ramps.

2) Analysis using space-time diagrams suggests that some lesioned axons have multiple regions of differing abnormal refractoriness.

3) The collision paradigm demonstrated that lesioned axons generally appear to have normal conduction properties in the segment of axon that lies upstream from the lesion.

Chapter 7.
CONCLUSIONS AND FUTURE PERSPECTIVES.

The results presented in this thesis from studies of single myelinated fibres from the mammalian central nervous system (CNS), have provided the following major observations:

1) In contrast to the generally accepted view of the inverse relationship between conduction velocity and refractoriness, the refractory period of transmission (RPT) of BT/T1 and BS/T2 fibres in the optic pathway of the cat did not vary with their conduction velocity (CV). There were, however, indications that fibres with CV < 20 m/s may have a different relation between CV and RPT.

2) The CV of BT/T1 fibres appeared to change between the optic nerve (ON) and optic tract (OT). The CV in the majority of BT/T1 fibres increased in the OT compared to the ON, but in some fibres the CV decreased.

3) In fibres demyelinated by anti-galactocerebroside (anti-GC), recovery from conduction block appeared to occur before remyelination. The process of recovery appeared to occur in two phases. Initially recovery from block coincided with an increase in the number of axons conducting impulses abnormally. This was followed by the re-establishment of normal conduction parameters in most axons.

4) In the lesioned ON, particularly those subjected to the severe pressure lesion, evidence was obtained suggesting that retinal ganglion cells (RGCs) of the BT/T1 class had abnormal visual response properties in response to injury, which led them to be characterised as non-brisk RGCs.

5) The collision paradigm was used to investigate the spatio-temporal location of the regional RPTs (rRPT). The study of normal axons by this method led to the development of space-time analysis to explain the complex interaction of the orthodromic and two antidromic impulses. This paradigm and analysis were then applied to the lesioned optic axons, permitting investigation of the location, extent and heterogeneity of conduction parameters along the axon.

These observations posed a number of further questions which need to be investigated in the following ways:

1) There is need for a study of fibres with a wider range of diameters, to establish the exact nature of the relationship of CV and RPT, for example in small diameter fibres with CV < 20 m/s. Particular attention needs to be focussed on determining if there is a point of discontinuity in the relationship and the exact nature of the relationship for fibres with CVs below the point of discontinuity.

If such a discontinuity occurs, then it needs to be explained in terms of channel properties and/or nodal structure. A parallel morphological study may be able to elicit relevant changes in structure that reflect the changes in conduction properties.

2) A more comprehensive examination of changes in CV along the single optic fibres is needed. The use of multiple electrodes along the optic pathway is necessary to establish accurate measurements of CVs in particular segments of the fibres. The exact placement and number of electrodes, particularly in the area of the optic chiasm (OX) may be crucial to determining the degree of change in CV and locating the region where such changes might occur.

A further point of interest is whether these changes in CV are of functional significance. There has been a long standing question about the nature of timing of impulses in the visual system. Because the retinal axons are unmyelinated and therefore have long latencies, and because the distances from cell body to the optic nerve head vary over some millimetres in the eye, impulses generated at the same time, but at different points on the retina would tend to reach higher visual centres at different times, unless there are compensatory mechanisms in the optic pathway.

There have been some studies of possible compensatory changes in the diameter of axons within the retina. These have demonstrated only minor changes. The anatomy of the pathway at the point where the ON exits the orbit through the optic foramen, may provide a fundamental restriction of an excessive compensatory increase in the diameter of retinal axons. Therefore, if there are compensatory mechanisms, these may be anatomically more feasible in the central pathways and may parallel known compensatory mechanisms for the ipsi and contralateral projections of the RGCs.

3) Recovery of conduction prior to remyelination has been sometimes, but not always observed in the peripheral nervous system (PNS) and to a lesser extent in the CNS. The molecular and cellular events that underlie this recovery are not known. Various mechanisms for the recovery of conduction in the absence of myelin have been suggested, however, the evidence required to provide a definitive answer is likely to come from a correlative study of electrophysiological changes and associated morphological changes in a model where recovery and remyelination reliably occur. The anti-GC lesion of the CNS may provide such a model and gain insights into the human neuropathophysiology of human CNS demyelinating diseases. The morphological studies would ideally make use of immunohistochemical and freeze fracture techniques, which allow the visualisation of Na+ channels and other relevant molecules.

4) The pressure lesion provided a number of insights into the responses of RGC to severe injury, such as partial degeneration and lesions of variable refractoriness. Further, the phenomenon of "sick BTs" could provide insight into the pre-synaptic inputs of RGCs which generate the visual responses of the ganglion cells. The behaviour of the "sick BTs" needs to be correlated to morphological changes in the cell body and dendritic structure of the RGC. The techniques for such a study are well-established. They include the use of intracellular recording techniques to both characterise the visual responses of the RGC and to fill the cells for subsequent morphological studies.

5) The collision paradigm needs to be further developed with the use of additional electrodes and different electrode placements, so that the spatial extent of the lesion can be definitively determined. This will enable the accurate calculation of CV within the various sections of the axon. Such calculations would lead to a precise knowledge of the spatial location and conduction properties of the lesion.

Given the ability to establish the conduction properties of the lesioned fibre, and given that it was ascertained by this study that the fibres upstream from the anti-GC lesion retained their normal conduction parameters, the normal segment of the optic fibre can be used as an internal control. This would be particularly powerful tool in the pharmacological investigation of the restoration of conduction in demyelinated axons.

While there is clearly more work to be done, these advances in our understanding of conduction in normal and lesioned central fibres may ultimately provide approaches to the more effective restoration of conduction in human demyelinating neuropathies.

REFERENCES

ADRIAN, E. D. (1921). The recovery process of excitable tissues. Part II. *J.Physiol.* 55, 193-225.

ADRIAN, E. D. & LUCAS, K. (1912). On the summation of propagating disturbances in nerve and muscle. *J.Physiol.* **44**, 68-124.

AEBERSOLD, H., CREUTZFELDT, O. D., KUHNT, U. & SANIDES, D. (1981). Representation of the visual field in the optic tract and optic chiasma of the cat. *Exp.Brain Res.* **42**, 127-145.

AWISZUS, F. (1990). Effects of a slow potassium permeability on repetitive activity of the frog node of Ranvier. *Biol.Cybern.* **63**, 155-159.

BAKER, G. E. & STRYKER, M. P. (1990). Retinofugal fibres change conduction velocity and diameter between the optic nerve and tract in ferrets. *Nature* **344**, 342-345.

BAKER, M., BOSTOCK, H., GRAFE, P. & MARTIUS, P. (1987). Function and distribution of three types of rectifying channel in rat spinal root myelinated axons. *J.Physiol.Lond.* **383**, 45-67.

BALL, A. P., HOPKINSON, R. B., FARRELL, I. D., HUTCHISON, J. G., PAUL, R., WATSON, R. D., PAGE, A. J. & PARKER, (1979). Human botulism caused by Clostridium botulinum type E: the Birmingham outbreak. *Q.J.Med.* **48**, 473-491.

BARRES, B. A., CHUN, L. L. & COREY, D. P. (1988). Ion channel expression by white matter glia: I. Type 2 astrocytes and oligodendrocytes. *Glia* **1**, 10-30.

BARRES, B. A., CHUN, L. L. & COREY, D. P. (1989). Glial and neuronal forms of the voltage-dependent sodium channel: characteristics and cell-type distribution. *Neuron* **2**, 1375-1388.

BARRETT, E. F. & BARRETT, J. N. (1982). Intracellular recording from vertebrate myelinated axons: mechanism of the depolarizing afterpotential. *J.Physiol.Lond.* **323**, 117-144.

BARRON, K. D. (1975). Ultrastructural changes in dendrites of central neurons during axon reaction. *Adv.Neurol.* **12**, 381-399.

BATTISTA, A. F. & ALBAN, E. (1983). Effect of graded ligature compression on nerve conduction. *Exp.Neurol.* **80**, 186-194.

BERTHOLD, C. H. (1978). Morphology of normal peripheral axons. In *Physiology and Pathobiology of Axons*, ed. WAXMAN, S. G., pp. 3-63. New York: Raven Press.

BEVAN, S., CHIU, S. Y., GRAY, P. T. & RITCHIE, J. M. (1985). The presence of voltage-gated sodium, potassium and chloride channels in rat cultured astrocytes. *Proc.R.Soc.Lond.B.Biol.Sci.* **225**, 299-313.

BEVER, C. T. J. (1994). The current status of studies of aminopyridines in patients with multiple sclerosis. *Ann.Neurol.* **36 Suppl**, S118-S121.

BISHOP, G. H. & CLARE, M. H. (1955). Organisation and distribution of fibres in the optic tract of the cat. *J.Comp.Neurol.* **103**, 269-304.

BISHOP, G. H. & HEINBECKER, P. (1928). Correlation between threshold and conduction rate. *Proc.Soc.Exp.Biol.Med.* **26**, 241-243.

BISHOP, G. H., CLARE, M. H. & LANDAU, W. M. (1969). Further analysis of fiber groups in the optic tract of the cat. *Exp.Neurol.* **24**, 386-399.

BISHOP, P. O. & MCLEOD, J. G. (1954). Nature of potentials associated with synaptic transmission in lateral geniculate of cat. *J.Neurophysiol.* **17**, 387-414.

BISHOP, P. O., JEREMY, D. & LANCE, J. W. (1953). The optic nerve. Properties of a central tract. *J.Physiol.* **121**, 415-432.

BISHOP, P. O., BURKE, W. & DAVIS, R. (1962a). Single-unit recording from antidromically activated optic radiation neurons. *J.Physiol.* **162**, 432-450.

BISHOP, P. O., BURKE, W. & DAVIS, R. (1962b). The interpretation of the extracellular response of single lateral geniculate cells. *J.Physiol.* **162**, 451-472.

BISHOP, P. O., BURKE, W. & DAVIS, R. (1962c). The identification of single units in central visual pathways. *J.Physiol.* **162**, 409-431.

BISHOP, P. O., KOZAK, W. & VAKKUR, G. J. (1962d). Some quantitative aspects of the cat's eye: axis and plane reference, visual field co-ordinates and optics. *J.Physiol.* **163**, 466-502.

BLACK, I. B. (1993). Viktor Hamburger Award review. Environmental regulation of brain trophic interactions. *Int.J.Dev.Neurosci.* **11**, 403-410.

BLACK, J. A., FOSTER, R. E. & WAXMAN, S. G. (1981). Freeze-fracture ultrastructure of rat C.N.S. and P.N.S. nonmyelinated axolemma. *J.Neurocytol.* **10**, 981-993.

BLACK, J. A., WAXMAN, S. G. & FOSTER, R. E. (1982). Spatial heterogeneity of the axolemma of non-myelinated fibers in the optic disc of the adult rat. Freeze-fracture observations. *Cell Tissue Res.* **224**, 239-246.

BLACK, J. A., WAXMAN, S. G. & HILDEBRAND, C. (1984). Membrane specialization and axo-glial association in the rat retinal nerve fibre layer: freeze-fracture observations. *J.Neurocytol.* **13**, 417-430.

BLACK, J. A., WAXMAN, S. G. & HILDEBRAND, C. (1985). Axo-glial relations in the retina-optic nerve junction of the adult rat: freeze-fracture observations on axon membrane structure. *J.Neurocytol.* **14**, 887-907.

BLACK, J. A., WAXMAN, S. G. & SMITH, M. E. (1987). Macromolecular structure of axonal membrane during acute experimental allergic encephalomyelitis in rat and guinea pig spinal cord. *J.Neuropathol.Exp.Neurol.* **46**, 167-184.

BLACK, J. A., FRIEDMAN, B., WAXMAN, S. G., ELMER, L. W. & ANGELIDES, K. J. (1989). Immuno-ultrastructural localization of sodium channels at nodes of Ranvier and perinodal astrocytes in rat optic nerve. *Proc.R.Soc.Lond.* **B238**, 39-51.

BLACK, J. A., KOCSIS, J. D. & WAXMAN, S. G. (1990). Ion channel organization of the myelinated fiber. *Trends.Neurosci.* **13**, 48-54.

BLACK, J. A., FELTS, P., SMITH, K. J., KOCSIS, J. D. & WAXMAN, S. G. (1991). Distribution of sodium channels in chronically demyelinated spinal cord axons: immuno-ultrastructural localization and electrophysiological observations. *Brain Res.* **544**, 59-70.

BLAIR, E. A. & ERLANGER, J. (1933). A comparison of the characteristics of axons through their individual electrical responses. *Am.J.Physiol.* **106**, 524-564.

BLAIR, E. A. & ERLANGER, J. (1936). On the process of excitation by brief shocks in axons. *Am.J.Physiol.* **114**, 309-316.

BLAKEMORE, W. F. & MURRAY, J. A. (1981). Quantitative examination of internodal length of remyelinated nerve fibres in the central nervous system. *J.Neurol.Sci.* **49**, 273-284.

BLAKEMORE, W. F. & SMITH, K. J. (1983). Node-like axonal specializations along demyelinated central nerve fibres: ultrastructural observations. *Acta Neuropathol.Berl.* **60**, 291-296.

BLIGHT, A. R. (1985). Computer simulation of action potentials and afterpotentials in mammalian myelinated axons: the case for a lower resistance myelin sheath. *Neuroscience* **15**, 13-31.

BLIGHT, A. R. & SOMEYA, S. (1985). Depolarizing afterpotentials in myelinated axons of mammalian spinal cord. *Neuroscience* **15**, 1-12.

BLUNT, M. J., WENDELL-SMITH, C. P. & BALDWIN, F. (1965). Glia-nerve fibre relationships in mammalian optic nerve. *J. Anat. Lond.* **99**, 1-11.

BOSTOCK, H. & GRAFE, P. (1985). Activity-dependent excitability changes in normal and demyelinated rat spinal root axons. *J.Physiol.Lond.* **365**, 239-257.

BOSTOCK, H. & SEARS, T. A. (1976). Continuous conduction in demyelinated mammalian nerve fibers. *Nature* **263**, 786-787.

BOSTOCK, H. & SEARS, T. A. (1978). The internodal axon membrane: electrical excitability and continuous conduction in segmental demyelination. *J.Physiol.Lond.* **280**, 273-301.

BOSTOCK, H., SHERRATT, R. M. & SEARS, T. A. (1978). Overcoming conduction failure in demyelinated nerve fibres by prolonging action potentials. *Nature* **274**, 385-387.

BOSTOCK, H., HALL, S. M. & SMITH, K. J. (1980). Demyelinated axons can form `nodes' prior to remyelination. *J.Physiol.Lond.* **308**, 21P-23P.

BOSTOCK, H., SEARS, T. A. & SHERRATT, R. M. (1981). The effects of 4-aminopyridine and tetraethylammonium ions on normal and demyelinated mammalian nerve fibres. *J.Physiol.Lond.* **313**, 301-315.

BOSTOCK, H., SEARS, T. A. & SHERRATT, R. M. (1983). The spatial distribution of excitability and membrane current in normal and demyelinated mammalian nerve fibres. *J.Physiol.Lond.* **341**, 41-58.

BOWE, C. M., KOCSIS, J. D., TARG, E. F. & WAXMAN, S. G. (1987a). Physiological effects of 4-aminopyridine on demyelinated mammalian motor and sensory fibers. *Ann.Neurol.* **22**, 264-268.

BOWE, C. M., KOCSIS, J. D. & WAXMAN, S. G. (1987b). The association of the supernormal period and the depolarizing afterpotential in myelinated frog and rat sciatic nerve. *Neuroscience* **21**, 585-593.

BOYCOTT, A. E. (1904). On the number of nodes of Ranvier in different stages of the growth of nerve fibres in the frog. *J.Physiol.* **30**, 370-380.

BOYCOTT, B. B. & WASSLE, H. (1974). The morphological types of ganglion cells of the domestic cat's retina. *J.Physiol.Lond.* **240**, 397-419.

BOYD, I. A. & DAVEY, M. R. (1968). *Composition of Peripheral Nerves*. Edinburgh: E. & S. Livingstone Ltd..

BOYD, I. A. & KALU, K. U. (1979). Scaling factor relating conduction velocity and diameter for myelinated afferent nerve fibres in the cat hind limb. *J.Physiol.Lond.* **289**, 277-297.

BRAUN, M. & SCHMIDT, R. F. (1966). Potential changes recorded from the frog motor nerve terminal during its activation. *Pflugers Arch.Gesamte.Physiol.Menschen.Tiere.*

BRIGANT, J. L. & MALLART, A. (1982). Presynaptic currents in mouse motor endings. *J.Physiol.Lond.* **333**, 619-636.

BRILL, M. H., WAXMAN, S. G., MOORE, J. W. & JOYNER, R. W. (1977). Conduction velocity and spike configuration in myelinated fibres: computed dependence on internode distance. *J.Neurol.Neurosurg.Psychiatry* **40**, 769-774.

BRISMAR, T. (1980). Potential clamp analysis of membrane currents in rat myelinated nerve fibres. *J.Physiol.Lond.* **298**, 171-184.

BRISMAR, T. (1981). Specific permeability properties of demyelinated rat nerve fibres. *Acta Physiol.Scand.* **113**, 167-176.

BRISMAR, T. & GILLY, W. F. (1987). Synthesis of sodium channels in the cell bodies of squid giant axons. *Proc.Natl.Acad.Sci.U.S.A.* **84**, 1459-1463.

BULLOCK, T. H. (1951). Facilitation of conduction rate in nerve fibres. *J.Physiol.* **114**, 87-89.

BUNGE, R. P. (1968). Glial cells and the central myelin sheath. *Physiol.Rev.* **48**, 197-251.

BURKE, W. (1986). The function of optic nerve fibre groups in the cat studied by means of selective block. In *Visual Neuroscience*, eds. PETTIGREW, J. D., SANDERSON, K. J. & LEVICK, W. R., pp. 97-110. Cambridge U.K.: Cambridge University Press.

BURKE, W., BURNE, J. A. & MARTIN, P. R. (1985). Selective block of Y optic nerve fibres in the cat and the occurrence of inhibition in the lateral geniculate nucleus. *J.Physiol.Lond.* **364**, 81-92.

BURKE, W., COTTEE, L. J., GARVEY, J., KUMARASINGHE, R. & KYRIACOU, C. (1986). Selective degeneration of optic nerve fibres in the cat produced by a pressure block. *J.Physiol.Lond.* **376**, 461-476.

BURKE, W., COTTEE, L. J., HAMILTON, K., KERR, L., KYRIACOU, C. & MILOSAVLJEVIC, M. (1987). Function of the Y optic nerve fibres in the cat: do they contribute to acuity and ability to discriminate fast motion?. *J.Physiol.Lond.* **392**, 35-50.

BURKE, W., DREHER, B., MICHALSKI, A., CLELAND, B. G. & ROWE, M. H. (1992). Effects of selective pressure block of Y-type optic nerve fibers on the receptive-field properties of neurons in the striate cortex of the cat. *Vis.Neurosci.* **9**, 47-64.

CARLSTEDT, T. (1977). Observations on the morphology at the transition between the peripheral and the central nervous system in the cat. IV. Unmyelinated fibres in S1 dorsal rootlets. *Acta Physiol.Scand.Suppl.* **446**, 61-72.

CARONI, P. & SCHWAB, M. E. (1988). Two membrane protein fractions from rat central myelin with inhibitory properties for neurite growth and fibroblast spreading. *J.Cell Biol.* **106**, 1281-1288.

CARROLL, W. M., JENNINGS, A. R. & MASTAGLIA, F. L. (1984). Experimental demyelinating optic neuropathy induced by intra-neural injection of galactocerebroside antiserum. *J.Neurol.Sci.* **65**, 125-135.

CARROLL, W. M., JENNINGS, A. R. & MASTAGLIA, F. L. (1985). Galactocerebroside antiserum causes demyelination of cat optic nerve. *Brain Res.* **330**, 378-381.

CARROLL, W. M., JENNINGS, A. R. & MASTAGLIA, F. L. (1990). The origin of remyelinating oligodendrocytes in antiserum-mediated demyelinative optic neuropathy. *Brain* **113**, 953-973.

CHAO, T. I., SKACHKOV, S. N., EBERHARDT, W. & REICHENBACH, A. (1994). Na+ channels of Muller (glial) cells isolated from retinae of various mammalian species including man. *Glia* **10**, 173-185.

CHARCOT, J. M. (1877). *Lectures on the Diseases of the Nervous System.* London: The Sydenham Society.

CHIU, S. Y. (1980). Asymmetry currents in the mammalian myelinated nerve. *J.Physiol.Lond.* **309**, 499-519.

CHIU, S. Y. & RITCHIE, J. M. (1981). Evidence for the presence of potassium channels in the paranodal region of acutely demyelinated mammalian single nerve fibres. *J.Physiol.Lond.* **313**, 415-437.

CHIU, S. Y. & RITCHIE, J. M. (1982). Evidence for the presence of potassium channels in the internode of frog myelinated nerve fibres. *J.Physiol.Lond.* **322**, 485-501.

CHIU, S. Y. & RITCHIE, J. M. (1984). On the physiological role of internodal potassium channels and the security of conduction in myelinated nerve fibres. *Proc.R.Soc.Lond.Biol.* **220**, 415-422.

CHIU, S. Y. & SCHWARZ, W. (1987). Sodium and potassium currents in acutely demyelinated internodes of rabbit sciatic nerves. *J.Physiol.Lond.* **391**, 631-649.

CHIU, S. Y., RITCHIE, J. M., ROGART, R. B. & STAGG, D. (1979). A quantitative description of membrane currents in rabbit myelinated nerve. *J.Physiol.Lond.* **292**, 149-166.

CHIU, S. Y., SCHRAGER, P. & RITCHIE, J. M. (1984). Neuronal-type Na+ and K+ channels in rabbit cultured Schwann cells. *Nature* **311**, 156-157.

CLELAND, B. G. & LEVICK, W. R. (1974a). Brisk and sluggish concentrically organized ganglion cells in the cat's retina. *J.Physiol.Lond.* **240**, 421-456.

CLELAND, B. G. & LEVICK, W. R. (1974b). Properties of rarely encountered types of ganglion cells in the cat's retina and an overall classification. *J.Physiol.Lond.* **240**, 457-492.

CLELAND, B. G., DUBIN, M. W. & LEVICK, W. R. (1971). Sustained and transient neurones in the cat's retina and lateral geniculate nucleus. *J.Physiol.Lond.* **217**, 473-496.

CLELAND, B. G., LEVICK, W. R. & WASSLE, H. (1975). Physiological identification of a morphological class of cat retinal ganglion cells. *J.Physiol.Lond.* **248**, 151-171.

CLIFFORD JONES, R. E., LANDON, D. N. & MCDONALD, W. I. (1980). Remyelination during optic nerve compression. *J.Neurol.Sci.* **46**, 239-243.

COHEN, R. A. & FISHER, M. (1989). Amantadine treatment of fatigue associated with multiple sclerosis. *Arch.Neurol.* **46**, 676-680.

COLE, K. S. & CURTIS, H. J. (1939). Electrical impedance of the squid giant axon during activity. *J.Gen.Physiol.* **22**, 649-670.

COOMBS, J. S., CURTIS, D. R. & ECCLES, J. C. (1957a). The generation of impulses in motoneurones. *J.Physiol.* **139**, 232-264.

COOMBS, J. S., CURTIS, D. R. & ECCLES, J. C. (1957b). The interpretation of spike potentials of motoneurones. *J.Physiol.* **139**, 198-231.

COPPIN, C. M. & JACK, J. J. (1972). Internodal length and conduction velocity of cat muscle afferent nerve fibres. *J.Physiol.Lond.* **222**, 92P-93P.

COTTRELL, D. F. (1984). Conduction velocity and axonal diameter of alimentary C fibres. *Q.J.Exp.Physiol.* **69**, 355-364.

CRAGG, B. G. & THOMAS, P. K. (1964). Changes in nerve conduction in experimental allergic neuritis. *J.Neurol.Neurosurg.Psychiat.* **27**, 106-115.

DAVIS, F. A. (1972). Impairment of repetitive impulse conduction in experimentally demyelinated and pressure-injured nerves. *J.Neurol.Neurosurg.Psychiatry* **35**, 537-544.

DAVIS, F. A. & SHAUF, C. L. (1981). Approaches to the development of pharmacological interventions in multiple sclerosis. In *Advances in Neurology Vol.31: Demyelinating Disease*, eds. WAXMAN, S. G. & RITCHIE, J. M., pp. 505-510.

DAVIS, F. A., BECKER, F. O., MICHAEL, J. A. & SORENSEN, E. (1970). Effect of intravenous sodium bicarbonate, disodium edetate (Na2EDTA), and hyperventilation on visual and oculomotor signs in multiple sclerosis. *J.Neurol.Neurosurg.Psychiatry* **33**, 723-732.

DAVIS, F. A., STEFOSKI, D. & RUSH, J. (1990). Orally administered 4-aminopyridine improves clinical signs in multiple sclerosis [see comments]. *Ann.Neurol.* **27**, 186-192.

DENNY-BROWN, D. & BRENNER, C. (1944). Paralysis of nerve induced by direct pressure and by tourniquet. *Arch. Neurol. Psych.* **51**, 1-26.

DODT, E. (1956). Geschwindigkeit der Nervenleitung innerhalb der Netzhaut. *Experientia* **12**, 34-35.

DONOVAN, A. (1967). The nerve fibre composition of the cat optic nerve. *J.Anat.* **101**, 1-11.

DOWLING, J. E. & BOYCOTT, B. B. (1966). Organization of the primate retina: electron microscopy. *Proc.R.Soc.Lond.B.Biol.Sci.* **166**, 80-111.

DUBOIS, J. M. (1981). Evidence for the existence of three types of potassium channels in the frog Ranvier node membrane. *J.Physiol.Lond.* **318**, 297-316.

DUGANDZIJA NOVAKOVIC, S., KOSZOWSKI, A. G., LEVINSON, S. R. & SHRAGER, P. (1995). Clustering of Na+ channels and node of Ranvier formation in remyelinating axons. *J.Neurosci.* **15**, 492-503.

DUN, F. T. (1955). The delay and blockage of sensory impulses in the dorsal root ganglion. *J.Physiol.* **127**, 252-264.

DURON, B., BERNARD, J. F. & LE BARS, P. (1984). Absolute refractory period of the ulnar nerve motor fibers in the human newborn. *Neurosci.Lett.* **45**, 95-98.

ENG, D. L., GORDON, T. R., KOCSIS, J. D. & WAXMAN, S. G. (1988). Development of 4-AP and TEA sensitivities in mammalian myelinated nerve fibers. *J.Neurophysiol.* **60**, 2168-2179.

ENG, D. L., GORDON, T. R., KOCSIS, J. D. & WAXMAN, S. G. (1990). Current-clamp analysis of a time-dependent rectification in rat optic nerve. *J.Physiol.Lond.* **421**, 185-202.

ENGLAND, J. D., GAMBONI, F., LEVINSON, S. R. & FINGER, T. E. (1990). Changed distribution of sodium channels along demyelinated axons. *Proc.Natl.Acad.Sci.U.S.A.* **87**, 6777-6780.

ENGLAND, J. D., GAMBONI, F. & LEVINSON, S. R. (1991). Increased numbers of sodium channels form along demyelinated axons. *Brain Res.* **548**, 334-337.

ENROTH-CUGELL, C. & ROBSON, J. G. (1966). The contrast sensitivity of retinal ganglion cells of the cat. *J.Physiol.* **187**, 517-552.

ERLANGER, J. & BLAIR, E. A. (1934). Manifestations of segmentation in myelinated axons. *Am.J.Physiol.* **110**, 287-311.

ERLANGER, J. & GASSER, H. S. (1937). *Electrical signs of nervous activity*. Philadelphia: University of Pennsylvania Press.

EUGENE, D. & TAXI, J. (1991). Effects of axotomy on synaptic transmission and structure in frog sympathetic ganglia. *J.Neurocytol.* **20**, 404-419.

FEIGIN, I. & OGATA, J. (1971). Schwann cells and peripheral myelin within human central nervous tissues: the mesenchymal character of Schwann cells. *J.Neuropathol.Exp.Neurol.* **30**, 603-612.

FERN, R. & HARRISON, P. J. (1991). The effects of compression upon conduction in myelinated axons of the isolated frog sciatic nerve. *J.Physiol.Lond.* **432**, 111-122.

FERNALD, R. & CHASE, R. (1971). An improved method for plotting retinal landmarks and focusing the eyes. *Vision Res.* **11**, 95-96.

FITZGIBBON, T. & FUNKE, K. (1994). Retinal ganglion cell axon diameter spectrum of the cat: mean axon diameter varies according to retinal position. *Vis.Neurosci.* **11**, 425-439.

FORBES, A., RAY, L. H. & GRIFFITH, F. R. J. (1923). The nature of the delay in the response to the second of two stimuli in nerve and in the nerve-muscle preparation. *Am.J.Physiol.66* **553**, 617

FOSTER, R. E., WHALEN, C. C. & WAXMAN, S. G. (1980). Reorganization of the axon membrane in demyelinated peripheral nerve fibers: morphological evidence. *Science* **210**, 661-663.

FOSTER, R. E., CONNORS, B. W. & WAXMAN, S. G. (1982). Rat optic nerve: electrophysiological, pharmacological and anatomical studies during development. *Brain Res.* **255**, 371-386.

FOX, D. A. & RUAN, D. Y. (1989). Time- and frequency-dependent effects of potassium channel blockers on large and medium diameter optic tract axons. *Brain Res.* **498**, 229-242.

FRAHER, J. P. (1978). Quantitative studies on the maturation of central and peripheral parts of individual ventral motoneuron axons. II. Internodal length. *J.Anat.* **127**, 1-15.

FRANKENHAEUSER, B. & HUXLEY, A. F. (1964). The action potential in the myelinated nerve fibre of Xenopus Laevis as computed on the basis of voltage clamp data. *J.Physiol.* **171**, 302-315.

FREEMAN, B. (1978). Myelin sheath thickness and conduction latency groups in the cat optic nerve. *J.Comp.Neurol.* **181**, 183-196.

FRIED, K. & ERDELYI, G. (1984). Short internodal lengths of canine pulp axons in the young adult cat. *Brain Res.* **303**, 141-145.

FRISEN, L. (1973). [Optokinetic nystagmus in neurological focal diagnosis]. *Lakartidningen.* **70**, 1306-1308.

FUKUDA, Y. & STONE, J. (1974). Retinal distribution and central projections of Y-, X-, and W-cells of the cat's retina. *J.Neurophysiol.* **37**, 749-772.

FULLER, J. H. & SCHLAG, J. D. (1976). Determination of antidromic excitation by the collision test: problems of interpretation. *Brain Res.* **112**, 283-298.

FUNCH, P. G. & FABER, D. S. (1984). Measurement of myelin sheath resistances: implications for axonal conduction and pathophysiology. *Science* **225**, 538-540.

FUORTES, M. G. F., FRANK, K. & BECKER, M. C. (1957). Steps in the production of motorneuron spikes. *J.Gen.Physiol.* **40**, 735-752.

GALLYAS, F. (1979). Silver staining of myelin by means of physical development. *Neurol.Res.* **1**, 203-209.

GASSER, H. S. (1950). Unmedullated fibers originating in dorsal root ganglia. *J.Gen.Physiol.* **33**, 651-690.

GASSER, H. S. & ERLANGER, J. (1925). The nature of conduction of an impulse in the relatively refractory period. *Am.J.Physiol.* **73**, 613-635.

GASSER, H. S. & ERLANGER, J. (1927). The role played by the sizes of the constituent fibres of a nerve trunk in determining the form of its action potential wave. *Am.J.Physiol.* **80**, 522-547.

GASSER, H. S. & ERLANGER, J. (1929). The role of fiber size in the establishment of a nerve block by pressure or cocaine. *Am.J.Physiol.* **88**, 581-591.

GASSER, H. S. & GRUNDFEST, H. (1939). Axon diameters in relation to the spike dimensions and the conduction velocity in mammalian A fibers. *Am.J.Physiol.* **127**, 393-414.

GE, X. X., SPECTOR, G. J. & CARR, C. (1982). The pathophysiology of compression injuries of the peripheral facial nerve. *Laryngoscope* **92**, 1-15.

GEORGE, S. A., MASTRONARDE, D. N. & DUBIN, M. W. (1984). Prior activity influences the velocity of impulses in frog and cat optic nerve fibers. *Brain Res.* **304**, 121-126.

GILLIATT, R. W. & WILLISON, R. G. (1963). The refractory and supernormal periods of the human median nerve. *J.Neurol.Neurosurg.Psychiat.* **26**, 136-147.

GLEDHILL, R. F., HARRISON, B. M. & MCDONALD, W. I. (1973). Pattern of remyelination in the CNS. *Nature* **244**, 443-444.

GOLDMAN, L. & ALBUS, J. S. (1968). Computation of impulse conduction in myelinated fibers; theoretical basis of the velocity-diameter relation. *Biophys.J.* **8**, 596-607.

GOLDSTEIN, S. S. (1978). Models of conduction in nonuniform axons. In *Physiology and Pathobiology of Axons*, ed. WAXMAN, S. G., pp. 227-236. New York: Raven Press.

GOLDSTEIN, S. S. & RALL, W. (1974). Changes of action potential shape and velocity for changing core conductor geometry. *Biophys.J.* **14**, 731-757.

GORDON, T. R., KOCSIS, J. D. & WAXMAN, S. G. (1988). Evidence for the presence of two types of potassium channels in the rat optic nerve. *Brain Res.* **447**, 1-9.

GOTCH, F. (1910). The delay of the electrical response of nerve to a second stimulus. *J.Physiol.Lond.* **40**, 250-274.

GOTCH, F. & BURCH, G. J. (1899). The electrical response of nerve to two stimuli. *J.Physiol.* **24**, 410-426.

GRAFSTEIN, B. & FORMAN, D. S. (1980). Intracellular transport in neurons. *Physiol.Rev.* **60**, 1167-1283.

GRAHAM, H. T. (1934). Supernormality, a modification of the recovery process in nerve. *Am.J.Physiol.*

GRISSMER, S. (1986). Properties of potassium and sodium channels in frog internode. *J.Physiol.Lond.* **381**, 119-134.

GROSSFELD, R. M. (1991). Axon-glia exchange of macromolecules. *Ann.N.Y.Acad.Sci.* **633**, 318-330.

GUILLERY, R. W., POLLEY, E. H. & TORREALBA, F. (1982). The arrangement of axons according to fiber diameter in the optic tract of the cat. *J.Neurosci.* **2**, 714-721.

HADA, J. & HAYASHI, Y. (1990). Retinal X-afferents bifurcate to lateral geniculate X-cells and to the pretectum or superior colliculus in cats. *Brain Res.* **515**, 149-154.

HALL, S. M. & GREGSON, N. A. (1971). The in vivo and ultrastructural effects of injection of lysophosphatidyl choline into myelinated peripheral nerve fibres of the adult mouse. *J.Cell Sci.* **9**, 769-789.

HALLIDAY, A. M. & MCDONALD, W. I. (1977). Pathophysiology of demyelinating disease. *Br.Med.Bull.* **33**, 21-27.

HALLIDAY, A. M., MCDONALD, W. I. & MUSHIN, J. (1972). Delayed visual evoked response in optic neuritis. *Lancet* **1**, 982-985.

HAMASAKI, D. I. & MAGUIRE, G. W. (1985). A neural pathway for the shift response in the cat. *Brain Res.* **337**, 51-58.

HAMMOND, P. (1978a). Inadequacy of nitrous oxide/oxygen mixtures for maintaining anaesthesia in cats: satisfactory alternatives. *Pain* **5**, 143-151.

HAMMOND, P. (1978b). Inadequacy of nitrous oxide/oxygen mixtures for maintaining anaesthesia in cats: satisfactory alternatives. *Pain* **5**, 143-151.

HENDRY, I. A., STACH, R. & HERRUP, K. (1974). Characteristics of the retrograde axonal transport system for nerve growth factor in the sympathetic nervous system. *Brain Res.* **82**, 117-128.

HILDEBRAND, C. (1989). Myelin sheath remodelling in remyelinated rat sciatic nerve. *J.Neurocytol.* **18**, 285-294.

HILDEBRAND, C. & WAXMAN, S. D. (1983). Regional node-like membrane specializations in non-myelinatedaxons of rat retinal nervefibre layer. *Brain Res.* **258**, 23-32.

HILDEBRAND, C., REMAHL, S. & WAXMAN, S. G. (1985). Axo-glial relations in the retina-optic nerve junction of the adult rat: electron-microscopic observations. *J.Neurocytol.* **14**, 597-617.

HILL, A. V. (1936). Excitation and accommodation in nerve. *Proc.Roy.Soc.B.* **119**, 305-355.

HILLE, B. (1967). The selective inhibition of delayed potassium currents in nerve by tetraethylammonium ion. *J.Gen.Physiol.* **50**, 1287-1302.

HILLE, B. (1992). *Ionic channels of excitable membranes*. Sunderland, MA: Sinauer Ass. Inc..

HIRANO, A. & DEMBITZER, H. M. (1978). Morphology of normal central myelinated axons. In *Physiology and Pathobiology of axons*, ed. WAXMAN, S. G., pp. 65-82. New York: Raven Press.

HODES, R. (1953). Linear relationship between fiber diameter and velocity of conduction in giant axon of squid. *J.Neurophysiol.* **16**, 145-154.

HODGKIN, A. L. (1937a). Evidence for electrical transmission in nerve. Part II. *J.Physiol.* **90**, 211-232.

HODGKIN, A. L. (1937b). Evidence for electrical transmission in nerve. Part I. *J.Physiol.* **90**, 183-210.

HODGKIN, A. L. (1964). *The conduction of a nervous impulse*. Springfield, Illinios: Charles C. Thomas.

HODGKIN, A. L. & HUXLEY, A. F. (1952). A quantitative description of membrane current and its application to conduction and excitation in nerve. *J.Physiol.* **117**, 500-544.

HOFFMANN, K. P. (1973). Conduction velocity in pathways from retina to superior colliculus in the cat: a correlation with receptive-field properties. *J.Neurophysiol.* **36**, 409-424.

HOGAN, M. J., ALVARADO, A. B. & WEDDELL, J. E. (1971). *Histology of the human eye*. Philadelphia: W.B.Saunders.

HOLDER, J., STAMPFLI, R. & TASAKI, I. (1952). The role of the potential wave spreading along the myelinated nerve fiber in excitation and conduction. *Am.J.Physiol.* **170**, 375-389.

HOPF, H. C. & LOWITZSCH, K. (1973). Relative refractory periods of motor nerve fibres. In *Neuromuscular Diseases, Proceedings of International Symposium*, eds. KUNZE, K. & DESMEDT, J. E., pp. 264-267. Basel: Karger.

HORACKOVA, M., NONNER, W. & STAMPFLI, R. (1968). Action potentials and voltage clamp currents of single rat Ranvier nodes. *Proc. Int. Union Physiol. Sci.* **7**, 198

HORCHOLLE-BOSSAVIT, G., JAMI, L., PETIT, J. & SCOTT, J. J. (1987). Activation of cat motor units by paired stimuli at short intervals. *J.Physiol.Lond.* **387**, 385-399.

HOWE, J. R. & RITCHIE, J. M. (1990). Sodium currents in Schwann cells from myelinated and non-myelinated nerves of neonatal and adult rabbits. *J.Physiol.Lond.* **425**, 169-210.

HOWE, J. F., CALVIN, W. H. & LOESER, J. D. (1976). Impulses reflected from dorsal root ganglia and from focal nerve injuries. *Brain Res.* **116**, 139-144.

HUGHES, A. (1975). A quantitative analysis of the cat retinal ganglion cell topography. *J.Comp.Neurol.* **163**, 107-128.

HUGHES, A. (1981). Population magnitudes and distribution of the major modal classes of cat retinal ganglion cell as estimated from HRP filling and a systematic survey of the soma diameter spectra for classical neurones. *J.Comp.Neurol.* **197**, 303-339.

HUGHES, A. (1985). New perspectives in retinal organisation. *Prog.Ret. Res.* **4**, 243-313.

HUGHES, A. & WASSLE, H. (1976). The cat optic nerve: fibre total count and diameter spectrum. *J.Comp.Neurol.* **169**, 171-184.

HURSCH, J. B. (1939a). Conduction velocity and diameter of nerve fibres. *Am.J.Physiol.* **127**, 131-139.

HURSCH, J. B. (1939b). The properties of growing nerve fibers. *Am.J.Physiol.* **127**, 140-153.

HUTCHINSON, N. A., KOLES, Z. J. & SMITH, R. S. (1970). Conduction velocity in myelinated nerve fibres of Xenopus laevis. *J.Physiol.Lond.* **208**, 279-289.

HUXLEY, A. F. (1959). Ion movements during nerve activity. *Ann.N.Y.Acad.Sci.* **81**, 221-246.

HUXLEY, A. F. & STAMPFLI, R. (1949). Evidence for saltatory conduction in peripheral myelinated nerve fibres. *J.Physiol.* **108**, 315-339.

ILLING, R. B. & WASSLE, H. (1981). The retinal projection to the thalamus in the cat: a quantitative investigation and a comparison with the retinotectal pathway. *J.Comp.Neurol.* **202**, 265-285.

ILYIN, V. I., KATINA, I. E., LONSKII, A. V., MAKOVSKY, V. S. & POLISHCHUK, E. V. (1980). The Cole-Moore effect in nodal membrane of the frog Rana ridibunda: evidence for fast and slow potassium channels. *J.Membr.Biol.* **57**, 179-193.

ISHISE, J. & ROSENBLUTH, J. (1987). Nodal and paranodal structure during Wallerian degeneration in frog spinal nerve. *Brain Res.* **418**, 85-97.

JACK, J. J. (1975). Physiology of peripheral nerve fibres in relation to their size. *Br.J.Anaesth.* **47 suppl**, 173-182.

JACK, J. J. (1976). Electrophysiological properties of peripheral nerve fibres. In *The Peripheral Nerve*, ed. LANDON, D. N., pp. 740-818. Chapman and Hall: London.

JOE, E. H. & ANGELIDES, K. (1992). Clustering of voltage-dependent sodium channels on axons depends on Schwann cell contact. *Nature* **356**, 333-335.

KAJI, R. & SUMNER, A. J. (1989). Effect of digitalis on central demyelinative conduction block in vivo. *Ann.Neurol.* **25**, 159-165.

KAJI, R., SUZUMURA, A. & SUMNER, A. J. (1988). Physiological consequences of antiserum-mediated experimental demyelination in CNS. *Brain* **111**, 675-694.

KAJI, R., HAPPEL, L. & SUMNER, A. J. (1990). Effect of digitalis on clinical symptoms and conduction variables in patients with multiple sclerosis. *Ann.Neurol* **28**, 582-584.

KATZ, B. & MILEDI, R. (1965). Propagation of electric activity in motor nerve terminals. *Pro.Roy.Soc.B.* **161**, 453-482.

KHODOROV, B. I. & TIMIN, E. N. (1975). Nerve impulse propagation along nonuniform fibres. *Prog.Biophys.Mol.Biol.* **30**, 145-184.

KIMURA, J. (1981). Refractory period measurement in the clinical domain. In *Advances in Neurology, Vol 31, Demyelinating disease*, eds. WAXMAN, S. G. & RITCHIE, J. M., pp. 239-266. New York: Raven Press.

KIRK, D. L., CLELAND, B. G., WASSLE, H. & LEVICK, W. R. (1975). Axonal conduction latencies of cat retinal ganglion cells in central and peripheral retina. *Exp.Brain Res.* **23**, 85-90.

KIRK, D. L., LEVICK, W. R. & CLELAND, B. G. (1976a). The crossed or uncrossed destination of axons of sluggish-concentric and non-concentric cat retinal ganglion cells, with an overall synthesis of the visual field representation. *Vision Res.* **16**, 233-236.

KIRK, D. L., LEVICK, W. R., CLELAND, B. G. & WASSLE, H. (1976b). Crossed and uncrossed representation of the visual field by brisk-sustained and brisk-transient cat retinal ganglion cells. *Vision Res.* **16**, 225-231.

KOCSIS, J. D. & WAXMAN, S. G. (1980). Absence of potassium conductance in central myelinated axons. *Nature* **287**, 348-349.

KOCSIS, J. D. & WAXMAN, S. G. (1981). Action potential electrogenesis in mammalian central axons. *Adv.Neurol.* **31**, 299-312.

KOCSIS, J. D., SWADLOW, H. A., WAXMAN, S. G. & BRILL, M. H. (1979). Variation in conduction velocity during the relative refractory and supernormal periods: a mechanism for impulse entrainment in central axons. *Exp.Neurol.* **65**, 230-236.

KOCSIS, J. D., MALENKA, R. C. & WAXMAN, S. G. (1981). Enhanced parallel fiber frequency-following after reduction of postsynaptic activity. *Brain Res.* **207**, 321-331.

KOCSIS, J. D., MALENKA, R. C. & WAXMAN, S. G. (1983). Effects of extracellular potassium concentration on the excitability of the parallel fibres of the rat cerebellum. *J.Physiol.Lond.* **334**, 225-244.

KOENIG, H., BUNGE, M. B. & BUNGE, R. P. (1962). Nucleic acid and protein metabolism in white matter. *Arch.Neurol.* **6**, 177-193.

KOLB, H., NELSON, R. & MARIANI, A. (1981). Amacrine cells, bipolar cells and ganglion cells of the cat retina: a Golgi study. *Vision Res.* **21**, 1081-1114.

KOLES, Z. J. & RASMINSKY, M. (1972). A computer simulation of conduction in demyelinated nerve fibres. *J.Physiol.Lond.* **227**, 351-364.

KOSUGI, Y., YANAGAWA, N. & IKEBE, J. (1988). A new collision method for the detection of axonal hazard. *IEEE.Trans.Biomed.Eng* **35**, 277-279.

KRNJEVIC, K. & MILEDI, R. (1959). Presynaptic failure of neuromuscular propagation in rats. *J.Physiol.* **149**, 1-22.

KUFFLER, S. W. (1953). Discharge patterns and functional organization of mammalian retina. *J.Neurophysiol.* **16**, 37-68.

LAFONTAINE, S., RASMINSKY, M., SAIDA, T. & SUMNER, A. J. (1982). Conduction block in rat myelinated fibres following acute exposure to anti-galactocerebroside serum. *J.Physiol.Lond.* **323**, 287-306.

LANDON, D. N. (1981). Structure of the normal peripheral myelinated nerve fibres. In *Demyelniating Disease:Basic and Clinical Electrophysiology*, eds. WAXMAN, S. G. & RITCHIE, J. M., pp. 25-49. New York: Raven Press.

LANDON, D. N. & HALL, S. (1976). The myelinated nerve fibre. In *The Peripheral Nerve*, ed. LANDON, D. N., pp. 1-105. Chapman and Hall: London.

LANDON, D. N. & LANGLEY, O. K. (1971). The local chemical environment of nodes of Ranvier: a study of cation binding. *J.Anat.* **108**, 419-432.

LATIES, A. M. & SPRAGUE, J. M. (1966). The projection of optic fibers to the visual centers in the cat. *J.Comp.Neurol.* **127**, 35-70.

LEHMANN, H. J. (1969). The refractory period of peripheral nerve fibres under pathological conditions. *Electroencephalogr.Clin.Neurophysiol.* **26**,

LEHMANN, H. J. & ULE, G. (1964). Electrophysiological findings and structural changes in circumspect inflammation of peripheral nerves. *Prog.Brain Res.* **6**, 169-173.

LEINFELDER, D. J. (1938). Retrograde degeneneration in the optic nerves and retinal ganglion cells. *Trans. Am. Opthal. Soc.* **36**, 307-315.

LEVICK, W. R. (1972). Another tungsten microelectrode. *Med.biol.Engng Comput* **10**, 510-515.

LEVICK, W. R. & THIBOS, L. N. (1983). Receptive fields of cat ganglion cells: classification and construction. In *Progress in Retinal Research, Vol. 2*, eds. OSBORNE, N. & CHADER, G., pp. 267-319. Oxford: Pergamon Press.

LIEBERMAN, A. R. (1971). The axon reaction: a review of the principal features of perikaryal responses to axon injury. *Int.Rev.Neurobiol.* **14**, 49-124.

LILLE, R. S. (1920). The recovery of transmissivity in passive iron wires as a model of recovery processes in irritable living systems. Part 1. *J.Gen.Physiol.* **3**, 107-128.

LILLE, R. S. (1925). Factors affecting transmission and recovery in the passive iron nerve model. *J.Gen.Physiol.* **7**, 473-507.

LIVERANT, S. & MEIRI, H. (1990). Colchicine prevents recovery of nerve conduction at chronic demyelination. *Brain Res.* **519**, 50-56.

LOMBET, A., LADURON, P., MOURRE, C., JACOMET, Y. & LAZDUNSKI, M. (1985). Axonal transport of the voltage-dependent Na+ channel protein identified by its tetrodotoxin binding site in rat sciatic nerves. *Brain Res.* **345**, 153-158.

LUCAS, K. (1910). On the recovery of muscle and nerve after the passage of a propagating disturbance. *J.Physiol.* **41**, 368-408.

LUCAS, K. (1912). The process of excitation in nerve and muscle. *Pro.Roy.Soc.B.* **85**, 495-524.

LUDWIN, S. K. (1978). Central nervous system demyelination and remyelination in the mouse: an ultrastructural study of cuprizone toxicity. *Lab.Invest.* **39**, 597-612.

LUDWIN, S. K. (1981). Pathology of demyelination and remyelination. In *Demyelinating disease: Basic and Clinical Electrophysiology*, eds. WAXMAN, S. G. & RITCHIE, J. M., New York: Raven Press.

LUDWIN, S. K. (1988). Remyelination in the central nervous system and the peripheral nervous system. *Adv.Neurol.* **47**, 215-254.

MACGREGOR, R. J., SHARPLESS, S. K. & LUTTGES, M. W. (1975). A pressure vessel model for nerve compression. *J.Neurol.Sci.* **24**, 299-304.

MAFEI, L. & FIORENTINI, A. (1981). Electroretinographic responses to alternating gratings before and after section of the optic nerve. *Science* **211**, 953-955.

MASTRONARDE, D. N. (1983). Interactions between ganglion cells in cat retina. *J.Neurophysiol.* **49**, 350-365.

MCDONALD, W. I. (1963). The effects of experimental demyelination on conduction in peripheral nerve: a histological and electrophysiological study. II Electrophysiological observations. *Brain* **86**, 501-524.

MCDONALD, W. I. (1974). Remyelination in relation to clinical lesions of the central nervous system. *Br.Med.Bull.* **30**, 186-189.

MCDONALD, W. I. & OHLRICH, G. D. (1971). Quantitative anatomical measurements on single isolated fibres from the cat spinal cord. *J.Anat.* **110**, 191-202.

MCDONALD, W. I. & SEARS, T. A. (1969). Effect of demyelination on conduction in the central nervous system. *Nature* **221**, 182-183.

MCDONALD, W. I. & SEARS, T. A. (1970). The effects of experimental demyelination on conduction in the central nervous system. *Brain* **93**, 583-598.

MCILWAIN, J. T. (1964). Receptive fields of optic tract axons and lateral geniculate nucleus cells: peripheral extent and barbituate sensitivity. *J.Neurophysiol.* **27**, 1154-1173.

MEIRI, H., PRI CHEN, S. & KORCZYN, A. D. (1985). Sodium channel localization in rat sciatic nerve following lead-induced demyelination. *Brain Res.* **359**, 326-331.

MOLL, C., MOURRE, C., LAZDUNSKI, M. & ULRICH, J. (1991). Increase of sodium channels in demyelinated lesions of multiple sclerosis. *Brain Res.* **556**, 311-316.

MOORE, J. W., JOYNER, R. W., BRILL, M. H., WAXMAN, S. D. & NAJAR JOA, M. (1978). Simulations of conduction in uniform myelinated fibers. Relative sensitivity to changes in nodal and internodal parameters. *Biophys.J.* **21**, 147-160.

MORAN, O. & MATEU, L. (1983). Loosening of paranodal myelin by repetitive propagation of action potentials. *Nature* **304**, 344-345.

MOTOKAWA, K., OIKAWA, T. & TASAKI, K. (1957). Studies of neuronal processes in the retina by antidromic stimulation. *Jap.J.Physiol.* **7**, 119-131.

MOYANO, H. F. & MOLINA, J. C. (1980). Axonal projections and conduction properties of olfactory peduncle neurons in the rat. *Exp.Brain Res.* **39**, 241-248.

MULLER, F., WASSLE, H. & VOIGT, T. (1988). Pharmacological modulation of the rod pathway in the cat retina. *J.Neurophysiol.* **59**, 1657-1672.

MURRAY, J. A. & BLAKEMORE, W. F. (1980). The relationship between internodal length and fibre diameter in the spinal cord of the cat. *J.Neurol.Sci.* **45**, 29-41.

NAMEROW, N. S. & THOMPSON, L. R. (1969). Plaques, symptoms, and the remitting course of multiple sclerosis. *Neurology* **19**, 765-774.

NEUMCKE, B., SCHWARZ, J. R. & STAMPFLI, R. (1987). A comparison of sodium currents in rat and frog myelinated nerve: normal and modified sodium inactivation. *J.Physiol.Lond.* **382**, 175-191.

NEUMCKE, B. & STAMPFLI, R. (1982). Sodium currents and sodium-current fluctuations in rat myelinated nerve fibres. *J.Physiol.Lond.* **329**, 163-184.

NJA, A. & PURVES, D. (1978). The effects of nerve growth factor and its antiserum on synapses in the superior cervical ganglion of the guinea-pig. *J.Physiol.Lond.* **277**, 55-75.

NOEBELS, J. L., MARCOM, P. K. & JALILIAN TEHRANI, M. H. (1991). Sodium channel density in hypomyelinated brain increased by myelin basic protein gene deletion. *Nature* **352**, 431-434.

NUWER, M. R. & NAMEROW, N. S. (1981). Somatosensory evoked potential testing in multiple sclerosis. *Adv.Neurol.* **31**, 183-199.

OCHOA, J., FOWLER, T. J. & GILLIATT, R. W. (1972). Anatomical changes in peripheral nerves compressed by a pneumatic tourniquet. *J.Anat.* **113**, 433-455.

OCHS, S. (1972). Rate of fast axoplasmic transport in mammalian nerve fibres. *J.Physiol.Lond.* **227**, 627-645.

OGAWA, T. & TAKAHASHI, Y. (1981). Retinotectal connections within the superficial layers of the cat's superior colliculus. *Brain Res.* **217**, 1-11.

OGAWA, T., IMAZAWA, Y. & CHU, S. (1969). Electrophysiological tracings of intraretinal optic nerve fibers in the cat. *Tohoku J.exp.Med.* **98**, 215-222.

PAINTAL, A. S. (1965). Effects of temperature on conduction in single vagal and saphenous myelinated nerve fibres of the cat. *J.Physiol.* **180**, 20-49.

PAINTAL, A. S. (1966). The influence of diameter of medullated nerve fibres of cats on the rising and falling phases of the spike and its recovery. *J.Physiol.Lond.* **184**, 791-811.

PAINTAL, A. S. (1978). Conduction properties of normal peripheral mammalian axons. In *Physiology and Pathobiology of Axons*, ed. WAXMAN, S. G., pp. 131-144. New York: Raven Press.

PEICHL, L. & WASSLE, H. (1981). Morphological identification of on- and off-centre brisk transient (Y) cells in the cat retina. *Proc.R.Soc.Lond.Biol.* **212**, 139-153.

PELLEGRINO, R. G. & RITCHIE, J. M. (1984). Sodium channels in the axolemma of normal and degenerating rabbit optic nerve. *Proc.R.Soc.Lond.Biol.* **222**, 155-160.

PETTIGREW, J. D., COOPER, M. L. & BLASDEL, G. G. (1979). Improved use of tapetal reflection for eye-position monitoring. *Invest.Ophthalmol.Vis.Sci.* **18**, 490-495.

PLAUT, G. S. (1987). Effectiveness of amantadine in reducing relapses in multiple sclerosis. *J.R.Soc.Med.* **80**, 91-93.

POLMAN, C. H., BERTELSMANN, F. W., DE WAAL, R., VAN DIEMEN, H. A., UITDEHAAG, B. M., VAN LOENEN, A. C. & KOETSIER, J. C. (1994). 4-Aminopyridine is superior to 3,4-diaminopyridine in the treatment of patients with multiple sclerosis. *Arch.Neurol.* **51**, 1136-1139.

POLYAK, S. (1957). *The vertebrate visual system.* Chicago: University of Chicago Press.

POULTER, M. O., HASHIGUCHI, T. & PADJEN, A. L. (1989). Dendrotoxin blocks accommodation in frog myelinated axons. *J.Neurophysiol.* **62**, 174-184.

POWELL, H. C. & MYERS, R. R. (1986). Pathology of experimental nerve compression. *Lab.Invest.* **55**, 91-100.

PRINCE, J. H., DIESEM, C. D., EGLITIS, I. & RUSKELL, G. L. (1960). *Anatomy and Histology of the eye and orbit in domestic animals*. Springfield, Illinois: Charles C. Thomas.

PRINEAS, J. W. & CONNELL, F. (1978). The fine structure of chronically active multiple sclerosis plaques. *Neurology* **28**, 68-75.

PRINEAS, J. W. & CONNELL, F. (1979). Remyelination in multiple sclerosis. *Ann.Neurol.* **5**, 22-31.

PUMPHERY, R. J. & YOUNG, J. Z. (1938). The rates of conduction of nerve fibres of various diameters in cephalopods. *J.Exp.Biol.* **15**, 453-466.

PURVES, D. (1976). Functional and structural changes in mammalian sympathetic neurones following colchicine application to post-ganglionic nerves. *J.Physiol.Lond.* **259**, 159-175.

PURVES, D., SNIDER, W. D. & VOYVODIC, J. T. (1988). Trophic regulation of nerve cell morphology and innervation in the autonomic nervous system. *Nature* **336**, 123-128.

PURVES, D. & LICHTMAN, J. W. (1985). Trophic effects of targets on neurons. In *Principles of Neural Development*, Sunderland MA: Sinauer Associated Inc., pp 155-178.

QUANDT, F. N. & DAVIS, F. A. (1992). Action potential refractory period in axonal demyelination: a computer simulation. *Biol.Cybern.* **67**, 545-552.

QUERFURTH, H. W., ARMSTRONG, R. & HERNDON, R. M. (1987). Sodium channels in normal and regenerated feline ventral spinal roots. *J.Neurosci.* **7**, 1705-1716.

QUICK, D. C., KENNEDY, W. R. & DONALDSON, L. (1979). Dimensions of myelinated nerve fibers near the motor and sensory terminals in cat tenuissimus muscles. *Neuroscience* **4**, 1089-1096.

QUICK, D. C. & WAXMAN, S. G. (1977). Specific staining of the axon membrane at nodes of Ranvier with ferric ion and ferrocyanide. *J.Neurol.Sci.* **31**, 1-11.

RAFF, M. C., MILLER, R. H. & NOBLE, M. (1983). A glial progenitor cell that develops in vitro into an astrocyte or an oligodendrocyte depending on culture medium. *Nature* **303**, 390-396.

RAINE, C. S. (1984). The neuropathology of myelin diseases. In *Myelin*, ed. MORELL, P., pp. 259-310. New York: Plenum Press.

RANCK, J. B. J. (1975). Which elements are excited in electrical stimulation of mammalian central nervous system: a review. *Brain Res.* **98**, 417-440.

RASMINSKY, M. (1973). The effects of temperature on conduction in demyelinated single nerve fibers. *Arch.Neurol.* **28**, 287-292.

RASMINSKY, M. & SEARS, T. A. (1972). Internodal conduction in undissected demyelinated nerve fibres. *J.Physiol.Lond.* **227**, 323-350.

RAYMOND, S. A. & LETTVIN, J. Y. (1978). Aftereffects of activity in peripheral axons as a clue to nervous coding. In *Physiology and Pathobiology of Axons*, ed. WAXMAN, S. G., pp. 203-225. New York: Raven Press.

REINOSO-SUAREZ, F. (1961). *Topographischer Hirnatlas der Katze*. Darmstadt: Herausgegben von E. Merck AG.

RITCHIE, J. M. (1982). On the relation between fibre diameter and conduction velocity in myelinated nerve fibres. *Proc.R.Soc.Lond.Biol.* **217**, 29-35.

RITCHIE, J. M. (1992). Voltage-gated ion channels in Schwann cells and glia. *Trends.Neurosci.* **15**, 345-351.

RITCHIE, J. M. & CHIU, S. Y. (1981). Distribution of sodium and potassium channels in mammalian myelinated nerve. In *Advances in Neurology, Vol. 31. Demyelinating diseases*, eds. WAXMAN, S. G. & RITCHIE, J. M., pp. 329-342. New York: Raven Press.

RITCHIE, J. M. & RANG, H. P. (1983). Extraneuronal saxitoxin binding sites in rabbit myelinated nerve. *Proc.Natl.Acad.Sci.U.S.A.* **80**, 2803-2807.

RITCHIE, J. M. & ROGART, R. B. (1977). Density of sodium channels in mammalian myelinated nerve fibers and nature of the axonal membrane under the myelin sheath. *Proc.Natl.Acad.Sci.U.S.A.* **74**, 211-215.

RITCHIE, J. M., RANG, H. P. & PELLEGRINO, R. (1981). Sodium and potassium channels in demyelinated and remyelinated mammalian nerve. *Nature* **294**, 257-259.

RITCHIE, J. M., BLACK, J. A., WAXMAN, S. G. & ANGELIDES, K. J. (1990). Sodium channels in the cytoplasm of Schwann cells. *Proc.Natl.Acad.Sci.U.S.A.* **87**, 9290-9294.

ROBERTS, W. J. & SMITH, D. O. (1973). Analysis of threshold currents during microstimulation of fibres in the spinal cord. *Acta Physiol.Scand.* **89**, 384-394.

RODIECK, R. W. (1979). Visual pathways. *Annu.Rev.Neurosci.* **2**, 193-225.

RODIECK, R. W., PETTIGREW, J. D., BISHOP, P. O. & NIKARA, T. (1967). Residual eye movements in receptive-field studies of paralyzed cats. *Vision Res.* **7**, 107-110.

ROPER, J. & SCHWARZ, J. R. (1989). Heterogeneous distribution of fast and slow potassium channels in myelinated rat nerve fibres. *J.Physiol.Lond.* **416**, 93-110.

ROSENBERG, G. A. & APPENZELLER, O. (1988). Amantadine, fatigue, and multiple sclerosis. *Arch.Neurol.* **45**, 1104-1106.

ROSENBLUTH, J. (1976). Intramembranous particle distribution at the node of Ranvier and adjacent axolemma in myelinated axons of the frog brain. *J.Neurocytol.* **5**, 731-745.

ROSENBLUTH, J. (1981). Freeze-fracture approaches to ionphore localization in normal and myelin-deficient nerves. In *Advances in Neurology, Vol. 31. Demyelinating disease*, eds. WAXMAN, S. G. & RITCHIE, J. M., pp. 391-418. Raven Press: New York.

ROSENBLUTH, J. (1985). Intramembranous particle patches in myelin-deficient rat axons. *Neurosci.Lett.* **62**, 19-24.

ROSENBLUTH, J. & BLAKEMORE, W. F. (1984). Structural specializations in cat of chronically demyelinated spinal cord axons as seen in freeze-fracture replicas. *Neurosci.Lett.* **48**, 171-177.

ROWE, M. H. (1990). Reduced conduction velocity of retinal Y-cell axons following early partial removal of their synaptic targets. *Brain Res.* **514**, 119-127.

ROWE, M. H. & STONE, J. (1976). Properties of ganglion cells in the visual streak of the cat's retina. *J.Comp.Neurol.* **169**, 99-125.

RUBINSTEIN, C. T. & SHRAGER, P. (1990). Remyelination of nerve fibers in the transected frog sciatic nerve. *Brain Res.* **524**, 303-312.

RUIT, K. G., OSBORNE, P. A., SCHMIDT, R. E., JOHNSON, E. M.,JR. & SNIDER, W. D. (1990). Nerve growth factor regulates sympathetic ganglion cell morphology and survival in the adult mouse. *J.Neurosci.* **10**, 2412-2419.

RUSHTON, W. A. H. (1951). A theory of the effects of fibre size in medullated nerve. *J.Physiol.* **115**, 101-122.

SAIDA, T. (1985). Myelin antigens and immune-mediated demyelination of peripheral nerve. In *The Pathology of the Myelinated Axon*, eds. ADACHI, M., HIRANO, A. & ARONSON, S. M., pp. 195-227. New York: Igaku Shoin.

SAIDA, K., SAIDA, T., BROWN, M. J. & SILBERBERG, D. H. (1979). In vivo demyelination induced by intraneural injection of anti-galactocerebroside serum: a morphologic study. *Am.J.Pathol.* **95**, 99-116.

SAIDA, K., SUMNER, A. J., SAIDA, T., BROWN, M. J. & SILBERBERG, D. H. (1980). Antiserum-mediated demyelination: relationship between remyelination and functional recovery. *Ann.Neurol.* **8**, 12-24.

SAIDA, K., SAIDA, T., KAYAMA, H. & NISHITANI, H. (1984). Rapid alterations of the axon membrane in antibody-mediated demyelination. *Ann.Neurol.* **15**, 581-589.

SAITO, H. A. (1983). Morphology of physiologically identified X-, Y-, and W-type retinal ganglion cells of the cat. *J.Comp.Neurol.* **221**, 279-288.

SANDERS, F. K. (1948). The thickness of the myelin sheaths of normal and regenerating peripheral nerve fibres. *Proc.Roy.Soc.B.* **135**, 323

SCHALOW, G. (1989). Efferent and afferent fibres in human sacral ventral nerve roots: basic research and clinical implications. *Electromyogr.Clin.Neurophysiol.* **29**, 33-53.

SCHAUF, C. L. (1987). Amantadine restores impulse conduction across demyelinated nerve segments. *Clin.Exp.Pharmacol.Physiol.* **14**, 273-281.

SCHAUF, C. L. & DAVIS, F. A. (1974). Impulse conduction in multiple sclerosis: a theoretical basis for modification by temperature and pharmacological agents. *J.Neurol.Neurosurg.Psychiatry* **37**, 152-161.

SCHNAPP, B. J. & REESE, T. S. (1986). New developmants in understanding rapid axonal transport. *Trends.Neurosci.* **9**, 155-162.

SCHWARZ, J. R., CORRETTE, B. J., MANN, K. & WIETHOLTER, H. (1991). Changes of ionic channel distribution in myelinated nerve fibres from rats with experimental allergic neuritis. *Neurosci.Lett.* **122**, 205-209.

SEARS, T. A. & BOSTOCK, H. (1981). Conduction failure in demyelination: is it inevitable?. *Adv.Neurol.* **31**, 357-375.

SELEKTOR, L. I. & KHODOROV, B. I. (1979). [Nerve impulse conduction along myelinated fibers while internodal vary (mathematical model)]. *Biofizika.* **24**, 910-916.

SERGOTT, R. C., BROWN, M. J., SILBERBERG, D. H. & LISAK, R. P. (1984). Antigalactocerebroside serum demyelinates optic nerve in vivo. *J.Neurol.Sci.* **64**, 297-303.

SHEFNER, J. M. & DAWSON, D. M. (1990). The use of sensory action potentials in the diagnosis of peripheral nerve disease. *Arch.Neurol.* **47**, 341-348.

SHERRATT, R. M., BOSTOCK, H. & SEARS, T. A. (1980). Effects of 4-aminopyridine on normal and demyelinated mammalian nerve fibres. *Nature* **283**, 570-572.

SHRAGER, P., CHIU, S. Y. & RITCHIE, J. M. (1985). Voltage-dependent sodium and potassium channels in mammalian cultured Schwann cells. *Proc.Natl.Acad.Sci.U.S.A.* **82**, 948-952.

SHRAGER, P. (1987). The distribution of sodium and potassium channels in single demyelinated axons of the frog. *J.Physiol.Lond.* **392**, 587-602.

SHRAGER, P. (1989). Sodium channels in single demyelinated mammalian axons. *Brain Res.* **483**, 149-154.

SMALL, R. K., RIDDLE, P. & NOBLE, M. (1987). Evidence for migration of oligodendrocyte--type-2 astrocyte progenitor cells into the developing rat optic nerve. *Nature* **328**, 155-157.

SMITH, K. J. & HALL, S. M. (1980). Nerve conduction during peripheral demyelination and remyelination. *J.Neurol.Sci.* **48**, 201-219.

SMITH, R. S. & KOLES, Z. J. (1970). Myelinated nerve fibers: computed effect of myelin thickness on conduction velocity. *Am.J.Physiol.* **219**, 1256-1258.

SMITH, K. J. & SCHAUF, C. L. (1981a). Size-dependent variation of nodal properties in myelinated nerve. *Nature* **293**, 297-299.

SMITH, K. J. & SCHAUF, C. L. (1981b). Effects of gallamine triethiodide on membrane currents in amphibian and mammalian peripheral nerve. *J.Pharmacol.Exp.Ther.* **217**, 719-726.

SMITH, E. J., BLAKEMORE, W. F. & MCDONALD, W. I. (1979). Central remyelination restores secure conduction. *Nature* **280**, 395-396.

SMITH, K. J., BLAKEMORE, W. F. & MCDONALD, W. I. (1981). The restoration of conduction by central remyelination. *Brain* **104**, 383-404.

SMITH, K. J., BOSTOCK, H. & HALL, S. M. (1982). Saltatory conduction precedes remyelination in axons demyelinated with lysophosphatidyl choline. *J.Neurol.Sci.* **54**, 13-31.

SONTHEIMER, H., FERNANDEZ MARQUES, E., ULLRICH, N., PAPPAS, C. A. & WAXMAN, S. G. (1994). Astrocyte Na+ channels are required for maintenance of Na+/K(+)-ATPase activity. *J.Neurosci.* **14**, 2464-2475.

SPEHLMANN, R. (1967). Compound action potentials of cat optic nerve produced by stimulation of optic tracts and of optic nerve. *Exp.Neurol.* **19**, 156-165.

SRINIVASAN, Y., ELMER, L., DAVIS, J., BENNETT, V. & ANGELIDES, K. (1988). Ankyrin and spectrin associate with voltage-dependent sodium channels in brain. *Nature* **333**, 177-180.

STAMPFLI, R. (1981). Overview of studies on the physiology of conduction in myelinated nerve fibres. In *Advances in Neurology, Vol. 31. Demyelinating disease*, eds. WAXMAN, S. G. & RITCHIE, J. M., pp. 11-23. New York: Raven Press.

STEPHANOVA, D. I. (1988). Systematic paranodal demyelination of nerve fibers: computer simulations. *Electromyogr.Clin.Neurophysiol.* **28**,

STEPHANOVA, D. I. (1989). Conduction along myelinated and demyelinated nerve fibres during the recovery cycle: model investigations. *Biol.Cybern.* **62**, 83-87.

STERLING, P., FREED, M. & SMITH, R. G. (1986). Microcircuitry and functional architecture of the cat retina. *Trends.Neurosci.* **9**, 186-192.

STONE, J. (1965). A quantitative analysis of the distribution of ganglion cells in the cat's retina. *J.Comp.Neurol.* **124**, 337-352.

STONE, J. (1966). The naso-temporal division of the cat's retina. *J.Comp.Neurol.* **126**, 585-600.

STONE, J. & FREEMAN, R. B. (1971). Conduction velocity groups in the cat's optic nerve classified according to their retinal origin. *Exp.Brain Res.* **13**, 489-497.

STONE, J. & FUKUDA, Y. (1974). Properties of cat retinal ganglion cells: a comparison of W-cells with X- and Y-cells. *J.Neurophysiol.* **37**, 722-748.

STONE, J. & HANSEN, S. M. (1966). The projection of the cat's retina on the lateral geniculate nucleus. *J.Comp.Neurol.* **126**, 601-624.

STONE, J. & HOFFMANN, K. P. (1972). Very slow-conducting ganglion cells in the cat's retina: a major, new functional type?. *Brain Res.* **43**, 610-616.

STONE, J. & HOLLANDER, H. (1971). Optic nerve axon diameters measured in the cat retina: some functional considerations. *Exp.Brain Res.* **13**, 498-503.

SUMITOMO, I., IDE, K., IWAMA, K. & ARIKUNI, T. (1969). Conduction velocity of optic nerve fibers innervating lateral geniculate body and superior colliculus in the rat. *Exp.Neurol.* **25**, 378-392.

SUMNER, B. E. (1977). Ultrastructural responses of the hypoglossal nucleus to the presence in the tongue of botulinum toxin, a quantitative study. *Exp.Brain Res.* **30**, 313-321.

SUMNER, B. E. & WATSON, W. E. (1971). Retraction and expansion of the dendritic tree of motor neurones of adult rats induced in vivo. *Nature* **233**, 273-275.

SUR, M. & SHERMAN, S. M. (1982). Retinogeniculate terminations in cats: morphological differences between X and Y cell axons. *Science* **218**, 389

SUZUKI, K., ANDREWS, J. M., WALTZ, J. M. & TERRY, R. D. (1969). Ultrastructural studies of multiple sclerosis. *Lab.Invest.* **20**, 444-454.

SWADLOW, H. A., ROSENE, D. L. & WAXMAN, S. G. (1978). Characteristics of interhemispheric impulse conduction between prelunate gyri of the rhesus monkey. *Exp.Brain Res.* **33**, 455-467.

SWADLOW, H. A. (1982). Antidromic activation: measuring the refractory period at the site of axonal stimulation. *Exp.Neurol.* **75**, 514-519.

SWADLOW, H. A. & WAXMAN, S. G. (1976). Variations in conduction velocity and excitability following single and multiple impulses of visual callosal axons in the rabbit. *Exp.Neurol.* **53**, 128-150.

TACKMANN, W., SPALKE, G. & OGINSZUS, H. J. (1976). Quantitative histometric studies and relation of number and diameter of myelinated fibres to electrophysiological parameters in normal sensory nerves of man. *J.Neurol.* **212**, 71-84.

TAIT, T. (1910). The relation between refractory phase and electric charge. *Quart.J.Exp.Physiol.* **III**, 221-232.

TAKAHASHI, K. (1965). Slow and fast groups of pyramidal tract cells and their respective membrane properties. *J.Neurophysiol.* **28**, 908-924.

TASAKI, I. (1939). The electro-saltatory transmission of the nerve impulse and the effects of narcosis upon the nerve fiber. *Am.J.Physiol.* **127**, 211-227.

TASAKI, I. (1949). Collision of two nerve impulses in the nerve fibre. *Biochim.Biophys.Acta* **3**, 494-497.

TASAKI, I. (1953). *Nervous Transmission.* Springfield, Illinois: C.C.Thomas.

TASAKI, I. (1955). New measurements of the capacity and the resistance of the myelin sheath and nodal membrane of the isloated frog nerve fibre. *Am.J.Physiol.* **181**, 639-650.

TASAKI, I. (1982). *Physiology and Electrochemistry of nerve fibers.* New York: Academic Press.

TASAKI, I. & TAKEUCHI, T. (1941). Der am Ranvierschen knoten entstehende aktionsstrom und seine bedeutung fur die erregungsleitung. *Pflugers Arch.Gesamte Physiol.Menschen Tiere* **244**, 696-711.

TASAKI, I. & TAKEUCHI, T. (1942). Weitere Studien uber den Aktionsstrom der markhaltigen Nervenfaser und ueber die elektrosaltatorische Uebertragung des Nervenimpulses. *Pfluegers Arch. Gesamte Physiol. Menschen Tiere* **245**, 764-782.

THOMAS, R. C. (1972). Electrogenic sodium pump in nerve and muscle cells. *Physiol.Rev.* **52**, 563-594.

TITMUS, M. J. & FABER, D. S. (1990). Axotomy-induced alterations in the electrophysiological characteristics of neurons. *Prog.Neurobiol.* **35**, 1-51.

TRAUGOTT, V. & RAINE, C. S. (1984). The neurology of myelin diseases. In *Myelin*, ed. MORELL, P., pp. 311-335. New York: Plenum Press.

VAKKUR, G. J., BISHOP, P. O. & KOZAK, W. (1963). Visual optics in the cat, including posterior nodal distance and retinal landmarks. *Vision Res.* **3**, 289-314.

VAN DIEMEN, H. A., POLMAN, C. H., VAN DONGEN, T. M., VAN LOENEN, A. C., NAUTA, J. J., TAPHOORN, M. J., VAN WALBEEK, H. K. & KOETSIER, J. C. (1992). The effect of 4-aminopyridine on clinical signs in multiple sclerosis: a randomized, placebo-controlled, double-blind, cross-over study. *Ann.Neurol.* **32**, 123-130.

VANEY, D. I. (1991). Many diverse types of retinal neurons show tracer coupling when injected with biocytin or Neurobiotin. *Neurosci.Lett.* **125**, 187-190.

VENES, J. L., COLLINS, W. F. & TAUB, A. (1971). Nitrous oxide: an anesthetic for experiments in cats. *Am.J.Physiol.* **220**, 2028-2031.

VIZOSO, A. D. & YOUNG, J. Z. (1948). Internode length and fibre diameter in regenerating nerves. *J.Anat.* **82**, 110-134.

WASSLE, H., LEVICK, W. R. & CLELAND, B. G. (1975). The distribution of the alpha type of ganglion cells in the cat's retina. *J.Comp.Neurol.* **159**, 419-438.

WASSLE, H., BOYCOTT, B. B. & ILLING, R. B. (1981). Morphology and mosaic of on- and off-beta cells in the cat retina and some functional considerations. *Proc.R.Soc.Lond.Biol.* **212**, 177-195.

WASSLE, H., PEICHL, L. & BOYCOTT, B. B. (1983). A spatial analysis of on- and off-ganglion cells in the cat retina. *Vision Res.* **23**, 1151-1160.

WAXMAN, S. G. (1972). Regional differentiation of the axon: a review with special reference to the concept of the multiplex neuron. *Brain Res.* **47**, 269-288.

WAXMAN, S. G. (1974). Ultrastructural differentiation of the axon membrane at synaptic and non-synaptic central nodes of Ranvier. *Brain Res.* **65**, 338-342.

WAXMAN, S. G. (1977). Conduction in myelinated, unmyelinated, and demyelinated fibers. *Arch.Neurol.* **34**, 585-589.

WAXMAN, S. G. (1981). Clinicopathological correlations in multiple sclerosis and related diseases. In *Advances in Neurology, Vol. 31. Demyelinating disease*, eds. WAXMAN, S. G. & RITCHIE, J. M., pp. 169-182. Raven Press: New York.

WAXMAN, S. G. (1987). Rules governing membrane organisation and axon-glial interactions during development of myelinated fibers. In *Progress in Brain Research. Vol. 71*, eds. SEIL, F. J., HERBERT, E. & CARLSON, B. M., pp. 121-142. Elsevier Science Publishers: Amsterdam.

WAXMAN, S. G. & BENNETT, M. V. (1972). Relative conduction velocities of small myelinated and non-myelinated fibres in the central nervous system. *Nature New Biol.* **238**, 217-219.

WAXMAN, S. G. & BRILL, M. H. (1978). Conduction through demyelinated plaques in multiple sclerosis: computer simulations of facilitation by short internodes. *J.Neurol.Neurosurg.Psychiatry* **41**, 408-416.

WAXMAN, S. G. & FOSTER, R. E. (1980). Ionic channel distribution and heterogeneity of the axon membrane in myelinated fibers. *Brain Res.* **203**, 205-234.

WAXMAN, S. G. & MELKER, R. J. (1971). Closely spaced nodes of Ranvier in the mammalian brain. *Brain Res.* **32**, 445-448.

WAXMAN, S. G. & RITCHIE, J. M. (1985). Organization of ion channels in the myelinated nerve fiber. *Science* **228**, 1502-1507.

WAXMAN, S. G. & WOOD, S. L. (1984). Impulse conduction in inhomogeneous axons: effects of variation in voltage-sensitive ionic conductances on invasion of demyelinated axon segments and preterminal fibers. *Brain Res.* **294**, 111-122.

WAXMAN, S. G., BLACK, J. A., KOCSIS, J. D. & RITCHIE, J. M. (1989). Low density of sodium channels supports action potential conduction in axons of neonatal rat optic nerve. *Proc.Natl.Acad.Sci.U.S.A.* **86**, 1406-1410.

WAXMAN, S. G., BLACK, J. A., DUNCAN, I. D. & RANSOM, B. R. (1990). Macromolecular structure of axon membrane and action potential conduction in myelin deficient and myelin deficient heterozygote rat optic nerves. *J.Neurocytol.* **19**, 11-28.

WELLER, R. O. (1967). An electron microscopic study of hypertrophic neuropathy of Dejerine and Sottas. *J.Neurol.Neurosurg.Psychiatry* **30**, 111-125.

WILLIAMS, R. W. & CHALUPA, L. M. (1983). An analysis of axon caliber within the optic nerve of the cat: evidence of size groupings and regional organization. *J.Neurosci.* **3**, 1554-1564.

WISNIEWSKI, H. & RAINE, C. S. (1971). An ultrastructural study of experimental demyelination and remyelination. V. Central and peripheral nervous system lesions caused by diphtheria toxin. *Lab.Invest.* **25**, 73-80.

WOLLNER, D. A. & CATTERALL, W. A. (1986). Localization of sodium channels in axon hillocks and initial segments of retinal ganglion cells. *Proc.Natl.Acad.Sci.U.S.A.* **83**, 8424-8428.